

**Pathogenicity of a minimal organism:
Role of protein phosphorylation in
*Mycoplasma pneumoniae***

Dissertation

zur Erlangung des mathematisch-naturwissenschaftlichen Doktorgrades

„Doctor rerum naturalium“

der Georg-August-Universität Göttingen

vorgelegt von

Sebastian Schmidl

aus Bad Hersfeld

Göttingen 2010

Mitglieder des Betreuungsausschusses:

Referent: Prof. Dr. Jörg Stülke

Koreferent: PD Dr. Michael Hoppert

Tag der mündlichen Prüfung: 02.11.2010

“Everything should be made as simple as possible, but not simpler.”

(Albert Einstein)

Danksagung

Zunächst möchte ich mich bei Prof. Dr. Jörg Stülke für die Ermöglichung dieser Doktorarbeit bedanken. Nicht zuletzt durch seine freundliche und engagierte Betreuung hat mir die Zeit viel Freude bereitet. Des Weiteren hat er mir alle Freiheiten zur Verwirklichung meiner eigenen Ideen gelassen, was ich sehr zu schätzen weiß.

Für die Übernahme des Korreferates danke ich PD Dr. Michael Hoppert sowie Prof. Dr. Heinz Neumann, PD Dr. Boris Görke, PD Dr. Rolf Daniel und Prof. Dr. Botho Bowien für das Mitwirken im Thesis-Komitee. Der Studienstiftung des deutschen Volkes gilt ein besonderer Dank für die finanzielle Unterstützung dieser Arbeit, durch die es mir unter anderem auch möglich war, an Tagungen in fernen Ländern teilzunehmen.

Prof. Dr. Michael Hecker und der Gruppe von Dr. Dörte Becher (Universität Greifswald) danke ich für die freundliche Zusammenarbeit bei der Durchführung von zahlreichen Proteomics-Experimenten. Ein ganz besonderer Dank geht dabei an Katrin Gronau, die mich in die Feinheiten der 2D-Gelelektrophorese eingeführt hat. Außerdem möchte ich mich bei Andreas Otto für die zahlreichen Proteinidentifikationen in den letzten Monaten bedanken. Nicht zu vergessen ist auch meine zweite Außenstelle an der Universität in Barcelona. Dr. Maria Lluch-Senar und Dr. Jaume Piñol gilt ein besonderer Dank bei der morphologischen Untersuchungen von Mutanten sowie zahlreichen lustigen Abenden auf Tagungen.

Für die gute Arbeitsatmosphäre und tatkräftige Unterstützung im Labor möchte ich mich bei Julia Busse bedanken. Speziell natürlich für die unzähligen Slot Blots. Ein besonderer Dank geht auch an Hinnerk Eilers für die vielen anregenden Diskussionen rund um die kleinen Biester. Viel Erfolg in Umeå! Meinem Nachfolger Arne Schmeisky wünsche ich alles Gute und hoffe, dass er das Mycoplasmen-Mekka weiterhin gut vertreten wird. Dr. Petra Neumann-Staubitz danke ich für die vielen unterhaltsamen Gespräche im S2-Labor. Mal sehen, ob ihr Schilderwahn einmal ein Ende nimmt! Weiterhin bedanke ich mich bei meinen alteingesessenen sowie neuen Mitstreitern Katrin Gunka, Christine Diethmaier, Christoph Wrede, Nico Pietack, Lope A. Flórez, Martin Lehnik, Frederik Meyer und Fabian Rothe, die in den letzten 3 Jahren viel zu einer entspannten und kreativen Arbeitsatmosphäre beigetragen haben. Ein großer Dank für die Erleichterung des Laboraltages geht auch an unsere „Pufferella“ Bärbel Herbst. Möge sie wieder zu ihrer alten Stärke zurückfinden! Bei der Praktikantin Sandra Appelt,

den Bachelor-Studenten Stephanie Großhennig, Miriam Bothe und Daniel Reuß sowie den Diplomanden Meike Ridderbusch und Pavel Dutow bedanke ich mich für die tatkräftige Unterstützung bei vielen Projekten. Hoffentlich haben sie meinen kleinen Exkurs in die „Advanced and Applied Mycoplasmaology“ gut überstanden!?! Außerdem danke ich noch all jenen, die ich nicht namentlich erwähnen konnte, die mich aber dennoch bei der Erstellung dieser Arbeit unterstützt haben.

Mein ganz spezieller Dank gilt meiner Familie. Ohne die moralische Unterstützung meiner Eltern und meiner Schwester hätte ich weder mein Studium noch meine Doktorarbeit schaffen können. Dafür ein riesengroßes Dankeschön! Zum Schluss gilt mein Dank meiner Freundin Anke, die mich immer wieder neu motiviert und so sehr an mich glaubt.

Contents

Contents	I
List of abbreviations	III
List of publications.....	VII
Summary.....	1
1. Introduction.....	3
(A) <i>Mycoplasma</i> and <i>Spiroplasma</i>	3
(B) Aims of this work	30
2. The stability of cytoadherence proteins in <i>Mycoplasma pneumoniae</i> requires activity of the protein kinase PrkC	31
3. The phosphoproteome of the minimal bacterium <i>Mycoplasma pneumoniae</i>: Analysis of the complete known Ser/Thr kinome suggests the existence of novel kinases.....	52
4. <i>In vitro</i> phosphorylation of key metabolic enzymes from <i>Bacillus subtilis</i>: PrkC phosphorylates enzymes from different branches of basic metabolism	109
5. Upregulation of thymidine kinase activity compensates for loss of thymidylate synthase activity in <i>Mycoplasma pneumoniae</i>	128
6. Interactions between glycolytic enzymes of <i>Mycoplasma pneumoniae</i>....	146
7. The hidden pathway: Impact of the glycerophosphodiesterase GlpQ on virulence of <i>Mycoplasma pneumoniae</i>	161
8. Discussion.....	205

9. References..... 219

10. Appendix..... 245

Curriculum vitae 263

List of abbreviations

5FdUMP	5-fluorodeoxyuridine monophosphat
A	adenine
Å	ångström
ABC	adenosine 5'-triphosphate binding cassette
ADP	adenosine 5'-diphosphate
Amp	ampicillin
Asn	asparagine
ATP	adenosine 5'-triphosphate
B2H	bacterial two-hybrid
bp	base pair
BSA	bovine serum albumin
C	cytosine
Ca ²⁺	calcium cation
Cam	chloramphenicol
cAMP	cyclic adenosine 5'-monophosphate
CDP- <i>Star</i>	disodium 2-chloro-5-(4-methoxyspiro {1,2-dioxetane-3,2'-(5'-chloro)tricyclo[3.3.1.1 ^{3,7}]decan}-4-yl) phenyl phosphate
CH ₃ CN	acetonitrile
CHAPS	3-[(3-cholamidopropyl)dimethylammonio]-1-propanesulfonate
ChIP-chip	chromatin immunoprecipitation with microarray technology
Cho	choline
Ci	curie
cm	centimeter
CM	cell membrane
cm ²	square centimeter
CMP	cytidine 5'-monophosphate
co	control
CO ₂	carbon dioxide
CoA	coenzyme A
COG	cluster of orthologous groups of proteins
Cys	cysteine
Da	dalton
DHAP	dihydroxyacetone phosphate
DIG	digoxigenin
DNA	deoxyribonucleic acid
dT	thymidine
dTDP	thymidine 5'-diphosphate
dTMP	thymidine 5'-monophosphate
DTT	dithiothreitol
dTTP	thymidine 5'-triphosphate
dU	deoxyuridine
dUMP	deoxyuridine 5'-monophosphate
EDTA	ethylenediaminetetraacetic acid
Erm	erythromycine
ESI	electrospray ionization
<i>et al.</i>	and others
FAD	flavin adenine dinucleotide

Fig.	figure
G	guanine
g	gram
G3P	glycerol 3-phosphate
Glc	glucose
Glu	glutamic acid
Gly	glycerol
Gm	gentamicin
GPC	glycerophosphorylcholine
GTP	guanosine 5'-triphosphate
h	hour
H	hydrogen
H ₂ O	water
HCl	hydrochloric acid
HEPES	4-(2-hydroxyethyl)-1-piperazineethanesulfonic acid
His	histidine
HIV	human immunodeficiency virus
HMW	high molecular weight
HPLC	high performance liquid chromatography
HPrK	HPr kinase
i.d.	in diameter
<i>i.e.</i>	that is
IPG	immobilized power of hydrogen gradient
IPTG	isopropyl-β-D-1-thiogalactopyranoside
IS	insertion sequence
Kan	kanamycin
kb	kilobase
KCl	potassium chloride
KClO ₄	potassium perchlorate
kDa	kilodalton
KOH	potassium hydroxide
kPa	kilopascal
l	liter
LB	lysogeny broth
LC	liquid chromatography
Leu	leucine
M	marker
M	molar
m/z	mass-to-charge ratio
mg	milligram
Mg ²⁺	magnesium cation
MgCl ₂	magnesium chloride
μg	microgram
μl	microliter
μm	micrometer
μM	micromolar
min	minute
ml	milliliter
mm	millimeter
mM	millimolar

mmol	millimole
MMR	multiple mutation reaction
Mn ²⁺	manganese cation
MnCl ₂	manganese chloride
MPN	<i>Mycoplasma pneumoniae</i>
mRNA	messenger ribonucleic acid
MS	mass spectrometry
MW	molecular weight
na	not available
NaCl	sodium chloride
NAD ⁺ /NADH	nicotinamide adenine dinucleotide (oxidized/reduced form)
NADPH	nicotinamide adenine dinucleotide phosphate (reduced form)
NaF	sodium fluoride
NaH ₂ PO ₄	monosodium phosphate
NaOH	sodium hydroxide
nd	not detectable
ng	nanogram
NH ₄ HCO ₃	ammonium bicarbonate
Ni ²⁺	nickel cation
nl	nanoliter
nm	nanometer
nmol	nanomole
ns	no significant difference
N-terminal	amino-terminal
OH	hydroxyl group
ORF	open reading frame
P	phosphate
p.s.i.	pound per square inch
PAGE	polyacrylamide gel electrophoresis
PBS	phosphate buffered saline
PCA	perchloric acid
PCR	polymerase chain reaction
PEI	polyethylenimine
PEP	phosphoenolpyruvate
<i>Pfu</i>	<i>Pyrococcus furiosus</i>
pH	power of hydrogen
Phe	phenylalanine
pI	isoelectric point
ppm	parts per million
PrkC	protein kinase C
PrpC	protein phosphatase of the PP2C family
PRPP	phosphoribosyl pyrophosphate
pS	phosphoserine
pT	phosphothreonine
PTS	phosphotransferase system
RNA	ribonucleic acid
RNase	ribonuclease
rRNA	ribosomal ribonucleic acid
s	second
sa	similar amount

SDS	sodium dodecyl sulfate
Ser	serine
Spec	spectinomycin
SSC	saline sodium citrate
Str	streptomycin
<i>Strep</i>	Streptavidin (<i>Streptomyces avidinii</i>)
T	thymine
Tab.	table
TAP	tandem affinity purification
TCA	tricarboxylic acid
Tet	tetracycline
Thr	threonine
TLC	thin layer chromatography
Tn	transposon
Tris	tris(hydroxymethyl)aminomethane
tRNA	transfer ribonucleic acid
Trp	tryptophan
TY	tryptophan yeast
Tyr	tyrosine
U	uracil
UDP	uridine 5'-diphosphate
UMP	uridine 5'-monophosphate
Urd	uridine
UTP	uridine 5'-triphosphate
v	version
vol/vol	volume per volume (volume percent)
vs.	versus
w/o	without
wt	wild type
wt/vol	weight per volume (percentage solution)
X-Gal	5-bromo-4-chloro-3-indolyl- β -D-galactopyranoside
zip	zipper
Zn ²⁺	zinc cation
ZnCl ₂	zinc chloride

List of publications

- Stülke, J., H. Eilers, and S. R. Schmidl.** 2009. *Mycoplasma* and *Spiroplasma*. Encyclopedia of Microbiology (M. Schaechter, ed.), Elsevier, Oxford. p. 208-219.
- Schmidl, S. R., K. Gronau, C. Hames, J. Busse, D. Becher, M. Hecker, and J. Stülke.** 2010. The stability of cytoadherence proteins in *Mycoplasma pneumoniae* requires activity of the protein kinase PrkC. *Infect. Immun.* **78**: 184-192.
- Schmidl, S. R., K. Gronau, N. Pietack, M. Hecker, D. Becher, and J. Stülke.** 2010. The phosphoproteome of the minimal bacterium *Mycoplasma pneumoniae*: Analysis of the complete known Ser/Thr kinome suggests the existence of novel kinases. *Mol. Cell. Proteomics* **9**: 1228-1242.
- Pietack, N., D. Becher, S. R. Schmidl, M. H. Saier, M. Hecker, F. M. Commichau, and J. Stülke.** 2010. *In vitro* phosphorylation of key metabolic enzymes from *Bacillus subtilis*: PrkC phosphorylates enzymes from different branches of basic metabolism. *J. Mol. Microbiol. Biotechnol.* **18**: 129-140.
- Wang, L., C. Hames, S. R. Schmidl, and J. Stülke.** 2010. Upregulation of thymidine kinase activity compensates for loss of thymidylate synthase activity in *Mycoplasma pneumoniae*. *Mol. Microbiol.* **77**: 1502-1511.
- Dutow, P., S. R. Schmidl, M. Ridderbusch, and J. Stülke.** 2010. Interactions between glycolytic enzymes of *Mycoplasma pneumoniae*. *J. Mol. Microbiol. Biotechnol.* accepted.
- Schmidl, S. R., A. Otto, M. Lluch-Senar, J. Piñol, J. Busse, D. Becher, and J. Stülke.** The hidden pathway: Impact of the glycerophosphodiesterase GlpQ on virulence of *Mycoplasma pneumoniae*. *PLoS Pathogens* submitted.

Summary

Mycoplasma pneumoniae is a human pathogen that belongs to the Mollicutes, a group of bacteria with the smallest genomes that are capable of independent life. The reductive evolution of the Mollicutes is reflected by their limited regulatory features for gene expression. Thus, posttranslational regulation might be important for *M. pneumoniae* to adapt to environmental changes. Among the very few regulatory proteins retained is the HPr kinase (HPrK), which phosphorylates the phosphocarrier protein HPr at the Ser-46 residue. This phosphorylation event is a major signal to trigger carbon catabolite repression in less degenerated bacteria. However, the function of HPr(Ser-P) in *M. pneumoniae* is unknown. For the protein phosphatase PrpC, an implication in the dephosphorylation of HPr(Ser-P) could be shown. In addition to HPrK, the *M. pneumoniae* *prkC* gene encodes another serine/threonine protein kinase C.

The determination of the complete phosphoproteome of *M. pneumoniae* by two-dimensional gel electrophoresis and mass spectrometry allowed the detection of 63 phosphorylated proteins, including many enzymes of central carbon metabolism and proteins related to host cell adhesion. It was also possible to detect 16 phosphorylation sites, among them 8 serine and 8 threonine residues. However, a comparison with the phosphoproteomes of other bacteria revealed that there is only a weak conservation of phosphorylation sites, even if the same proteins are phosphorylated in related organisms. There is only one exception: The phosphorylation of phosphosugar mutases on a conserved serine residue, which could be detected in all studied organisms from archaea and bacteria to man. In the case of the phosphosugar mutase ManB in *M. pneumoniae*, it could be shown that this protein undergoes autophosphorylation. In conclusion, the results indicate that protein phosphorylation seems to be highly specific for each individual organism.

For a more detailed analysis of the phosphorylation network in *M. pneumoniae*, the phosphoproteomes of the wild type strain and of three isogenic mutants that are affected in the two protein kinases HPrK and PrkC and in the protein phosphatase PrpC were compared. Examination of the phosphorylation profile of the *hprK* mutant revealed that only HPr is phosphorylated by HPrK, whereas six proteins, including the major adhesin P1 and two cytoadherence proteins HMW1 and HMW3, were affected by the loss of PrkC. In contrast, inactivation of PrpC that antagonizes PrkC-dependent phosphorylation resulted in more intensive phosphorylation of the same target proteins.

The phenotypic characterization of *prkC* mutant cells revealed a nonadherent growth type along with a loss of cytotoxicity toward HeLa cells. Thus, posttranslational modification of cytoadherence proteins by PrkC is essential for cell adhesion and virulence in *M. pneumoniae*.

The phosphoproteomic analysis demonstrated that several glycolytic enzymes are subject to phosphorylation. *M. pneumoniae* uses glycolysis as the major pathway for the generation of energy by substrate-level phosphorylation. Using a bacterial two-hybrid approach, the enolase was identified as the central glycolytic enzyme of *M. pneumoniae* due to its ability to directly interact with all other glycolytic enzymes. Moreover, most of the glycolytic enzymes performed self-interactions. The results support the idea that glycolysis proceeds in a well structured manner even in a minimal organism.

In its natural habitat, *M. pneumoniae* thrives on pulmonary surfaces that are mainly composed of phosphatidylcholine. This phospholipid can be integrated directly into the cell membrane or serve as precursor for cellular processes. *M. pneumoniae* possesses two potential glycerophosphodiesterases, MPN420 (GlpQ) and MPN566, that are able to cleave deacylated phospholipids to glycerol 3-phosphate and choline. Further glycerol 3-phosphate utilization by enzymes of the glycerol metabolism is crucial for the cytotoxicity of *M. pneumoniae* due to hydrogen peroxide release. Biochemical studies showed that GlpQ is active as a glycerophosphodiesterase, whereas MPN566 has no enzymatic activity *in vitro*. Mutants affected in either glycerophosphodiesterase revealed that inactivation of *mpn566* did not result in any phenotype. In contrast, the *glpQ* mutant exhibited a growth defect in glucose-supplemented medium. Moreover, the lack of GlpQ resulted in an absence of hydrogen peroxide formation in the presence of deacylated phospholipids and a loss of cytotoxicity toward HeLa cells. These observations imply that GlpQ is important for the pathogenicity of *M. pneumoniae*, but also for other functions in the cell. Indeed, proteomic and transcriptomic analyses of the wild type and the *glpQ* mutant strain suggested a GlpQ-dependent transcription regulation, which led to higher or lower protein amounts of the glycerol facilitator, a subunit of a metal ion ABC transporter, and three lipoproteins. Interestingly, all genes subject to GlpQ-dependent control have a conserved potential *cis*-acting element upstream of the coding region. Nevertheless, it is open for speculation whether GlpQ or a transcription factor that is controlled by GlpQ is responsible for this regulation.

Chapter 1

Introduction

(A) Mycoplasma and Spiroplasma

This chapter is part of the following publication:

Stülke, J., H. Eilers, and S. R. Schmidl. 2009. *Mycoplasma and Spiroplasma*. Encyclopedia of Microbiology (M. Schaechter, ed.), Elsevier, Oxford. p. 208-219.

Author contributions:

This review was written by JS, HE, and SRS. SRS performed the systematics of the Mollicutes, on which the first two chapters are based as well as partial researches on biochemistry, genetics, and molecular biology of the Mollicutes.

Defining statement

Mycoplasma and *Spiroplasma* species are bacteria that lack a cell wall (the Mollicutes). These organisms evolved in close association with their eukaryotic hosts, resulting in an extreme genome reduction. In this article, the biology of the Mollicutes is discussed with special emphasis on their pathogenicity, cell biology, and molecular biology.

Introduction

Mycoplasmas and spiroplasmas are two important genera of the bacterial group called Mollicutes. The name Mollicutes - *soft skin* - reflects the major collective characteristic of these bacteria - the lack of a cell wall - which at the same time distinguishes them from all other bacteria with the exception of the chlamydiae. The lack of a cell wall is caused by the absence of genes encoding enzymes for peptidoglycan biosynthesis. The lack of a cell wall is closely linked to another characteristic feature of the Mollicutes - their cells are usually pleomorphic. Again, there is no rule without exception: The cells of the genus *Spiroplasma* have a helical shape (see “Cytology of the Mollicutes”).

Another important feature of the Mollicutes is their close association with eukaryotic host organisms. In nature, Mollicutes are never found as free-living organisms. Hosts are either animals including humans (*Mycoplasma*, *Ureaplasma*) or plants and insects (*Spiroplasma*, *Phytoplasma*) (Table 1). *Mycoplasma* species usually cause mild diseases such as atypical pneumonia (*Mycoplasma pneumoniae*) or nongonococcal urethritis (*Mycoplasma genitalium*). However, there is an interesting exception: *Mycoplasma alligatoris*, a pathogen of alligators, causes lethal infections. Although the infections caused by Mollicutes are rarely lethal, Mollicutes pathogenic for plants and animals cause a significant economic loss in agriculture. This is true for cattle in Africa that are infected by *Mycoplasma mycoides* as well as for rice crops in some regions of Southeast Asia that are infected by phytoplasmas. These losses not only have an economic dimension but also a significant effect on human nutrition in the affected regions. *Mycoplasma* species such as *Mycoplasma hyorhinis* or *Acholeplasma laidlawii* are major sources of cell culture contamination and have gained increasing

interest. These infections are often discovered only late in the course of an experiment and can invalidate the scientific research.

The close association of Mollicutes with eukaryotic hosts and their adaptation to habitats with a good nutrient supply and relatively constant growth conditions led to a remarkable process of reductive genome evolution. The organism with the smallest known genome capable of independent life (if provided with rich artificial medium) is *M. genitalium*, a human pathogen. This organism has a genome size of only 580 kb and encodes about 480 proteins, as compared to about 4 million bp and 4000 genes for bacteria such as *Escherichia coli* or *Bacillus subtilis*. These small genomes made the Mollicutes important tools for the new discipline of synthetic biology (see “Genomic comparisons of Mollicutes”).

The systematics of the Mollicutes

Evolution of the Mollicutes. The analysis and comparison of 16S rRNA sequences revealed that the Mollicutes belong to the Gram-positive bacteria with genomes of low GC content. Ironically, most members of this phylum are characterized by their thick Gram-positive cell wall, and the group is therefore referred to as the Firmicutes. This bacterial phylum includes the lactic acid bacteria (such as *Streptococcus* and *Lactobacillus*), spore-forming bacteria (*Bacillus* and *Clostridium*) and their close relatives (*Listeria* and *Staphylococcus*). As can be seen in the phylogenetic tree of the Firmicutes (Fig. 1), the Mollicutes form a sister group to the large *Bacillus*/lactic acid bacteria group. It is believed that the first Mollicutes emerged some 600 million years ago and that significant loss of ancestral genomic sequences was a major force in the evolution of the Mollicutes.

The Mollicutes are subdivided in several ways. Three traditional classifications rely on genetic or physiological properties of the bacteria, whereas more recent classification schemes are based on the similarity of the 16S rRNA or conserved protein families.

Tab. 1. The systematic groups of the Mollicutes.

Order	Genus	Genome size	Sterol requirement	Characteristics	Habitat
Mycoplasmatales	<i>Mycoplasma</i>	580-1350 kb	Yes	Growth optimum: 37°C UGA as Trp codon	Humans, animals
	<i>Ureaplasma</i>	760-1170 kb	Yes	Urea hydrolysis UGA as Trp codon	Humans, animals
Entomoplasmatales	<i>Entomoplasma</i>	790-1140 kb	Yes	Growth optimum: 30°C	Insects, plants
	<i>Mesoplasma</i>	870-1100 kb	No	Growth optimum: 30°C UGA as Trp codon	Insects, plants
	<i>Spiroplasma</i>	780-2200 kb	Yes	Growth optimum: 30-37°C UGA as Trp codon Helical motile filaments	Insects, plants
Anaeroplasmatales	<i>Anaeroplasma</i>	1500-1600 kb	Yes	Obligate anaerobes	Bovine/ovine rumen
	<i>Asteroleplasma</i>	1500 kb	No	Obligate anaerobes	Bovine/ovine rumen
Acholeplasmatales	<i>Acholeplasma</i>	1500-1650 kb	No	Growth optimum: 30-37°C UGA as stopp codon	Animals, plants, insects
	<i>Phytoplasma</i>	640-1185 kb	Not known	Uncultured <i>in vitro</i> UGA as stopp codon	Insects, plants

Two large groups of Mollicutes can be distinguished based on their host organisms. Although most Mollicutes infect exclusively animal hosts, there are other representatives (*Spiroplasma* and *Phytoplasma*) that are capable of infecting both plant and insect hosts. Another conventional way of classifying the Mollicutes is based on their requirement for sterols. Most genera need sterols for growth, whereas this is not the case for the members of the genus *Acholeplasma* (see Table 1). However, this requirement can only be determined for those Mollicutes that can be cultivated, and many (perhaps most) representatives have not yet been cultured, including all species of the genus *Phytoplasma*. Another peculiarity of most Mollicutes is their codon usage: They use the UGA codon to specify tryptophan rather than as a stop codon as in the universal genetic code. Only the genera *Acholeplasma* and *Phytoplasma* among the Mollicutes use UGA as a stop codon. Because this is the ancestral property, it can be assumed that *Acholeplasma* and *Phytoplasma* represent the more ancestral Mollicutes. This conclusion is supported by a phylogenetic tree based on a concatenated alignment of 30 protein families present in all Mollicutes that places the genus *Phytoplasma* at the bottom of the tree (Fig. 1). The genus *Acholeplasma* is not included in this analysis because of the lack of genome sequence information. It is interesting to note that the genus *Mycoplasma* is paraphyletic, and that genera such as *Spiroplasma*, *Mesoplasma*, and *Ureaplasma* have specific relatives among the different *Mycoplasma* clades (Fig. 1).

For practical reasons, the Mollicutes are grouped in four orders that do not represent the phylogenetic relationships. An overview of these taxa is provided in Table 1.

Mycoplasma. As mentioned earlier, the genus *Mycoplasma* is a paraphyletic collection of Mollicutes that are widespread in nature as parasites of humans, mammals, birds, reptiles, and fish. The first representative of the genus *Mycoplasma* was identified in 1898 as the causative agent of contagious bovine pleuropneumonia (*M. mycoides*). The human pathogens *Mycoplasma hominis* and *M. pneumoniae* were discovered in 1937 and 1944, respectively. Even now, new species are being identified: In 1981, *M. genitalium* was isolated from a patient suffering from nongonococcal urethritis, and more recently, *Mycoplasma penetrans* and *Mycoplasma fermentans* were found to be associated with HIV infections.

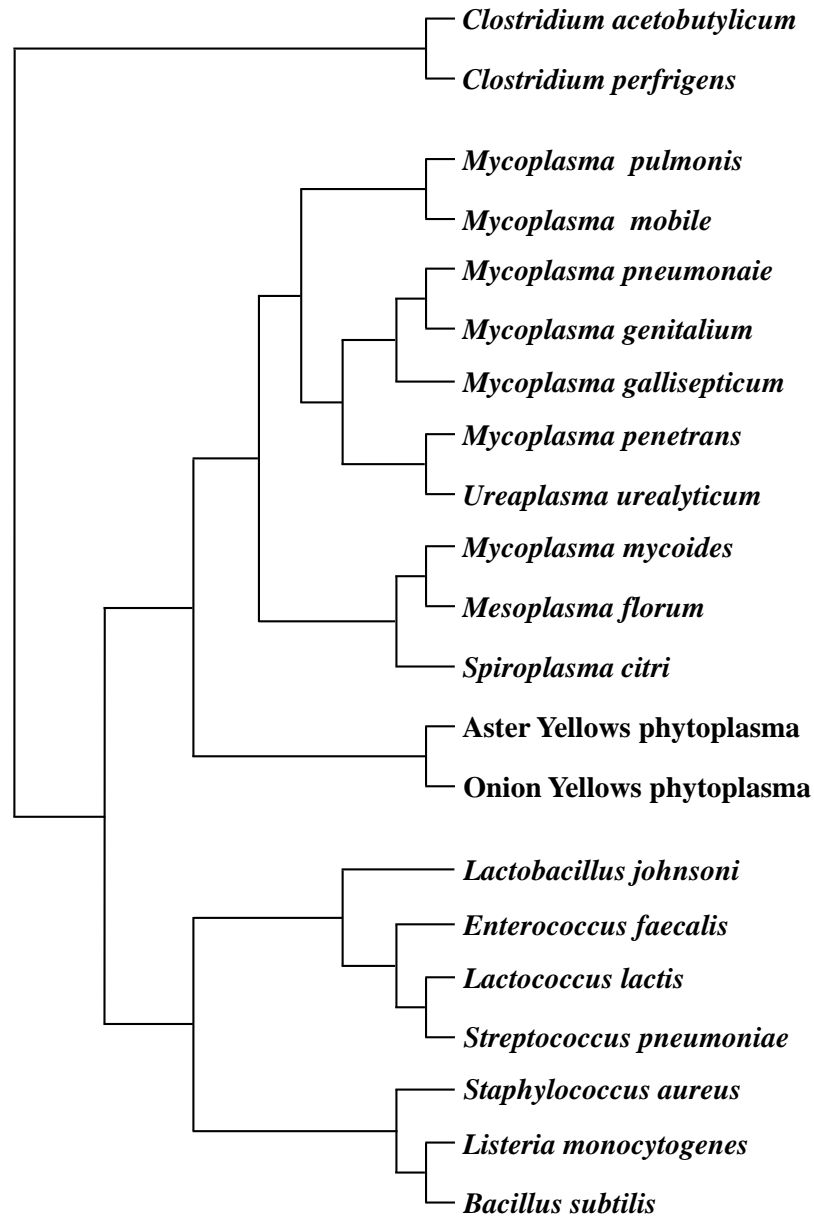


Fig. 1. Unrooted phylogenetic tree of the Firmicutes with special emphasis to the Mollicutes. The tree is based on a concatenated alignment of 31 universal protein families. Reproduced from Ciccarelli *et al.* (2006).

The primary habitats of human and animal mycoplasmas are the mucous surfaces of the respiratory and urogenital tracts, the eyes, the alimentary canal, and mammary glands. In addition, cell cultures are an artificial habitat for many *Mycoplasma* species. The mycoplasmas exhibit a rather strict host and tissue specificity, probably reflecting their highly specific metabolic demands and their parasitic lifestyle. For example, *M. pneumoniae* and *M. genitalium* are preferentially detected in the respiratory and urogenital tracts, respectively.

If cultivated in the laboratory, mycoplasmas as well as other Mollicutes require complex media containing sugars, amino acids, nucleotides, and vitamins. It has so far been impossible to cultivate them on chemically defined media.

The complete genome sequences of ten species of the genus *Mycoplasma* have been determined so far. This large interest in the variability of the *Mycoplasma* genetic complement is stimulated by the interest in creating artificial organisms based on the *Mycoplasma* species (*i.e.*, synthetic biology; see “Genomic comparisons of Mollicutes”). The genome sequences revealed the reason for the complex nutritional requirements of the mycoplasmas: They lack the genes for many biosynthetic pathways and are thus dependent on their host or on the artificial medium to provide these required nutrients. Another interesting feature revealed by genome sequences is that only very few known regulatory proteins are present. Again, this is reflective of their close adaptation to one single natural habitat and a result of the reductive evolution: While a metabolically versatile bacterium such as *Pseudomonas aeruginosa* that is capable of thriving in a wide variety of environments reserves as much as 10% of its genome for regulatory genes, only a handful of these genes is found in the mycoplasmas (see “Gene expression in the Mollicutes”).

Pathogenicity has been most intensively studied with *M. pneumoniae*. In contrast to most other pathogenic bacteria, *M. pneumoniae* and other Mollicutes do not seem to produce any exo- or endotoxins. However, a recent study suggests the formation of a protein similar to ADP-ribosylating and vacuolating cytotoxin. However, this observation has not been confirmed by other groups. A major factor contributing to cytotoxicity and thus to pathogenicity of *M. pneumoniae* is the formation of hydrogen peroxide. The synthesis of hydrogen peroxide by mycoplasmas is most strongly increased if the bacteria are supplied with glycerol. This can be attributed to the oxidase activity of the enzyme that oxidizes glycerol 3-phosphate. This enzyme, glycerol-3-phosphate oxidase, uses water rather than NAD^+ (as in typical glycerol-3-phosphate dehydrogenases) as the electron acceptor. The hydrogen peroxide formed by *M. pneumoniae* acts in concert with endogenous toxic oxygen molecules generated by the host cells and induces oxidative stress in the respiratory epithelium. The effects of the peroxide on the host cells include loss of reduced glutathione, denaturation of hemoglobin, peroxidation of erythrocyte lipids, and eventually the lysis of the cells. Another result of infection by *M. pneumoniae* is the release of

proinflammatory cytokines by the host cells. It has been suggested that cytokine production leads to chronic pulmonary diseases such as bronchial asthma.

The significance of glycerol metabolism in hydrogen peroxide production and virulence has been convincingly demonstrated by a series of studies that started with an analysis of the differences between European and African strains of *M. mycoides*, the causative agent of contagious bovine pleuropneumonia. Glycerol transport is highly efficient in the African isolates, whereas it is barely detectable in the European isolates. Because glycerol catabolism gives rise to the formation of hydrogen peroxide, it is not surprising that hydrogen peroxide production is high in the African strains but low in the European isolates of *M. mycoides*. In consequence, the African strains are highly virulent to cattle, whereas their European relatives are harmless. It has been hypothesized that intracellular formation of large quantities of hydrogen peroxide would be toxic for the producing cells themselves. Accordingly, the cellular localization of the responsible enzyme, GlpO, was studied in *M. mycoides* and it was found to be located in the cell membrane. The inactivation of GlpO by antibodies results in the loss of cytotoxicity of *M. mycoides* toward bovine epithelial cells. Given that hydrogen peroxide in concentrations similar to those produced by *M. mycoides* is not cytotoxic, it was concluded that GlpO is not only inserted in the bacterial cell membrane, but also in the membrane of the host cell to inject the cytotoxic hydrogen peroxide directly into the epithelial cells. This may cause oxidative stress and subsequent cell death.

Plant pathogenic Mollicutes: *Spiroplasma* and *Phytoplasma*. The genera *Spiroplasma* and *Phytoplasma* contain plant pathogenic Mollicutes that shuttle between plant and insect hosts. *Spiroplasma citri* was identified in 1971 as a causative agent of citrus stubborn disease. Phytoplasmas were first described in 1967 as the probable cause of plant yellow diseases. Originally, it was speculated that these diseases are of viral origin, and only in 1967 it became clear that these pathogens are *Mycoplasma*-like organisms. While spiroplasmas can be cultivated in the laboratory, no cultivation of any representative of the phytoplasmas has been reported. Therefore, no valid species description for members of the genus *Phytoplasma* is available. Moreover, *Spiroplasma* cells have a spiral morphology, whereas phytoplasmas are pleomorphic.

Spiroplasma species live in the phloem sieve tubes of their host plants. They are transmitted by insect vectors that feed on the phloem sap. Multiplication of the bacteria occurs both in the plant and in the insect hosts. The most intensively studied representative of the genus, *S. citri*, infects periwinkle (*Catharanthus roseus*) and its vector, the leafhopper *Circulifer haematoceps*. Unfortunately, no genome sequences of any *Spiroplasma* species are so far publicly available, although the *Spiroplasma kunkelii* genome has recently been sequenced.

The spiroplasmas are unique among the Mollicutes for their helical cell morphology, and also by their unique mechanism of locomotion. The genetic determinants for this distinct morphology and movement are so far unknown. Although the spiroplasmas have a shape that is similar to that of the members of the genus *Spirillum*, they are different because they do not possess flagella. Propulsion is generated by a propagation of kink pairs down the length of the cell, caused by a processive change of cell helicity. In addition, these waves of kinks seem to be initiated always by the same end of the cell suggesting cell polarity. Cell polarity can also be concluded from the results of diverse microscopic studies that showed heterogeneity of both ends: One end is tapered with a tip-like structure called terminal organelle and the other one is blunt or round.

An interesting aspect of the *S. citri* lifecycle is the differential utilization of carbohydrates as source of carbon and energy in the two hosts. *S. citri* possesses the genetic equipment for the utilization of sorbitol, trehalose, glucose, and fructose as carbon sources, which are mainly catabolized to acetate. The two habitats of *S. citri* differ significantly in their carbon source availability. While glucose and fructose are predominant in phloem sieve tubes of plants, trehalose is the major sugar in the hemolymph of the vector insect, the leafhopper *C. haematoceps*. The glucose and trehalose permeases of the *S. citri* phosphotransferase system (PTS) share a common IIA domain encoded by the *crr* gene, which might be involved in the rapid physiological adaptation to changing carbon supplies. The glucose and fructose found in the plant sieve tubes are both derived from the cleavage of sucrose by the plant enzyme invertase. A transposon mutagenesis study with *S. citri* revealed that mutants devoid of a functional *fruR* gene encoding the transcriptional activator of the fructose utilization operon are no longer phytopathogenic. The fructose operon of *S. citri* contains three genes, *fruR*, *fruA*, and *fruK* encoding the transcription activator, the fructose-specific

permease of the PTS, and the fructose-1-phosphate kinase, respectively. Mutations in the *fruA* and *fruK* genes also resulted in decreased phytopathogenicity. However, these mutant strains could revert, and this reversion also restored severe symptoms upon plant infection. Thus, fructose utilization and pathogenicity are intimately linked in *S. citri*. In contrast to mutations affecting fructose utilization, a *ptsG* mutation abolishing glucose transport into the cell does not result in reduced pathogenicity of *S. citri*. The reason for the differential implication of the two sugars in pathogenicity was studied by nuclear magnetic resonance analysis and it turned out that the bacteria use fructose preferentially, whereas the glucose accumulated in the leaf cells of the infected plants. This led to the following model. In noninfected plants, both fructose and glucose are formed by invertase. Fructose inhibits this enzyme resulting in a very low activity. In contrast, no inhibition occurs in infected plants because of fructose utilization by *S. citri*. The accumulating glucose that is not used by the bacteria results in inhibition of photosynthesis and thus in the different symptoms.

Transmission from an infected plant to an insect vector occurs by the uptake of bacteria along with the phloem sap. Inside the leafhopper, the bacteria have to pass the intestine midgut lining to multiply in the hemolymph, and then infect the salivary glands. Infection of the salivary glands is important because transmission from the insect to a host plant occurs by inoculation of the saliva into the damaged plant during feeding. It was shown that certain adhesins are necessary for transmissibility of *S. citri* from an infected plant to a vector, and that the genes coding for these adhesins are located on plasmids not existing in all *S. citri* strains.

In contrast to the spiroplasmas whose members are pathogenic to a broad range of plants and insects, the phytoplasmas form their own group among the Mollicutes that is strictly pathogenic to plants. Like the plantpathogenic spiroplasmas, they inhabit the phloem sieve tubes of their host plants after infection by an insect vector (usually belonging to the family of Cicadelli), but they depend completely on their host and so far it has been impossible to cultivate them *in vitro*. However, the genome sequences of three members of this group, *Candidatus Phytoplasma asteris* onion yellows strain (OY-M), aster yellows *Phytoplasma* strain witches broom (AY-WB), and *Candidatus Phytoplasma australiense* have been determined.

Compared to other members of the Mollicutes, the phytoplasmas have some unique features. They exhibit shapes that range from rounded pleomorphic cells, with an average diameter of 200-800 μm , to filaments. Their genomes lack all known genes coding for cytoskeleton or flagellum elements, suggesting that translocation of cells *in planta* is a passive event caused by the flow of phloem sap. As other Mollicutes, the phytoplasmas lack genes for the *de novo* synthesis of amino acids, fatty acids, or nucleotides, but they also lack some genes considered to be essential in all bacteria, such as *ftsZ* encoding a tubulin-like protein. As FtsZ is involved in cell division, the mechanism of division in the phytoplasmas lacking it must be completely different from that of other bacteria. Although living in an environment that is rich in carbon sources, neither of the sequenced *Phytoplasma* possesses genes coding for sugar-specific components of the PTS. In contrast, *S. citri* and *S. kunkelii*, which thrive in the same environment as the phytoplasmas, contain three PTS for the import of glucose, fructose, and the insect-specific sugar trehalose (see earlier). However, *Phytoplasma* possesses the maltose-binding protein MalE. This protein may bind other sugars as well, but genes for enzymes making these sugars available for glycolysis are absent. Sucrose, the main sugar in the phloem sap of plants, could be used as a source of carbon and energy, but in sequenced phytoplasmas the gene for sucrose phosphorylase, which is important for sucrose degradation, is absent or fragmented. In general, phytoplasmas possess fewer genes related to carbon metabolism than the other Mollicutes. Energy generation in phytoplasmas seems to be restricted to glycolysis because ATP synthases are absent. OY-M *Phytoplasma* contains a P_{2C}-ATPase, which is common in eukaryotic cells but unique among prokaryotes. Another remarkable feature that makes the phytoplasmas unique among the Mollicutes is their ability to synthesize phospholipids, supporting a closer phylogenetic relationship to *Acholeplasma*, which do not require sterols.

Biochemistry of the Mollicutes

Cytology of the Mollicutes. The Mollicutes differ from other bacteria not only because they lack a cell wall but also by dint of their small cell sizes. A typical cell of *M. pneumoniae* is 1-2 μm long and 0.1-0.2 μm wide (Fig. 2). In contrast, a typical rod-shaped bacterial cell (such as *E. coli* or *B. subtilis*) is 1-4 μm in length and 0.5-1 μm in diameter.

The absence of a cell wall has serious consequences for the osmotic stability of the Mollicute cells. They are much more sensitive to changes of the osmotic conditions than bacteria possessing a cell wall. The parasitic lifestyle of the Mollicutes may be directly related to their osmotic sensitivity: The hosts provide them with osmotically constant conditions that would not be found in the external environment. For example, *M. genitalium* is a parasite of the human urogenital tract, and its transmission by sexual contact ensures minimal exposure of the bacteria to an external, osmotically variable, environment. With the exception of the phytoplasmas and acholeplasmas, the Mollicutes are unable to produce fatty acids for membrane biosynthesis and are therefore dependent on exogenously provided fatty acids, which are then used for phospholipid synthesis. The lack of fatty acid synthesis is accompanied by the absence of a fatty acid desaturase, which is required to adapt the membrane fluidity to lower temperatures. To overcome this difficulty, most Mollicutes incorporate large amounts of sterols, which serve as a very effective buffer of membrane fluidity (see Table 1).

The lack of a cell wall has also consequences for the cellular morphology of the Mollicutes. The cells are pleomorphic; however, they are not small amoebas! The Mollicutes exhibit a variety of morphologies, such as pear-shaped cells, flask-shaped cells with terminal tip structures (see below), filaments of various lengths, and in the case of *Spiroplasma* species the cells are helical.

The mycoplasmas have a flask- or club-like shape with a terminal organelle, the so-called tip structure (see Fig. 2). This tip structure is a complex and specialized attachment organelle that has evolved to facilitate the parasitic existence of the mycoplasmas. The tip structure is made up of a network of adhesins, interactive proteins, and adherence accessory proteins, which cooperate structurally and functionally to mobilize and concentrate adhesins at the tip of the cell. The major adhesin of *M. pneumoniae* is the 170 kDa P1 protein that is responsible for the interaction of the bacteria with the host cells. In addition, the tip structure is important for the internalization of intracellular Mollicutes such as *M. penetrans* and *M. genitalium*. *M. penetrans* is capable of actively entering different types of animal cells, even those with minimal phagocytic activity. This may protect the bacterial cells against the host immune system. The formation of the tip structure in *M. pneumoniae* depends on the activity of the P41 protein that serves as an anchor protein. In the absence of this protein, multiple terminal organelles form at lateral sites of the cell and

the terminal organelles are not attached to the body of the cell. In *Mycoplasma mobile*, there is also a terminal structure that is referred to as the “jellyfish” structure made up of a “bell” with dozens of flexible tentacles. Several components of this structure have been identified. With the exception of the glycolytic enzyme phosphoglycerate kinase, these *M. mobile* proteins are all absent from the genome of *M. pneumoniae* suggesting that the two species found individual solutions for the assembly of the terminal organelle.

Mycoplasma species are able to glide on solid surfaces with the help of their terminal attachment organelle. Terminal organelles that are detached from the body of the *M. pneumoniae* cell are released by some mutants. These detached organelles are still capable of gliding demonstrating that this organelle acts as a novel engine that allows cellular movement. The fastest gliding *Mycoplasma* species, *M. mobile*, contains a dedicated 349 kDa “leg” protein that is required for gliding. This protein is composed of an oval base with three successive flexible extensions that may support movement. Movement is thought to occur by repeated catching and releasing of sialic acid on solid surfaces and is driven by the hydrolysis of ATP. This ATP hydrolysis may be catalyzed by the glycolytic enzyme phosphoglycerate kinase that is part of the terminal organelle in *M. mobile*.

As other bacteria, the Mollicutes divide by binary fission. Again, the terminal organelle seems to be very important for this process: Cell division in *M. pneumoniae* is preceded by the formation of a second tip structure adjacent to the existing one. The two terminal organelles then separate leading eventually to cytokinesis. Among the proteins known to be important for bacterial cell division is the tubulin-like GTP-hydrolyzing FtsZ protein that forms a ring at the division site. Until recently, FtsZ proteins were found in any newly analyzed genome, and the *ftsZ* gene is essential in most bacteria, including *E. coli* and *B. subtilis*. Therefore, FtsZ was considered to be indispensable for all life. However, it recently turned out that some Mollicutes such as *M. mobile*, *Ureaplasma urealyticum*, and the two sequenced phytoplasmas lack *ftsZ* genes, suggesting that its function is dispensable at least in some Mollicutes. In many bacteria, the FtsA protein is required for the recruitment of the proteins that form the septum for cell division. Interestingly, this protein is absent from all the pleomorphic Mollicutes, whereas it has been detected in *S. kunkelii*. This may be related to the helical morphology of these bacteria.

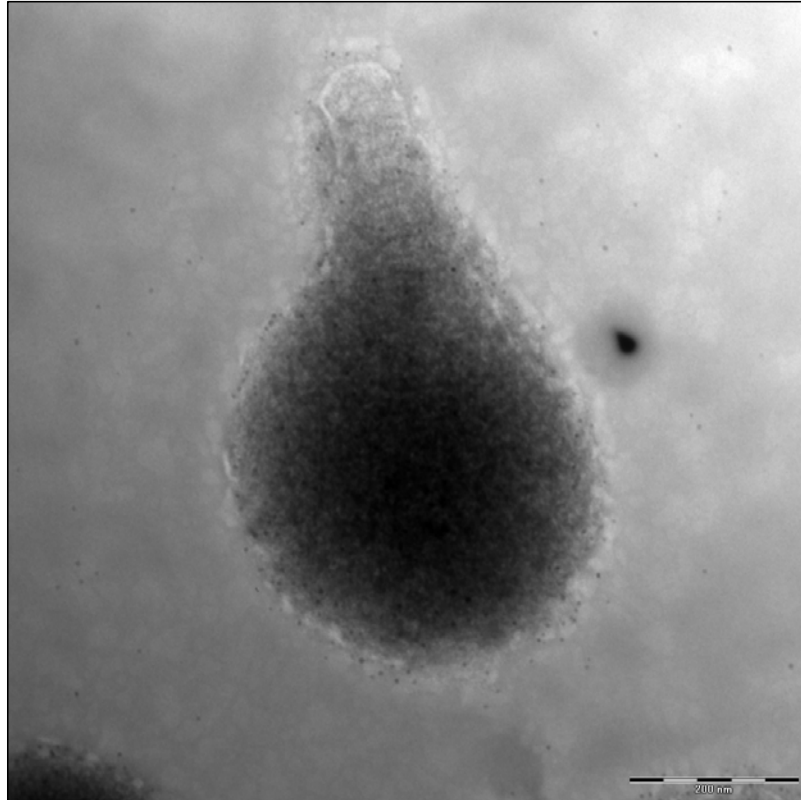


Fig. 2. Electron micrograph of a cell of *M. pneumoniae*. The terminal organelle (also called the tip structure) is visible in the upper part of the cell. Scale bar, 200 nm.

Metabolism of the Mollicutes. The reductive evolution of the Mollicutes is reflected in their limited metabolic properties. Of the central metabolic pathways, that is, glycolysis, the pentose phosphate shunt, and the tricarboxylic acid (TCA) cycle, only glycolysis seems to be operative in most Mollicutes. Most striking is the lack of many energy-yielding systems in the Mollicutes. No quinones or cytochromes were found in any representative. The electron transport system is flavin-terminated. Thus, ATP is produced by substrate-level phosphorylation, a less efficient mechanism as compared to oxidative phosphorylation.

As observed for *M. genitalium* glyceraldehyde-3-phosphate dehydrogenase, the glycolytic kinases of several Mollicute species have functions in addition to that in glycolysis. These enzymes can use not only ADP/ATP but also other nucleoside diphosphate/triphosphate couples. Thus, these enzymes (phosphofructokinase, phosphoglycerate kinase, pyruvate kinase, and acetate kinase) compensate for the lack of the normally essential *ndk* gene encoding nucleoside diphosphate kinase that is required for nucleotide biosynthesis.

Glycolysis is not the only source of ATP formation by substrate level phosphorylation in the Mollicutes. Pyruvate can be oxidized to acetyl-CoA by pyruvate dehydrogenase. Acetyl-CoA can be further catabolized by phosphotransacetylase and acetate kinase in an additional substrate-level phosphorylation resulting in the formation of acetate. An alternative pathway of pyruvate consumption is its reduction to lactate, leading to the regeneration of NAD⁺.

A recent study with *M. pneumoniae* demonstrated that glucose is the carbon source allowing the fastest growth of these bacteria. In addition, *M. pneumoniae* can utilize glycerol and fructose. Interestingly, mannitol is not used even though the genetic equipment to utilize this carbohydrate seems to be complete. Obviously, one or more of the required genes are not expressed or inactive.

Glucose and fructose are transported into the cells by the PTS. This system is made up of general soluble components and sugar-specific membrane-bound permeases. The general components, enzyme I and HPr, transfer a phosphate group from phosphoenolpyruvate to the sugar permease, which phosphorylates the sugar concomitant to its transport.

The arginine dihydrolase pathway can be found also in some *Spiroplasma* and *Mycoplasma* species. Arginine hydrolysis by this pathway results in the production of ornithine, ATP, CO₂, and ammonia. The pathway uses three enzymes: Arginine deiminase, ornithine carbamoyl transferase, and carbamate kinase. The degradation of arginine is coupled to equimolar generation of ATP by substrate-level phosphorylation. The role of this pathway as a sole energy-generating source in mycoplasmas is questionable. However, the existence of an arginine-ornithine antiport system in *Spiroplasma melliferum* requiring no ATP for arginine import into the cells supports an energetic advantage in arginine utilization.

Mollicutes possess very limited metabolic and biosynthetic activities for amino acids, carbohydrates, and lipids as compared to “conventional” bacteria. *M. pneumoniae* scavenges nucleic acid precursors and does not synthesize purines or pyrimidines *de novo*. These may be provided by RNA and DNA that have been degraded by potent mycoplasmal nucleases. Furthermore, both *M. genitalium* and *M. pneumoniae* lack all the genes involved in amino acid synthesis, making them totally dependent on the exogenous supply of amino acids from the host or from the artificial culture medium. The mycoplasmas have also lost most of the genes involved in cofactor biosynthesis;

therefore, to cultivate them *in vitro*, the medium has to be supplemented with essentially all the vitamins.

Being dependent on the exogenous supply of many nutrients would predict that mycoplasmas need many transport systems. Surprisingly, *M. genitalium* and *M. pneumoniae* possess a only small number of transport proteins (34 and 44 proteins, respectively) compared to the 281 transport and binding proteins annotated in *E. coli* and almost 400 in *B. subtilis*. The apparent low substrate specificity of some of the Mollicute transport systems, such as those for amino acids, may also contribute to the significant gene reduction observed.

Although Mollicutes produce hydrogen peroxide, *M. pneumoniae* and *M. genitalium* lack the genes dealing with oxidative stress, such as those encoding catalase, peroxidase, and superoxide dismutase. A thioredoxin reductase system, identified in the mycoplasmas, may protect them from reactive oxygen compounds.

A major problem for the research with Mollicutes is the difficulty of cultivating them *in vitro*. Only a minority of the Mollicutes existing in nature have been cultivated so far. For example, none of the phytoplasmas infecting insects or plants has been cultivated *in vitro*. To overcome the metabolic deficiencies of the mycoplasmas, complex media are used for their cultivation. The media are usually based on beef heart infusion, peptone, yeast extract, and serum with various supplements. Serum has been shown to provide, among other nutrients, fatty acids and sterols that are required for membrane synthesis. The requirement for sterols has served as an important taxonomic criterion distinguishing the sterol-nonrequiring mycoplasmas, particularly the *Acholeplasma* species, from the sterol-requiring ones. For most mycoplasmas, the pH is adjusted to a slightly alkaline value, conditions that imitate those in the eukaryotic host. A common approach to improve *in vitro* cultivation of fastidious mycoplasmas is based on coculture with eukaryotic cell lines (cell-assisted growth). In this way, some spiroplasmas, such as the Colorado potato beetle *Spiroplasma*, were first successfully cocultivated with insect cell lines.

Genetics and molecular biology of the Mollicutes

Gene expression in the Mollicutes. The basic mechanisms of gene expression have been studied poorly in the Mollicutes. They possess a conventional bacterial RNA polymerase, but unlike most other bacteria, they encode only one sigma factor of the

RNA polymerase. Thus, diversity of promoters and RNA polymerase holoenzymes are not used for regulatory purposes in the Mollicutes. The transcription start sites have been identified for several *M. pneumoniae* genes, and it turned out that the -10 region of these promoters is similar to that recognized by the housekeeping sigma factors of other bacteria such as *E. coli* or *B. subtilis*. In contrast, there is no conserved -35 region. These observations were confirmed by a recent analysis of the sequence determinants that are required for promoter activity in front of the *M. pneumoniae ldh* gene encoding lactate dehydrogenase. The -10 region is essential for transcription initiation, whereas the -35 region could be mutated without any consequences. Thus, the single *M. pneumoniae* RNA polymerase holoenzyme recognizes only the -10 region for promoter recognition.

Another peculiarity of the *M. pneumoniae* transcription machinery is the lack of the termination factor Rho, and correspondingly, the absence of Rho-dependent transcription terminators. Surprisingly, a bioinformatic analysis of bacterial genomes and the free energy values of RNAs around the end of open reading frames suggest that the Mollicutes do also not contain functional Rho-independent transcription terminators. This raises the important question of how transcription is terminated in the Mollicutes or whether it is terminated at all. The answer came from Northern blot experiments aimed at the identification of *in vivo* transcripts, and this answer is ambiguous. Indeed, defined transcripts were observed in a few cases, such as the *M. genitalium* and *M. pneumoniae ftsZ* gene clusters or the *M. pneumoniae ptsH* gene. The existence of these defined transcripts implies that there are also defined transcription terminators present. However, these terminators may be very rare. This might explain the observation that unrelated genes are expressed as parts of one transcription unit in the Mollicutes. Moreover, most attempts to determine transcript sizes by Northern blot analysis in the Mollicutes have failed. This is probably the result of mRNA length polymorphisms, which prevent the detection of clearly defined RNA species.

Most genes in the Mollicutes have the same orientation on the chromosome, and the intergenic regions are usually quite short if present at all. The transcription of most of these large gene clusters is colinear with replication. This genome organization also favors polycistronic transcription of large gene clusters.

The lack of defined mRNA species results not only from the absence of transcription terminators but also from the weak conservation of sequences that mediate transcription initiation: A -10 region made up of only Ts and As is statistically overrepresented in the AT-rich Mollicute genome. Indeed, the -10 regions predicted from the analysis of many start points occur about 2900 times in the 816 kb genome of *M. pneumoniae*. This large number of possible transcription initiation sites is also reflected by the observation of substantial antisense transcription in both *M. genitalium* and *M. pneumoniae*.

In bacteria, regulation is usually exerted at the level of transcription. In the Mollicutes, only one example of transcription regulation is clearly documented: This is the regulation of the *S. citri* fructose operon by the transcription activator FruR (see “Plant pathogenic Mollicutes: *Spiroplasma* and *Phytoplasma*”). Moreover, the induction of chaperone-encoding genes at elevated temperatures was demonstrated in several *Mycoplasma* species. By analogy to the mechanism of heat shock regulation by the repressor protein HrcA and the DNA operator element CIRCE, it was proposed that heat shock genes are under the control of HrcA in the Mollicutes. In addition to HrcA, the genomes of *M. genitalium* and *M. pneumoniae* encode only two other potential transcription factors that belong to the GntR and the Fur family, respectively. Unfortunately, the function of these regulators has so far not been studied.

It is interesting to note that *M. pneumoniae* contains only three potential regulators (less than 0.5% of all open reading frames), whereas environmental bacteria such as *Streptomyces coelicolor* and *P. aeruginosa* reserve about 10% of their genetic capacity to encode transcription factors. The low number of transcription factors in the Mollicutes and the weak stringency of transcription signals in the Mollicutes might therefore reflect their close adaptation to specific habitats that provide a good supply of nutrients and protect the bacteria from harmful environmental conditions. Moreover, the good supply of nutrients from external sources, that is, the host, may abolish the need for transcription regulation, that is, to switch off the expression of genes if their products are not required.

An additional mechanism of regulation is provided by riboswitches and regulatory RNAs. A guanine-specific riboswitch was detected in the untranslated region of the *Mesoplasma florum* *guaAB* operon suggesting that this RNA element governs the regulation of this operon via guanine.

Translation is one of the most prominent activities of the Mollicute cell: As much as 15% of the genome of the Mollicutes is devoted to translation-related functions. The principal mechanisms of translation in the Mollicutes are identical to those found in other bacteria. Because of the low genomic GC content, the codon usage is strongly biased toward AT-rich codons. With the exception of *Phytoplasma* and *Acholeplasma*, the Mollicutes decode the UGA codon as tryptophan instead of using it as a stop codon as in the universal genetic code. This poses severe problems for the expression of Mollicute proteins in heterologous hosts (see “Molecular biology and genetic tools for the Mollicutes”).

The mechanisms of translation initiation seem to differ among the Mollicutes. In some organisms such as *Mycoplasma capricolum* and *S. citri*, the open reading frames are preceded by canonical Shine-Dalgarno sequences that form base pairs with the 3' end of the 16S rRNA. In contrast, many genes of *M. pneumoniae* and *M. genitalium* lack such a sequence, and moreover, leaderless mRNAs are common in these bacteria. The molecular mechanisms of translation initiation in *M. pneumoniae* and its close relatives still await elucidation.

Posttranslational protein modification. In many bacteria including the mycoplasmas, the HPr protein of the PTS cannot only be phosphorylated by enzyme I, but is also the target of a regulatory phosphorylation on Ser-46 by a metabolite-activated protein kinase, HPrK. The phosphorylation of HPr on Ser-46 in “less degenerated” Firmicutes leads to carbon catabolite repression. So far, the functions of HPrK and ATP-dependent phosphorylation of HPr have not been studied in the Mollicutes. In contrast, much work has been devoted to the biochemical characterization of HPrK from *M. pneumoniae*. Unlike its equivalent from other bacteria, this protein is active at very low ATP concentrations. As in related proteins, it contains an essential Walker A motif for ATP binding. Mutations in this region severely affect both the kinase and the phosphatase activities of the protein. Fluorescence studies revealed that the *M. pneumoniae* HPrK has a significantly higher affinity for ATP than any other HPrK studied so far. This may explain why it is active even at low ATP concentrations. The *M. pneumoniae* HPrK was crystallized and its structure determined. As observed for homologous proteins, it forms a hexamer with the C-terminal domains in the active center.

In addition to HPrK, there is one other protein kinase in *M. pneumoniae* and many other Mollicutes, PrkC. The corresponding gene is clustered with the gene encoding a protein phosphatase of the PP2C family, PrpC. It was shown that PrpC is implicated in the dephosphorylation of HPr(Ser-P). PrkC is known to phosphorylate a wide variety of proteins in other Firmicutes; however, its targets and the role of PrkC-dependent phosphorylation in the Mollicutes remain to be studied.

Protein phosphorylation seems to be important for the biology of the Mollicutes. An analysis of the *M. genitalium* proteome revealed that each identified protein is present at an average of 1.22 spots on a two-dimensional gel, suggesting posttranslational modification of about 25% of all proteins. Given the importance of protein phosphorylation in all other living organisms, it seems safe to assume that a large portion of these modified proteins is actually phosphorylated. A phosphoproteome analysis of *M. genitalium* and *M. pneumoniae* identified 5 and 3% of the total protein complement of these bacteria, respectively, as phosphoproteins. Among these proteins are not only enzymes of central carbon metabolism such as enolase and pyruvate dehydrogenase subunits but also several cytoskeleton and cytoadherence proteins. It is tempting to speculate that PrkC may catalyze these phosphorylation events.

As in other bacteria, there is protein secretion in the Mollicutes. While some exported proteins carry typical signal peptides at their N-termini, there is no signal peptidase I present in the genome of the Mollicutes. This raises the possibility that so far uncharacterized proteins are active in protein secretion in the Mollicutes.

Genomic comparisons of Mollicutes. One of the questions that have been of interest to humans since its early days is the problem of what constitutes life. Only today, in the era of genome research, are we able to attempt an answer to this question. A major milestone in defining life was the identification of key features that characterize all living things and differentiate them from nonliving matter such as viruses and prions. Among these features are metabolism, autonomous replication, communication, and evolution. With the availability of genome sequences, it has become possible to determine the genetic equipment required for independent life. The Mollicutes are of special interest in this respect because they have the smallest genomes that allow independent life, at least under laboratory conditions.

Genome research with the Mollicutes is driven by two major challenges: (1) The identification of the minimal set of genes that is required for independent life and (2) the creation of artificial organisms that are based on this minimal gene set. The simplicity of the Mollicutes and the broad body of knowledge on their biology makes them ideal starting points for these research areas.

Several different strategies have been applied to identify the minimal gene set required for life. The most simple approach is based on the comparison of sequenced genomes of different organisms. It seems safe to assume that those genes that are conserved in different organisms are more important than those that appear only in certain species. The smallest genome of any independent living organism known so far is that of *M. genitalium*. This bacterium has a genome of 580 kb with 482 protein-coding genes and 39 genes coding for RNAs. *M. pneumoniae* has a genome of 816 kb with 779 genes coding for proteins and 40 RNA-coding genes. A comparison of the two genomes reveals an overlap of 477 genes common to both species. This suggests that *M. pneumoniae* is an “extended version” of *M. genitalium*. It is tempting to speculate that *M. genitalium* is further advanced on the pathway of reductive genome evolution. Indeed, some genes present in *M. pneumoniae* but not in *M. genitalium* such as the mannitol utilization genes are known to be nonfunctional in the former organism. Thus, *M. genitalium* seems to be very close to a true minimal organism.

A comparison of all sequenced Mollicute genomes reveals that only a small subset of their genes is part of a common gene pool. Only 156 genes are common to all Mollicute genomes that have so far been sequenced. This represents about one-third of the 482 open reading frames of *M. genitalium*. Interestingly, of the 156 genes of the Mollicute core genome, the large majority, that is, 124 genes, are shared by all Firmicutes. Thus, there is only a small set of 32 genes that is conserved in all Mollicutes but not in all Firmicutes. However, even these genes are shared by many members of the Firmicutes thus precluding the idea of a gene set unique to the Mollicutes. Moreover, a large fraction of the common Mollicute gene set forms the core genome of all bacteria (about 100 genes). Thus, the genome reduction of the Mollicutes obviously went down to a minimum that is absolutely required for cellular life. This is becoming clear if one takes into account that even unrelated bacteria such as *E. coli* (γ -proteobacterium) and *B. subtilis* (Firmicute) share about 1000 genes.

The core gene set of the Mollicutes is made up mainly of genes encoding proteins involved in essential cellular functions such as DNA topology, replication and repair, transcription, RNA modification and degradation, translation, protein folding, secretion, modification or degradation (Table 2). In addition, seven genes encoding potential GTP-binding proteins are conserved in all Mollicute genomes. A few conserved metabolic genes encode proteins involved in glycolysis, metabolite and ion transport, nucleotide, lipid, phosphate, and amino acid metabolism. Interestingly, not a single protein of completely unknown function is conserved among all Mollicutes. Moreover, the genes common to all Mollicutes act in the central processes of life. This implies that there are no genes common to all Mollicutes that are required for Mollicute-specific activities such as the formation of the terminal organelle. This is in good agreement with earlier studies that demonstrated a large variability in the protein composition of this organelle.

A second approach to determine the minimal gene set required for life uses an experimental setup. Global transposon mutagenesis studies with *M. genitalium* and *M. pneumoniae* revealed dispensable genes. For *M. genitalium*, about 100 genes could be disrupted. This implies that the remaining 382 genes are essential. In addition, five genes that are part of groups of redundant genes seem to be essential. It is believed that these 387 genes (plus the RNA-coding genes) constitute the essential gene set of *M. genitalium*. The difference between the 156 genes in the core gene set of the Mollicutes and the 387 genes that are essential for *M. genitalium* suggests that many of the additional genes are important under the specific ecological conditions of *M. genitalium*. This idea is supported by the presence of 110 genes of unknown function among the essential genes. This finding clearly demonstrates how much remains to be learned about the biology of *M. genitalium*, and surely about the other Mollicutes as well.

With information on the minimal gene set in hand, the logical next step will be to construct artificial organisms with this set of genes. In 2007 and 2008, two important technological steps have been made on the way to the construction of such minimal artificial life: First, the replacement of one genome by another, a process called genome transplantation, was demonstrated. Genomic DNA of *M. mycoides* large colony was used to replace the genome of *M. capricolum* by polyethylene glycol-mediated transformation. The second major achievement was the chemical synthesis and

assembly of the *M. genitalium* chromosome. Thus, an artificial chromosome can be synthesized and this DNA can be introduced into a living cell to provide the environment for the expression of this genome. The generation of an artificial minimal *Mycoplasma*-derived organism (“*Mycoplasma laboratorium*”) would be the logical next step and the ultimate proof of both these technologies and of our understanding for the minimal equipment of a living cell.

Tab. 2. The core gene set of the Mollicutes.

Function	Number of genes
Information pathways - Protein	
Ribosomal proteins	38
Translation factors	11
Amino acyl tRNA synthetases	19
Chaperones	2
Proteolysis	3
Protein modification	1
Protein secretion	5
Information pathways - RNA	
Transcription	7
RNA modification	8
RNA degradation and maturation	5
Information pathways - DNA	
Replication	7
Repair	8
DNA topology	3
Metabolism	
Basic carbon and energy metabolism	8
Amino acid metabolism	1
Nucleotide biosynthesis	6
Pyrophosphatase	1
Lipid metabolism	1
Miscellaneous functions	
Transport	7
GTP-binding proteins	7
Unknown proteins	7 (MG_009, 056, 132, 222, 366, 505, and 516)

Molecular biology and genetic tools for the Mollicutes. The detailed genetic analysis of the Mollicutes has been hampered for a long time by the lack of genetic tools that allow the efficient expression of UGA-containing Mollicute genes in heterologous hosts for purification and subsequent biochemical analysis, the stable introduction of foreign genetic material into a Mollicute cell, and either the targeted construction or the targeted isolation of desired mutant strains. During the past few years considerable progress has been made in the field of Mollicute genetics, making these organisms accessible for genetic studies.

The occurrence of UGA codons in the genes of Mollicutes has often prevented their expression in heterologous hosts for detailed biochemical analysis, because they serve as stop codons in *E. coli* and other expression hosts. To circumvent this problem, a variety of different but rather dissatisfying strategies had been employed, including the expression of UGA-containing genes in opal suppressor strains of *E. coli*, or in *S. citri* that also reads UGA as a tryptophan codon. As long as only few UGA codons are present in a gene, their sequential replacement by standard site-directed mutagenesis strategies might also be taken into consideration. However, the latter approach is time-consuming and cost-intensive with an increasing number of UGA codons. Recently, a strategy referred to as multiple mutation reaction (MMR) allowing the simultaneous replacement of multiple UGA codons in a single-step reaction was developed. This strategy is based on the use of 5'-phosphorylated oligonucleotides containing the desired mutations in a polymerase chain reaction (PCR). During the elongation steps, the external amplification primers are extended. As the mutation primers are designed to hybridize more strongly to their targets, the elongated amplification primers can then be ligated to the 5' ends of the mutation primer by a thermostable DNA ligase, yielding a DNA strand that contains the desired mutation. With this strategy, the simultaneous introduction of up to nine mutations in one single step is possible.

The majority of genetic tools that are well established in model organisms are unavailable for Mollicutes. Therefore, transposons are in common use for a variety of purposes. In combination with smart screening systems, they were used for the disruption of genes but also as carriers for the introduction of genetic material into the chromosome. The transposons Tn916 and Tn4001 and their improved derivatives can be used in Mollicutes. These transposons were originally isolated from *Enterococcus*

faecalis and *Staphylococcus aureus*, respectively, and have a broad host range. Tn916 is a conjugative 18 kb transposable element that contains the *xis-Tn/int-Tn* genes for excision/integration, followed by the *tetM* tetracycline resistance determinant and a set of genes (*tra*) required for intercellular transfer. Tn916 does not generate target duplications at its integration site, because it transposes by an excision/integration mechanism that is based on staggered nicks in the donor DNA. Tn4001 is a 4.5 kb composite transposon consisting of two identical IS256 elements flanking the gentamicin/kanamycin/tobramycin resistance conferring *aac-aphD* gene. Tn4001 has been used for transforming several *Mycoplasma* species. To increase the stability of transposon insertion mutants, mini-transposons on the basis of Tn4001 were constructed that have the transposase gene outside the transposable elements to prevent reexcision of the transposon after the first transposition event.

Until very recently, the targeted construction of gene knockout mutants via homologous recombination has only been reported in a few Mollicutes such as *M. genitalium*, *Mycoplasma gallisepticum*, *Mycoplasma pulmonis*, and *A. laidlawii*. In the absence of homologous recombination, the only remaining way to obtain gene knockouts is transposon mutagenesis. Because of the randomness of integration, the screening of large transposon mutant libraries for the loss or gain of a specific phenotype is required to isolate a gene knockout of interest. If no screenable phenotype can be expected to be associated with a gene of interest, the only known feature of the desired gene knockout is the specific DNA junction between the gene of interest and the transposon. Based on this idea, a strategy referred to as “haystack mutagenesis” has been designed that allows the targeted isolation of any viable transposon insertion strain out of an ordered library of transposon mutants. The concept of haystack mutagenesis is based on a saturating transposon mutagenesis to ensure that each dispensable gene is disrupted at a desired confidence level. Once the required number of transposon mutants has been isolated, they are arranged in pools of a reasonable size. These pools can then be screened by PCR using a gene-specific oligonucleotide and another one specific to the transposon for identifying the pool that contains the desired insertion. Subsequently, a similar screen at the level of the individual clones of the positive pool will identify the mutant of interest. This strategy has already been used for the isolation of several *M. pneumoniae* mutants. Alternatively, transposon mutant libraries can be screened for mutants that exhibit an interesting phenotype, such as loss of gliding motility.

The use of transposons is accompanied by the problem of changes of the genetic context at the site of integration that may cause undesired side effects. To avoid this problem, autonomously replicating plasmids have always been the vehicle of choice. Some early studies reported the isolation of naturally occurring plasmids from *M. mycoides*. These are small cryptic plasmids with a size in the range of 1.7-1.9 kb coding for replication functions only. Based on one of these plasmids, *M. mycoides*-*E. coli* shuttle vectors were developed. Further developments of artificial plasmid vectors were stimulated, when the first genome sequences became available that allowed the determination of the origins of replication of *Mycoplasma* chromosomes. Plasmid replicons have been constructed that contain the *oriC* sequences from *M. mycoides*, *M. capricolum*, and *Mycoplasma agalactiae*. Remarkably, a certain host specificity was observed for *oriC* plasmids, hampering the prediction the *oriC* compatibility between different *Mycoplasma* species and the derived plasmids. Nevertheless, with the genome sequence of many mycoplasmas at hand, the construction of stably replicating *oriC* plasmids for any desired *Mycoplasma* can be expected in the near future.

In the past there have been a couple of studies aimed at the definition of mycoplasmal promoters. The lack of clarity concerning the nature of gene expression/regulation signals in Mollicutes (see “Gene expression in the Mollicutes”) can only be answered in experiments that make use of promoter reporter systems. Such reporter systems based on the promoterless *lacZ* gene or on fluorescent proteins have been developed and used. They are used in two ways: The reporter genes can be randomly introduced into the chromosome to isolate random fusions with promoters; alternatively, the fusions can be prepared on plasmid vectors before their introduction into the genome. This second possibility allows the analysis of mutant promoter variants.

At present all required tools for the application of standard genetics to mycoplasmas are available. The biochemical *in vitro* analysis of individual proteins is no longer hampered by the genetic code of these organisms. Thus, interesting proteins can be easily studied. Similarly, antigenic surface proteins, which are often very large and thus contain many UGA codons can now easily be produced in heterologous hosts in sufficient amounts to be tested as vaccine candidates. Using the existing reporter systems, it will be possible to refine the mycoplasmal promoter concept, to discover

regulatory DNA sequences and, ultimately, unravel the signal transduction mechanisms that mediate the adaptive responses seen in a wide variety of DNA microarray analyses, but which are not yet understood at the molecular level. To confirm *in vitro* findings with purified proteins, targeted disruption of desired genes can presently be carried out in various representatives of the genus *Mycoplasma*, either by homologous recombination or by facilitated screening methods such as haystack mutagenesis.

Accompanying feature

Additional resources on the Mollicutes (key references, genome information, labs working on the Mollicutes, and information on important methods) can be found on an accompanying web page (<http://tinyurl.com/3vw8ca>).

Further reading

- Barré *et al.*** (2004) *Nucleic Acids Res.* **32**: D307-D310.
- Bové *et al.*** (2003) *Annu. Rev. Phytopathol.* **41**: 483-500.
- Christensen *et al.*** (2005) *Trends Plant Sci.* **10**: 526-535.
- Ciccarelli *et al.*** (2006) *Science* **311**: 1283-1287.
- Gibson *et al.*** (2008) *Science* **319**: 1215-1220.
- Glass *et al.*** (2006) *Proc. Natl. Acad. Sci. USA* **103**: 425-430.
- Halbedel and Stülke** (2007) *Int. J. Med. Microbiol.* **297**: 37-44.
- Krause and Balish** (2004) *Mol. Microbiol.* **51**: 917-924.
- Lee *et al.*** (2000) *Annu. Rev. Microbiol.* **54**: 221-255.
- Pollack** (2001) *Trends Microbiol.* **9**: 169-175.
- Razin and Herrmann** (2002) Kluwer Academic/Plenum Publishers, New York.
- Sirand-Pugnet *et al.*** (2007) *Res. Microbiol.* **158**: 754-766.
- Waites and Talkington** (2004) *Clin. Microbiol. Rev.* **17**: 697-728.

(B) Aims of this work

The close adaptation of *M. pneumoniae* to human mucosal surfaces did not only result in a reductive evolution of metabolic capabilities but also affected the regulation of protein biosynthesis and activity. The most prominent regulatory modification of a protein both in bacteria and in eukaryotes is posttranslational modification via protein phosphorylation (Boekhorst *et al.*, 2008; Jers *et al.*, 2008).

In *M. pneumoniae*, the phosphorylation of HPr by HPrK was the first regulatory event and the first covalent protein modification described for any *Mycoplasma* strain (Halbedel *et al.*, 2004; Merzbacher *et al.*, 2003; Steinhauer *et al.*, 2002). Later on, the implication of PrpC in HPr(Ser-P) dephosphorylation was discovered (Halbedel *et al.*, 2006) and phylogenetic studies suggested that PrkC may be another protein kinase in *M. pneumoniae*. A recent publication demonstrated that many proteins of *M. pneumoniae* are subject to protein phosphorylation (Su *et al.*, 2007). Interestingly, the phosphorylation of HPr escaped the authors of this study. Moreover, these authors do not have the mutants affected in kinases and the phosphatase.

To understand the role of HPrK and other enzymes implicated in protein phosphorylation/dephosphorylation, it was therefore intended to analyze the phosphoproteome of the *M. pneumoniae* wild type strain and of three isogenic mutants that are affected in the two protein kinases HPrK and PrkC and in the protein phosphatase PrpC using two-dimensional gel electrophoresis. Similarly, the regulatory output of protein phosphorylation was studied more directly by unraveling the phosphorylation effect on cell morphology and virulence.

In a second part of this work two proteins encoding paralogous glycerophosphodiesterases (GlpQ/MPN420 and MPN566) were to be characterized. These enzymes cleave glycerol 3-phosphate diesters present in phospholipids to produce glycerol 3-phosphate that can be utilized by enzymes of the glycerol metabolism (Hames *et al.*, 2009). A first experiment was the analysis of the biochemical activity of the two glycerophosphodiesterases *in vitro*. To analyze the impact of glycerophosphodiesterases on the pathogenicity of *M. pneumoniae*, *glpQ* and *mpn566* mutant strains had to be isolated. These mutants allowed the verification of hydrogen peroxide production and their cytotoxicity toward HeLa cells. Furthermore, a detailed proteome analysis of the mutants should provide the basis for a better understanding of regulatory mechanisms of gene expression in *M. pneumoniae*.

Chapter 2

The stability of cytodherence proteins in *Mycoplasma pneumoniae* requires activity of the protein kinase PrkC

The work described in this chapter was published in:

Schmidl, S. R., K. Gronau, C. Hames, J. Busse, D. Becher, M. Hecker, and J. Stülke. 2010. The stability of cytodherence proteins in *Mycoplasma pneumoniae* requires activity of the protein kinase PrkC. *Infect. Immun.* **78**: 184-192.

Author contributions:

This study was designed and interpreted by SRS, CH, and JS. CH isolated the *prkC* transposon mutant. SRS performed all experiments, but JB contributed substantially to the expression analysis of cytodherence genes. The proteomic analysis was done in collaboration with KG, DB, and MH, University of Greifswald. SRS and JS wrote the paper.

Abstract

Mycoplasma pneumoniae belongs to the Mollicutes, a group of bacteria that have strongly reduced genomes, but that are nevertheless capable of independent life. With only three transcription factors, the regulatory features of these bacteria are very limited. Thus, posttranslational regulation might be important for *M. pneumoniae*. In addition to the highly specific HPr kinase, the *M. pneumoniae prkC* gene encodes the serine/threonine protein kinase C. In order to study the function(s) of this kinase, we isolated an *M. pneumoniae* mutant affected in PrkC. This mutation resulted in nonadherent growth and loss of cytotoxicity. Examination of the phosphorylation profile of the *prkC* mutant suggested that phosphorylation of cytodherence proteins was affected by the loss of this kinase. In contrast, inactivation of the *prpC* gene affecting the protein phosphatase that antagonizes PrkC-dependent phosphorylation resulted in more intensive phosphorylation of the cytodherence proteins HMW1 and HMW3 of the major adhesin P1 and of the surface protein MPN474. Moreover, loss of PrkC affects not only the phosphorylation state of the cytodherence proteins but also their intracellular accumulation. However, the expression of the corresponding genes was not affected by PrkC, suggesting that PrkC-dependent phosphorylation results in stabilization of the cytodherence proteins. The HMW proteins and P1 are part of the so-called terminal organelle of *M. pneumoniae* that is involved in gliding motility, cell division, and adhesion to host epithelial tissues. Our observations suggest that the posttranslational modification of cytodherence proteins by PrkC is essential for the development and function of the *M. pneumoniae* terminal organelle.

Introduction

Mycoplasma pneumoniae belongs to the Mollicutes, *i.e.*, cell wall-less bacteria. These organisms are among the smallest self-replicating living beings capable of a host-independent existence. *M. pneumoniae* is a pathogenic bacterium that causes atypical pneumonia and extrapulmonary infections, such as autoimmune disorders, asthma, and arthritis (Atkinson *et al.*, 2008; Stülke *et al.*, 2009; Waites and Talkington, 2004).

M. pneumoniae and its close relative *Mycoplasma genitalium* have recently attracted much attention, not only with respect to the elucidation of pathogenicity mechanisms, but also because the small genomes of these bacteria define the lower limit of naturally existing independent life. The analysis of the minimal gene complement of *M. pneumoniae* and *M. genitalium* is one of the sources of synthetic biology, a new discipline of biology (Gibson *et al.*, 2008; Glass *et al.*, 2006).

However, life is not static and not determined only by a defined set of genes. A very important feature is the control of biological activities in response to changing environmental conditions. Only this control enables organisms to adapt to different habitats and to survive suboptimal conditions. In *M. pneumoniae*, the regulatory potential seems to be rather limited. In bacteria, regulation of gene expression is achieved mainly at the level of transcription, by alternative sigma factors of the RNA polymerase, by transcription repressors and activators, or by RNA switches. The annotation of the *M. pneumoniae* genome revealed only one sigma factor and three putative transcriptional repressors. No two-component regulatory system is present (Dandekar *et al.*, 2000). This set of transcription factors corresponds to only 0.5% of the protein-coding genes of *M. pneumoniae*. In contrast, versatile environmental bacteria, such as *Streptomyces coelicolor* and *Pseudomonas aeruginosa*, reserve as much as 10% of their coding capacity for transcription regulation (Greenberg, 2000).

A second way to control biochemical activities is the posttranslational modification of proteins, and protein phosphorylation is the most common protein modification. For a long time, it has been thought that bacteria prefer to phosphorylate proteins on histidine and aspartate residues, whereas eukaryotes phosphorylate serine, threonine, and tyrosine residues. In the past few years, protein phosphorylation on these amino acids was found to be common in bacteria as well (Jers *et al.*, 2008).

In *M. pneumoniae*, protein phosphorylation has been studied with the phosphotransferase system (PTS). This system uses the phosphate group of phosphoenolpyruvate to phosphorylate consecutively its components, enzyme I, HPr, the glucose permease, and the incoming glucose (Halbedel *et al.*, 2004). The HPr protein of the PTS is not only subject to enzyme I-dependent phosphorylation on His-15, but it is also phosphorylated on Ser-46 by the HPr kinase at the expense of ATP (Steinhauer *et al.*, 2002). The molecular role of HPr phosphorylation on Ser-46 has not yet been identified with *M. pneumoniae*; in other bacteria this phosphorylation is crucial

for carbon catabolite repression (Görke and Stülke, 2008). Dephosphorylation of HPr(Ser-P) in *M. pneumoniae* requires the protein phosphatase PrpC, the product of the MPN247 gene (Halbedel *et al.*, 2006). This gene is clustered with another gene that potentially encodes a protein kinase (PrkC). This gene cluster is conserved in all Firmicutes, *i.e.*, in gram-positive bacteria with a low GC content of their genomic DNA (this group includes the Mollicutes). In other Firmicutes, PrkC has been shown to be a protein kinase involved in many functions, such as phosphorylation of glycolytic enzymes, virulence, and germination (Faucher *et al.*, 2008; Kristich *et al.*, 2007; Lomas-Lopez *et al.*, 2007; Shah *et al.*, 2008). However, the potential protein kinase PrkC of *M. pneumoniae* has so far not been the subject of any studies.

To date, phosphorylation of HPr by the HPr kinase is the best-studied protein phosphorylation event of *M. pneumoniae* (Allen *et al.*, 2003; Halbedel and Stülke, 2005; Halbedel *et al.*, 2006; Merzbacher *et al.*, 2004; Steinhauer *et al.*, 2002). However, in addition to HPr, several other proteins are phosphorylated in these bacteria. Among these proteins are HMW1 and HMW2, large cytoadherence proteins that were shown to be phosphorylated on serine and threonine residues (Dirksen *et al.*, 1994; Krebs *et al.*, 1995). Recently, a proteomic approach was used to identify phosphorylated proteins in *M. genitalium* and *M. pneumoniae* (Su *et al.*, 2007). This study identified 18 phosphoproteins in *M. pneumoniae*, among them the surface protein MPN474, the cytoadherence protein HMW3, and several metabolic enzymes. Unfortunately, none of the previously identified phosphoproteins was found by the phosphoproteome approach. Until now, it has not been known, which kinases are responsible for these phosphorylation events. Moreover, the function of these phosphorylations has not been addressed.

In this work, we have studied the function of PrkC in *M. pneumoniae* by genetic and proteomic methods. The analysis of a *prkC* mutant revealed that this kinase is required for adherent growth of the cells on solid surfaces and for cytotoxicity toward eukaryotic cells. Moreover, we provide evidence that PrkC-dependent protein phosphorylation is crucial for the stability of a group of high molecular weight cytoadherence proteins.

Materials and Methods

Bacterial strains, oligonucleotides, and growth conditions. The *M. pneumoniae* strains used in this study were *M. pneumoniae* M129 (ATCC 29342) in the 32nd broth passage and its isogenic mutant derivatives GPM11 (*prkC*::mini-Tn, Gm^R), GPM51 (*hprK*::mini-Tn, Gm^R) (Halbedel *et al.*, 2006), GPM68 (*prpC*::mini-Tn, Gm^R) (Halbedel *et al.*, 2006), and GPM70 (*mpn474*::mini-Tn, Gm^R) (Hegermann *et al.*, 2008). The oligonucleotides used in this study are listed in Table S1 in the supplemental material. *M. pneumoniae* was grown at 37°C in 150-cm² tissue culture flasks containing 100 ml of modified Hayflick medium with glucose [1% (wt/vol)] as the carbon source as described previously (Halbedel *et al.*, 2004). Strains harboring transposon insertions were cultivated in the presence of 80 g/ml gentamicin.

Preparation of whole cell extracts. A 100-ml culture was washed twice with cold phosphate-buffered saline (PBS) (137 mM NaCl, 2.7 mM KCl, 10 mM sodium hydrogen phosphate, 2 mM potassium dihydrogenphosphate, pH 7.4). The cells were harvested with 1.5 ml PBS by scraping them off the surface of the flask. The cells were then centrifuged for 4 min at 15,000 × g at 4°C. The pellet was resuspended in 150 µl of PBS. The protein concentration was determined and adjusted to 1 µg/l in PBS containing sodium dodecyl sulfate-polyacrylamide gel electrophoresis (SDS-PAGE) loading dye. Cells of the *M. pneumoniae prkC* mutant GPM11 were harvested by centrifugation of the culture. The pellets were washed twice with 1.5 ml PBS, and the cells were resuspended as described above.

Visualization of protein phosphorylation. In order to detect phosphorylated proteins, cell extracts were separated on 6% SDS polyacrylamide gels. The gels were subsequently stained with Pro-Q Diamond (Invitrogen) and Flamingo fluorescent dye (Bio-Rad) to visualize the phosphoproteins and all proteins, respectively (Eymann *et al.*, 2007). Pro-Q staining was detected using a Molecular Imager FX (Bio-Rad). Flamingo signals were detected using a Typhoon 9400 image scanner. Relative quantification of the phosphosignal intensities was performed using Image J software v1.42 (Abramoff *et al.*, 2004).

Protein identification by MS. Gel pieces were washed twice with 200 µl 20 mM NH₄HCO₃/30% (vol/vol) acetonitrile for 30 min at 37°C and dried in a vacuum centrifuge (Concentrator 5301, Eppendorf). Trypsin solution (10 ng/µl trypsin in 20 mM ammonium bicarbonate) was added until gel pieces stopped swelling, and

digestion was allowed to proceed for 16 to 18 h at 37°C. Peptides were extracted from gel pieces by incubation in an ultrasonic bath for 15 min in 20 µl high-performance liquid chromatography-grade water and transferred into micro vials for mass spectrometric analysis. Peptides were separated by liquid chromatography and measured online by electrospray ionization mass spectrometry (MS) using a nanoAcquity ultra-performance liquid chromatography system (Waters, Milford, MA) coupled to an LTQ Orbitrap mass spectrometer (Thermo Fisher Scientific, Waltham, MA). Peptides were desalted onto a trap column (Symmetry C₁₈, Waters). Elution was performed in an analytical column (BEH130 C₁₈, Waters) with a binary gradient of buffer A [0.1% (vol/vol) acetic acid] and B [100% (vol/vol) acetonitrile, 0.1% (vol/vol) acetic acid] over a period of 80 min with a flow rate of 400 nl/min. The LTQ Orbitrap was operated in data-dependent tandem MS (MS-MS) mode using multistage activation for phospho-relevant masses. Proteins were identified by searching all MS-MS spectra in .dta format against all *M. pneumoniae* proteins (extracted from the NCBI database [http://www.ncbi.nlm.nih.gov/sites/entrez?Db=genome&Cmd=Retrieve&dopt=Protein+Table&list_uids=113]) using SEQUEST (Bioworks 3.3.1/Sequest version 2.7, revision 11; Thermo Electron). Initial mass tolerances for peptide identification on MS and MS-MS peaks were 10 ppm and 1 Da, respectively. Up to two missed tryptic cleavages were allowed. Methionine oxidation (+15.99492 Da) was set as a variable modification. Proteins were identified by at least two peptides by applying a stringent SEQUEST filter (Xcorr versus charge state of 1.90 for singly charged ions, 2.2 for doubly charged ions, 3.3 for triply charged ions, and 3.75 for higher-charged ions). Phosphorylated peptides that passed this filter were examined manually and accepted only when b- or y-ions confirmed the phosphorylation site.

Western blot analysis. For Western blot analysis, *M. pneumoniae* cell extracts were separated on SDS polyacrylamide gels (6% to 12%). After electrophoresis, the proteins were transferred onto a polyvinylidene difluoride membrane (Bio-Rad) by electroblotting. The proteins of interest were detected with polyclonal antibodies raised against these proteins. The antibodies used in this study are listed in Table S2 in the supplemental material. Antibodies were visualized by using anti-rabbit immunoglobulin G-alkaline phosphatase secondary antibodies (Promega) and the CDP-*Star* detection system (Roche Diagnostics). The quantification was performed using Image J software v1.42 (Abramoff *et al.*, 2004).

Southern blot analysis. For the preparation of *M. pneumoniae* chromosomal DNA, cells of a 100-ml culture were harvested as described previously (Halbedel *et al.*, 2004). The cell pellet was resuspended in 750 μ l 50 mM Tris-HCl, pH 8.0, and 25 mM EDTA, and RNase A was added to a final concentration of 25 μ g/ml. After an incubation step at 37°C for 15 min, 50 μ l proteinase K (25 mg/ml) and 75 μ l 10% SDS were added. The mixture was incubated at 50°C until the lysate was clarified and subsequently cooled down on ice. To precipitate debris, 300 μ l 5 M NaCl was added, and the mixture was incubated for 20 min on ice. The precipitate was pelleted by centrifugation (25 min, 15,000 \times g, 4°C), and the resulting supernatant was mixed with 500 μ l isopropanol to precipitate the chromosomal DNA. The DNA pellet was washed with 70% ethanol and finally resolved in 300 μ l Tris-EDTA buffer. Digests of chromosomal DNA were separated using 1% agarose gels, transferred onto a positively charged nylon membrane (Roche Diagnostics) (Sambrook *et al.*, 1989), and probed with digoxigenin (DIG)-labeled riboprobes obtained by *in vitro* transcription with T7 RNA polymerase (Roche Diagnostics) using PCR-generated fragments as templates. Primer pairs for the amplification of *prkC* and *aac-ahpD* gene fragments were CH74/SH89 and SH62/SH63, respectively (see Table S1 in the supplemental material). The reverse primers contained a T7 RNA polymerase recognition sequence. *In vitro* RNA labeling, hybridization, and signal detection were carried out according to the manufacturer's instructions (DIG RNA labeling kit and detection chemicals, Roche Diagnostics).

Analysis of mRNA amounts. Preparation of total *M. pneumoniae* RNA was done as described previously (Halbedel *et al.*, 2004). For slot blot analysis, serial twofold dilutions of the RNA extract in 10 \times SSC (1 \times SSC is 0.15 M NaCl plus 0.015 M sodium citrate) (2 μ g to 0.25 μ g) were blotted onto a positively charged nylon membrane using a PR 648 slot blot manifold (Amersham Biosciences). Equal amounts of yeast tRNA (Roche) and *M. pneumoniae* chromosomal DNA served as controls. DIG-labeled riboprobes were obtained by *in vitro* transcription from PCR products that cover open reading frame internal sequences using T7 RNA polymerase (Roche). The reverse primers used to generate the PCR products contained a T7 promoter sequence (see Table S1 in the supplemental material). The quantification was performed using Image J software v1.42 (Abramoff *et al.*, 2004).

HeLa cell cytotoxicity assay. HeLa cells were grown in 24-well plates with 2.5×10^4 cells per well in 700 μ l Dulbecco modified Eagle medium for 24 h at 37°C and 5% CO₂. The *M. pneumoniae* cultures were grown for 96 h at 37°C. The *M. pneumoniae* cells were then washed three times with 67.6 mM HEPES, pH 7.3; 140 mM NaCl; and 7 mM MgCl₂. The *M. pneumoniae* cells were resuspended with a 0.4- by 20-mm needle. Depending on the size of the pellet, they were resuspended in 5 to 8 ml buffer. The cell suspensions were adjusted to an A₅₅₀ of 0.1 and centrifuged for 5 min at 15,000 \times g at 4°C. The pellet was resuspended in 125 μ l of modified Hayflick medium with a 0.4- by 20-mm needle. The cells were then pipetted onto the lawn of HeLa cells and incubated for 2 h at 37°C and 5% CO₂. Then the supernatant was removed and replaced by 700 μ l Dulbecco modified Eagle medium, and the cells were incubated. The cytotoxicity assays were performed in triplicate.

Results

Isolation of an *M. pneumoniae prkC* mutant. To get more insights into the function of the protein kinase PrkC (MPN248), we attempted to isolate *prkC* mutants. This was done using “haystack mutagenesis” (Halbedel *et al.*, 2006). This strategy is based on an ordered collection of pooled random transposon insertion mutants that can be screened for junctions between the transposon and the gene of interest due to transposon insertion. Sixty-four pools containing 2,976 individual mutants (Halbedel *et al.*, 2006) were used in a PCR to detect junctions between the *prkC* gene and the mini-transposon using the oligonucleotides CH35 and SH29 for *prkC* and the mini-transposon, respectively (Fig. 3A). For one pool that gave a positive signal, colony PCR with the 50 individual mutants resulted in the identification of one *prkC* mutant. The presence of the transposon insertion in *prkC* was verified by Southern blot analysis using a *prkC*-specific probe (Fig. 3B). To test whether this strain contained only a unique transposon insertion, we did another Southern blotting using a probe specific for the *aac-aphD* resistance gene present on the mini-transposon. As shown in Fig. 3B, only a single band hybridizing with this probe was detected; moreover, this fragment had the same size as that of the *XhoI* fragment hybridizing to the *prkC* probe (Fig. 3B). The isolated *prkC* mutant strain was designated GPM11. The position of the transposon insertion in the *prkC* gene of *M. pneumoniae* GPM11 was determined by DNA sequencing. The *prkC* gene was disrupted between nucleotides 313 and 314, resulting in

a truncated protein of 106 amino acids, with one additional amino acid and the following stop codon encoded by the inserted mini-transposon. The disruption destroyed the kinase domain of PrkC (amino acids 80 to 256), suggesting that no active PrkC is present in the mutant strain.

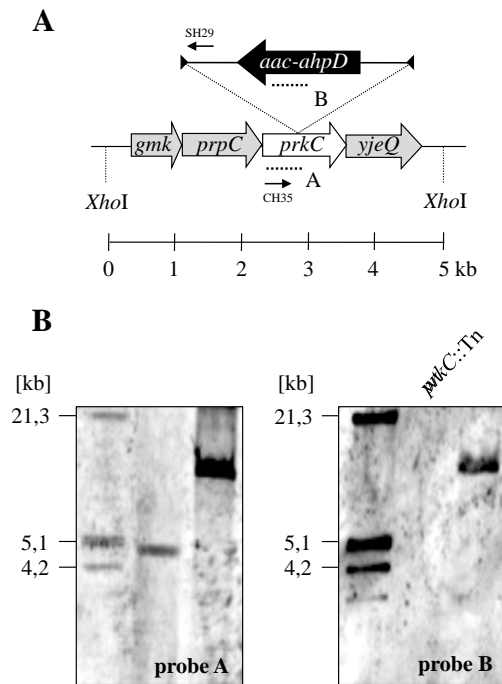


Fig. 3. Isolation of a *M. pneumoniae* *prkC* transposon insertion mutant. (A) Schematic representation of the genomic region surrounding the *prkC* gene in *M. pneumoniae* and site of the transposon insertion in the *prkC* knockout strain GPM11. The annealing sites of oligonucleotides used for the determination of the transposon insertion site are indicated by arrows. Probes hybridizing to internal fragments of the *prkC* and the *aac-ahpD* genes are depicted as dotted lines. (B) Southern blot analysis to confirm the single insertion of the mini-transposon into the *prkC* gene of strain GPM11. Chromosomal DNA of the wild type and of strain GPM11 was digested using *XhoI*. Blots were hybridized with the *prkC*-specific probe (left) and a probe hybridizing to the *aac-ahpD* gene of the mini-transposon (right). DIG-labeled DNA molecular size marker III (Roche Applied Science) served as a standard.

Implication of PrkC in adherent growth and cytotoxicity. For an initial characterization of the *prkC* mutant strain GPM11, we observed growth of this strain in modified Hayflick medium. A comparison of the growths of the wild type and the *prkC* mutant strain revealed that both strains grow at the same rate in the presence of glucose as the carbon source (data not shown). However, in contrast to its isogenic wild type, GPM11 was unable to attach to the surface of the culture flask, and the cells grew as a suspension in liquid medium.

This loss of adherent growth suggested that the *prkC* mutant might also be impaired in cytotoxicity. To assess the cytotoxicity of the *prkC* mutant strain, we infected confluent HeLa cell cultures with *M. pneumoniae* cells (multiplicity of infection of two). The cytotoxicity of the *prkC* mutant was compared to that of wild type strain M129 and *M. pneumoniae* GPM68, which is affected in *prpC*, the protein phosphatase that is thought to be the antagonist of PrkC. As shown in Fig. 4, the HeLa cells underwent lysis after 6 days upon infection with wild type *M. pneumoniae*. In contrast, a large portion of viable cells was observed after infection of the cell culture with *prkC* mutant GPM11. In contrast, cytotoxicity induced by *prpC* mutant strain GPM68 was equivalent to that of the wild type strain (Fig. 4B). These data clearly demonstrate that PrkC is required for host cell damage, whereas PrpC is not. This suggests that PrkC-dependent protein phosphorylation is an important factor for cytotoxicity.

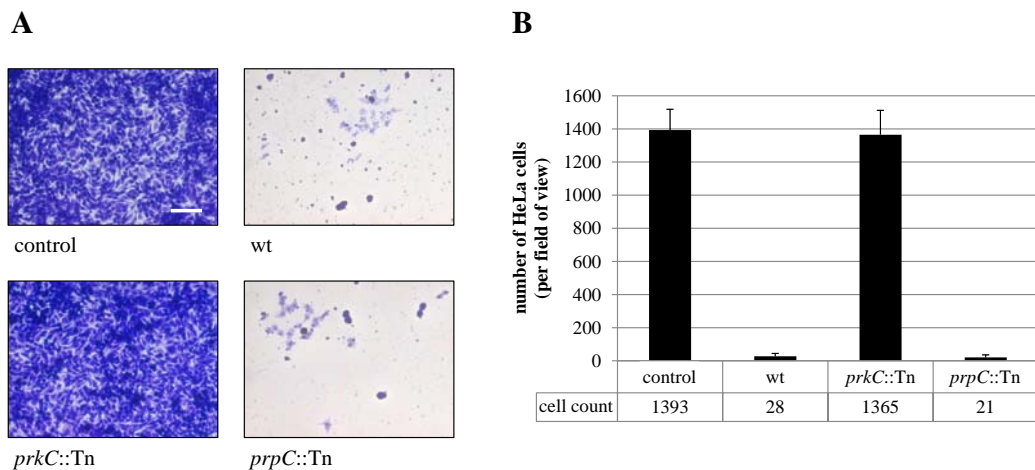


Fig. 4. Cytotoxicity of *M. pneumoniae* toward HeLa cell cultures. (A) Infection assay with the *M. pneumoniae* *prkC*::Tn strain GPM11 and the *prpC*::Tn strain GPM68. HeLa cell culture without *M. pneumoniae* (left top; control); HeLa cell culture incubated with wild type *M. pneumoniae* (right top; wt); HeLa cell culture incubated with the *prkC* or *prpC* mutant (bottom; *prkC*::Tn or *prpC*::Tn, respectively). After 6 days, HeLa cell cultures were stained with crystal violet and photographed. Scale bar, 0.1 mm. (B) Quantification of HeLa cells after infection with wild type *M. pneumoniae* or the *prkC* or *prpC* mutant. The cell count of surviving cells is indicated as the number of viable cells per field of view, quantified by crystal violet staining after 6 days of incubation. An uninfected HeLa cell culture served as a control. Error bars indicate the standard deviation (based on three independent experiments).

Identification of proteins that are subject to PrkC-dependent phosphorylation. The loss of adherent growth and cytotoxicity in the *prkC* mutant suggested that proteins that are phosphorylated by PrkC might be involved in these functions. To identify such proteins, we separated whole cell extracts of *M. pneumoniae* by SDS-PAGE. The proteins were consecutively stained with Pro-Q Diamond, a dye for the detection of Ser/Thr/Tyr-phosphorylated proteins, and with Flamingo fluorescence stain for the detection of the total proteins. For this analysis, we compared the wild type strain M129 and the *prkC* mutant GPM11. As a control, we used the *prpC* mutant GPM68. Since PrpC is thought to be the antagonist of PrkC, we expected to observe a more intense phosphorylation of PrkC target proteins with this mutant. In addition, we used a mutant affected in the other identified protein kinase of *M. pneumoniae*, HPrK (GPM51), and a mutant deficient in the surface protein MPN474, which is not thought to be implicated in protein phosphorylation (GPM70) (Krebes *et al.*, 1995). Several of the proteins that are involved in cytoadherence in *M. pneumoniae* are very large proteins, such as HMW1, HMW2, and HMW3. It has been shown that these proteins are phosphorylated in *M. pneumoniae* (Krebes *et al.*, 1995; Su *et al.*, 2007). Therefore, we decided to analyze specifically the phosphorylation pattern of large proteins by using 6% SDS-polyacrylamide gels. A comparison of the total protein patterns in the wild type and the *prkC* mutant strain revealed that the quantity of four proteins was severely reduced (Fig. 5A). These protein bands were identified by MS as the three high molecular weight proteins HMW1, HMW2, and HMW3 and the major adhesin P1. The amounts of these four proteins in the *prpC* mutant were indistinguishable from those of the wild type strain, suggesting that PrkC is necessary for their accumulation in the cell. The quantitative analysis of the Pro-Q Diamond signal intensities for the detection of phosphorylated proteins revealed that the bands of these proteins were absent or much weaker in the *prkC* mutant (Fig. 5B and C). In contrast, the phosphorylation signals of HMW1, HMW3, and P1 were more intense in the *prpC* phosphatase mutant than in the wild type (Fig. 5C). This observation indicated the accumulation of phosphorylated protein that cannot be dephosphorylated by the cognate protein phosphatase. In turn, this suggests that these proteins are targets of PrkC-dependent phosphorylation and that phosphorylation plays a role in their accumulation. In addition, one protein with an apparent molecular mass of 160 kDa accumulates in the *prpC* mutant and shows also a

new very strong phosphorylation signal in this mutant (Fig. 5B). This protein is the acidic surface protein MPN474.

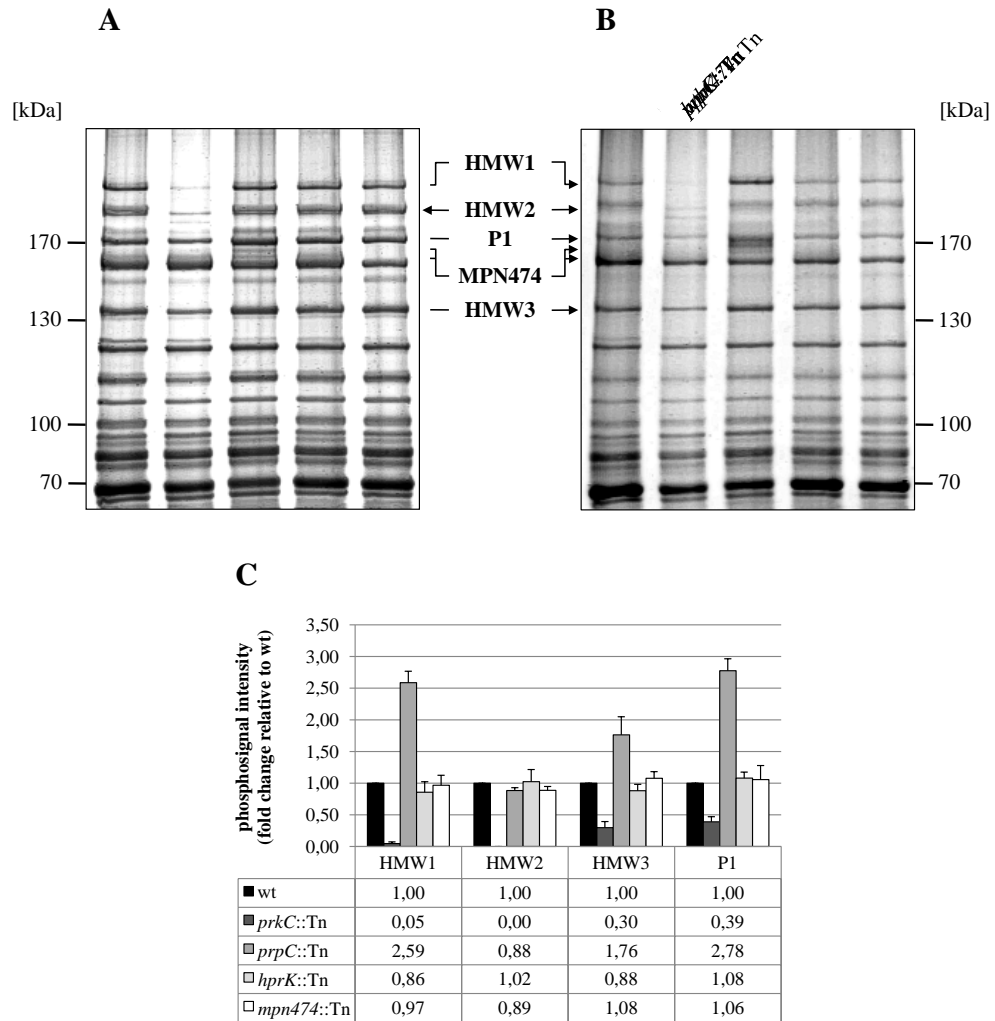


Fig. 5. Comparison of protein profile and *in vivo* phosphorylation patterns in *M. pneumoniae* wild type and mutant cells. Whole cell extracts of the *M. pneumoniae* wild type and different mutant strains were analyzed by SDS-PAGE and stained with Pro-Q Diamond (Invitrogen) and Flamingo fluorescent dye (Bio-Rad) for visualization of phosphoproteins and all proteins, respectively. Ten µg of extract was applied to each lane. Interesting protein bands were cut out and identified by MS. Protein bands with changes in the phosphorylation signal or the protein amount are indicated by arrows. Total protein (A) (Flamingo fluorescent stain); phosphoproteins (B) (Pro-Q Diamond stain). (C) Relative quantification of phosphosignal intensity. The graph shows the changes relative to the phosphorylation signal of the corresponding protein in the *M. pneumoniae* wild type. Error bars indicate the standard deviation (based on three independent experiments). Note that the protein amount of HMW1-3 and P1 is also decreased in the *prkC* mutant.

Impact of PrkC on the accumulation of cytodherence proteins. It has been shown that HMW2 mutants of *M. pneumoniae* are impaired in the accumulation of other cytodherence proteins, such as HMW1, HMW3, and MPN309 (P65) (Balish *et al.*, 2003). Since the amounts of the HMW proteins were reduced in the *prkC* mutant, we determined the cellular amounts of other cytodherence proteins by use of specific polyclonal antibodies raised against these proteins (Table 3 provides a summary of the results). As controls, we used the elongation factor G (FusA) and the MPN567 (P200) protein, which is required for gliding motility (Jordan *et al.*, 2007). The amounts of both proteins were virtually identical in all strains tested in this study (Fig. 6C).

Tab. 3. Summary of Western blot analyses with a *prkC*::Tn mutant (GPM11).

<i>M. pneumoniae</i> locus tags	SwissProt accession no.	Protein	Signal in Western blot (%) ^a	Protein function
MPN141	P11311	P1	35	Adhesin
MPN142	Q50341	P40	40	Involved in cytodherence
MPN227	P75544	FusA	100	Elongation factor G
MPN309	P53663	P65	9	Adhesin-related protein
MPN310	P75471	HMW2	0	Cytodherence high molecular weight protein 2
MPN310	P75471	HMW2-S (P28)	0	Adhesin-related protein, HMW2 fragment
MPN311	P75470	P41	8	Adhesin-related protein
MPN312	P75469	P24	41	Adhesin-related protein
MPN447	Q50365	HMW1	20	Cytodherence high molecular weight protein 1
MPN452	Q50360	HMW3	22	Cytodherence high molecular weight protein 3
MPN453	P75330	P30	34	Adhesin
MPN474	P75310	MPN474	104	Coiled coil protein, putative structural protein involved in cytoskeleton
MPN567	P75211	P200	96	Involved in cytodherence

^a The protein amount in the *prkC* mutant relative to that in the wild type strain (100%) is indicated.

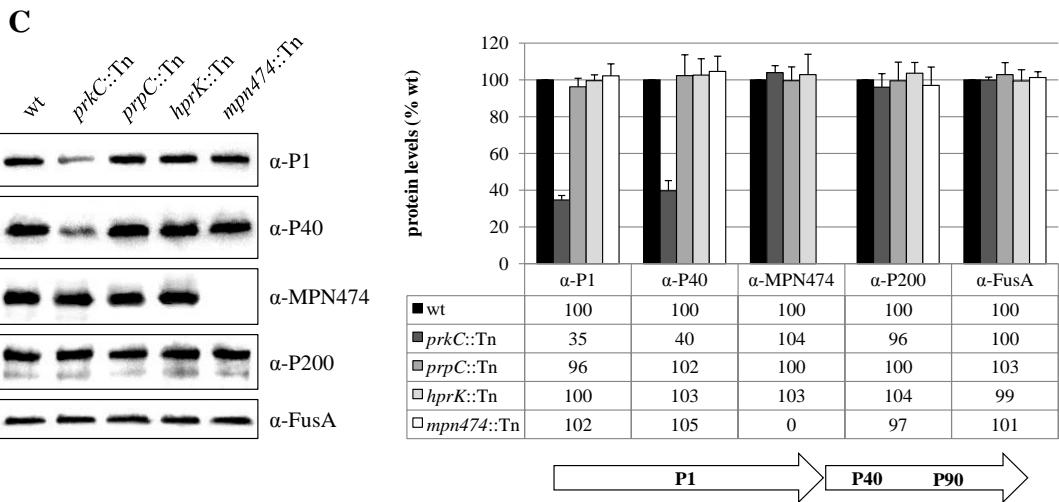
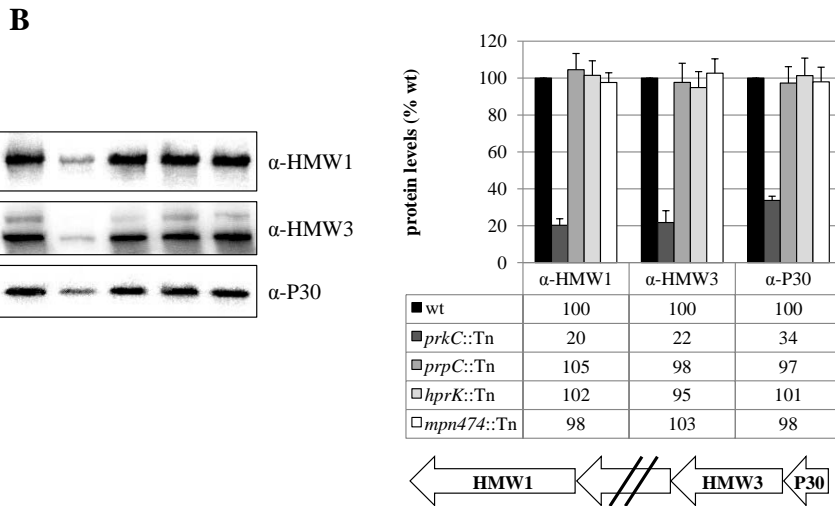
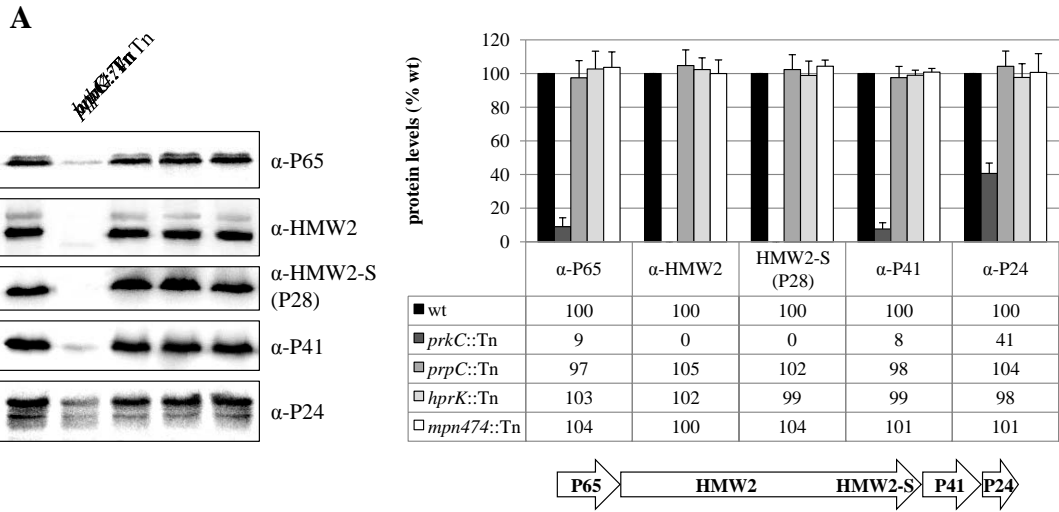


Fig. 6. Western blot analyses of expression profiles of *M. pneumoniae* cytodherence proteins. Whole cell extracts of the *M. pneumoniae* wild type and different mutant strains were separated by SDS-PAGE and blotted onto a polyvinylidene difluoride membrane. Cytadherence proteins were detected by using polyclonal rabbit antibodies raised against proteins of the P65 operon (A), the HMW gene cluster (B), and major adhesins (C). A polyclonal rabbit antibody raised against *M. pneumoniae* elongation factor G (FusA) was used as the control. Ten μg of extract was applied to each lane. The names of antibodies are given next to each blot. α , anti. HMW1, HMW2, HMW3, MPN474, P1, and P200 were analyzed by 6% SDS-PAGE, and the other proteins by 12% SDS-PAGE. The graphs show the quantification of Western blot signals relative to that for the *M. pneumoniae* wild type. Error bars indicate the standard deviation (based on three independent experiments). The organization of the different operons is shown by arrows. Note that there are four genes between *hmw3* and *hmw1*, which is indicated (panel B). Moreover, *mpn474*, *p200*, and *fusA* are not part of operons (panel C).

First, we studied the proteins encoded by one gene cluster containing the gene encoding HMW2 (the so-called P65 operon). As shown in Fig. 6A, the cellular amounts of all these proteins are significantly reduced in the *prkC* mutant. In fact, the HMW2 protein and HMW2-S (also called P28), a second translation product of the same mRNA (Boonmee *et al.*, 2009), are nearly completely absent in the *prkC* mutant strain. The accumulation of all the proteins encoded by the gene cluster is not affected by a disruption of the *prpC* gene (Fig. 6A). Thus, the phosphorylation of these proteins seems to be essential for their accumulation. The so-called HMW gene cluster encodes the HMW1, HMW3, and MPN453 (P30) proteins. As observed for HMW2, the two high molecular weight proteins encoded by this gene cluster are much less abundant in the *prkC* mutant, whereas none of the other tested mutations had any effect. The accumulation of MPN453 was also somewhat reduced but to a lesser extent (Fig. 6B). Finally, we assayed the amounts of the major adhesins MPN141 (P1) and MPN142 (P40) and of the surface protein MPN474, which was shown to be phosphorylated by PrkC (Fig. 5). As shown for the large cytodherence proteins, many fewer adhesins were detected in the *prkC* mutant than in the wild type or all other strains. In contrast, the cellular amounts of MPN474 were not affected by the *prkC* mutation. As expected, the antibodies do not cross-react with any protein in the MPN247 mutant strain GPM70.

Transcription of the genes encoding cytodherence proteins in mutants affecting protein phosphorylation. The virtual absence of cytodherence proteins in the *prkC* mutant can be explained by two alternative scenarios: (1) The expression of the corresponding genes and the accumulation of their mRNAs might require some kind of

PrkC-dependent protein phosphorylation and (2) the proteins might be translated to a lesser extent or be subject to rapid degradation. To distinguish between these possibilities, we compared the amounts of the mRNAs of the cytoadherence genes in the wild type strain M129 and in our set of mutants that are affected in protein (de)phosphorylation. For this purpose, we isolated RNA from cultures grown in modified Hayflick medium supplemented with glucose and performed slot blot analyses.

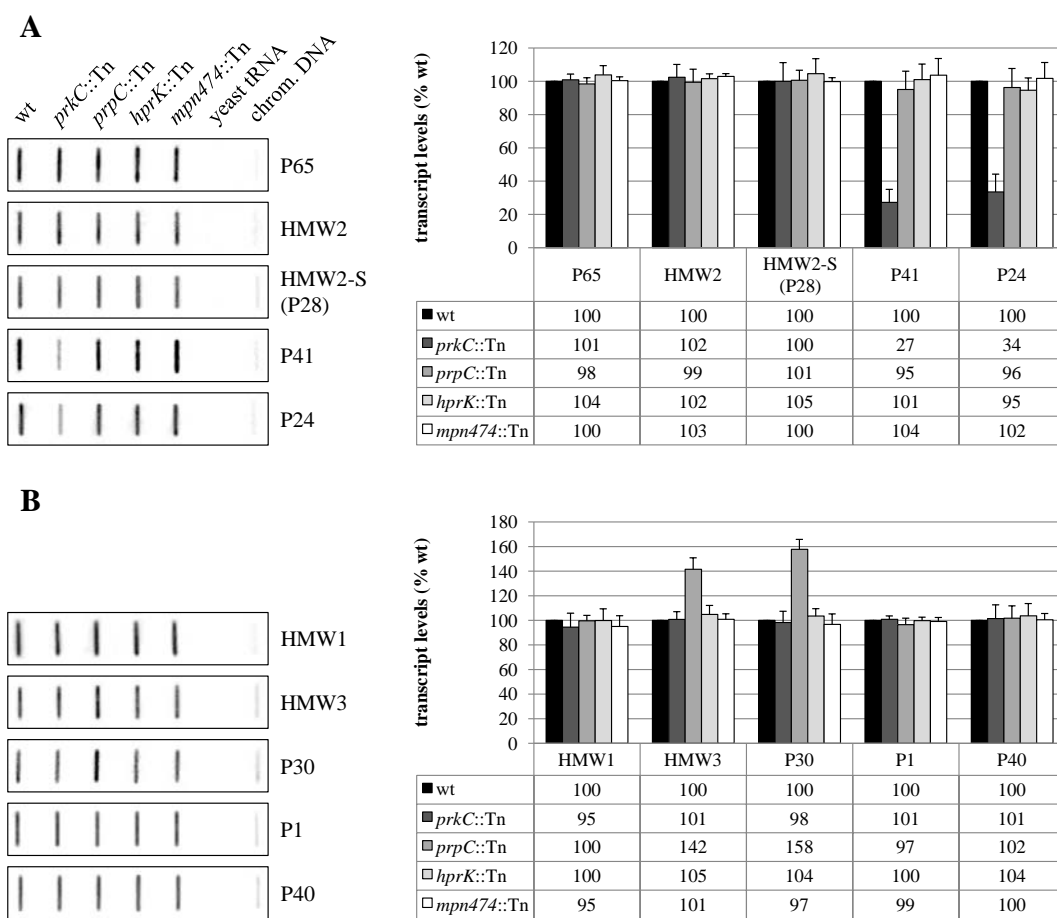


Fig. 7. Expression of cytoadherence genes in *M. pneumoniae* wild type and mutant cells. Slot blot analyses with whole RNA extracts of the *M. pneumoniae* wild type and different mutant strains. A dilution series of RNA extracts was blotted onto a positively charged nylon membrane and probed with a DIG-labeled riboprobe specific for an internal part of a particular open reading frame. Names of riboprobes are given next to each blot. Signals obtained with 1 μ g of RNA are shown. Yeast tRNA and *M. pneumoniae* chromosomal DNA served as controls. Expression profiles of the genes of the P65 operon are shown (A), and the analyses of cytoadherence genes of the HMW gene cluster and the major adhesins are also shown (B). The graphs show the quantification of transcript levels relative to that for the *M. pneumoniae* wild type. Error bars indicate the standard deviation (based on three independent experiments).

For the P65 operon, we observed similar amounts of mRNA for the two proximal genes of the operon, MPN309 (encoding P65) and *hmw2* (encoding HMW2) in the wild type and in the kinase and phosphatase mutants (Fig. 7A). This observation is in sharp contrast to the strongly reduced amounts of the corresponding proteins in the *prkC* mutant (Fig. 7A). For the two distal genes of the operon, MPN311 (P41) and MPN312 (P24), we observed a slight reduction of mRNA amounts in the *prkC* mutant (Fig. 7A). These reduced mRNA levels might explain the weak reduction of P24 protein accumulation, but they are not sufficient to account for the strongly reduced P41 amounts in the *prkC* mutant strain GPM11.

The genes of the HMW and the adhesin (P1 and P40) operons were all expressed at similar levels in the wild type as well as in the *prkC*, *hprK*, and *prpC* mutant strains (Fig. 7B). Again, the mRNA amounts were not affected by the *prkC* mutation, whereas the protein amounts were strongly reduced (Fig. 6C). This is in good agreement with the observations for the P65 operon and supports the conclusion that PrkC-dependent protein phosphorylation is implicated in the stability of the cytoadherence and adhesion proteins in *M. pneumoniae*.

Discussion

Protein phosphorylation is a major mechanism to control the activities of proteins. This posttranslational modification has been observed with all organisms, for which it has been studied, including the minimal bacteria *M. genitalium* and *M. pneumoniae* (Su *et al.*, 2007; this work). However, the physiological consequences of protein phosphorylation events in bacteria, as well as the responsible kinases, have remained largely unknown.

So far, only a few classes of serine/threonine protein kinases have been identified and characterized for bacteria. *M. pneumoniae* contains two of these protein kinases, HPrK and PrkC (Steinhauer *et al.*, 2002; this work). While HPrK is generally thought to phosphorylate only one specific substrate, the HPr protein of the phosphotransferase system, a variety of substrates have been proposed for PrkC and its homologues in different gram-positive bacteria. In *Bacillus subtilis*, PrkC was shown to phosphorylate the elongation factors Tu and G, the small-ribosome-associated GTPase CpgA, and the potential stressosome component YezA (Absalon *et al.*, 2009; Shah *et al.*, 2008). PrkC is required for germination of *B. subtilis* spores in response to

muropeptides (Shah *et al.*, 2008). The extracellular PASTA domain of PrkC senses these muropeptides (Shah *et al.*, 2008). Since *M. pneumoniae* neither sporulates nor possesses a peptidoglycan cell wall, it is not surprising that the PrkC protein of this bacterium does not contain a PASTA domain. Thus, it is safe to assume that *M. pneumoniae* PrkC has a function(s) that differs completely from that described for *B. subtilis*. Indeed, this work provides evidence that PrkC is required for adhesive growth of *M. pneumoniae*, and a *prkC* mutant has lost cytotoxicity. This is reminiscent of observations that have been made with several other pathogenic Firmicutes. In *Streptococcus pyogenes*, the homolog of PrkC is required for adherence to host cells and for invasion (Jin and Pancholi, 2006). Similarly, the kinase of *Enterococcus faecalis* is implicated in persistence in the intestine of mice (Kristich *et al.*, 2007). In contrast, PrkC of *Staphylococcus aureus* was reported to phosphorylate glycolytic enzymes (Lomas-Lopez *et al.*, 2007).

While the importance of PrkC-dependent protein phosphorylation is well established for many bacteria, the molecular consequences of the primary phosphorylation events have not been studied so far. Most often, protein phosphorylation results in a shift of a protein's activity (Johnson and Barford, 1993).

In this work, we observed that PrkC-dependent phosphorylation of large cytoadherence proteins is required for the stability of these complexes. It is unknown, which of these proteins is responsible for the destabilization of cytoadherence proteins in the *prkC* mutant, but our studies revealed that HMW1, HMW3, the major adhesin P1, and the surface protein MPN474 are subject to PrkC-dependent phosphorylation. This conclusion is supported not only by the absence of these proteins in cell extracts of the *prkC* mutant but also by the increased intensity of phosphorylation signals for these proteins in the *prpC* mutant strain. PrpC is the protein phosphatase that reverses PrkC-dependent protein phosphorylation. Thus, our work confirms and extends earlier reports on the phosphorylation of cytoadherence proteins (Krebes *et al.*, 1995; Su *et al.*, 2007). We cannot exclude, however, the possibility that an additional kinase(s) might phosphorylate HMW3 and P1 (Fig. 5C). It is well established that the cytoadherence proteins show reciprocal dependency in their stabilities, *i.e.*, mutations in one of the corresponding genes result in destabilization and delocalization of the other proteins of the attachment structure (Balish and Krause, 2006; Popham *et al.*, 1997; Willby *et al.*, 2004). Specifically, HMW1 was shown to be required for HMW2 and P1 localization

and stability. In turn, HMW2 is necessary for the stabilization of HMW3 and P65. As shown in this work, it has been suggested previously that the interdependence of the proteins of the attachment organelle does not involve reduced transcription (Popham *et al.*, 1997). Taken together, these findings establish that phosphorylation of the HMW proteins by PrkC is a prerequisite for their stability and perhaps for their proper localization in the attachment structure. This is the first time that protein phosphorylation was shown to increase the stability of a protein.

M. pneumoniae has only limited regulatory potential. These bacteria may use, in addition to three potential transcription regulators, protein phosphorylation to adapt to changes in environmental conditions. An analysis of the *M. pneumoniae* genome revealed the presence of two genes for serine/threonine kinases, *i.e.*, *hprK* and *prkC*, encoding the HPr kinase and protein kinase C (PrkC), respectively. Based on our present knowledge, it appears that these two proteins represent the total serine/threonine kinome of *M. pneumoniae*. It will be interesting to study how PrkC activity is triggered and whether other proteins are targets of this pleiotropic protein kinase.

Acknowledgments

We are grateful to Richard Herrmann for the gift of antibodies. Hinnerk Eilers is acknowledged for helpful discussions. This work was supported by Deutsche Forschungsgemeinschaft and the Fonds der Chemischen Industrie. S.R.S. was supported by a personal grant from the Studienstiftung des Deutschen Volkes.

Supplemental material

Tab. S1. Oligonucleotides used in this study.

Oligonucleotide	Sequence (5'→3') ^a
CH35	GCTCAACTTGATTAATTTAAAACAATGG
CH74	<u>CTAATACGACTCACTATAGGGAGAGGTGTTCAAACTGTGGAGG</u>
SH29	ATGAGTGAGCTAACTCACAG
SH62	TAGAATTTTATGGTGGTAGAG
SH63	<u>CTAATACGACTCACTATAGGGAGA</u> ACACTATCATAACCACTACC
SH89	TAGAGCTCGATGGCACTAAATTTAAAGATTGG
SS60	GCTACTGCATACGATCCCAATC
SS61	<u>CTAATACGACTCACTATAGGGAGAC</u> CATAGTAAGCGTTGGGATCGG
SS62	GCACTGGGTTTGATGATGGG
SS63	<u>CTAATACGACTCACTATAGGGAGAC</u> CCTGGTTAGCTGCAATCTGTTC
SS64	GAAGCGCAACCAACTAACGC
SS65	<u>CTAATACGACTCACTATAGGGAGAG</u> TTGTTGGGACAGATCAGCAC
SS66	GATGATGAAGCTGACATCATCATAG
SS67	<u>CTAATACGACTCACTATAGGGAGAG</u> TGTATTCCGTGCCACCAATAAC
SS68	CTAACACTAAAACGGGTACGAATTG
SS69	<u>CTAATACGACTCACTATAGGGAGAG</u> CCACAAGTGTTTCTGATGTCAC
SS70	CTGAGGAAAATCCCGAACAGATC
SS71	<u>CTAATACGACTCACTATAGGGAGAG</u> GCTGGTACATCTGCTTCCAAAC
SS72	GCCAACAGCGACATTAACAGC
SS73	<u>CTAATACGACTCACTATAGGGAGAC</u> AGTATCACTGCAGAGCTTATAAAC
SS74	GTATGGTAAGCTAGCACAAAAGATC
SS75	<u>CTAATACGACTCACTATAGGGAGAG</u> TTGATCAGCTTGCTGTTCCGG
SS76	CTTGGATTCTCATCCTCACCG
SS77	<u>CTAATACGACTCACTATAGGGAGAG</u> GGTGCAGCCCCACTCAAAC
SS78	GCGAGCGGGTGGTTCG
SS79	<u>CTAATACGACTCACTATAGGGAGAG</u> CCTTGTAAGCACTCGCTTCC
SS80	CCTGAATGCTAGTGCTGTTTCAG
SS81	<u>CTAATACGACTCACTATAGGGAGAG</u> TTGAGGTGGGAAACCAGTAC
SS86	GCACGCATCTTAAAGCTGTTGG
SS87	<u>CTAATACGACTCACTATAGGGAGAC</u> ACTGTCAGCGTGCTCTGC
SS92	GCTAGCTTCTTCACTTACCGG
SS93	<u>CTAATACGACTCACTATAGGGAGAG</u> TTAACGTTCCCTTCGTTACCATTG

^a The sequence of the T7-promotor is underlined.

Tab. S2. Antibodies used in this study.

<i>M. pneumoniae</i> locus tags	Protein	Antibody number	Dilution
MPN141	P1	449	1:1000
MPN146	P40	66450	1:250
MPN227	FusA	66708	1:3000
MPN309	P65	66578	1:3000
MPN310	HMW2	28050	1:2000
MPN310	HMW2-S (P28)	86236	1:1000
MPN311	P41	86630	1:1000
MPN312	P24	85910	1:250
MPN447	HMW1	84267	1:10000
MPN452	HMW3	65376	1:5000
MPN453	P30	123	1:50000
MPN474	MPN474	41804	1:20000
MPN567	P200	65020	1:10000

Chapter 3

The phosphoproteome of the minimal bacterium *Mycoplasma pneumoniae*: Analysis of the complete known Ser/Thr kinome suggests the existence of novel kinases

The work described in this chapter was published in:

Schmidl, S. R., K. Gronau, N. Pietack, M. Hecker, D. Becher, and J. Stülke. 2010.

The phosphoproteome of the minimal bacterium *Mycoplasma pneumoniae*: Analysis of the complete known Ser/Thr kinome suggests the existence of novel kinases. *Mol. Cell. Proteomics* **9**: 1228-1242.

Author contributions:

This study was designed and interpreted by SRS and JS. SRS performed the phosphoproteome experiments in *M. pneumoniae*. NP contributed to the investigation of the autophosphorylation event of phosphosugar mutases, especially in *B. subtilis*. The phosphoproteome analysis was done in collaboration with KG, MH, and DB, University of Greifswald. KG and DB helped substantially with the evaluation of the phosphorylation sites. SRS and JS wrote the paper.

Abstract

Mycoplasma pneumoniae belongs to the Mollicutes, the group of organisms with the smallest genomes that are capable of host-independent life. These bacteria show little regulation in gene expression, suggesting an important role for the control of protein activities. We have studied protein phosphorylation in *M. pneumoniae* to identify phosphorylated proteins. Two-dimensional gel electrophoresis and mass spectrometry allowed the detection of 63 phosphorylated proteins, many of them enzymes of central carbon metabolism and proteins related to host cell adhesion. We identified 16 phosphorylation sites, among them 8 serine and 8 threonine residues, respectively. A phosphoproteome analysis with mutants affected in the two annotated protein kinase genes or in the single known protein phosphatase gene suggested that only one protein (HPr) is phosphorylated by the HPr kinase, HPrK, whereas four adhesion-related or surface proteins were targets of the protein kinase C, PrkC. A comparison with the phosphoproteomes of other bacteria revealed that protein phosphorylation is evolutionarily only poorly conserved. Only one single protein with an identified phosphorylation site, a phosphosugar mutase (ManB in *M. pneumoniae*), is phosphorylated on a conserved serine residue in all studied organisms from archaea and bacteria to man. We demonstrate that this protein undergoes autophosphorylation. This explains the strong conservation of this phosphorylation event. For most other proteins, even if they are phosphorylated in different species, the actual phosphorylation sites are different. This suggests that protein phosphorylation is a form of adaptation of the bacteria to the specific needs of their particular ecological niche.

Introduction

Bacteria of the group called Mollicutes are unique among all living organisms because of their small genome that nevertheless allows them to grow independently from any host cell. The two most intensively studied representatives of the Mollicutes are *Mycoplasma genitalium* and *Mycoplasma pneumoniae* with genome sizes of 580 and 816 kb, respectively. The approximately 475 protein-coding and 43 RNA-coding genes of *M. genitalium* define the lower limit of the genetic equipment that permits independent life. The small genomes of the Mollicutes reflect their adaptation to rarely changing ecosystems, such as lung epithelia for *M. pneumoniae* (Stülke *et al.*, 2009).

Furthermore, *M. pneumoniae* has only limited metabolic capabilities: This bacterium can utilize only a few carbon sources (glucose, fructose, and glycerol) (Halbedel *et al.*, 2004), and its only way to produce ATP is by substrate level phosphorylation in glycolysis. The citric acid cycle, respiration, and most anabolic reactions are not carried out by *M. pneumoniae* (Halbedel *et al.*, 2007).

M. pneumoniae is a human pathogen that causes usually mild infections such as atypical pneumonia; however, the infections may be severe in children and elderly people. In addition, *M. pneumoniae* is involved in extrapulmonary complications, such as erythema multiforme and pediatric encephalitis (Atkinson *et al.*, 2008; Jacobs, 1997; Waites and Talkington, 2004).

The close adaptation of *M. pneumoniae* to human mucosal surfaces did not only result in a reductive evolution of metabolic capabilities but also affected the regulation of protein biosynthesis and activity: In contrast to versatile environmental bacteria such as *Pseudomonas aeruginosa* that reserve about 10% of their coding capacity for regulators of gene expression, *M. pneumoniae* encodes only three potential transcription regulators (less than 0.5% of all genes) (Stülke *et al.*, 2009). This absence of regulation at the level of gene expression suggests that the control of protein activities might play an important role in *M. pneumoniae* and other Mollicutes.

An important way to control the activity of a protein is posttranslational modification with protein phosphorylation being the most prominent regulatory modification both in bacteria and in eukaryotes (Boekhorst *et al.*, 2008; Jers *et al.*, 2008). Studies on the phosphoproteome have been performed for several bacteria, including the model organisms *Escherichia coli* and *Bacillus subtilis*. In both bacteria, about 5% of all proteins can be phosphorylated on Ser, Thr, or Tyr residues (Eymann *et al.*, 2007; Lévine *et al.*, 2006; Macek *et al.*, 2008; Macek *et al.*, 2007). Interestingly, there is a high level of species specificity with respect to the phosphoproteome: A comparison of the phosphoproteomes of *B. subtilis*, *E. coli*, and *Lactococcus lactis* revealed only eight proteins that are phosphorylated in all three species. Six of these proteins are involved in sugar metabolism, and two are translation factors. Of these eight proteins, only one, phosphoglucosamine mutase, is phosphorylated at a conserved residue (Soufi *et al.*, 2008).

In *M. pneumoniae*, only the phosphorylation of the HPr protein of the phosphoenolpyruvate:sugar phosphotransferase system by the HPr kinase has been

studied to some detail (Allen *et al.*, 2003; Halbedel *et al.*, 2004; Steinhauer *et al.*, 2002). Once phosphorylated, HPr can be dephosphorylated by a protein phosphatase, PrpC (Halbedel *et al.*, 2006). The corresponding *prpC* gene is in many Gram-positive bacteria clustered with the gene for a protein kinase, *prkC*, suggesting that PrkC and PrpC form a functional couple with opposing activities. Evidence for this idea was provided by the observation that the two proteins from *B. subtilis* have identical targets *in vitro* (Absalon *et al.*, 2009). The *prpC/prkC* gene cluster also exists in *M. pneumoniae*; however, the targets of the corresponding proteins are so far unknown. Previous studies with *M. pneumoniae* demonstrated that several proteins implicated in adhesion to the host cell are subject to protein phosphorylation *in vivo* (Dirksen *et al.*, 1994; Krebs *et al.*, 1995; Schmidl *et al.*, 2010). These proteins, HMW1 and HMW2, are important for the virulence of *M. pneumoniae* because adhesion is the first step in the interaction with the host. A recent proteomics study resulted in the identification of 18 phosphorylated proteins in *M. pneumoniae*, among them adhesion and surface proteins and metabolic enzymes (Su *et al.*, 2007). Unfortunately, none of the previously known phosphoproteins were detected in this study. Moreover, Ser-46 in HPr is still the only known phosphorylation site in *M. pneumoniae* (with the exception of phosphorylated His and Cys residues in phosphotransferase system proteins), and the (de)phosphorylation of HPr is the only event, for which the kinase and the phosphatase are known. Finally, nothing is known about protein tyrosine phosphorylation in *M. pneumoniae* and other Mollicutes.

We are interested in the elucidation of the molecular networks that allow life of *M. pneumoniae* as a minimal organism. The analysis of these bacteria is hampered by their slow growth and by the lack of efficient genetic systems that allow the elucidation of gene functions. We have established a technique, haystack mutagenesis, that can be used to isolate mutants of *M. pneumoniae* (Halbedel *et al.*, 2006). In this work, we have studied the phosphoproteome of the *M. pneumoniae* wild type strain and of three isogenic mutants that are affected in the two protein kinases, HPr kinase (HPrK) and protein kinase C (PrkC), and in the protein phosphatase PrpC. We identified 63 phosphorylated proteins. However, most of these proteins are phosphorylated by so far unknown kinases. An in-depth analysis of the only universally conserved phosphoprotein, a phosphosugar mutase, revealed that this enzyme autophosphorylates.

Experimental procedures

Bacterial strains and growth conditions. The *M. pneumoniae* strains used in this study were *M. pneumoniae* M129 (ATCC 29342) in the 32nd broth passage and its isogenic mutant derivatives GPM11 (*prkC*::mini-Tn, Gm^R) (Schmidl *et al.*, 2010), GPM51 (*hprK*::mini-Tn, Gm^R) (Halbedel *et al.*, 2006), and GPM68 (*prpC*::mini-Tn, Gm^R) (Halbedel *et al.*, 2006). *M. pneumoniae* was grown at 37°C in 150-cm² tissue culture flasks containing 100 ml of modified Hayflick medium with glucose (1%, wt/vol) as the carbon source as described previously (Halbedel *et al.*, 2004). Strains harboring transposon insertions were cultivated in the presence of 80 µg/ml gentamicin. *B. subtilis* 168 (*trpC2*; laboratory collection) was grown in LB and in minimal medium containing succinate and glutamate/ammonium as basic sources of carbon and nitrogen, respectively (Faires *et al.*, 1999). The media were supplemented with tryptophan (at 50 mg/liter) and glucose (0.5%, wt/vol). *B. subtilis* was transformed with plasmid DNA or PCR products according to the two-step protocol (Kunst and Rapoport, 1995). Transformants were selected on sporulation medium plates (Faires *et al.*, 1999) containing erythromycin plus lincomycin (2 and 25 µg/ml, respectively) and/or spectinomycin (100 µg/ml).

Preparation of cell extracts. After 4 days of incubation at 37°C, the culture medium was removed from the *M. pneumoniae* cell layer, and the cells were washed twice with 20 ml of cold PBS. After washing, cells were collected by scraping into 1.5 ml of PBS and subsequent centrifugation (5 min, 15,000 × g, 4°C). The cell pellet was resuspended in 500 µl of 10 mM Tris-HCl, pH 7.5, and the cells were disrupted by sonication (3 × 10 s, 50 watts, 4°C). Cell debris were sedimented by centrifugation (10 min, 15,000 × g, 4°C), and the resulting supernatant was centrifuged again (30 min, 24,000 × g, 4°C) to remove disturbing particles. The protein concentration of the supernatant was determined using the Bio-Rad dye binding assay with bovine serum albumin as the standard.

Two-dimensional SDS-polyacrylamide gel electrophoresis. Two-dimensional separation of proteins was performed as described previously (Halbedel *et al.*, 2007). For separation in the first dimension, IPG strips with a linear pH range of 4-7, 4.5-5.5, or 6-11 were used (ImmobilineTM DryStrip, Amersham Biosciences). The gels were subsequently stained with Pro-Q Diamond (Invitrogen) and FlamingoTM fluorescent dye (Bio-Rad) to visualize the phosphoproteins and all proteins, respectively. Image

analysis, spot quantification, and determination of putative phosphorylated protein spots were performed as described previously (Eymann *et al.*, 2007). The determination of phosphorylated proteins was based on the Pro-Q/Flamingo log ratio. Phosphoprotein spots were cut from the gel and identified by mass spectroscopy.

Protein identification by mass spectrometry. Gel pieces were washed twice with 200 μ l of 20 mM NH_4HCO_3 , 30% (v/v) CH_3CN for 30 min at 37°C and dried in a vacuum centrifuge (Concentrator 5301, Eppendorf). Trypsin solution (10 ng/ μ l trypsin in 20 mM ammonium bicarbonate) was added until gel pieces stopped swelling, and digestion was allowed to proceed for 16-18 h at 37°C. Peptides were extracted from gel pieces by incubation in an ultrasonic bath for 15 min in 20 μ l of HPLC grade water and transferred into microvials for mass spectrometric analysis. Peptides were separated by liquid chromatography and measured on line by ESI-mass spectrometry using a nanoACQUITY UPLCTM system (Waters) coupled to an LTQ OrbitrapTM mass spectrometer (Thermo Fisher Scientific, Waltham, MA). Peptides were desalted onto a trap column (Symmetry[®] C₁₈, Waters). Elution was performed onto an analytical column (BEH130 C₁₈, Waters) by a binary gradient of buffer A [0.1% (v/v) acetic acid] and B [100% (v/v) acetonitrile, 0.1% (v/v) acetic acid] over a period of 50 min with a flow rate of 400 nl/min. The LTQ Orbitrap was operated in data-dependent MS/MS mode using multistage activation for phosphorelevant masses. Proteins were identified by searching all MS/MS spectra in .dta format against all 689 *M. pneumoniae* proteins (extracted from the NCBI database) using SorcererTM-SEQUENT[®] (SEQUENT version 2.7 revision 11, Thermo Electron) including Scaffold_2_05_02 (Proteome Software Inc., Portland, OR). SEQUEST was searched with a fragment ion mass tolerance of 1.00 Da and a parent ion tolerance of 10 ppm. Up to two missed tryptic cleavages were allowed. Methionine oxidation (+15.99492 Da), cysteine carbamidomethylation (+57.021465 Da), and phosphorylation (+79.966331 Da) were set as variable modifications. For protein identification, a stringent SEQUEST filter for peptides was used (Xcorr versus charge state: 1.90 for singly, 2.2 for doubly, and 3.3 for triply charged ions and ΔCn value greater than 0.10), and at least two peptides per proteins were required. With this method, all identified proteins had a protein probability score greater than 99.9%. Protein probabilities were assigned by the Protein Prophet algorithm (Nesvizhskii *et al.*, 2003). Phosphorylated peptides that had a peptide probability score greater than 95.0% as specified by the Peptide Prophet algorithm

(Keller *et al.*, 2002) were examined manually and accepted only when b- or y-ions confirmed the identification. All spectra with Scaffold-annotated b- and y-ions series are provided as screen shots in the supplemental material (see supplemental Fig. S3).

Analysis of protein conservation and structure prediction. To address the potential conservation of phosphorylation sites, multiple sequence alignments were performed using the EXPRESSO alignment server that takes available structures into account (Armougom *et al.*, 2006). Structural models of the phosphoproteins were created using SWISS-MODEL in the automated mode and Swiss-PdbViewer v4.0.1 (Guex and Peitsch, 1997; Kiefer *et al.*, 2009). Ordered and disordered regions of proteins were predicted using the DisEMBL v1.5 web server (Linding *et al.*, 2003).

Cloning procedures. *E. coli* DH5 α (Sambrook *et al.*, 1989) was used for cloning experiments and protein expression. *E. coli* was grown in LB medium. LB plates were prepared by addition of 17 g of Bacto agar/liter (Difco) to LB (Sambrook *et al.*, 1989). Transformation of *E. coli* and plasmid DNA extraction were performed using standard procedures (Sambrook *et al.*, 1989). Restriction enzymes, T4 DNA ligase, and DNA polymerases were used as recommended by the manufacturers. DNA fragments were purified from agarose gels using the QIAquick Gel Extraction kit (Qiagen). *Pfu* DNA polymerase was used for the polymerase chain reaction as recommended by the manufacturer. DNA sequences were determined using the dideoxy chain termination method (Sambrook *et al.*, 1989). Standard procedures were used to transform *E. coli* (Sambrook *et al.*, 1989), and transformants were selected on LB plates containing ampicillin (100 μ g/ml).

Plasmid constructions. Plasmids for the overexpression and purification of the phosphosugar mutases GlmM and ManB from *B. subtilis* and *M. pneumoniae*, respectively, were constructed as follows. The coding sequence of the genes was amplified by PCR with gene-specific primers (listed in supplemental Table S3) using chromosomal DNA of *B. subtilis* 168 and *M. pneumoniae* M129 as the template. The PCR products were digested as shown in supplemental Table S4 and cloned into the appropriately linearized expression vector pWH844 (Schirmer *et al.*, 1997). These plasmids allowed the expression of the phosphosugar mutases carrying an N-terminal His₆-tag. The resulting plasmids pGP1401 and pGP656 are listed in supplemental Table S4. In *M. pneumoniae*, the UGA specifies a tryptophan; however, in *E. coli*, it is a stop codon. The *manB* gene contains three UGA codons that were replaced by the

multiple mutation reaction (Hames *et al.*, 2005) using the phosphorylated mutagenic oligonucleotides SS109, SS110, and SS111 (see supplemental Table S3) and plasmid pGP656 as the template. The resulting plasmid was pGP657 (see supplemental Table S4). The phosphorylation sites of GlmM and ManB were replaced by alanine residues. For this purpose, the combined chain reaction (Bi and Stambrook, 1998) was applied with the mutagenic primers NP116 and SS112 (see supplemental Table S3) and plasmids pGP1401 and pGP657. The resulting plasmids are pGP1405 (*glmM*) and pGP658 (*manB*) (see supplemental Table S4). All plasmid inserts were verified by DNA sequencing.

The plasmids pGP400 and pGP1403 were used to express the wild type and S100A mutant forms of GlmM, respectively, in *B. subtilis*. For the construction of pGP400, the *glmM* gene was amplified using the oligonucleotides NP108/NP109. The PCR product was digested with *Bam*HI and *Sal*I and cloned into pBQ200 (Martin-Verstraete *et al.*, 1994) digested with the same enzymes. For the construction of the plasmid encoding the S100A GlmM variant, mutagenesis was performed using the combined chain reaction with NP116 as the mutagenic primer and NP108/NP109. The resulting PCR product was cloned into pBQ200 as described for the wild type allele. The resulting plasmid was pGP1403.

Overexpression and purification of recombinant proteins. *E. coli* DH5 α transformed with the appropriate expression vector was used as host for the overexpression of recombinant proteins. Expression was induced by the addition of isopropyl 1-thio- β -D-galactopyranoside (final concentration, 1 mM) to exponentially growing cultures (A_{600} of 0.6). Cells were lysed using a French press (20,000 p.s.i., 138,000 kilopascals; Spectronic Instruments). After lysis, the crude extracts were centrifuged at 15,000 \times g for 1 h. For purification of His₆-tagged proteins, the resulting supernatants were passed over a Ni²⁺ HiTrap chelating column (4-ml bed volume; GE Healthcare) followed by elution with an imidazole gradient (from 0 to 500 mM imidazole in a buffer containing 10 mM Tris-HCl, pH 7.5, 600 mM NaCl, 10 mM β -mercaptoethanol) over 30 ml at a flow rate of 0.5 ml/min. After elution, the fractions were tested for the desired protein using 12.5% SDS-PAGE. The relevant fractions were combined and dialyzed overnight. Protein concentration was determined using the Bio-Rad dye binding assay where bovine serum albumin served as the standard.

Assays for protein phosphorylation. Protein phosphorylation assays were carried out with purified proteins in assay buffer [25 mM Tris-HCl, pH 7.6, 1 mM dithiothreitol, 0.4 mM [γ - 32 P]ATP (480 Ci/mmol), divalent cations as indicated] using purified target proteins. The assays were carried out at 37°C for 30 min followed by thermal inactivation of the protein (10 min at 95°C). The assay mixtures were analyzed on 16% SDS-polyacrylamide gels. Proteins were visualized by Coomassie staining. Radioactive protein spots were detected using a phosphorimaging system (Storm 860, GE Healthcare).

Allelic replacement of *B. subtilis glmM* gene. To delete the chromosomal copy of the *glmM* gene, the long flanking homology PCR technique was used (Wach, 1996). Briefly, a cassette carrying the *spc* resistance gene was amplified from plasmid pDG1726 (Guérout-Fleury *et al.*, 1995). DNA fragments of about 1,000 bp flanking the *glmM* gene at its 5' and 3' ends were amplified. The 3' end of the upstream fragment as well as the 5' end of the downstream fragment extended into *glmM* in a way that all expression signals of genes up- and downstream of the *glmM* remained intact. The joining of the two fragments to the resistance cassette was performed in a second PCR as described previously (Jordan *et al.*, 2006). In this reaction, we used the primer pair spec-fwd/spec-rev (Jordan *et al.*, 2006) for the amplification and joining of the *spc* cassette. The PCR product was directly used to transform *B. subtilis* carrying plasmids that express different alleles of *glmM*. The integrity of the regions flanking the integrated resistance cassette was verified by sequencing PCR products of about 1,000 bp amplified from chromosomal DNA of the resulting mutants.

Results

Phosphoproteome of growing *M. pneumoniae* cells. In a previous study on protein phosphorylation in *M. pneumoniae*, no phosphorylation sites were determined, and no mutants affected in the players of protein phosphorylation were studied (Su *et al.*, 2007). To get a more comprehensive insight into protein phosphorylation in *M. pneumoniae*, we decided to analyze the phosphoproteome of the wild type strain M129 and of three isogenic mutants defective in the two annotated protein kinases and the single annotated protein phosphatase of *M. pneumoniae*.

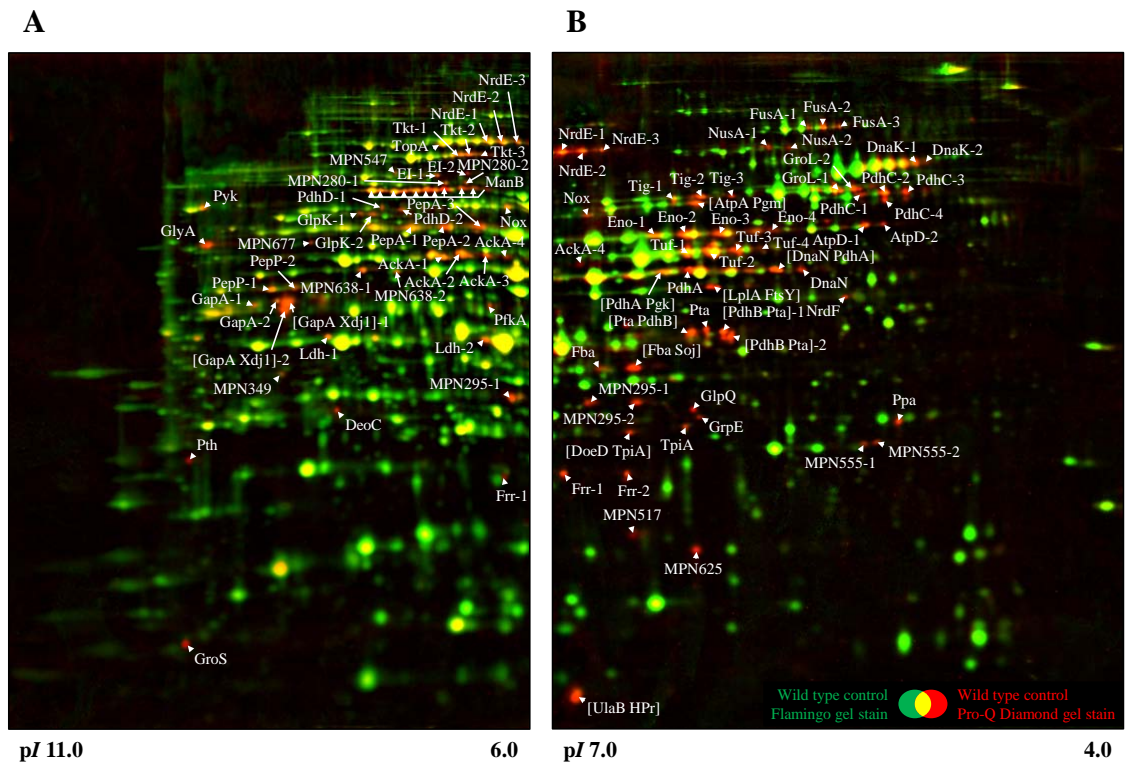


Fig. 8. Dual channel image of total protein amount (Flamingo fluorescent dye-stained; green) and phosphorylated proteins (Pro-Q Diamond-stained; red) of stationary phase *M. pneumoniae* cells. About 125 μ g of a total protein extract of *M. pneumoniae* grown in modified Hayflick medium supplemented with glucose were subjected to two-dimensional gel electrophoresis using either an 18-cm IPG strip with a linear pH gradient of pI 6–11 (A) or pI 4–7 (B) in the first dimension. Dual channel images were obtained using the software DECODON Delta2D v3.6. Spots with high Pro-Q Diamond/Flamingo log ratios representing phosphorylated proteins (Eymann *et al.*, 2007) are indicated on the gel. Multiple protein spots corresponding to the same original protein are distinguished by appended digits (e.g. Tuf-1 and Tuf-2). Protein spots were cut from the gel and identified by MS/MS (see Table 4 and supplemental Table S5).

The wild type strain M129 was grown in modified Hayflick medium with glucose as the principal carbon source, and cells were harvested in the late logarithmic phase. Protein extracts were prepared as described under “Experimental procedures” and the proteins were separated by two-dimensional gel electrophoresis (see Fig. 8). Traditional two-dimensional gels cover only the neutral and acidic proteins (pH range, 4-7). However, the theoretical proteome of *M. pneumoniae* shows a high number of more basic proteins that might escape detection (see supplemental Fig. S1). To include these basic proteins, we performed the isoelectric focusing in two pH ranges, 4-7 and 6-11. The gels were stained with Pro-Q Diamond and Flamingo fluorescent dye

to detect the phosphorylated proteins and the all proteins, respectively. The presence of more than 700 protein spots on the gels revealed that the proteome of *M. pneumoniae* was completely covered by our system (Jaffe *et al.*, 2004; Regula *et al.*, 2000). The identification of phosphorylated proteins revealed 58 phosphoproteins (see Table 4). We observed 36 phosphorylated proteins in the pH range from 4 to 7 and 27 phosphoproteins in the pH range from 6 to 11 with only five proteins (*i.e.* AckA, Frr, MPN295, Nox, and NrdE) detected in both gel systems. Of the proteins previously known to be phosphorylated, we detected HPr and, with the exception of the ribosomal protein S2 and the adhesin-related protein P65, all 17 phosphoproteins reported by Su *et al.* (2007).

In a next step, we tried to identify the phosphorylation sites in all phosphorylated peptides that had a peptide probability score greater than 95.0% as specified by the Peptide Prophet algorithm (see “Experimental procedures”). This analysis identified 12 phosphorylation sites in 10 phosphoproteins (see Table 4). These phosphorylations occurred on serine (eight sites) and threonine (four sites). Two proteins possessing two phosphorylation sites, NrdE and PepA, were phosphorylated on both a serine and a threonine residue. It is interesting to note that the individual NrdE molecules were phosphorylated only on one site: The two phosphopeptides for this protein were identified in different protein spots. In contrast, both PepA phosphopeptides were present in the protein from one spot, suggesting that this molecule was indeed doubly phosphorylated.

Phosphoproteome in *prpC* mutant. The *M. pneumoniae* genome encodes one protein phosphatase, PrpC. Previously, we have shown that PrpC dephosphorylates HPr(Ser-P) (Halbedel *et al.*, 2006). We considered that the analysis of the phosphoproteome in a *prpC* mutant might allow the identification of additional phosphorylated proteins that may have escaped our attention in the experiments with the wild type strain. Therefore, we cultivated the *prpC* mutant strain GPM68 as described above for the wild type and analyzed the protein phosphorylation pattern by two-dimensional gel electrophoresis. A comparison of the phosphoproteomes of the two strains revealed that all phosphoproteins detected in the wild type were also present in the *prpC* mutant. In addition, a few additional phosphoprotein spots were detected in the *prpC* mutant. These proteins had isoelectric points between 4 and 5 (data not shown). Therefore, we increased the resolution for these proteins by performing the isoelectric

focusing in the pH range from 4.5 to 5.5. In the *prpC* mutant, we observed five phosphoprotein spots that were not present in the wild type strain. The corresponding proteins were RpoE, the δ subunit of RNA polymerase, the adhesin-related protein P41, the high molecular weight cytoadherence protein HMW3, the uncharacterized protein MPN256, and the cell surface protein MPN474 (see Table 4 and Fig. 9). With the exception of RpoE, phosphorylation of these proteins seemed likely in the wild type strain, but was at the detection limit.

The analysis of the phosphorylated peptides that occur exclusively in the *prpC* mutant led to the identification of four additional phosphorylation sites. For P41, MPN256, and MPN474, phosphorylation occurred on a threonine residue. In addition, two different phosphorylation sites (Ser-87 and Thr-93) could be validated independently on the same phosphopeptide in the case of RpoE. However, the exact site could not be determined unambiguously, so it could only be assumed that phosphorylation occurred most likely on the threonine residue.

Effect of inactivation of Ser/Thr kinases on phosphoproteome.

M. pneumoniae encodes two known serine/threonine kinases, *i.e.* the HPr kinase HPrK and the protein kinase C PrkC. To analyze the impact of these kinases on protein phosphorylation on a global level, we analyzed the phosphoproteome in the corresponding mutant strains. As described for the wild type strain M129, the isogenic mutants GPM51 (*hprK*) and GPM11 (*prkC*) were grown in modified Hayflick medium, and cell extracts separated by two-dimensional gel electrophoresis.

In the *hprK* mutant, only one phosphoprotein spot appeared to be less intense as compared with the wild type (see Fig. 10). In the wild type strain, this spot contains two phosphorylated proteins, HPr and UlaB, a putative EIIB component of the phosphotransferase system. In the *hprK* mutant GPM51, this spot contained only the phosphorylated UlaB protein, whereas HPr was absent. This observation is in good agreement with the previous report that HPrK is the only kinase for HPr (Halbedel *et al.*, 2006). On the other hand, HPr is the only substrate that is phosphorylated by HPrK.

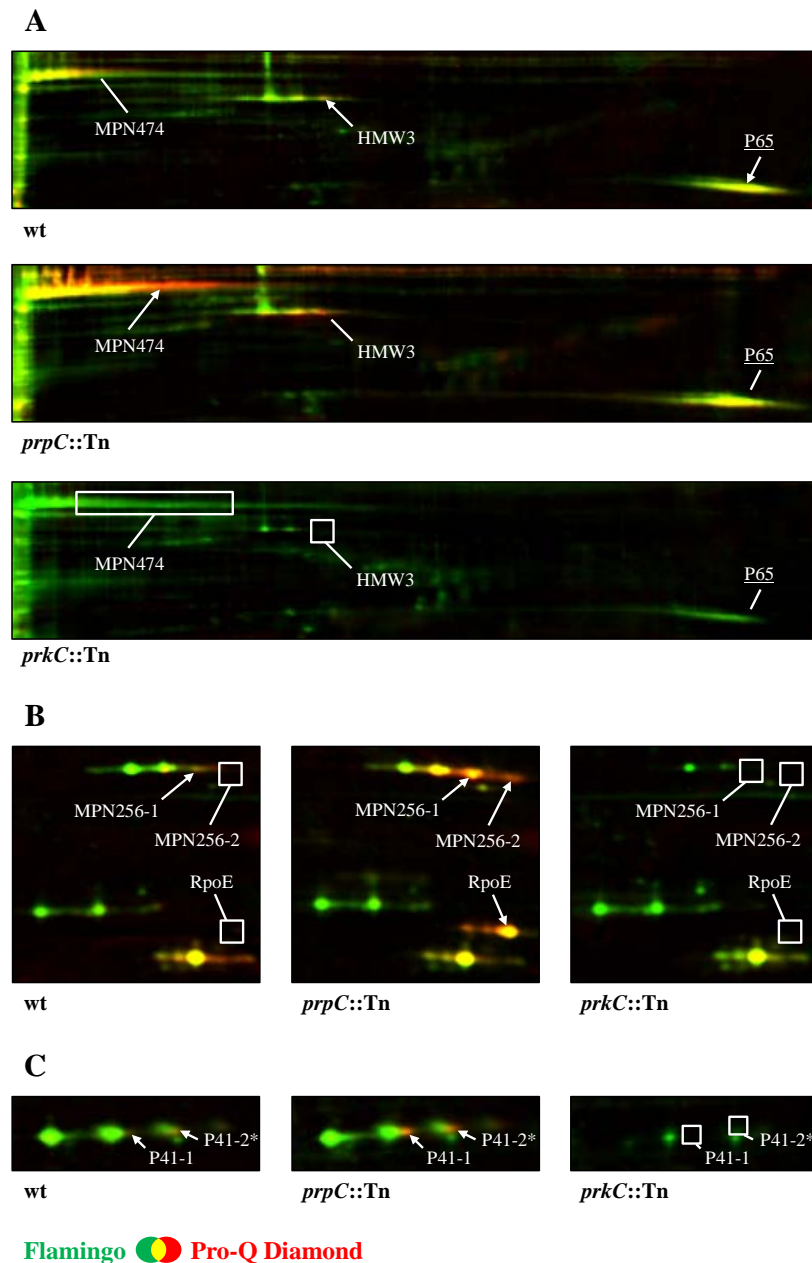


Fig. 9. PrpC/PrkC-dependent modification of cytoadherence proteins in *M. pneumoniae*. Shown are sections of dual channel images of Flamingo fluorescent dye- (green) and Pro-Q Diamond-stained (red) two-dimensional gels representing selected proteins in the *M. pneumoniae* wild type, *prpC::Tn* mutant, and *prkC::Tn* mutant. Proteins were separated on an 18-cm IPG strip with a linear pH gradient of pI 4.5-5.5 in the first dimension. The proteins HMW3, MPN474, P65 (A), MPN256, RpoE (B), and P41 (C) are shown. Putative phosphorylated proteins in the *M. pneumoniae* wild type as well as proteins with increased or new phosphorylation spots in the *prpC::Tn* mutant are indicated. Missing phosphorylation spots in the *M. pneumoniae* wild type and the *prkC::Tn* mutant are highlighted by a box. Protein amounts of HMW3, MPN256, and P41 (all represented by a triple protein spot) seem to be reduced as well as for the P65 protein (underlined) in the *prkC::Tn* mutant. Note that the P41 spot “2*” is only putative because of a low Pro-Q Diamond/Flamingo log ratio in the analyzed strains. Protein spots were cut from the gel and identified by MS/MS (see Table 4 and supplemental Table S5).

For the *prkC* mutant, we observed that the majority of phosphoproteins were not affected by the inactivation of this kinase. However, the phosphorylation or the accumulation of a few proteins was different in the *prkC* mutant as compared with the isogenic wild type. The large surface protein MPN474 was weakly phosphorylated in the wild type, and this protein was not at all phosphorylated in the *prkC* mutant, suggesting that MPN474 is a substrate for PrkC. This hypothesis is reinforced by the finding that MPN474 phosphorylation is strongly enhanced in the *prpC* phosphatase mutant (see Fig. 9A). Similarly, the so far uncharacterized protein MPN256 and the cytoadherence proteins HMW3 and P41 were phosphorylated in the wild type but not in the *prkC* mutant strain GPM11. As observed with MPN474, the intensity of the phosphoprotein spot of these proteins was strongly increased in the *prpC* mutant (see Fig. 9A and B). Thus, MPN256, HMW3, and P41 are novel targets of PrkC-dependent phosphorylation in *M. pneumoniae*.

The *prkC* mutation did not only affect protein phosphorylation but also the accumulation of some proteins. MPN256, a substrate of PrkC, was much less abundant in the *prkC* mutant as compared with the wild type. Similarly, the adhesion proteins P41 and HMW3 were present in reduced amounts in the *prkC* mutant. In addition, the adhesin-related protein P65 was less abundant in the *prkC* mutant. However, the phosphorylation signals for this protein in the wild type and the *prpC* mutant strains were below the threshold to conclude phosphorylation.

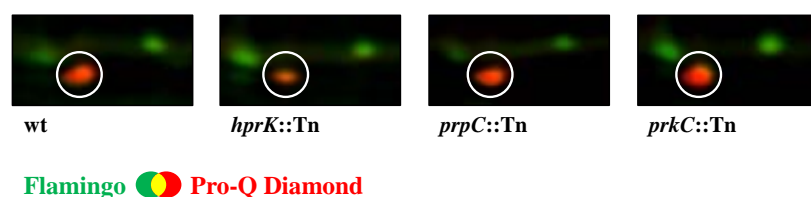


Fig. 10. Comparison of HPr phosphorylation pattern between different *M. pneumoniae* strains. Section of dual channel images of Flamingo fluorescent dye- (green) and Pro-Q Diamond-stained (red) two-dimensional gels displaying the phosphorylated spot of HPr in the *M. pneumoniae* wild type and different mutant strains. Proteins were separated on an 18-cm IPG strip with a linear pH gradient of pI 4-7 in the first dimension. Note that the HPr spot represents a multiprotein spot containing HPr and UlaB, whereas only UlaB could be detected in the *hprK::Tn* mutant (much lesser intensity of the phosphorylation spot).

Tab. 4. Phosphoproteins of *M. pneumoniae*.

For detailed MS/MS data, see supplemental Tables S5 and S6 and Fig. S3. pS, phosphoserine; pT, phosphothreonine.

Locus name	Protein name	Protein function	COG ^a	Phospho spots in two-dimensional gel	Phosphosite	Phosphopeptide sequence
MPN001	DnaN	DNA polymerase III subunit β	L	2		
MPN002	Xdj1	DnaJ-like protein	O	2		
MPN024 ^b	RpoE	RNA polymerase subunit δ	K	1	[Ser-87 or Thr-93]	Ip[SQAMFVT]KEIFEEGYEDLSNK
MPN025	Fba	Fructose-bisphosphate aldolase	G	2		
MPN050	GlpK	Glycerol kinase	C	2		
MPN053 ^c	HPr	Phosphocarrier protein	G	1		
MPN062	DeoD	Purine-nucleoside phosphorylase	F	1		
MPN063	DeoC	Deoxyribose-phosphate aldolase	F	1		
MPN066	ManB	Phosphomannomutase/phosphoglucomutase	G	10	Ser-149	(K)YHFDGGVNVTA p SHNPK
MPN082	Tkt	Transketolase	G	3		
MPN120	GrpE	Heat shock protein	O	1		
MPN154	NusA	Transcription elongation factor	K	2	Ser-503	PVVKPK p SVFSITVEADDSK
MPN221	Pth	Peptidyl-tRNA hydrolase	J	1		
MPN227	FusA	Elongation factor G	J	3		

Tab. 4. Continued.

Locus name	Protein name	Protein function	COG ^a	Phospho spots in two-dimensional gel	Phosphosite	Phosphopeptide sequence
MPN256 ^b	MPN256	Uncharacterized protein	S	2	Thr-200	FIDELDQIpTK
MPN261	TopA	DNA topoisomerase I	L	1	Ser-426	TVApSLMADCKK
MPN280	MPN280	Ribonuclease J	A	2		
MPN295	MPN295	Uncharacterized protein	S	2	Ser-63	YGPECEKSFLSLQpSK
MPN302	PfkA	Phosphofructokinase	G	1		
MPN303	Pyk	Pyruvate kinase	G	1		
MPN311 ^b	P41	Adhesin-related protein	M	1	Thr-223	TNNSIQQLEAEIQIPpTTHIK
MPN322	NrdF	Ribonucleoside-diphosphate reductase subunit β	F	1		
MPN324	NrdE	Ribonucleoside-diphosphate reductase subunit α	F	3	Thr-159, Ser-412	FQPApTPTFLNAGR VGNDIpSCNLGSLNIAK
MPN331	Tig	Trigger factor	O	3		
MPN349	MPN349	Uncharacterized protein	S	1		
MPN389	LplA	Lipoate-protein ligase A	H	1		
MPN390	PdhD	Pyruvate dehydrogenase E3 component	C	2		
MPN391	PdhC	Pyruvate dehydrogenase E2 component	C	4		
MPN392	PdhB	Pyruvate dehydrogenase E1 component subunit β	C	3		

Tab. 4. Continued.

Locus name	Protein name	Protein function	COG ^a	Phospho spots in two-dimensional gel	Phosphosite	Phosphopeptide sequence
MPN393	PdhA	Pyruvate dehydrogenase E1 component subunit α	C	3	Ser-205	TKLE p SAVSDLSTK
MPN394	Nox	NADH oxidase	H	1		
MPN420	GlpQ	Glycerophosphoryldiester phosphodiesterase	C	1		
MPN425	FtsY	Cell division protein homolog	U	1		
MPN428	Pta	Phosphotransacetylase	C	4		
MPN429	Pgk	Phosphoglycerate kinase	G	1		
MPN430	GapA	Glyceraldehyde-3-phosphate dehydrogenase	G	4	Ser-245	VPVLTG p SIVELCVALEK
MPN434	DnaK	Chaperone protein	O	2		
MPN452 ^b	HMW3	Cytadherence high molecular weight protein 3	M	1		
MPN470	PepP	Xaa-Pro aminopeptidase	E	2	Thr-317	LLCENAVI p TIEPGIYIPSVGGIR
MPN474 ^b	MPN474	Coiled coil surface protein	M	1	Thr-773	QNNEEL p TDKCSNIQNELHDLNR
MPN495	UlaB	Ascorbate-specific phosphotransferase enzyme IIB component	G	1		
MPN517	MPN517	Reductase homolog	C	1		
MPN528	Ppa	Inorganic pyrophosphatase	P	1		
MPN533	AckA	Acetate kinase	C	4		

Tab. 4. Continued.

Locus name	Protein name	Protein function	COG ^a	Phospho spots in two-dimensional gel	Phosphosite	Phosphopeptide sequence
MPN547	MPN547	Dihydroxyacetone kinase	C	1		
MPN555	MPN555	Uncharacterized protein	S	2		
MPN572	PepA	Cytosol aminopeptidase	E	3	Ser-249, Thr-420	YDMSGAAIVC p STVLALAK EGVPLIHCDIAS p TASIQDLGQGVLVR
MPN573	GroL	60-kDa chaperonin	O	2		
MPN574	GroS	10-kDa chaperonin	O	1		
MPN576	GlyA	Serine hydroxymethyltransferase	E	1		
MPN598	AtpD	ATP synthase subunit β	C	2		
MPN600	AtpA	ATP synthase subunit α	C	1		
MPN606	Eno	Enolase	G	4		
MPN625	MPN625	Osmotically inducible protein C-like protein	O	1		
MPN627	EI	Phosphotransferase system enzyme I	G	2		
MPN628	Pgm	Phosphoglycerate mutase	G	1		
MPN629	TpiA	Triose-phosphate isomerase	G	2		
MPN636	Frr	Ribosome-recycling factor	J	2		

Tab. 4. Continued.

Locus name	Protein name	Protein function	COG ^a	Phospho spots in two-dimensional gel	Phosphosite	Phosphopeptide sequence
MPN638	MPN638	Putative type I restriction enzyme specificity protein	V	2		
MPN665	Tuf	Elongation factor TU	J	4	Thr-383	EGGR p TVGAGSVTEVLE
MPN674	Ldh	L-Lactate dehydrogenase	C	2		
MPN677	MPN677	Uncharacterized protein	S	1		
MPN688	Soj	ParA family protein	D	1		

^a COG, cluster of orthologous groups of proteins; A, RNA processing and modification; C, energy production and conversion; D, cell cycle control, cell division, and chromosome partitioning; E, amino acid transport and metabolism; F, nucleotide transport and metabolism; G, carbohydrate transport and metabolism; H, coenzyme transport and metabolism; J, translation, ribosomal structure, and biogenesis; K, transcription; L, replication, recombination, and repair; M, cell wall, membrane, and envelope biogenesis; O, posttranslational modification, protein turnover, and chaperones; P, inorganic ion transport and metabolism; S, function unknown; U, intracellular trafficking, secretion, and vesicular transport; V, defense mechanisms.

^b Phosphoproteins only detectable in a *prpC*::Tn mutant (GPM68).

^c HPr (MPN053) not detectable in a *hprK*::Tn mutant (GPM51).

Classes of phosphorylated proteins. To get an impression of, which cellular processes are affected by protein phosphorylation, we grouped the proteins according to their functional categories (cluster of orthologous groups of proteins) (see Table 4). This analysis revealed that most phosphoproteins (36 proteins) are metabolic enzymes or transporters. 13 phosphorylated proteins are involved in cellular processes such as protein folding or envelope biogenesis. Nine of the phosphorylated proteins are required for the storage and processing of the genetic information, and the functions of five proteins are unknown.

Among the phosphorylated enzymes and transporters, a large number are involved in the central carbon metabolism (see Fig. 11). Of the glycolytic enzymes, all but the phosphoglucose isomerase are phosphorylated in *M. pneumoniae*. Moreover, all subunits of the pyruvate dehydrogenase and all three enzymes of overflow metabolism (Ldh, AckA, and Pta) are phosphoproteins. Of the enzymes of the pentose phosphate pathway, only the transketolase (Tkt) is phosphorylated in *M. pneumoniae*. In addition to glucose, *M. pneumoniae* can utilize glycerol and fructose. Although the enzymes that introduce fructose in the central metabolism are not phosphorylated, two glycerol 3-phosphate-forming enzymes are phosphoproteins.

Glycolytic enzymes are phosphorylated in many bacteria (see Table 5). A comparison of the phosphorylation pattern of these enzymes in different bacteria, however, revealed specific sets of phosphorylated glycolytic enzymes in each species. None of the glycolytic enzymes are phosphorylated in all species, and the phosphofructokinase is only phosphorylated in *M. pneumoniae* but not in any other bacterium studied so far. For some of the glycolytic phosphoproteins, the phosphorylation sites have been determined in multiple species. It is interesting to note that even if the same enzyme is phosphorylated in different species, the phosphorylation sites are not conserved. An exception is the pyruvate kinase that is phosphorylated on Ser-36 in a Gram-positive and in a Gram-negative bacterium (*B. subtilis* and *E. coli*, respectively) (Macek *et al.*, 2008; Macek *et al.*, 2007). However, phosphorylation of this enzyme was not detected in *L. lactis* (Soufi *et al.*, 2008), a close relative of both *B. subtilis* and *M. pneumoniae* (see “Discussion”).

Tab. 5. Phosphorylation events in glycolytic pathway of bacteria.

Bracketed letters indicate putative phosphorylation sites due to identification of the phosphopeptide.

Protein	Organism				
	<i>M. pneumoniae</i>	<i>B. subtilis</i>	<i>L. lactis</i>	<i>E. coli</i>	<i>C. jejuni</i>
Glucose-6-phosphate isomerase	No	Yes (Thr-39)	Yes (Ser-143)	Yes ([Ser-105], Thr-107)	No
Phosphofructokinase	Yes	No	No	No	No ^b
Fructose-bisphosphate aldolase	Yes	Yes (Thr-212, Thr-234)	Yes ([Thr-49, Ser-50], Ser-216)	No	Yes
Triose-phosphate isomerase	Yes	Yes (Ser-213)	No	No	Yes
Glyceraldehyde-3-phosphate dehydrogenase	Yes (Ser-245)	Yes ([Ser-148, Ser-151, Thr-153, Thr-154])	Yes (Ser-126, Ser-211, [Thr-212], Thr-321)	No	No

Tab. 5. Continued.

Protein	Organism				
	<i>M. pneumoniae</i>	<i>B. subtilis</i>	<i>L. lactis</i>	<i>E. coli</i>	<i>C. jejuni</i>
Phosphoglycerate kinase	Yes	Yes (Ser-183, Thr-299)	Yes (Ser-217)	Yes (Ser-192, Thr-196, Thr-199)	No
Phosphoglycerate mutase	Yes	Yes (Ser-62)	Yes (T94, S144)	Yes (S146)	No
Enolase	Yes	Yes (Thr-141, Ser-259, Tyr-281, Ser-325)	No	Yes ([Ser-372, Thr-375, Thr-379])	Yes ([Ser-180, Tyr-185])
Pyruvate kinase	Yes	Yes (Ser-36)	No	Yes (Ser-36)	Yes

^a *C. jejuni* does not encode for the glycolytic enzyme phosphofructokinase.

Autophosphorylation of single universally conserved phosphoprotein. As mentioned above, there is little conservation of the phosphorylation sites even if the same proteins are phosphorylated in fairly closely related organisms. There is only one exception to this notion, the phosphosugar mutase ManB (according to the nomenclature for *M. pneumoniae*). Phosphosugar mutases are phosphorylated in all domains of life from the archaeon *Halobacterium salinarum* and bacteria such as *M. pneumoniae* and *E. coli* to eukaryotes such as yeast, *Drosophila melanogaster*, and humans (Aivaliotis *et al.*, 2009; Li *et al.*, 2007; Macek *et al.*, 2008; Yu *et al.*, 2007; Zhai *et al.*, 2008).

The phosphoproteome analysis showed the presence of 10 phosphospots that do all correspond to ManB. The analysis of the phosphorylation site revealed that Ser-149 was phosphorylated in ManB of *M. pneumoniae* (see Fig. 12). This site was detected in all 10 spots, suggesting that ManB is subject to different posttranslational modifications that affect the isoelectric point of the protein. An alignment of the regions surrounding the phosphorylation site of these proteins revealed a very strong conservation of the region around the phosphorylated serine residue (see Fig. 13A). The motif (T/S)ASHN(P/R) is present in all proteins. This strong similarity suggests phylogenetic conservation of the phosphorylation site and also implies conservation of the phosphorylation mechanism (the kinase) and of the biological function of the phosphorylation event.

Because there are no conserved protein kinases in the three domains of life, we considered the possibility that ManB might autophosphorylate as it had been shown for the phosphoglucosamine mutase from *E. coli* (Jolly *et al.*, 2000). To test this idea, we purified ManB carrying an N-terminal His₆-tag and performed phosphorylation assays. As shown in Fig. 13B, the protein did indeed autophosphorylate in the presence of manganese. Only faint phosphorylation signals were observed in the presence of other divalent cations. A protein in which the phosphorylated serine residue was replaced by a non-phosphorylatable alanine did not autophosphorylate (Fig. 13C). This result demonstrates that ManB is phosphorylated on the same site *in vivo* and *in vitro* and supports the hypothesis of autophosphorylation. To demonstrate that autophosphorylation is not limited to the enzyme of *M. pneumoniae*, we also purified the phosphosugar mutase GlmM from *B. subtilis* and observed autophosphorylation for this protein as well. Again, no phosphorylation was detectable if the phosphorylated

serine residue [Ser-100 (Eymann *et al.*, 2007; Macek *et al.*, 2007)] was replaced by an alanine. Thus, autophosphorylation is the common mechanism of phosphorylation of these enzymes. This explains the unique conservation of a phosphorylation site.

The phosphosugar mutases play a key role in metabolism as shown by the fact that they are often essential. This is true for GlmM from *E. coli* and *B. subtilis* (Kobayashi *et al.*, 2003; Mengin-Lecreulx *et al.*, 1996). To test whether ManB of *M. pneumoniae* is also encoded by an essential gene, we attempted to isolate a *manB* mutant from an ordered collection of transposon insertions. In this collection, each viable mutant is included with a probability of 99.999% (Halbedel *et al.*, 2006; Halbedel and Stülke, 2007). No transposon insertion in *manB* was identified, suggesting that the gene is indeed essential. This finding is in good agreement with previous reports that no transposon insertion in *manB* could be isolated in *M. pneumoniae* and *M. genitalium* (Glass *et al.*, 2006; Hutchison III *et al.*, 1999).

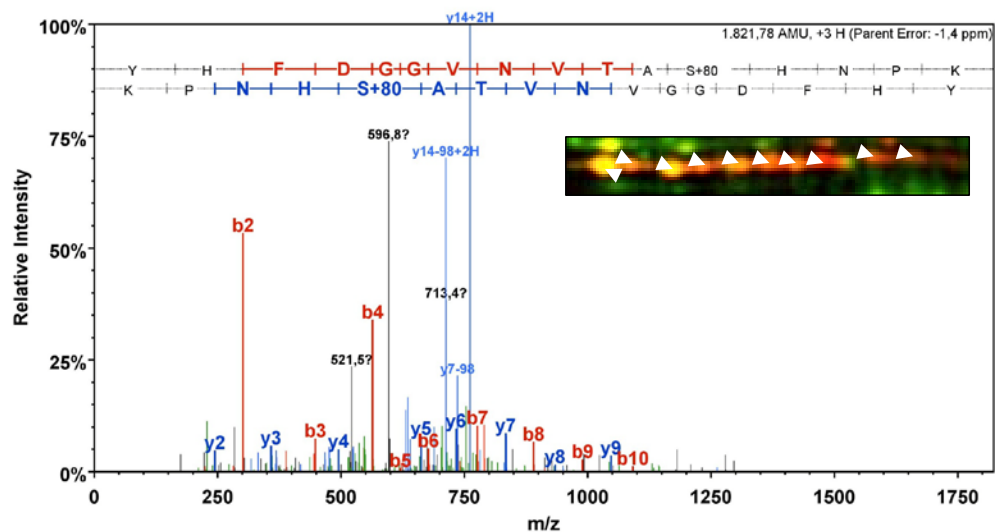


Fig. 12. MS/MS spectrum of serine-phosphorylated peptide from phosphomannomutase/phosphoglucomutase ManB (MPN066). The peptide was measured on line by ESI-mass spectrometry using a nanoACQUITY UPLC system coupled to an LTQ Orbitrap mass spectrometer (see “Experimental procedures”). The phosphorylation site (Ser-149) is located in the conserved phosphoserine signature of phosphosugar mutases. Detection of the same phosphorylated peptide in all 10 spots of ManB (enhanced image section) suggests further posttranslational modifications that affect the isoelectric point of the ManB protein.

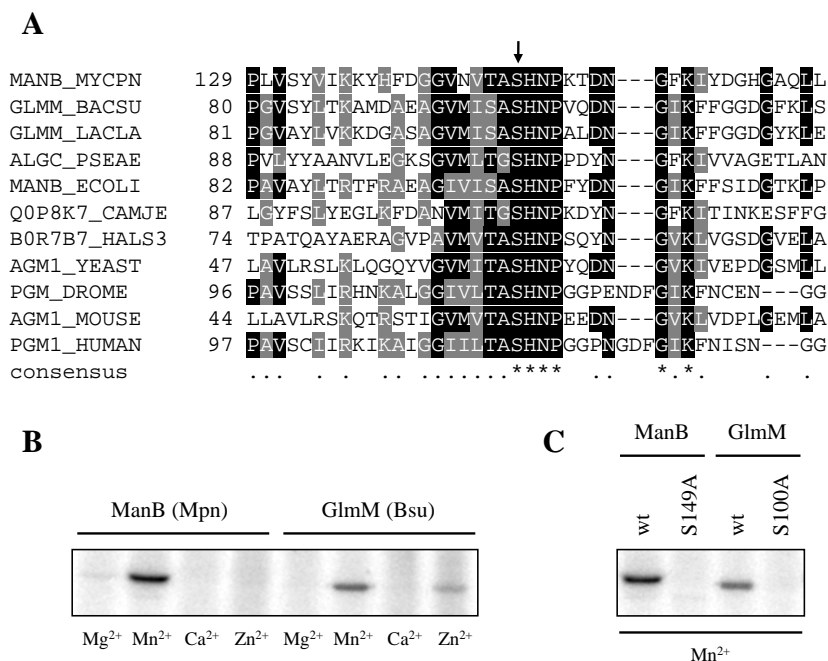


Fig. 13. Autophosphorylation on universally conserved serine residue in active site of phosphosugar mutases. (A) Multiple alignment of the conserved phosphoserine signature of phosphosugar mutases from all domains of life. Amino acids with similarities in at least two of the sequences are highlighted in gray, whereas amino acids that are identical in at least two of the sequences are depicted in a black background. The UniProtKB entry names of the aligned sequences are MANB_MYCPN (ManB, *M. pneumoniae*), GLMM_BACSU (GlmM; *B. subtilis*), GLMM_LACLA (GlmM; *L. lactis*), ALGC_PSEAE (AlgC; *P. aeruginosa*), MANB_ECOLI (ManB; *E. coli*), Q0P8K7_CAMJE (ManB; *C. jejuni*), B0R7B7_HALS3 (PMM1; *H. salinarum*), AGM1_YEAST (AGM1; *Saccharomyces cerevisiae*), PGM_DROME (PGM; *D. melanogaster*), AGM1_MOUSE (AGM1; *Mus musculus*), and PGM1_HUMAN (PGM1; *Homo sapiens*). The conserved active site phosphoserine is indicated by an arrow. (B) *M. pneumoniae* ManB and *B. subtilis* GlmM autophosphorylation assay in the presence of various divalent cations. About 5 µg of purified His₆-tagged ManB (lanes 1-4) or GlmM (lanes 4-8) were incubated in the presence of [³²P]ATP in an autophosphorylation assay (see “Experimental procedures”). Each reaction mixture was analyzed by SDS-PAGE and phosphorimaging analysis. Divalent cations (5 mM) used in the assays are indicated below the lanes. Bsu, *B. subtilis*; Mpn, *M. pneumoniae*. (C) Autophosphorylation assay of *M. pneumoniae* ManB (wild type (wt) and S149A) and *B. subtilis* GlmM (wild type and S100A) recombinant proteins. The four recombinant proteins were checked for autophosphorylation as described in (B). Autophosphorylation reactions were conducted in the presence of Mn²⁺ (5 mM) as divalent cation as it showed the strongest signal in (B).

The universal conservation of the phosphorylation site in phosphosugar mutases led us to conclude that this phosphorylation event might be essential. This hypothesis could not be addressed in *M. pneumoniae* because of the lack of genetic tools (Halbedel and Stülke, 2007). Therefore, we studied the role of this phosphorylation site for GlmM *B. subtilis*. The *glmM* gene and its variant encoding the S100A protein were established on multicopy plasmids in *B. subtilis*. In a strain expressing the wild type *glmM* gene from a plasmid, the chromosomal copy could be deleted by homologous recombination using a PCR fragment obtained by long flanking homology PCR. In contrast, a resistance cassette could not replace the chromosomal copy of *glmM* when the *glmM*-S100A allele was expressed from the plasmid. Thus, the phosphorylation of GlmM on Ser-100 seems to be essential for its function and thus for the survival of the bacteria.

Discussion

The analysis of the phosphoproteome of *M. pneumoniae* revealed substantial protein serine/threonine/tyrosine phosphorylation even in this minimal organism. We identified 63 phosphoproteins that account for nearly 10% of all proteins encoded by *M. pneumoniae*. This exceeds the percentage of phosphorylated proteins in other bacteria by far. For example, only 2.5% of all proteins of *B. subtilis* are known to be phosphorylated on a serine, threonine or tyrosine residue (Eymann *et al.*, 2007; Lévine *et al.*, 2006; Macek *et al.*, 2007). This raises the question whether protein phosphorylation is more common in *M. pneumoniae* than in other bacteria. It is tempting to speculate that the high rate of protein phosphorylation compensates for the obvious lack of transcriptional regulation in *M. pneumoniae*. However, this lack of regulation of gene expression allows the detection of the complete phosphoproteome in a single (or a few) experiment(s). Indeed, we detected about 500 CHAPS-soluble proteins that correspond to 80% of all 635 proteins that are in the pI range covered in this study (see supplemental Fig. S1). In other species with complex transcriptional regulation, only about 1,000 proteins are detectable under any specific condition, whereas the rest are required under specific growth conditions (Eymann *et al.*, 2004). For *B. subtilis* or *E. coli*, this corresponds to only 25% of all proteins. Thus, the higher coverage in our study is most probably due to the lack of transcription regulation in *M. pneumoniae*, but does not seem to reflect a higher impact of protein phosphorylation.

A striking feature of the phosphoproteomes of different bacteria is the phosphorylation of enzymes of the central metabolic pathways. In *M. pneumoniae*, metabolism is strongly reduced, and the major pathways are depicted in Fig. 11. The citric acid cycle and pathways of lipid, amino acid, and nucleotide metabolisms are absent in these bacteria. As in the other Firmicutes, most glycolytic enzymes are phosphorylated in *M. pneumoniae*. Unfortunately, the functions of these phosphorylations as well as the responsible kinases are so far unknown. It is interesting that all four subunits of the pyruvate dehydrogenase are phosphorylated in *M. pneumoniae*. In *B. subtilis*, there are different results concerning the pyruvate dehydrogenase. One study reports phosphorylation of PdhB (Macek *et al.*, 2007), whereas PdhC and PdhD were found to be phosphoproteins in another work (Eymann *et al.*, 2007). In contrast, none of the subunits is phosphorylated in *E. coli*, *Campylobacter jejuni*, and *L. lactis* (Macek *et al.*, 2008; Soufi *et al.*, 2008; Voisin *et al.*, 2007).

This work is the first global analysis of the effects of mutations in the complete set of annotated protein kinases on the phosphoproteome. We have shown that the HPr kinase has only one substrate, HPr. The phosphorylation of HPr on Ser-46 is a major signal to trigger carbon catabolite repression of catabolic genes and operons in *B. subtilis* and other Firmicutes (Görke and Stülke, 2008). If HPr(Ser-P) had the same function in *M. pneumoniae*, one would have expected major changes in the proteome of the *hprK* mutant as compared with the wild type strain. However, with the exception of HPr phosphorylation (see Fig. 10), no differences were detectable. This suggests that HPr phosphorylation on Ser-46 has a function different from that in the other bacteria. This conclusion is supported by three observations. First, HPr(Ser-P) acts as the cofactor for the pleiotropic transcription factor CcpA to cause catabolite repression. No protein similar to CcpA is encoded in the genome of any *Mycoplasma* species. Second, the phosphorylation of HPr on Ser-46 interferes with its participation in sugar transport due to the inhibition of enzyme I-dependent phosphorylation of His-15. This inhibition is relevant even in Gram-negative bacteria that also do not possess an equivalent of CcpA (Krausse *et al.*, 2009). However, in *M. pneumoniae*, these two phosphorylation events are not mutually exclusive (Halbedel and Stülke, 2005). Finally, although the activity of the HPr kinase of *B. subtilis* and most other bacteria is strongly controlled by the ATP and fructose 1,6-bisphosphate concentrations, the enzyme of *M. pneumoniae* is

constitutively active due to its high affinity to ATP (Merzbacher *et al.*, 2004). Thus, the phosphorylation of HPr on Ser-46 seems to serve other purposes in *M. pneumoniae*.

In addition to the HPr kinase, *M. pneumoniae* encodes only one protein kinase, PrkC. This kinase is implicated in a multitude of cellular functions in different bacteria, among them spore germination, virulence, and control of glycolysis (Kristich *et al.*, 2007; Lomas-Lopez *et al.*, 2007; Shah *et al.*, 2008). We found that PrkC has at least four targets in *M. pneumoniae*, the cell adhesion proteins HMW3 and P41, the cell surface protein MPN474, and the uncharacterized protein MPN256. These proteins are not phosphorylated in a *prkC* mutant, but their phosphorylation is enhanced if the protein phosphatase PrpC, the antagonist of PrkC, is not expressed (see Fig. 9). Moreover, HMW1 and P1, two very large proteins that were out of the detection window applied in this study, are likely to be phosphorylated by PrkC (Schmidl *et al.*, 2010). This suggests that PrkC might be required for cell adhesion in *M. pneumoniae*. Indeed, a *prkC* mutant strain is not capable of adherent growth and has lost toxicity to human host cells, most likely due to the defect in cell adhesion (Schmidl *et al.*, 2010). Thus, PrkC has a specific function in *M. pneumoniae* and phosphorylates a specific set of proteins.

As stated above, HPrK and PrkC are the only two annotated protein kinases in *M. pneumoniae*. However, they account for only five of 63 identified protein phosphorylation events. This suggests the existence of other, yet to be discovered protein kinases in *M. pneumoniae*. Alternatively, autophosphorylation might be more relevant than previously anticipated. Indeed, the only phosphorylation site that is universally conserved from archaea via bacteria such as *M. pneumoniae* to eukaryotes is the result of an autophosphorylation event in the catalytic site of phosphosugar mutases such as GlmM and ManB (Jolly *et al.*, 2000; Mengin-Lecreulx *et al.*, 1996; this work). This autophosphorylation is essential for the enzymatic activity of these enzymes, thus providing an explanation for the universal but highly exceptional conservation of the phosphorylation event at a conserved site. Interestingly, another ubiquitous protein, the heat shock protein DnaK (also called Hsp70) is also present as a phosphoprotein in all organisms that were studied so far. In *E. coli* and mycobacteria, DnaK is capable of autophosphorylating at a strongly conserved threonine residue (McCarty and Walker, 1991; Peake *et al.*, 1998; Preneta *et al.*, 2004; Zylicz *et al.*, 1983). This site is also present in the DnaK protein of *M. pneumoniae* (Thr-182), but it is not conserved in the

archaeal DnaK of *H. salinarum* (Aivaliotis *et al.*, 2009). It is therefore possible that DnaK autophosphorylates at a conserved site in bacteria and eukaryotes, whereas another phosphorylation mechanism occurs in archaea.

In this study, we unambiguously identified 16 phosphorylation sites. Phosphorylation on serine or threonine residues is equally distributed (eight phosphorylation sites each). Serine and threonine are also the predominant phosphorylation sites in other bacteria, and they are used with similar frequency as well (Macek *et al.*, 2008; Macek *et al.*, 2007; Soufi *et al.*, 2008). For eukaryotic phosphoproteins, it was shown that phosphorylations occur often in disordered regions and that the actual phosphorylation sites are not completely fixed in these regions (Iakoucheva *et al.*, 2004; Landry *et al.*, 2009). Indeed, seven of the 16 phosphorylation sites identified in this study are predicted to be localized in disordered regions (data not shown). An analysis of the regions surrounding the phosphorylation sites revealed the absence of defined amino acid sequence motifs. Rapid evolution and a corresponding lack of conservation of phosphorylation sites have recently also been observed for protein phosphorylation in yeast and other eukaryotes (Beltrao *et al.*, 2009; Holt *et al.*, 2009; Tan *et al.*, 2009). Taken together, these findings suggest that either the responsible protein kinases are quite nonspecific or that a large number of so far unidentified protein kinases exist in *M. pneumoniae*. An alternative explanation is offered by an analysis of the positions of the phosphorylation sites: Structural information is available for seven of the phosphoproteins with identified phosphorylation sites (see supplemental Fig. S2). All nine phosphorylation sites in these proteins are buried in the protein and are thus poorly accessible for protein kinases. This would suggest that these phosphorylation events are autophosphorylations as observed for ManB. Based on the structure of the *P. aeruginosa* phosphomannomutase/phosphoglucomutase (Regni *et al.*, 2002) (see Fig. 13), the site of autophosphorylation of ManB and GlmM is also buried in the inside of the protein.

The lack of conservation of phosphorylation sites was also observed in similar phosphoproteins from different bacteria. Only two strongly conserved phosphorylation sites were detected, Ser-46 in HPr and Ser-149 in ManB. Although HPr is phosphorylated by the ATP-dependent HPr kinase that is conserved in many bacteria (Steinhauer *et al.*, 2002; see Fig. 10), ManB is subject to autophosphorylation. Even among the glycolytic enzymes, only one identified phosphorylation site was conserved

between two species (Ser-36 in the pyruvate kinases from *B. subtilis* and *E. coli*). Because this latter site is conserved in *M. pneumoniae*, it is tempting to speculate that it is also phosphorylated in the Mollicutes. The observations reported in this work have important implications for the evolution of protein phosphorylation in bacteria: Protein phosphorylation events seem to be highly specific for each individual bacterial species; even among members of one bacterial phylum such as the Firmicutes, there is little conservation of protein phosphorylation. Moreover, one protein kinase may phosphorylate distinct sets of proteins in the different species. Finally, there may be a large number of protein kinases that have so far escaped discovery, and these kinases are likely to be specific for small groups of bacteria. In conclusion, protein phosphorylation may be one of the major features in the adaptation of bacteria to their individual ecological niche.

Acknowledgments

We are grateful to Julia Busse for excellent technical assistance. Robert Hertel is acknowledged for help with some experiments. This work was supported by grants of the Deutsche Forschungsgemeinschaft and the Fonds der Chemischen Industrie (to D. B., M. H., and J. S.). S. R. S. was supported by the Studienstiftung des Deutschen Volkes.

Supplemental material

Tab. S3. Primers used in this study.

Primer	Sequence (5'→3') ^{ab}	Mutation	Resulting plasmid
NP108	AAAGGATCCCTCACTTATTTAAAGGAGGAAA CAATCATGGGCAAGTATTTTGGAACAGACG	None	pGP400, pGP1403
NP109	TTTGTCTGACCTATCACTCTAATCCCATTTCTG ACCGG	None	pGP400, pGP1401, pGP1403, pGP1405
NP110	GGCTATTCTCCGGAGCAGCCGATTGTCA	None	-
NP111	CAGGAACGGACGACCAAAAGTTTTCCCG	None	-
NP112	CCTATCACCTCAAATGGTTCGCTGTAAAGGC CAGCTCAGGTGTAAGCTC	None	-
NP113	CCGAGCGCCTACGAGGAATTTGTATCGAGCG AAGACGAAAGAGCTGTGCGA	None	-
NP114	CATCGCCATCGCATCAGATGCTACGACGT	None	-
NP115	TATAAGACGCACGTGTAATCACGTCACCATC	None	-
NP116	P_GCAGAGGCGGGCGTCATGATTTCCGCTGC CCATAACCCAGTGCAGGATAACGGCATCAA	T298G	pGP1403, pGP1405
NP117	AAAGGATCCATGGGCAAGTATTTTGGAACAG ACG	None	pGP1401, pGP1405
spec-fwd (kan)	CAGCGAACCATTTGAGGTGATAGGGACTGGC TCGCTAATAACGTAACGTGACTGGCAAGAG	None	-
spec-rev (kan)	CGATACAAATTCCTCGTAGGCGCTCGGCGTA GCGAGGGCAAGGGTTTATTGTTTTCTAAAAT CTG	None	-
SH29	ATGAGTGAGCTAACTCACAG	None	-
SH30	CAATACGCAAACCGCCTC	None	-
SS107	AAAGGATCCATGAACAGTAACGCATACTTGG AAGC	None	pGP656-pGP658
SS108	TATACTGCAGCTAAGCTTTATCGAGGTTGAG CAATC	None	pGP656-pGP658
SS109	P_GAAAGTAAGGATACCTGGGAGTTAGCGCG	A846G	pGP657
SS110	P_CTTTGCATTGCCGAATGGAATCCGCAA C	A936G	pGP657
SS111	P_GATTACTATAACTGGACGGTACCACACAC CATTC	A1356G	pGP657
SS112	P_CGGTGAATGTCACTGCTCATAATCCTA AAACC	A445G, G446C	pGP658

Tab. S3. Continued.

Primer	Sequence (5'→3') ^{ab}	Mutation	Resulting plasmid
SS113	CAAGGCCACAATTGATTATGTCTTTG	None	-
SS114	GGTAACTTAGTGGAAGTCCACTTAAC	None	-

^a Restriction sites are underlined.

^b The “P” at the 5' end of primer sequences indicates phosphorylation.

Tab. S4. Plasmids used for analysis of phosphosugar mutases.

Plasmid	Relevant characteristics	Used restriction sites	Reference
pBQ200	Allows expression of proteins in <i>B. subtilis</i>	-	Martin-Verstraete <i>et al.</i> (1994)
pGP400	pBQ200- <i>glmM</i>	<i>Bam</i> HI + <i>Sal</i> I	This work
pGP656	pWH844- <i>manB</i>	<i>Bam</i> HI + <i>Pst</i> I	This work
pGP657	pWH844- <i>manB</i> ^a	<i>Bam</i> HI + <i>Pst</i> I	This work
pGP658	pWH844- <i>manB</i> (S149A)	<i>Bam</i> HI + <i>Pst</i> I	This work
pGP1401	pWH844- <i>glmM</i>	<i>Bam</i> HI + <i>Sal</i> I	This work
pGP1403	pBQ200- <i>glmM</i> (S100A)	<i>Bam</i> HI + <i>Sal</i> I	This work
pGP1405	pWH844- <i>glmM</i> (S100A)	<i>Bam</i> HI + <i>Sal</i> I	This work
pWH844	Allows overexpression of N-terminal His ₆ -tag fusion proteins in <i>E. coli</i> DH5α	-	Schirmer <i>et al.</i> (1997)

^a The three TGA opal codons in the wild type *manB* gene are mutated to TGG.

Tab. S5. Complete list of phosphospots identified from *M. pneumoniae* two-dimensional gels.

For general overview, see Table 4. pS, phosphoserine; pT, phosphothreonine.

#	Spot	Protein name	Locus name	UniProtKB accession number	Protein function	Molecular weight (Da)	Isoelectric point (pI)	Protein identification probability (%)	Number of unique peptides	Coverage (%)	Phosphorylation site	Phosphopeptide sequence	Experiment ^a
1	AckA-1	AckA	MPN533	P75245	Acetate kinase	43672.68	8.05	100.00	23	58.97			1, 2, 3, 4
2	AckA-2	AckA	MPN533	P75245	Acetate kinase	43672.68	8.05	100.00	22	55.38			1, 2, 3, 4
3	AckA-3	AckA	MPN533	P75245	Acetate kinase	43672.68	8.05	100.00	18	50.77			1, 2, 3, 4
4	AckA-4	AckA	MPN533	P75245	Acetate kinase	43672.68	8.05	100.00	16	43.85			1, 2, 3, 4
5	[AtpA Pgm]	AtpA	MPN600	Q50329	ATP synthase subunit α	57339.01	6.14	100.00	19	41.12			1, 2, 3, 4
		Pgm	MPN628	P75167	Phosphoglycerate mutase	56339.53	6.08	100.00	14	36.22			1, 2, 3, 4
6	AtpD-1	AtpD	MPN598	Q50331	ATP synthase subunit β	52204.62	5.36	100.00	28	86.32			1, 2, 3, 4
7	AtpD-2	AtpD	MPN598	Q50331	ATP synthase subunit β	52204.62	5.36	100.00	22	71.79			1, 2, 3, 4
8	DeoC	DeoC	MPN063	P09924	Deoxyribose-phosphate aldolase	24861.89	8.34	100.00	9	53.13			1, 2, 3, 4
9	[DoeD TpiA]	DeoD	MPN062	P75053	Purine-nucleoside phosphorylase	26266.66	6.78	100.00	15	77.73			1, 2, 3, 4
		TpiA	MPN629	P78010	Triosephosphate isomerase	26941.33	7.34	100.00	11	55.33			1, 2, 3, 4
10	DnaK-1	DnaK	MPN434	P75344	Chaperone protein	65058.30	5.28	100.00	34	51.09			1, 2, 3, 4
11	DnaK-2	DnaK	MPN434	P75344	Chaperone protein	65058.30	5.28	100.00	18	35.97			1, 2, 3, 4
12	DnaN	DnaN	MPN001	Q50313	DNA polymerase III subunit β	43829.01	5.74	100.00	23	59.74			1, 2, 3, 4
13	[DnaN PdhA]	DnaN	MPN001	Q50313	DNA polymerase III subunit β	43829.01	5.74	100.00	28	76.05			1, 2, 3, 4
		PdhA	MPN393	P75390	Pyruvate dehydrogenase E1 component subunit α	40568.44	6.22	100.00	10	30.45			1, 2, 3, 4
14	EI-1	EI	MPN627	P75168	Phosphotransferase system enzyme I	63909.70	7.92	100.00	31	47.03			1, 2, 3, 4
15	EI-2	EI	MPN627	P75168	Phosphotransferase system enzyme I	63909.70	7.92	100.00	12	27.62			1, 2, 3, 4
16	Eno-1	Eno	MPN606	P75189	Enolase	49197.47	6.11	100.00	24	64.69			1, 2, 3, 4
17	Eno-2	Eno	MPN606	P75189	Enolase	49197.47	6.11	100.00	25	70.18			1, 2, 3, 4
18	Eno-3	Eno	MPN606	P75189	Enolase	49197.47	6.11	100.00	20	60.96			1, 2, 3, 4
19	Eno-4	Eno	MPN606	P75189	Enolase	49197.47	6.11	100.00	17	55.26			1, 2, 3, 4
20	Fba	Fba	MPN025	P75089	Fructose-bisphosphate aldolase	31049.17	6.44	100.00	6	23.26			1, 2, 3, 4
21	[Fba Soj]	Fba	MPN025	P75089	Fructose-bisphosphate aldolase	31049.17	6.44	100.00	12	53.82			1, 2, 3, 4
		Soj	MPN688	Q50314	ParA family protein	30061.83	7.26	100.00	8	27.78			1, 2, 3, 4
22	Frr-1	Frr	MPN636	P75161	Ribosome-recycling factor	21653.51	8.87	100.00	12	63.04			1, 2, 3, 4

Tab. S5. Continued.

#	Spot	Protein name	Locus name	UniProtKB accession number	Protein function	Molecular weight (Da)	Isoelectric point (pI)	Protein identification probability (%)	Number of unique peptides	Coverage (%)	Phosphorylation site	Phosphopeptide sequence	Experiment ^a
23	Frr-2	Frr	MPN636	P75161	Ribosome-recycling factor	21653.51	8.87	100.00	10	62.50			1, 2, 3, 4
24	FusA-1	FusA	MPN227	P75544	Elongation factor G	76451.41	5.43	100.00	24	53.49			1, 2, 3, 4
25	FusA-2	FusA	MPN227	P75544	Elongation factor G	76451.41	5.43	100.00	37	71.22			1, 2, 3, 4
26	FusA-3	FusA	MPN227	P75544	Elongation factor G	76451.41	5.43	100.00	45	76.02			1, 2, 3, 4
27	GapA-1	GapA	MPN430	P75358	Glyceraldehyde-3-phosphate dehydrogenase	36782.40	8.85	100.00	20	68.84			1, 2, 3, 4
28	GapA-2	GapA	MPN430	P75358	Glyceraldehyde-3-phosphate dehydrogenase	36782.40	8.85	100.00	17	49.85			1, 2, 3, 4
29	[GapA Xdj1]-1	GapA	MPN430	P75358	Glyceraldehyde-3-phosphate dehydrogenase	36782.40	8.85	100.00	35	88.72	S245	VPVLTGpSIVELCVALEK	1, 2, 3, 4
		Xdj1	MPN002	Q50312	DnaJ-like protein	37109.23	9.44	100.00	13	36.25			1, 2, 3, 4
30	[GapA Xdj1]-2	GapA	MPN430	P75358	Glyceraldehyde-3-phosphate dehydrogenase	36782.40	8.85	100.00	27	86.05	S245	VPVLTGpSIVELCVALEK	1, 2, 3, 4
		Xdj1	MPN002	Q50312	DnaJ-like protein	37109.23	9.44	100.00	11	40.78			1, 2, 3, 4
31	GlpK-1	GlpK	MPN050	P75064	Glycerol kinase	56555.27	8.72	100.00	16	47.83			1, 2, 3, 4
32	GlpK-2	GlpK	MPN050	P75064	Glycerol kinase	56555.27	8.72	100.00	22	66.34			1, 2, 3, 4
33	GlpQ	GlpQ	MPN420	P75367	Glycerophosphoryldiester phosphodiesterase	28354.79	6.36	100.00	8	31.54			1, 2, 3, 4
34	GlyA	GlyA	MPN576	P78011	Serine hydroxymethyltransferase	45237.55	9.26	100.00	15	36.70			1, 2, 3, 4
35	GroL-1	GroL	MPN573	P78012	60-kDa chaperonin	58051.10	5.48	100.00	52	83.98			1, 2, 3, 4
36	GroL-2	GroL	MPN573	P78012	60-kDa chaperonin	58051.10	5.48	100.00	35	74.03			1, 2, 3, 4
37	GroS	GroS	MPN574	P75205	10-kDa chaperonin	12610.67	9.46	100.00	4	35.34			1, 2, 3, 4
38	GrpE	GrpE	MPN120	P78017	Heat shock protein	24690.28	8.81	100.00	12	46.54			1, 2, 3, 4
39	HMW3	HMW3	MPN452	Q50360	Cytadherence high molecular weight protein 3	73676.4	4.53	100.00	20	37.95			2
40	Ldh-1	Ldh	MPN674	P78007	L-Lactate dehydrogenase	33866.91	8.76	100.00	24	79.49			1, 2, 3, 4
41	Ldh-2	Ldh	MPN674	P78007	L-Lactate dehydrogenase	33866.91	8.76	100.00	21	75.64			1, 2, 3, 4
42	[LplA FtsY]	LplA	MPN389	P75394	Lipoate-protein ligase A	39169.02	6.14	100.00	25	67.26			1, 2, 3, 4
		FtsY	MPN425	P75362	Cell division protein homolog	38751.53	7.16	100.00	11	47.70			1, 2, 3, 4

Tab. S5. Continued.

#	Spot	Protein name	Locus name	UniProtKB accession number	Protein function	Molecular weight (Da)	Isoelectric point (pI)	Protein identification probability (%)	Number of unique peptides	Coverage (%)	Phosphorylation site	Phosphopeptide sequence	Experiment ^a
43	ManB-1	ManB	MPN066	P75050	Phosphomannomutase/ phosphoglucomutase	63175.24	8.39	100.00	10	18.23	S149	YHFDGGVNVTApSHNPK	1, 2, 3, 4
44	ManB-2	ManB	MPN066	P75050	Phosphomannomutase/ phosphoglucomutase	63175.24	8.39	100.00	20	52.17	S149	YHFDGGVNVTApSHNPK	1, 2, 3, 4
45	ManB-3	ManB	MPN066	P75050	Phosphomannomutase/ phosphoglucomutase	63175.24	8.39	100.00	23	54.69	S149	KYHFDGGVNVTApSHNPK	1, 2, 3, 4
46	ManB-4	ManB	MPN066	P75050	Phosphomannomutase/ phosphoglucomutase	63175.24	8.39	100.00	32	59.57	S149	YHFDGGVNVTApSHNPK	1, 2, 3, 4
47	ManB-5	ManB	MPN066	P75050	Phosphomannomutase/ phosphoglucomutase	63175.24	8.39	100.00	25	60.47	S149	YHFDGGVNVTApSHNPK	1, 2, 3, 4
48	ManB-6	ManB	MPN066	P75050	Phosphomannomutase/ phosphoglucomutase	63175.24	8.39	100.00	22	66.61	S149	YHFDGGVNVTApSHNPK	1, 2, 3, 4
49	ManB-7	ManB	MPN066	P75050	Phosphomannomutase/ phosphoglucomutase	63175.24	8.39	100.00	24	66.25	S149	YHFDGGVNVTApSHNPK	1, 2, 3, 4
50	ManB-8	ManB	MPN066	P75050	Phosphomannomutase/ phosphoglucomutase	63175.24	8.39	100.00	21	58.12	S149	YHFDGGVNVTApSHNPK	1, 2, 3, 4
51	ManB-9	ManB	MPN066	P75050	Phosphomannomutase/ phosphoglucomutase	63175.24	8.39	100.00	26	66.25	S149	YHFDGGVNVTApSHNPK	1, 2, 3, 4
52	ManB-10	ManB	MPN066	P75050	Phosphomannomutase/ phosphoglucomutase	63175.24	8.39	100.00	36	58.12	S149	YHFDGGVNVTApSHNPK	1, 2, 3, 4
53	MPN256-1	MPN256	MPN256	P75518	Uncharacterized protein	25722.9	4.18	100.00	14	67.71	T200	FIDELDQIpTK	2
54	MPN256-2	MPN256	MPN256	P75518	Uncharacterized protein	25722.9	4.18	100.00	7	48.88			2
55	MPN280-1	MPN280	MPN280	P75497	Ribonuclease J	64045.33	7.57	100.00	18	44.29			1, 2, 3, 4
56	MPN280-2	MPN280	MPN280	P75497	Ribonuclease J	64045.33	7.57	100.00	16	39.72			1, 2, 3, 4
57	MPN295-1	MPN295	MPN295	P75482	Uncharacterized protein	25684.16	8.08	100.00	16	60.91			1, 2, 3, 4
58	MPN295-2	MPN295	MPN295	P75482	Uncharacterized protein	25684.16	8.08	100.00	22	73.18	S63	YGPECEKSFLSLQpSK	1, 2, 3, 4
59	MPN349	MPN349	MPN349	P75429	Uncharacterized protein	31411.30	8.83	100.00	12	52.67			1, 2, 3, 4
60	MPN474	MPN474	MPN474	P75310	Coiled coil surface protein	118006.4	4.81	100.00	44	61.08	T773	QNNEELpTDKCSNIQNELHDLNR	2
61	MPN517	MPN517	MPN517	P75270	Reductase homolog	18856.85	7.26	100.00	7	42.17			1, 2, 3, 4

Tab. S5. Continued.

#	Spot	Protein name	Locus name	UniProtKB accession number	Protein function	Molecular weight (Da)	Isoelectric point (pI)	Protein identification probability (%)	Number of unique peptides	Coverage (%)	Phosphorylation site	Phosphopeptide sequence	Experiment ^a
62	MPN547	MPN547	MPN547	P75231	Dihydroxyacetone kinase	62398.49	8.20	100.00	39	75.63			1, 2, 3, 4
63	MPN555-1	MPN555	MPN555	P75223	Uncharacterized protein	22419.68	5.51	100.00	7	41.97			1, 2, 3, 4
64	MPN555-2	MPN555	MPN555	P75223	Uncharacterized protein	22419.68	5.51	100.00	11	55.44			1, 2, 3, 4
65	MPN625	MPN625	MPN625	P75170	Osmotical inducible protein C-like protein	15458.91	6.60	100.00	4	31.21			1, 2, 3, 4
66	MPN638-1	MPN638	MPN638	P75159	Putative type I restriction enzyme specificity protein	42623.25	8.51	100.00	24	66.67			1, 2, 3, 4
67	MPN638-2	MPN638	MPN638	P75159	Putative type I restriction enzyme specificity protein	42623.25	8.51	100.00	15	43.47			1, 2, 3, 4
68	MPN677	MPN677	MPN677	P75115	Uncharacterized protein	50554.18	8.89	100.00	12	36.94			1, 2, 3, 4
69	NrdE-1	NrdE	MPN324	P78027	Ribonucleoside-diphosphate reductase subunit α	82322.96	6.66	100.00	66	69.90	T159	FQPApTPTFLNAGR	1, 2, 3, 4
70	NrdE-2	NrdE	MPN324	P78027	Ribonucleoside-diphosphate reductase subunit α	82322.96	6.66	100.00	54	61.86	S412	VGNDIpSCNLGSLNIAK	1, 2, 3, 4
71	NrdE-3	NrdE	MPN324	P78027	Ribonucleoside-diphosphate reductase subunit α	82322.96	6.66	100.00	17	23.02			1, 2, 3, 4
72	NrdF	NrdF	MPN322	P75461	Ribonucleoside-diphosphate reductase subunit β	39388.04	5.36	100.00	19	71.98			1, 2, 3, 4
73	Nox	Nox	MPN394	P75389	NADH oxidase	52841.36	6.70	100.00	11	29.85			1, 2, 3, 4
74	NusA-1	NusA	MPN154	P75591	Transcription elongation factor	60235.03	5.77	100.00	43	80.00	S503	PVVVKPpSVFSITVEADDSK	1, 2, 3, 4
75	NusA-2	NusA	MPN154	P75591	Transcription elongation factor	60235.03	5.77	100.00	19	48.15			1, 2, 3, 4
76	P41	P41	MPN311	P75470	Adhesin-related protein	40555.6	4.64	100.00	9	42.58	T223	TNNSIQLEAEIQIPpTTHIK	2
77	PdhA	PdhA	MPN393	P75390	Pyruvate dehydrogenase E1 component subunit α	40568.44	6.22	100.00	19	53.63			1, 2, 3, 4
78	[PdhA Pgk]	PdhA	MPN393	P75390	Pyruvate dehydrogenase E1 component subunit α	40568.44	6.22	100.00	14	38.27	S205	TKLEpSAVSDLSTK	1, 2, 3, 4
		Pgk	MPN429	P78018	Phosphoglycerate kinase	44184.27	7.26	100.00	9	26.65			1, 2, 3, 4

Tab. S5. Continued.

#	Spot	Protein name	Locus name	UniProtKB accession number	Protein function	Molecular weight (Da)	Isoelectric point (pI)	Protein identification probability (%)	Number of unique peptides	Coverage (%)	Phosphorylation site	Phosphopeptide sequence	Experiment ^a
79	[PdhB Pta]-1	PdhB	MPN392	P75391	Pyruvate dehydrogenase E1 component subunit β	35891.67	6.54	100.00	15	57.19			1, 2, 3, 4
		Pta	MPN428	P75359	Phosphotransacetylase	35196.23	7.16	100.00	9	38.75			1, 2, 3, 4
80	[PdhB Pta]-2	PdhB	MPN392	P75391	Pyruvate dehydrogenase E1 component subunit β	35891.67	6.54	100.00	14	50.76			1, 2, 3, 4
		Pta	MPN428	P75359	Phosphotransacetylase	35196.23	7.16	100.00	7	27.50			1, 2, 3, 4
81	PdhC-1	PdhC	MPN391	P75392	Pyruvate dehydrogenase E2 component	42370.45	5.43	100.00	13	37.06			1, 2, 3, 4
82	PdhC-2	PdhC	MPN391	P75392	Pyruvate dehydrogenase E2 component	42370.45	5.43	100.00	15	37.06			1, 2, 3, 4
83	PdhC-3	PdhC	MPN391	P75392	Pyruvate dehydrogenase E2 component	42370.45	5.43	100.00	11	33.58			1, 2, 3, 4
84	PdhC-4	PdhC	MPN391	P75392	Pyruvate dehydrogenase E2 component	42370.45	5.43	100.00	8	18.41			1, 2, 3, 4
85	PdhD-1	PdhD	MPN390	P75393	Pyruvate dehydrogenase E3 component	49406.02	8.14	100.00	15	47.05			1, 2, 3, 4
86	PdhD-2	PdhD	MPN390	P75393	Pyruvate dehydrogenase E3 component	49406.02	8.14	100.00	11	38.29			1, 2, 3, 4
87	PepA-1	PepA	MPN572	P75206	Cytosol aminopeptidase	48758.12	8.23	100.00	38	75.73	S249 T420	YDMSGAAIVCpSTVLALAK EGVPLIHCDIASpTASIQDLGGVLR	1, 2, 3, 4
88	PepA-2	PepA	MPN572	P75206	Cytosol aminopeptidase	48758.12	8.23	100.00	22	56.18			1, 2, 3, 4
89	PepA-3	PepA	MPN572	P75206	Cytosol aminopeptidase	48758.12	8.23	100.00	18	49.44			1, 2, 3, 4
90	PepP-1	PepP	MPN470	P75313	Xaa-Pro aminopeptidase	39598.88	8.81	100.00	34	88.70	T317	LLCENAVIpTIEPGIYIPSVGGIR	1, 2, 3, 4
91	PepP-2	PepP	MPN470	P75313	Xaa-Pro aminopeptidase	39598.88	8.81	100.00	23	64.12			1, 2, 3, 4
92	PfkA	PfkA	MPN302	P75476	Phosphofructokinase	35966.53	7.30	100.00	6	24.39			1, 2, 3, 4
93	Ppa	Ppa	MPN528	P75250	Inorganic pyrophosphatase	21355.08	5.38	100.00	8	35.87			1, 2, 3, 4
94	Pta	Pta	MPN428	P75359	Phosphotransacetylase	35196.23	7.16	100.00	16	57.19			1, 2, 3, 4
95	[Pta PdhB]	Pta	MPN428	P75359	Phosphotransacetylase	35196.23	7.16	100.00	16	60.63			1, 2, 3, 4
		PdhB	MPN392	P75391	Pyruvate dehydrogenase E1 component subunit β	35891.67	6.54	100.00	11	47.71			1, 2, 3, 4
96	Pth	Pth	MPN221	P78034	Peptidyl-tRNA hydrolase	21403.30	9.91	100.00	6	38.83			1, 2, 3, 4
97	Pyk	Pyk	MPN303	P78031	Pyruvate kinase	57232.04	9.45	100.00	28	63.19			1, 2, 3, 4
98	RpoE	RpoE	MPN024	P75090	RNA polymerase subunit δ	17395.3	4.17	100.00	11	70.55	[S87 or T93]	Ip[SQAMFVT]KEIFEEGYEDLSNK	2
81	PdhC-1	PdhC	MPN391	P75392	Pyruvate dehydrogenase E2 component	42370.45	5.43	100.00	13	37.06			1, 2, 3, 4
99	Tig-1	Tig	MPN331	P75454	Trigger factor	51321.25	6.08	100.00	27	66.67			1, 2, 3, 4

Tab. S5. Continued.

#	Spot	Protein name	Locus name	UniProtKB accession number	Protein function	Molecular weight (Da)	Isoelectric point (pI)	Protein identification probability (%)	Number of unique peptides	Coverage (%)	Phosphorylation site	Phosphopeptide sequence	Experiment ^a
100	Tig-2	Tig	MPN331	P75454	Trigger factor	51321.25	6.08	100.00	25	52.03			1, 2, 3, 4
101	Tig-3	Tig	MPN331	P75454	Trigger factor	51321.25	6.08	100.00	16	30.18			1, 2, 3, 4
102	TopA	TopA	MPN261	P78032	DNA topoisomerase I	81914.21	9.52	100.00	48	64.84	S426	TVApSLMADCKK	1, 2, 3, 4
103	TpiA	TpiA	MPN629	P78010	Triose-phosphate isomerase	26941.33	7.34	100.00	12	56.97			1, 2, 3, 4
104	Tkt-1	Tkt	MPN082	P75611	Transketolase	72332.86	7.20	100.00	25	51.23			1, 2, 3, 4
105	Tkt-2	Tkt	MPN082	P75611	Transketolase	72332.86	7.20	100.00	20	37.35			1, 2, 3, 4
106	Tkt-3	Tkt	MPN082	P75611	Transketolase	72332.86	7.20	100.00	15	38.12			1, 2, 3, 4
107	Tuf-1	Tuf	MPN665	P23568	Elongation factor TU	43122.32	6.04	100.00	30	65.23	T383	EGGRpTVGAGSVTEVLE	1, 2, 3, 4
108	Tuf-2	Tuf	MPN665	P23568	Elongation factor TU	43122.32	6.04	100.00	24	64.97	T383	EGGRpTVGAGSVTEVLE	1, 2, 3, 4
109	Tuf-3	Tuf	MPN665	P23568	Elongation factor TU	43122.32	6.04	100.00	19	47.21	T383	EGGRpTVGAGSVTEVLE	1, 2, 3, 4
110	Tuf-4	Tuf	MPN665	P23568	Elongation factor TU	43122.32	6.04	100.00	7	22.08	T383	EGGRpTVGAGSVTEVLE	1, 2, 3, 4
111	[UlaB HPr]	UlaB	MPN495	Q9EXD8	Ascorbate-specific phosphotransferase enzyme IIB component	10320.41	8.61	100.00	4	55.79			1, 2, 3, 4
		HPr	MPN053	P75061	Phosphocarrier protein	9489.23	9.22	100.00	3	30.68			1, 2, 3

^a Phosphospot detected in different *M. pneumoniae* strains. 1, wild type; 2, *prpC*::Tn mutant; 3, *prkC*::Tn mutant; 4, *hprK*::Tn mutant.

Tab. S6. List of phosphopeptides.

For general overview, see Table 4. oM, oxidised methionine; pS, phosphoserine; pT, phosphothreonine.

#	Spot	Protein name	Locus name	UniProtKB accession number	Phosphopeptide sequence	Start aa	Stop aa	SEQUEST Xcorr	SEQUEST deltaCn	Observed m/z	Peptide mass (AMU)	Charge	Peptide identification probability (%)	Position	Mod. aa
1	[GapA Xdj1]-1	GapA	MPN430	P75358	VPVLTGpSIVELCVALEK	239	255	2.1403	0.7004	925.4895	1848.9634	2	95.00	245	S
2	[GapA Xdj1]-2	GapA	MPN430	P75358	VPVLTGpSIVELCVALEK	239	255	2.8309	0.7830	925.4899	1848.9641	2	95.00	245	S
3	ManB-1	ManB	MPN066	P75050	YHFDGGVNVTApSHNPK	138	153	3.4808	0.7661	608.2682	1821.7811	3	95.00	149	S
4	ManB-2	ManB	MPN066	P75050	YHFDGGVNVTApSHNPK	138	153	3.4107	0.8276	608.2686	1821.7824	3	95.00	149	S
5	ManB-3	ManB	MPN066	P75050	KYHFDGGVNVTApSHNPK	137	153	4.1654	0.4348	488.4794	1949.8865	4	95.00	149	S
6	ManB-4	ManB	MPN066	P75050	YHFDGGVNVTApSHNPK	138	153	3.0082	0.7313	608.2675	1821.7791	3	95.00	149	S
7	ManB-5	ManB	MPN066	P75050	YHFDGGVNVTApSHNPK	138	153	3.3379	0.7312	608.2715	1821.7910	3	95.00	149	S
8	ManB-6	ManB	MPN066	P75050	YHFDGGVNVTApSHNPK	138	153	3.5166	0.7365	608.2682	1821.7811	3	95.00	149	S
9	ManB-7	ManB	MPN066	P75050	YHFDGGVNVTApSHNPK	138	153	3.4299	0.7130	608.2709	1821.7891	3	95.00	149	S
10	ManB-8	ManB	MPN066	P75050	YHFDGGVNVTApSHNPK	138	153	3.5219	0.6994	608.2709	1821.7893	3	95.00	149	S
11	ManB-9	ManB	MPN066	P75050	YHFDGGVNVTApSHNPK	138	153	3.1959	0.7766	608.2673	1821.7783	3	95.00	149	S
12	ManB-10	ManB	MPN066	P75050	YHFDGGVNVTApSHNPK	138	153	3.2742	0.7367	608.2702	1821.7871	3	95.00	149	S
13	MPN256-1	MPN256	MPN256	P75518	FIDELDlQpTK	192	201	1.8676	0.4646	651.3056	1300.5955	2	95.00	200	T
14	MPN295-2	MPN295	MPN295	P75482	YGPECEKSFLSLQpSK	50	64	1.8583	0.6774	898.4016	1794.7875	2	95.00	63	S
15	MPN474	MPN474	MPN474	P75310	QNNNEELpTDKCSNIQNELHDLNR	767	788	3.8806	0.6714	903.0639	2706.1682	3	95.00	773	T
16	NrdE-1	NrdE	MPN324	P78027	FQPApTPTFLNAGR	155	167	1.9105	0.6332	750.3589	1498.7022	2	95.00	159	T
17	NrdE-2	NrdE	MPN324	P78027	VGNDlPSCNLGSLNIAK	407	422	2.1525	0.3036	849.3960	1696.7763	2	95.00	412	S
18	NusA-1	NusA	MPN154	P75591	PVVVKpSVFSITVEADDSK	497	515	3.2040	0.6335	709.3649	2125.0713	3	95.00	503	S
19	P41	P41	MPN311	P75470	TNNSIQLEAEIQlPpTTHIK	208	227	3.8887	0.7207	786.7265	2357.1560	3	95.00	223	T
20	[PdhA Pgk]	PdhA	MPN393	P75390	TKLEpSAVSDLSK	201	213	3.4406	0.2305	729.8603	1457.7050	2	95.00	205	S
21	PepA-1	PepA	MPN572	P75206	YDoMSGAAIVCpSTVLALAK	239	256	3.2690	0.6324	954.9456	1907.8756	2	95.00	249	S
22	PepA-1	PepA	MPN572	P75206	EGVPLIHCDIASpTASIQDLGGQVLVR	408	433	2.1490	0.3303	924.4661	2770.3749	3	95.00	420	T
23	PepP-1	PepP	MPN470	P75313	LLCENAVlPTIEPGIYIPSVGGIR	309	331	2.7570	0.7431	627.5862	2506.3136	4	95.00	317	T
24	RpoE	RpoE	MPN024	P75090	lPQAoMFVTKEIFEEGYEDLSNK	86	107	4.5815	0.6970	892.0717	2673.1917	3	95.00	87	S
25	RpoE	RpoE	MPN024	P75090	ISQAMFVpTKEIFEEGYEDLSNK	86	107	4.9395	0.7017	886.7402	2657.1970	3	95.00	93	T
26	TopA	TopA	MPN261	P78032	TVApSLMADCKK	423	433	1.9215	0.5958	623.7813	1245.5470	2	95.00	426	S
27	Tuf-1	Tuf	MPN665	P23568	EGGRpTVGAGSVTEVLE	379	394	3.4741	0.7097	820.8821	1639.7486	2	95.00	383	T

Tab. S6. Continued.

#	Spot	Protein name	Locus name	UniProtKB accession number	Phosphopeptide sequence	Start aa	Stop aa	SEQUEST Xcorr	SEQUEST deltaCn	Observed m/z	Peptide mass (AMU)	Charge	Peptide identification probability (%)	Position	Mod. aa
28	Tuf-2	Tuf	MPN665	P23568	EGGRpTVGAGSVTEVLE	379	394	3.2175	0.7339	820.8817	1639.7478	2	95.00	383	T
29	Tuf-3	Tuf	MPN665	P23568	EGGRpTVGAGSVTEVLE	379	394	2.9993	0.6668	820.8795	1639.7433	2	95.00	383	T
30	Tuf-4	Tuf	MPN665	P23568	EGGRpTVGAGSVTEVLE	379	394	3.2929	0.7727	820.8883	1639.7609	2	95.00	383	T

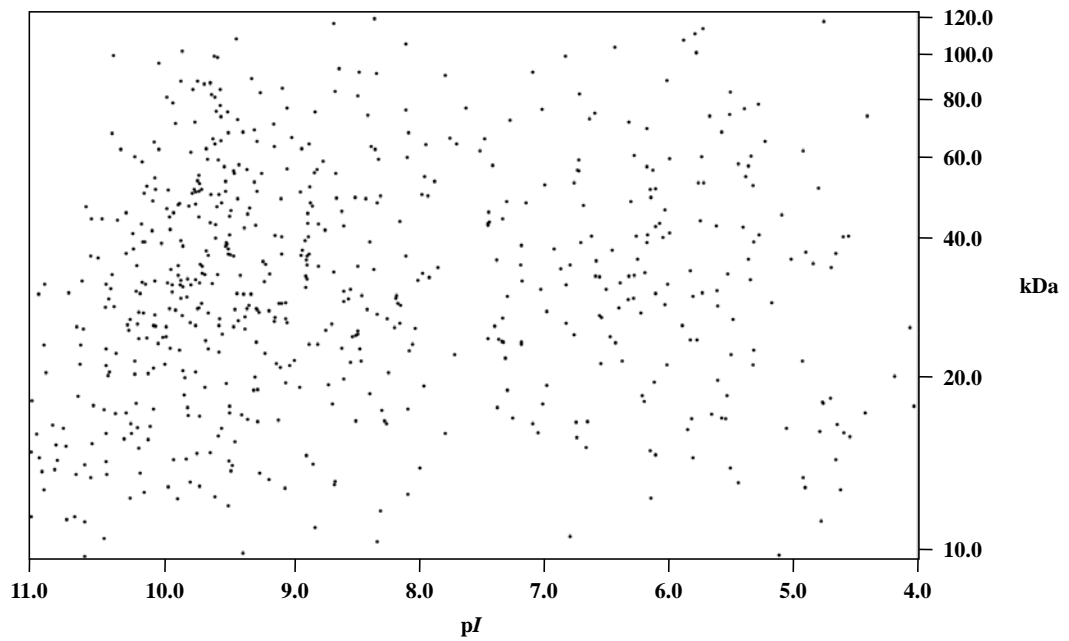
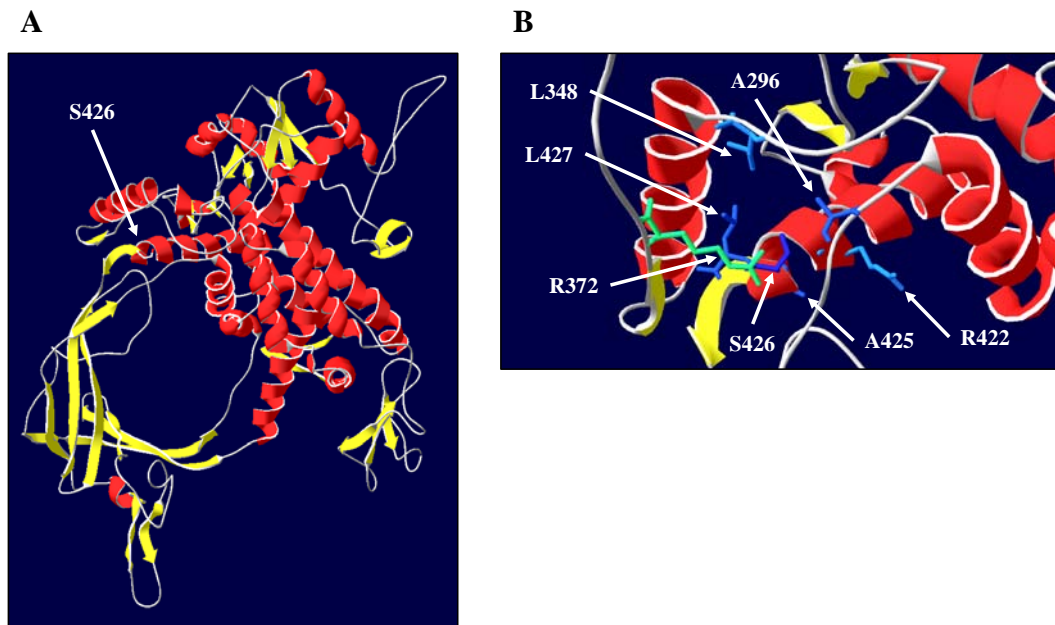


Fig. S1. Virtual two-dimensional protein map of *M. pneumoniae*. Based on the calculated molecular weight (MW) and theoretical isoelectric point (pI), each protein is localized in this virtual two-dimensional protein map of *M. pneumoniae* using the software JVirGel v2.2.3b (<http://www.jvirgel.de/>). NCBI reference sequence used for predicting MWs and pIs of the 689 proteins is NC_000912 (*M. pneumoniae* strain M129). The pI ranged from 4-11 and the molecular weight is adjusted from 8-125 kDa. About 635 proteins could be visualized with this set-up.

MPN261 - TopA - DNA topoisomerase I (S426)



MPN324 - NrdE - Ribonucleoside-diphosphate reductase subunit alpha (T159 & S412)

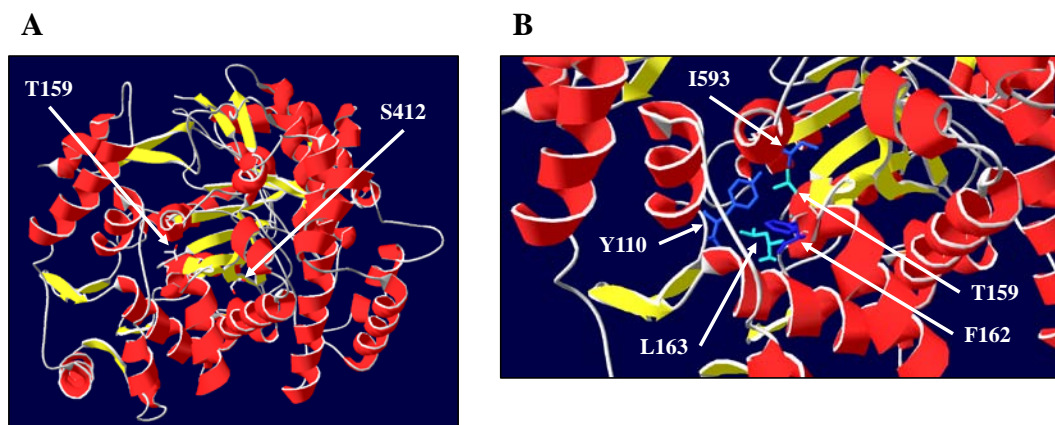
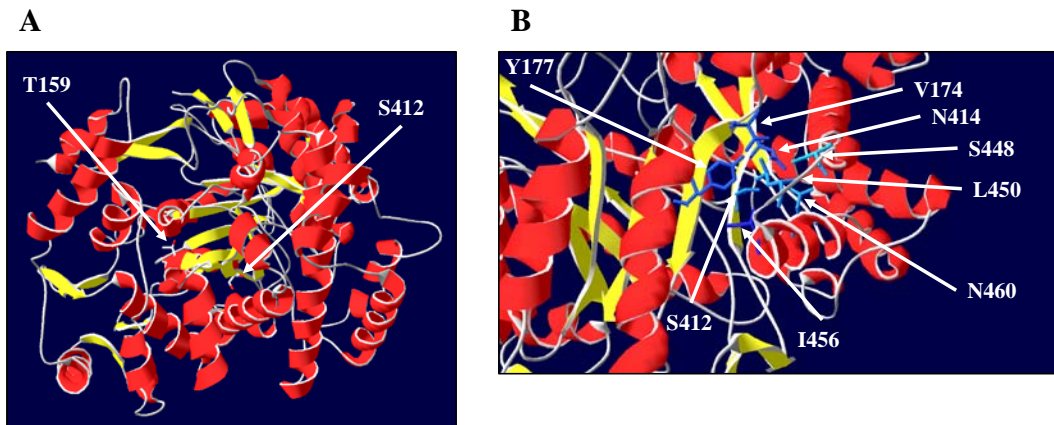


Fig. S2. Models of phosphoproteins based on homology with available structures. The models are based on the following PDB entries: 2GAI (MPN261, TopA), 1PEO (MPN324, NrdE), 1W85 (MPN393, PdhA), 1HDG (MPN430, GapA), 1PV9 (MPN470, PepP), 2J9A (MPN572, PepA), and 1OB2 (MPN665, Tuf). (A) Ribbon diagrams of phosphoproteins colored by secondary structure. As structural elements α -helices are shown in red and β -strands in yellow. Remaining elements are grey. The corresponding phosphorylation sites are highlighted on the model. (B) Close-up view of the phosphorylation sites with surrounding residues. Residues (distance of 1 Å) that possibly affect the phosphorylation are indicated. Additionally, each amino acid is colored by its relative accessibility. Dark blue color is attributed to completely buried amino acids, whereas red color is attributed to amino acids with at least 75% of their relative surface accessibility accessible.

MPN324 - NrdE - Ribonucleoside-diphosphate reductase subunit alpha (T159 & S412)



MPN393 - PdhA - Pyruvate dehydrogenase E1 component subunit alpha (S205)

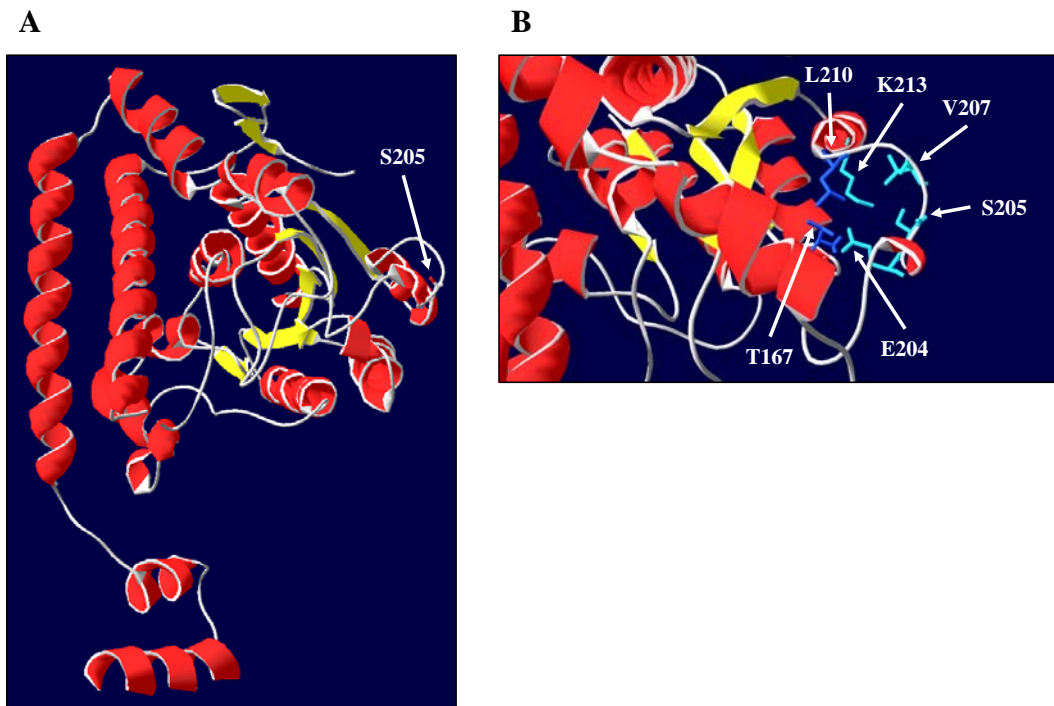
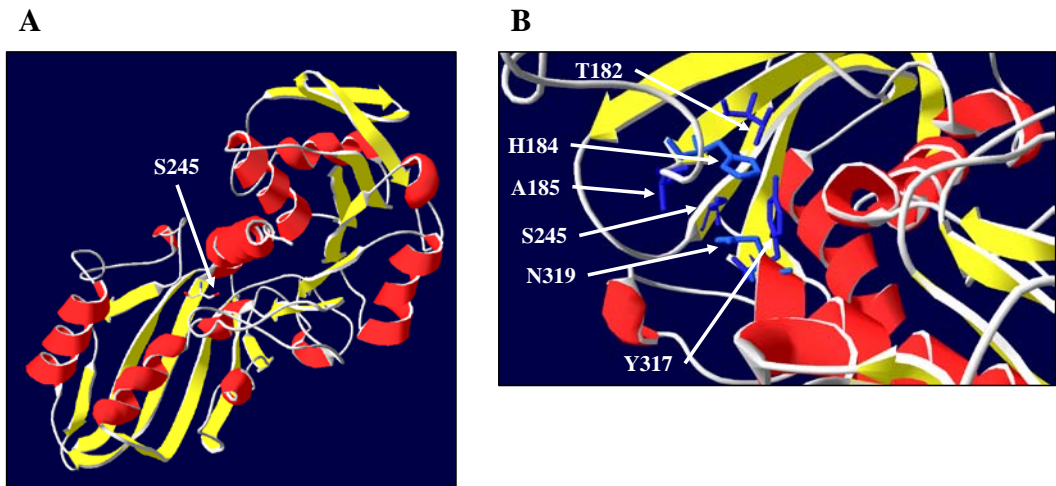
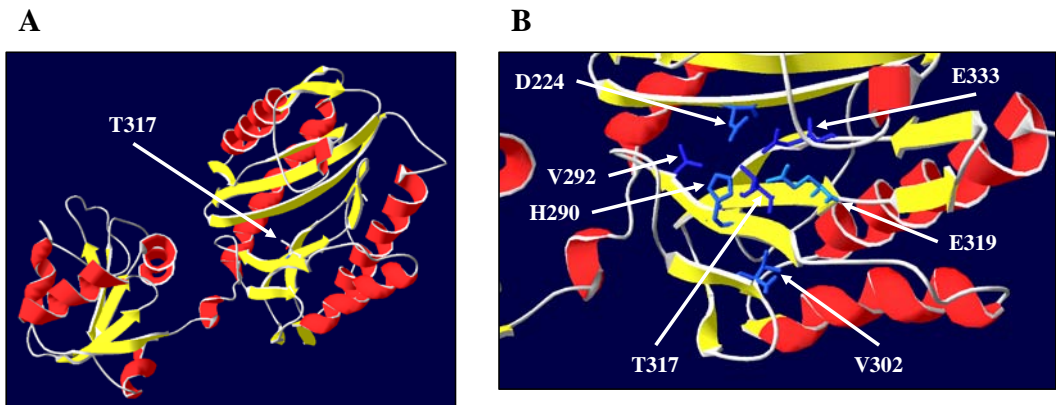


Fig. S2. Continued.

MPN430 - GapA - Glyceraldehyde-3-phosphate dehydrogenase (S245)



MPN470 - PepP - Xaa-Pro aminopeptidase (T317)



MPN572 - PepA - Cytosol aminopeptidase (S249 & T420)

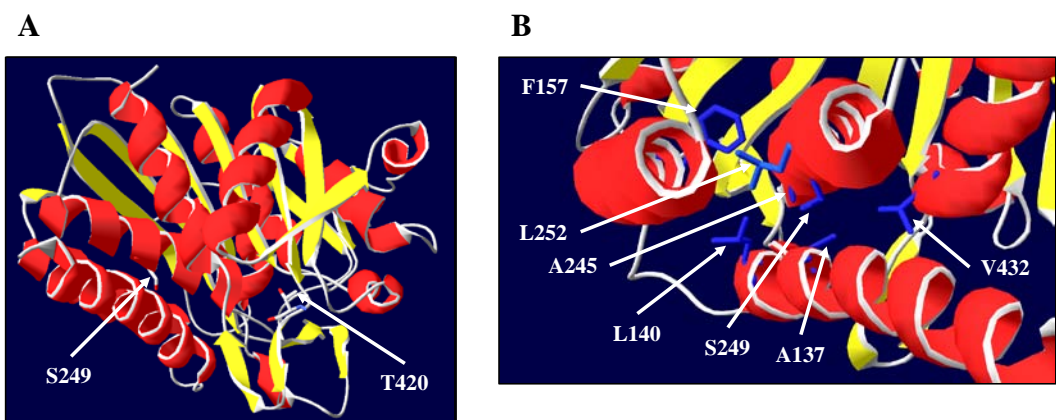
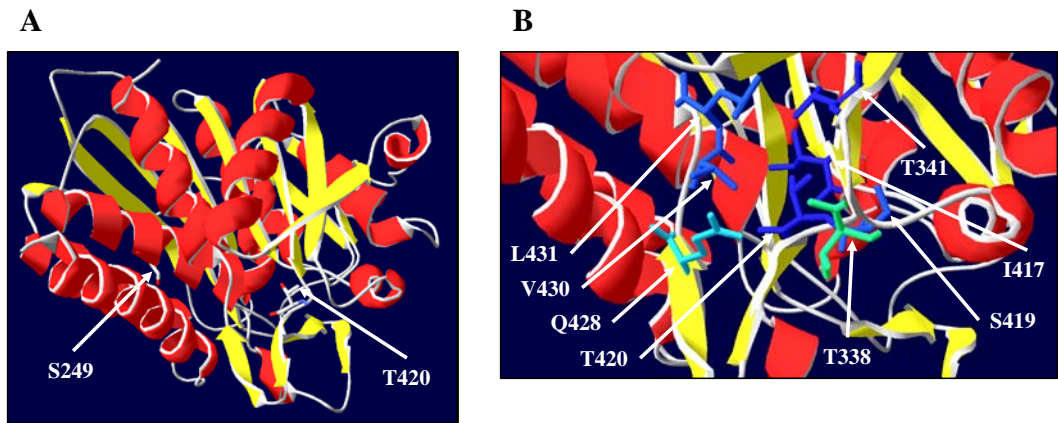


Fig. S2. Continued.

MPN572 - PepA - Cytosol aminopeptidase (S249 & T420)



MPN665 - Tuf - Elongation factor TU (T383)

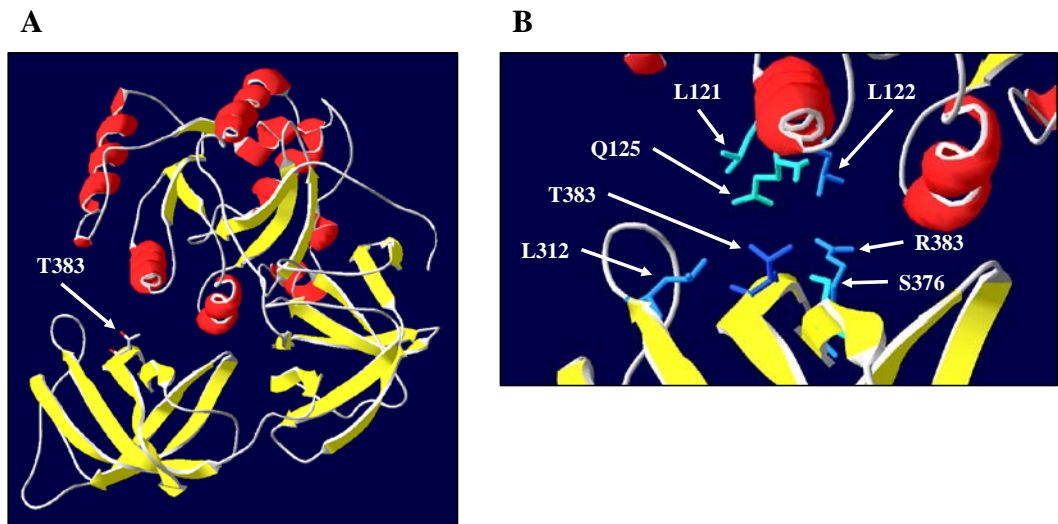
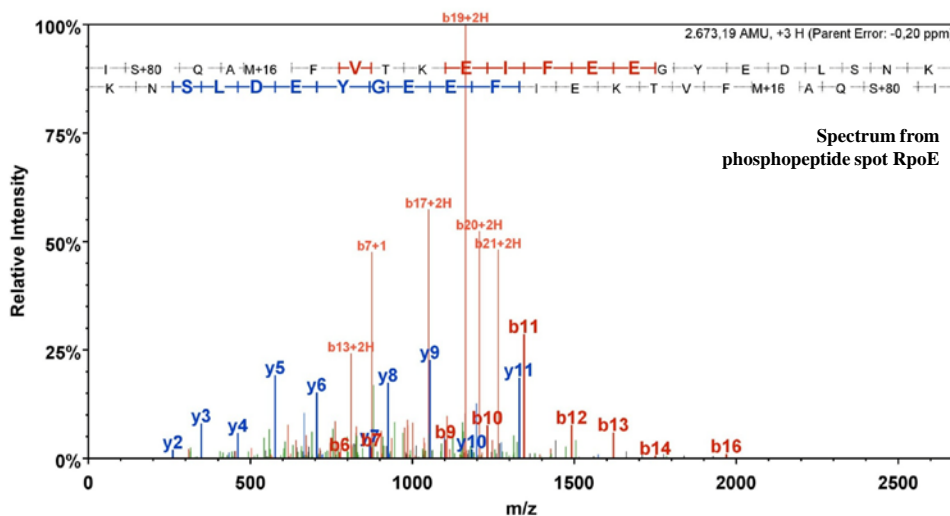


Fig. S2. Continued.

MPN024 - RpoE - RNA polymerase subunit delta



MPN024 - RpoE - RNA polymerase subunit delta

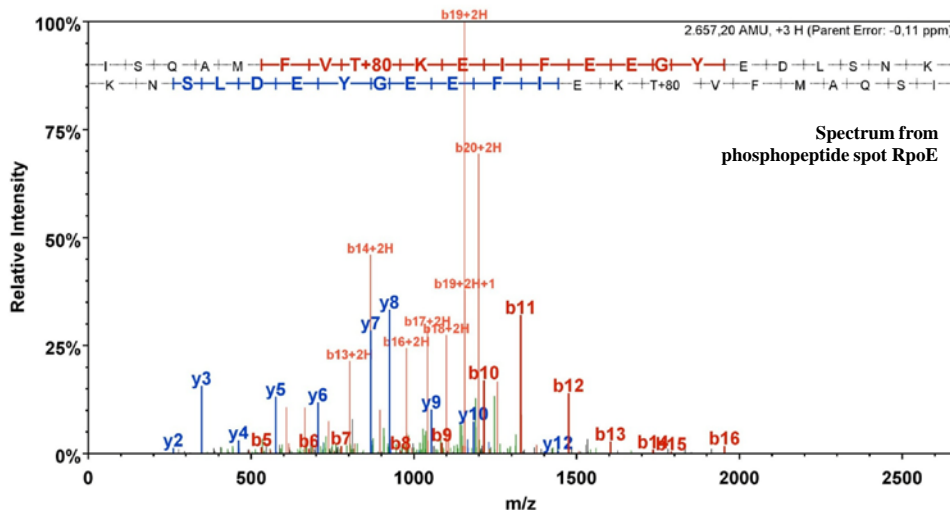
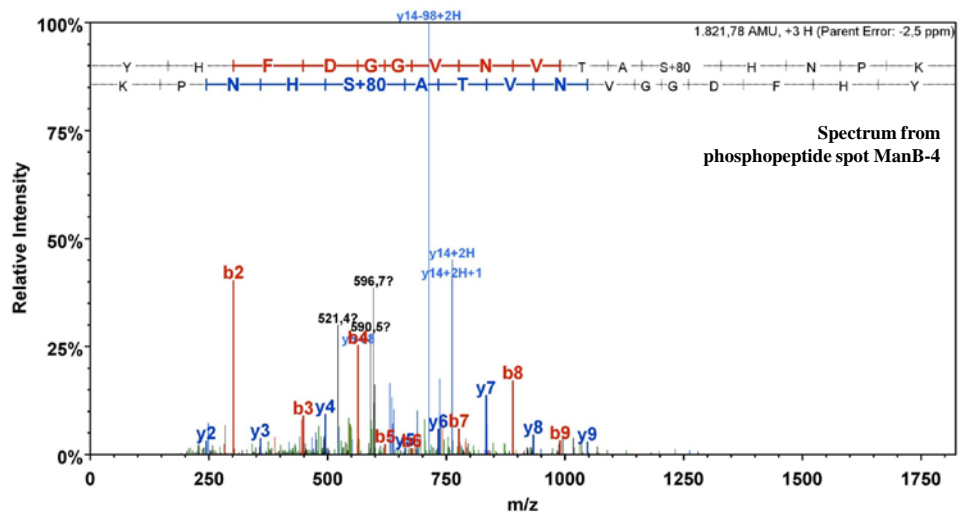
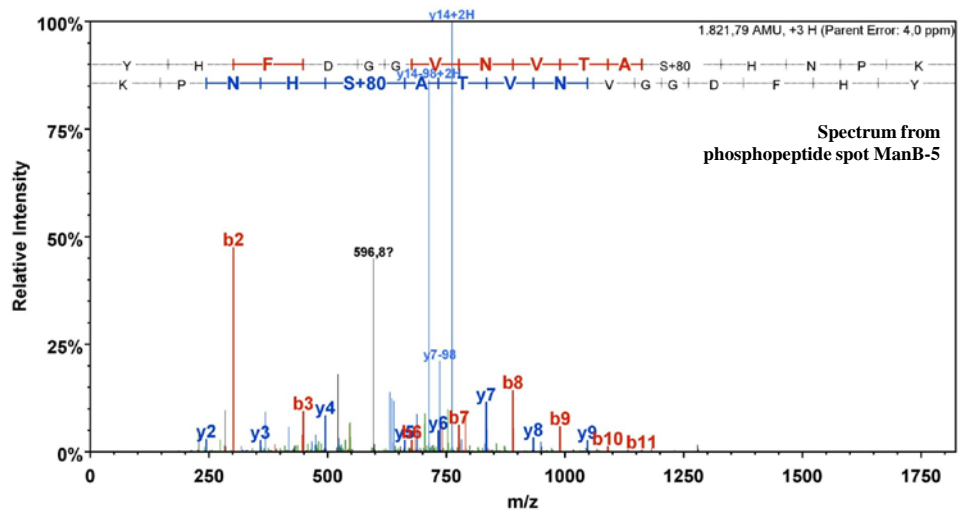


Fig. S3. Detailed MS/MS spectra of phosphorylated peptides. Peptides were measured online by ESI-mass spectrometry using a nanoACQUITY UPLC system coupled to an LTQ Orbitrap mass spectrometer (see “Experimental procedures”). Spectra are provided as screen shot with Scaffold annotated b- and y-ions series.

MPN066 - ManB - Phosphomannomutase/phosphoglucomutase



MPN066 - ManB - Phosphomannomutase/phosphoglucomutase



MPN066 - ManB - Phosphomannomutase/phosphoglucomutase

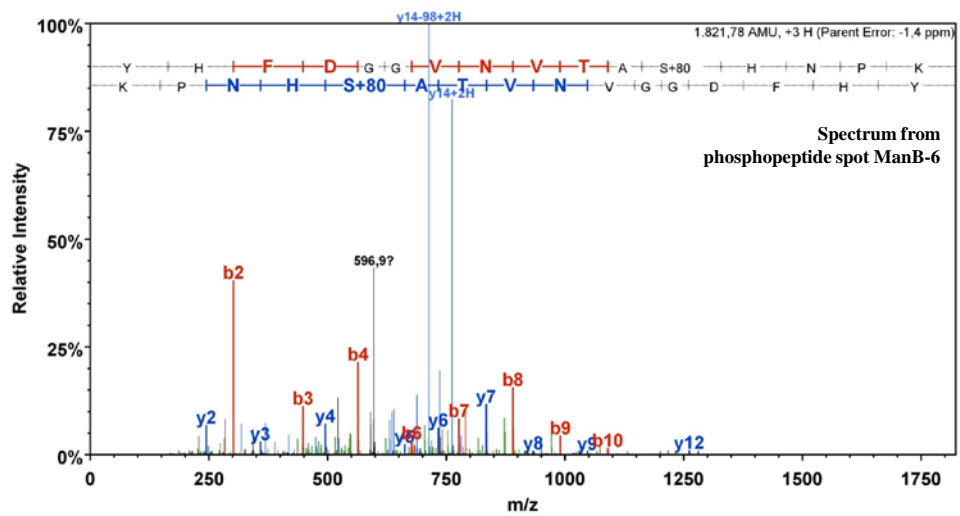
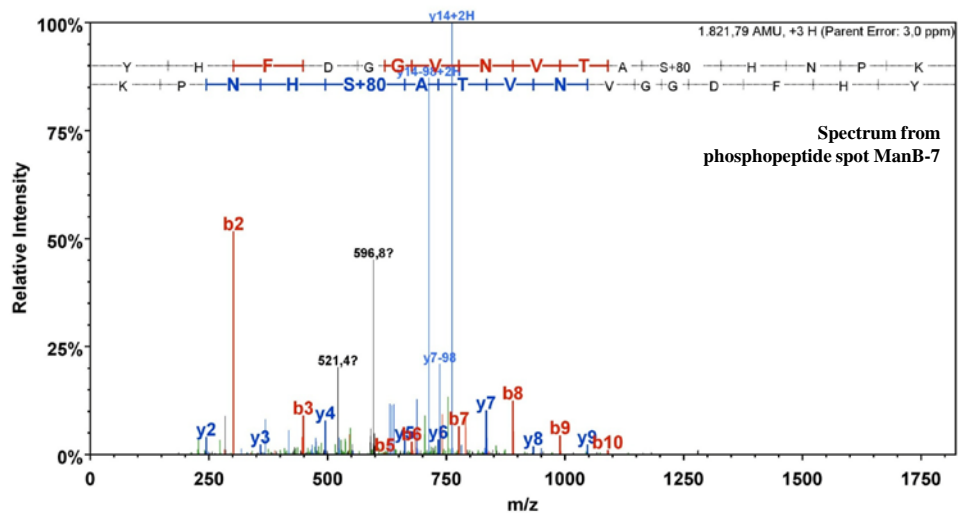
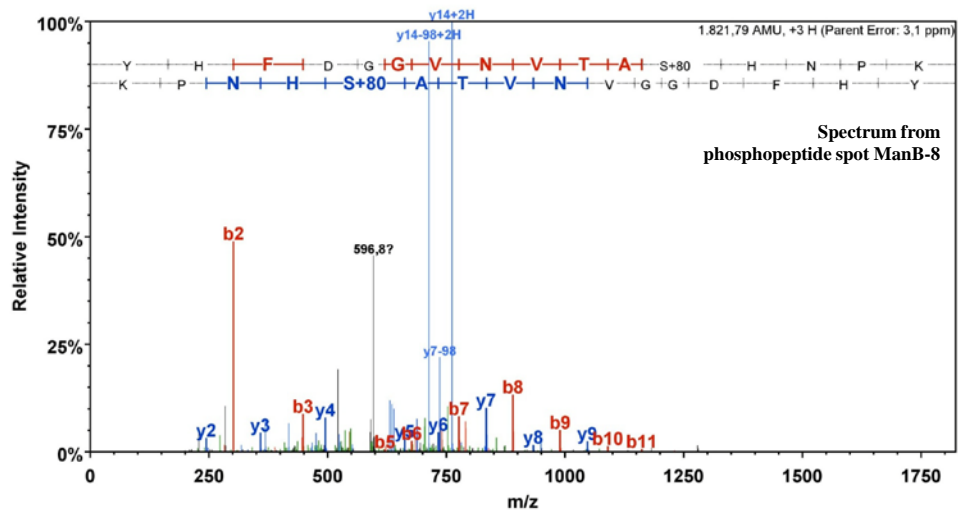


Fig. S3. Continued.

MPN066 - ManB - Phosphomannomutase/phosphoglucomutase



MPN066 - ManB - Phosphomannomutase/phosphoglucomutase



MPN066 - ManB - Phosphomannomutase/phosphoglucomutase

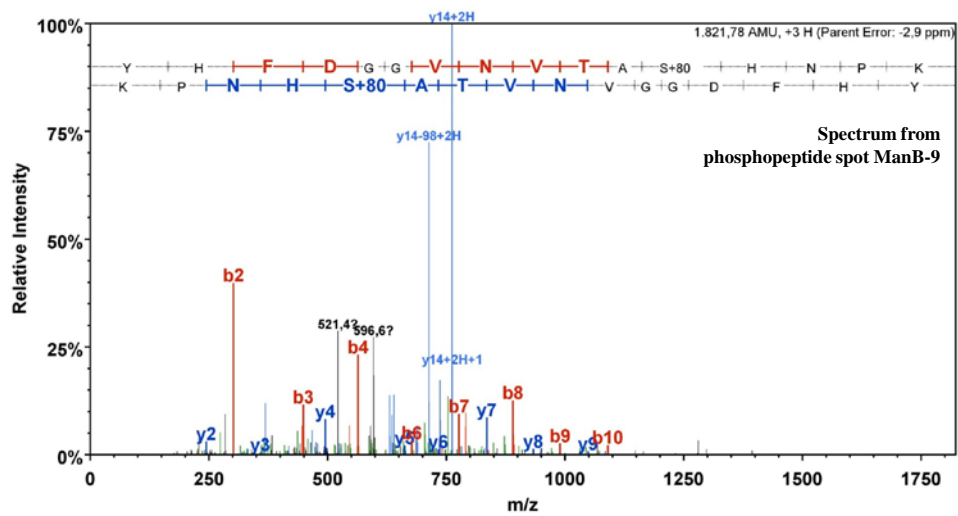
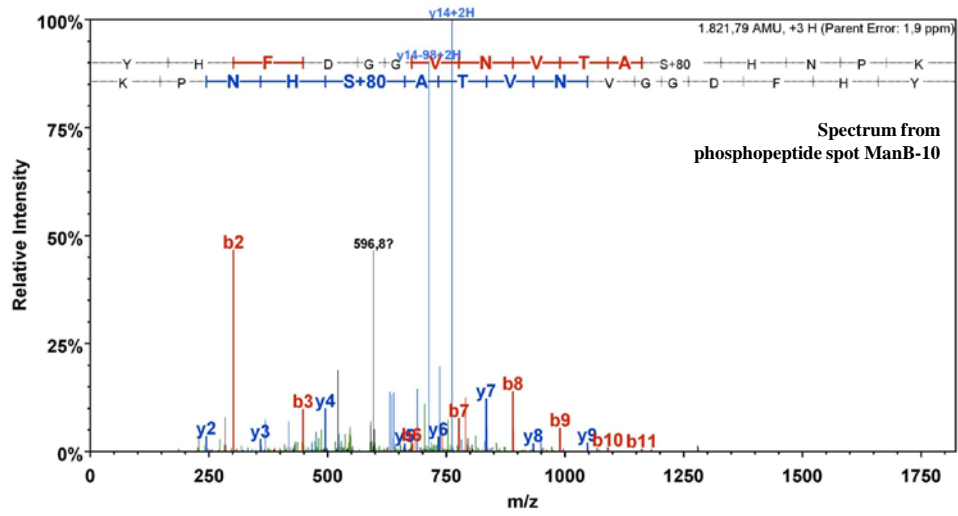
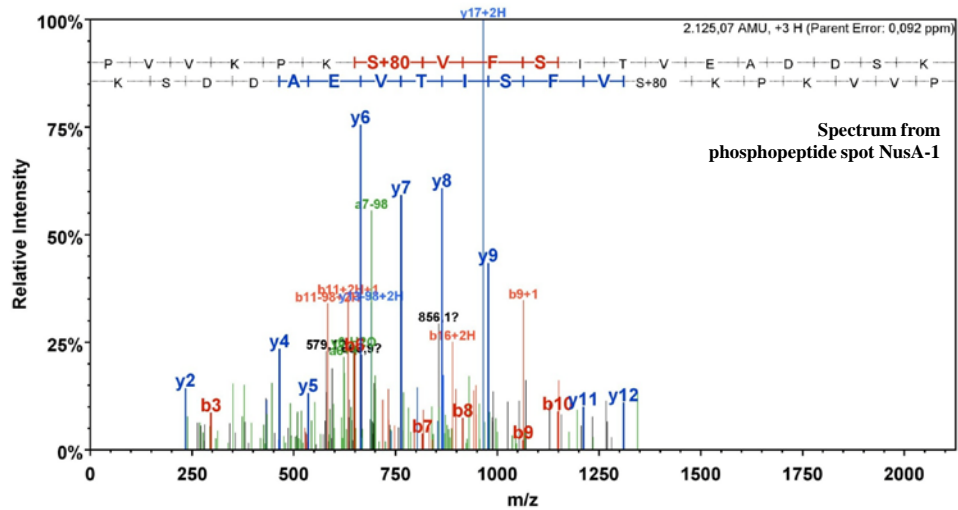


Fig. S3. Continued.

MPN066 - ManB - Phosphomannomutase/phosphoglucomutase



MPN154 - NusA - Transcription elongation factor



MPN256 - Uncharacterized protein

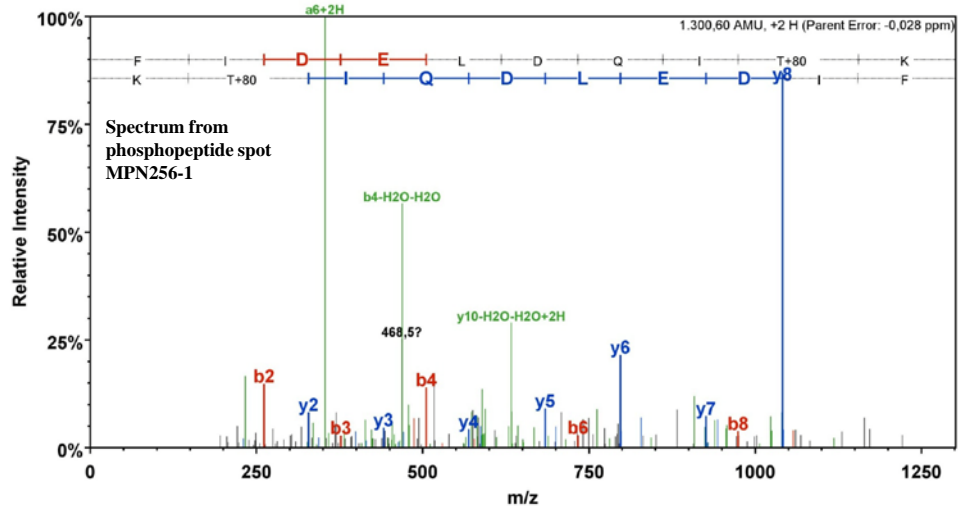
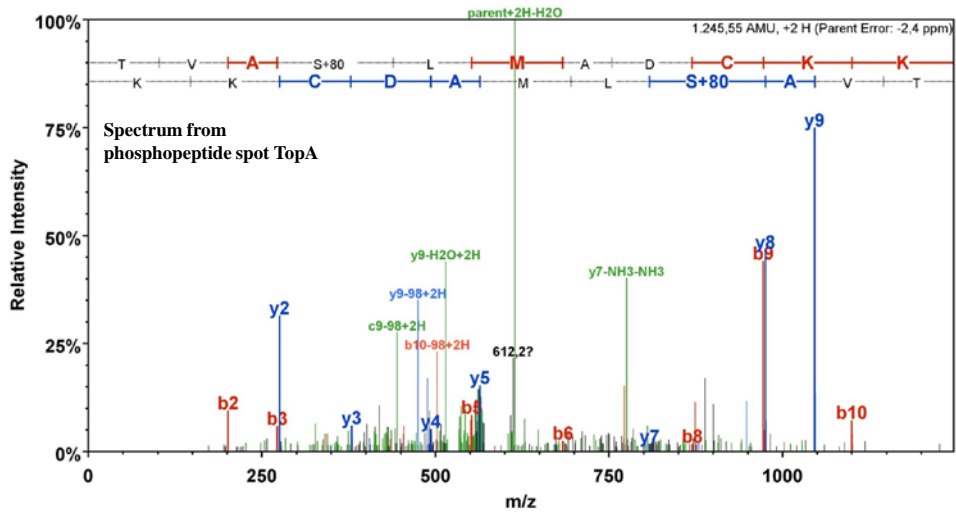
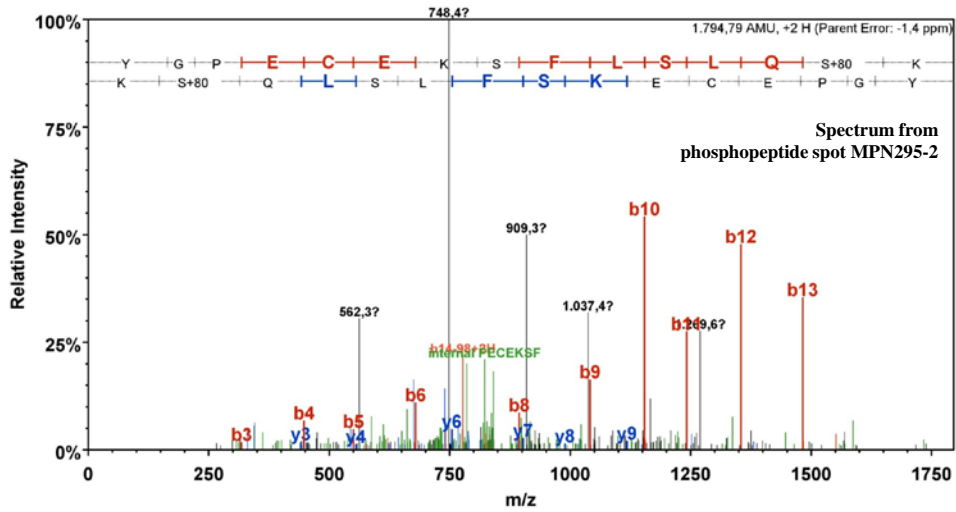


Fig. S3. Continued.

MPN261 - TopA - DNA topoisomerase I



MPN295 - Uncharacterized protein



MPN311 - P41 - Adhesin-related protein

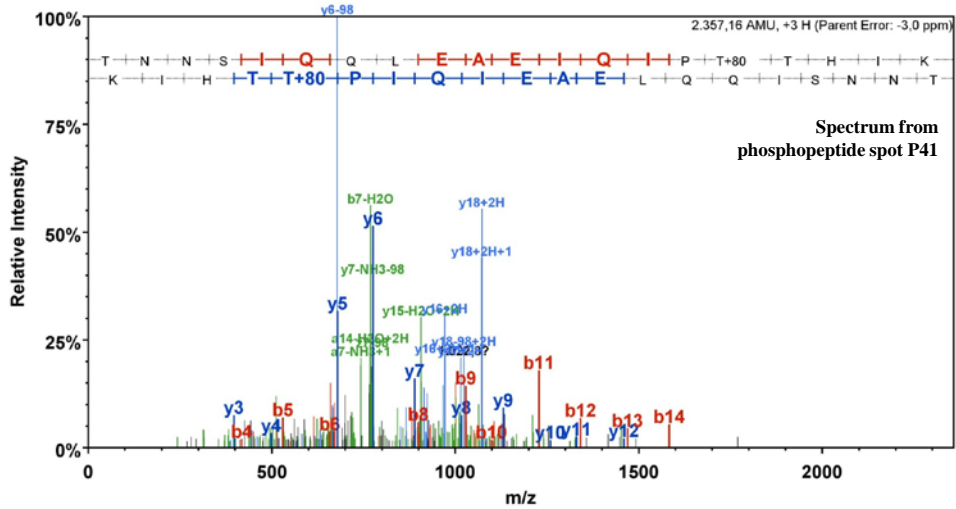
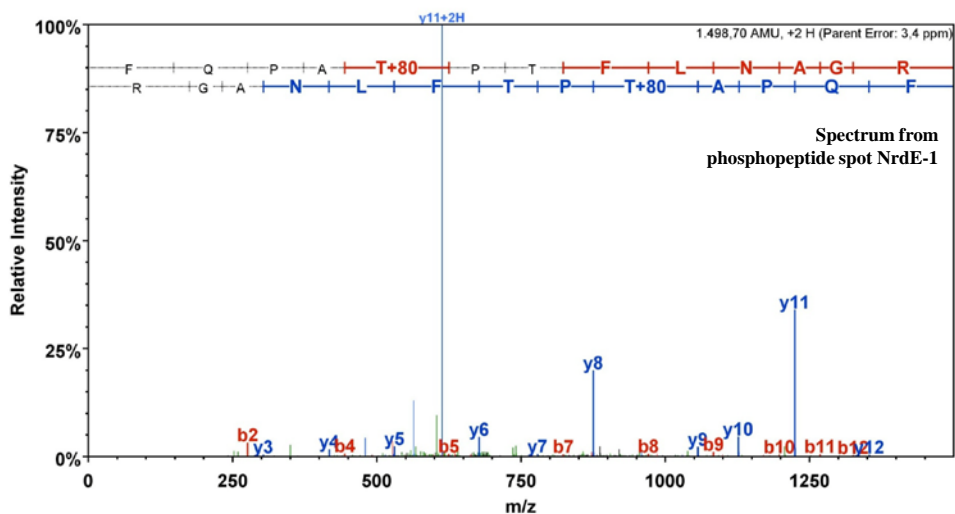
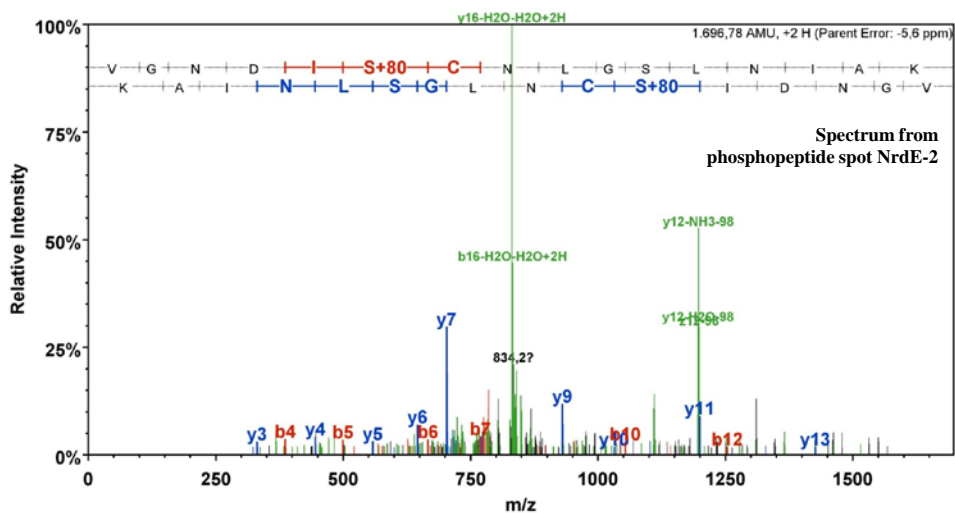


Fig. S3. Continued.

MPN324 - NrDE - Ribonucleoside-diphosphate reductase subunit alpha



MPN324 - NrDE - Ribonucleoside-diphosphate reductase subunit alpha



MPN393 - PdHA - Pyruvate dehydrogenase E1 component subunit alpha

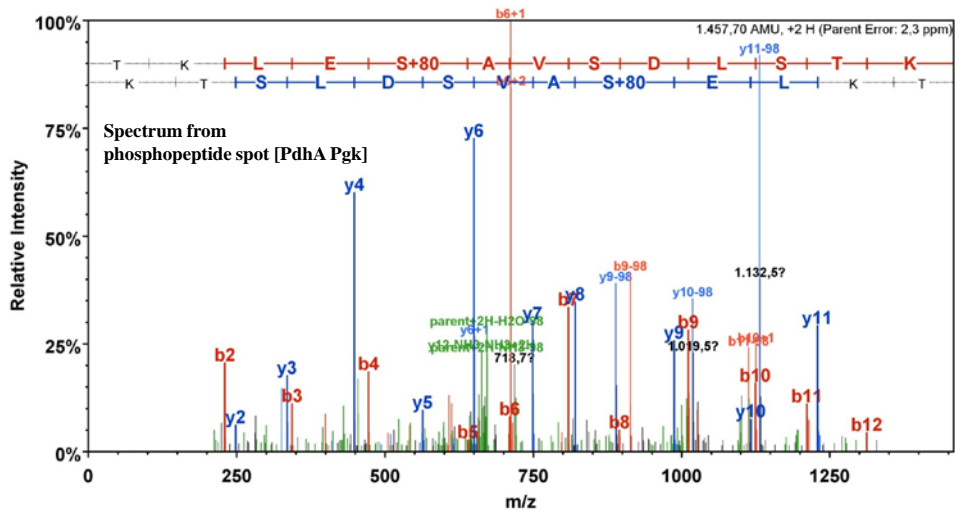
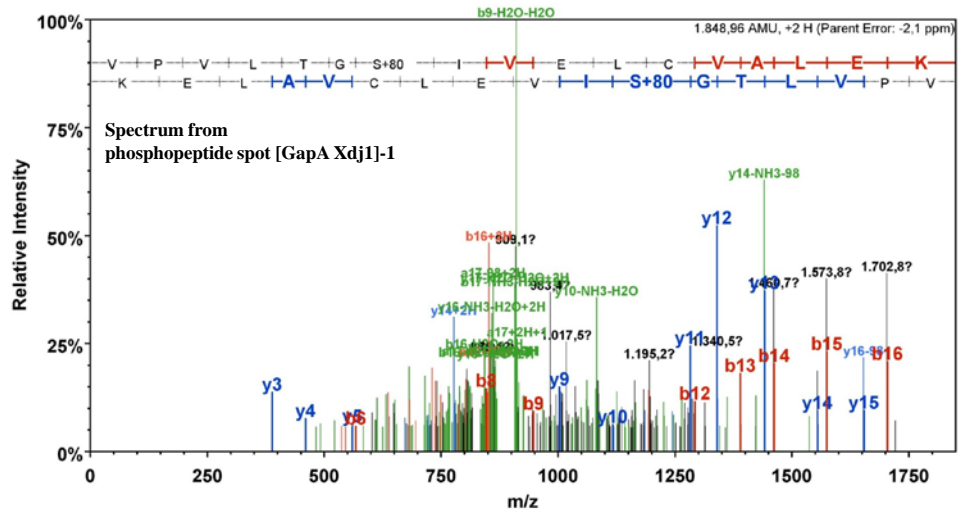
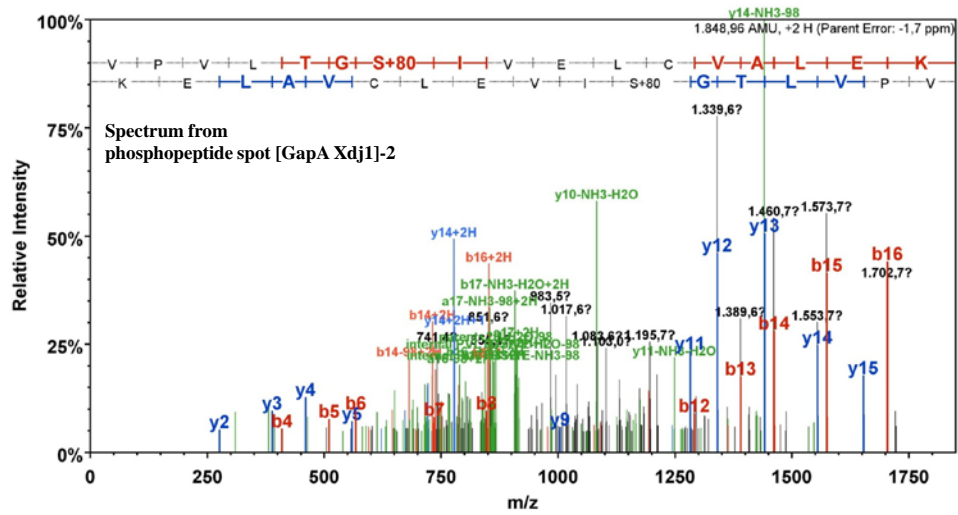


Fig. S3. Continued.

MPN430 - GapA - Glyceraldehyde-3-phosphate dehydrogenase



MPN430 - GapA - Glyceraldehyde-3-phosphate dehydrogenase



MPN470 - PepP - Xaa-Pro aminopeptidase

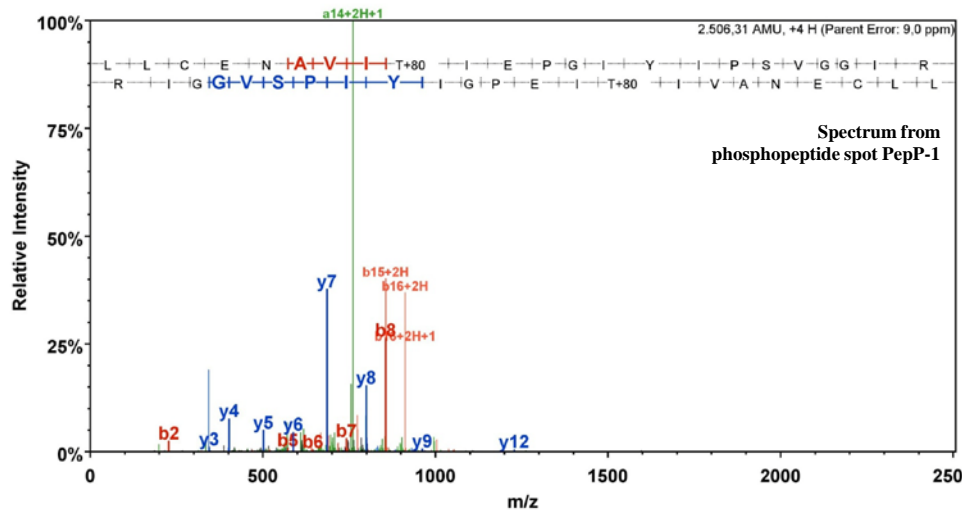
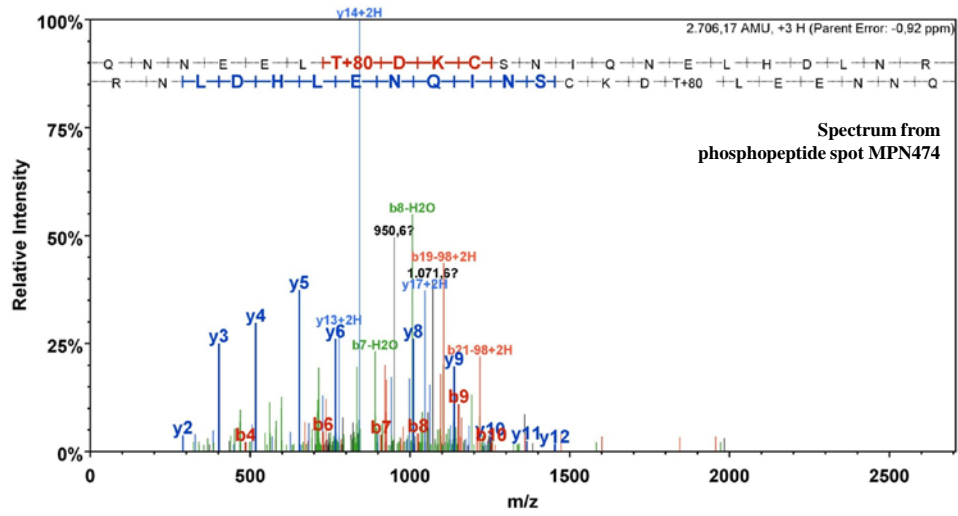
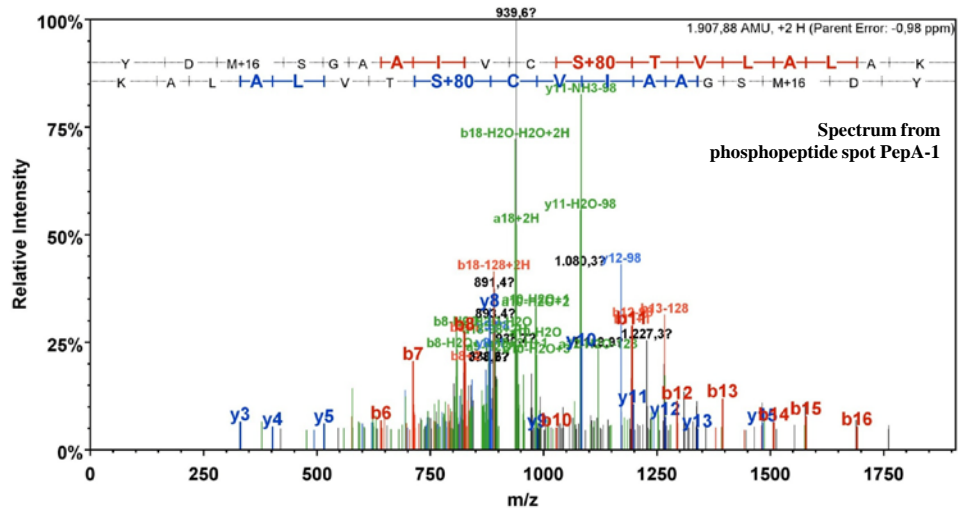


Fig. S3. Continued.

MPN474 - Coiled coil surface protein



MPN572 - PepA - Cytosol aminopeptidase



MPN572 - PepA - Cytosol aminopeptidase

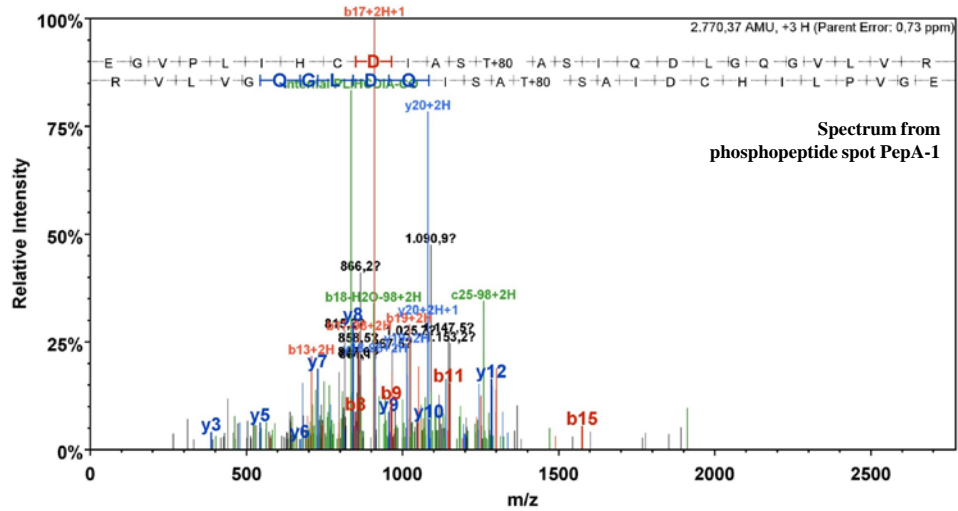
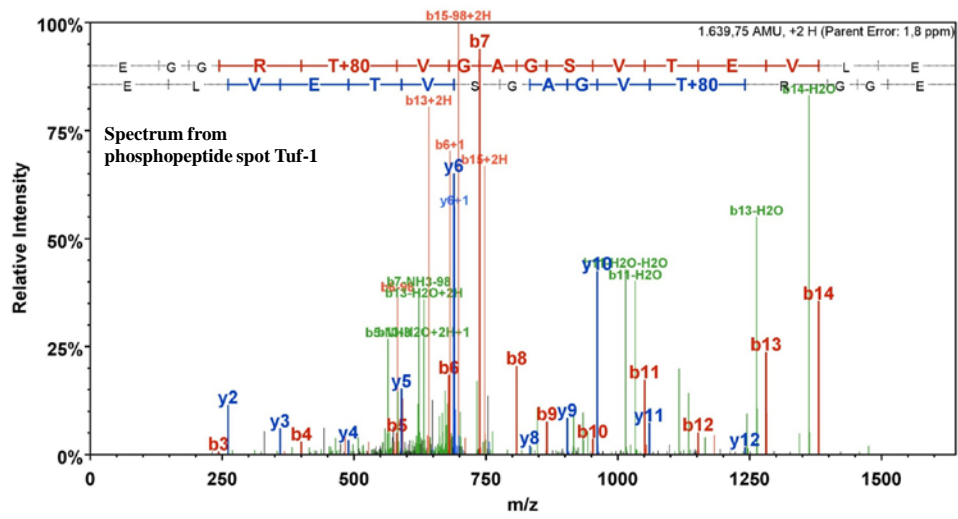
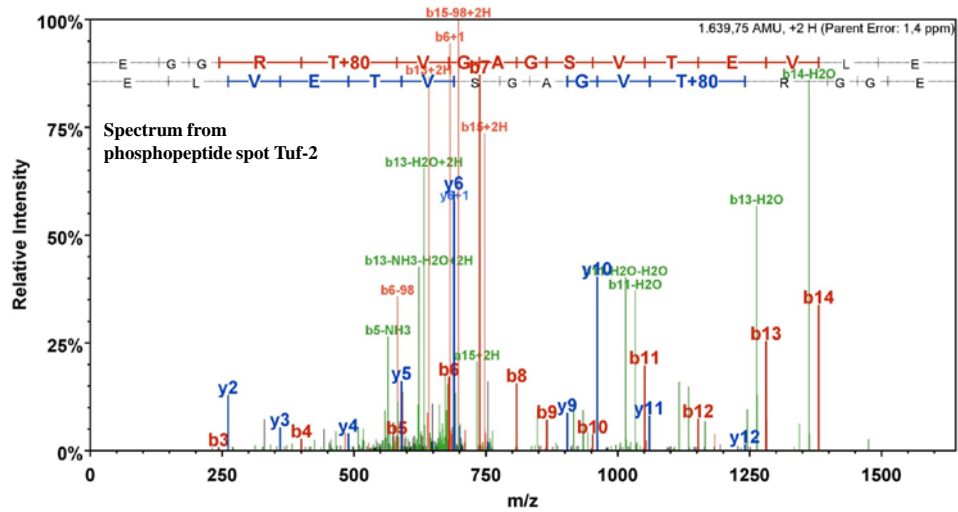


Fig. S3. Continued.

MPN665 - Tuf - Elongation factor TU



MPN665 - Tuf - Elongation factor TU



MPN665 - Tuf - Elongation factor TU

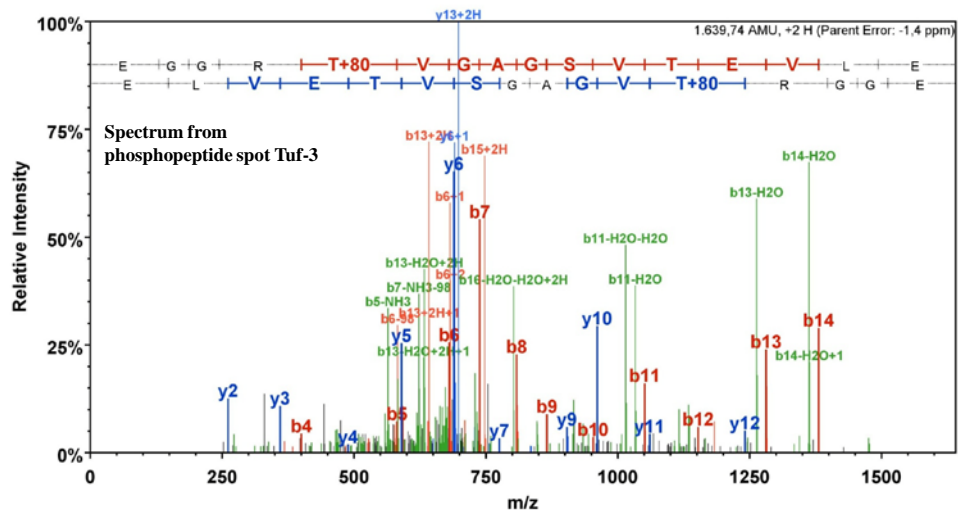
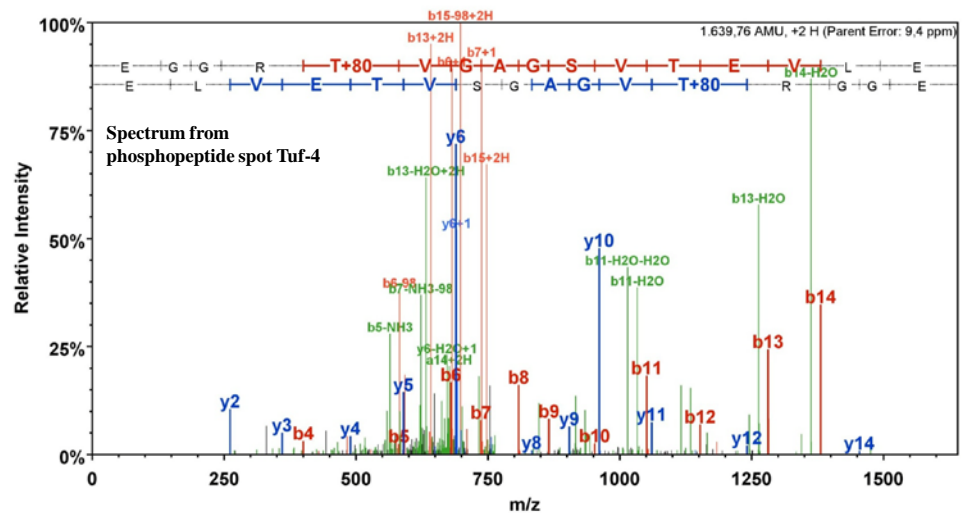


Fig. S3. Continued.

MPN665 - Tuf - Elongation factor TU



Chapter 4

***In vitro* phosphorylation of key metabolic enzymes from *Bacillus subtilis*: PrkC phosphorylates enzymes from different branches of basic metabolism**

The work described in this chapter was published in:

Pietack, N., D. Becher, S. R. Schmidl, M. H. Saier, M. Hecker, F. M. Commichau, and J. Stülke. 2010. *In vitro* phosphorylation of key metabolic enzymes from *Bacillus subtilis*: PrkC phosphorylates enzymes from different branches of basic metabolism. *J. Mol. Microbiol. Biotechnol.* **18**: 129-140.

Author contributions:

This study was designed and interpreted by NP, FMC, and JS. NP performed all *in vitro* phosphorylation experiments. SRS performed the phylogenetic analysis of PrkC homologues during an internship at the lab of MHS, University of California, San Diego. Determination of phosphorylation sites was done in collaboration with DB and MH, University of Greifswald. NP and JS wrote the paper.

Abstract

Phosphorylation is an important mechanism of protein modification. In the Gram-positive soil bacterium *Bacillus subtilis*, about 5% of all proteins are subject to phosphorylation, and a significant portion of these proteins is phosphorylated on serine or threonine residues. We were interested in the regulation of the basic metabolism in *B. subtilis*. Many enzymes of the central metabolic pathways are phosphorylated in this organism. In an attempt to identify the responsible protein kinase(s), we identified four candidate kinases, among them the previously studied kinase PrkC. We observed that PrkC is indeed able to phosphorylate several metabolic enzymes *in vitro*. Determination of the phosphorylation sites revealed a remarkable preference of PrkC for threonine residues. Moreover, PrkC often used several phosphorylation sites in one protein. This feature of PrkC-dependent protein phosphorylation resembles the multiple phosphorylations often observed in eukaryotic proteins. The HPr protein of the phosphotransferase system is one of the proteins phosphorylated by PrkC, and PrkC phosphorylates a site (Ser-12) that has recently been found to be phosphorylated *in vivo*. The agreement between *in vivo* and *in vitro* phosphorylation of HPr on Ser-12 suggests that our *in vitro* observations reflect the events that take place in the cell.

Introduction

Adaptation to changing environmental conditions is essential for life. The Gram-positive soil bacterium *Bacillus subtilis* is permanently exposed to changing conditions, such as nutrient limitations or various physical stresses. In principle, there are three different mechanisms by which bacteria can adapt their metabolism to the environment: (1) alterations of gene expression, (2) changing the stabilities of proteins, and (3) modulation of enzymatic activities. Regulation of gene expression is by far the most intensively studied regulatory mechanism. There is a huge collection of studies concerning the response of *B. subtilis* to environmental changes at the proteome and/or transcriptome levels (Blencke *et al.*, 2003; Eymann *et al.*, 2002; Moreno *et al.*, 2001). In the past few years, when transcriptome and proteome studies became very popular, most regulatory effects were attributed to changes in transcription. However, changes in transcription are not always accompanied by corresponding changes in metabolic fluxes

and vice versa (Schilling *et al.*, 2007). Thus, posttranslational regulatory mechanisms require our attention to fully understand regulatory phenomena.

In the past few years, it turned out that extensive protein phosphorylation not only on histidine, but also on serine, threonine, and tyrosine residues occurs in bacteria (Deutscher and Saier, 2005; Kennelly and Potts, 1996). In *B. subtilis*, phosphorylation on histidine residues occurs in the phosphotransferase system (PTS) as well as in PTS-controlled transcription regulators and glycerol kinase. The sensor kinases of the two-component regulatory systems constitute a second class of His-phosphorylated proteins (Fabret *et al.*, 1999; Reizer *et al.*, 1999). In the PTS, some phosphotransfer domains are phosphorylated on cysteine residues from which the phosphate is transferred to the incoming sugar. In contrast, the response regulators of the two-component systems are phosphorylated on aspartate residues by their cognate sensor kinases (Fabret *et al.*, 1999; Reizer *et al.*, 1999). Phosphorylation on serine residues has long been studied for the HPr protein of the PTS that is phosphorylated on Ser-46 by the metabolite-controlled HPr kinase/phosphorylase. HPr(Ser-P) then binds to the transcription factor CcpA and acts as a corepressor in carbon regulation (Görke and Stülke, 2008). Regulatory phosphorylation of proteins on serine (and threonine) residues is also well established for the modulators of sigma factor activity in sporulation and stress response (Min *et al.*, 1993; Yang *et al.*, 1996). Protein tyrosine phosphorylation is implicated in the control of the transcription repressor CtsR, of UDP-glucose dehydrogenases and of the single-stranded DNA-binding proteins (Grangeasse *et al.*, 2007). In total, about 200 proteins, representing 5% of all *B. subtilis* proteins, are now known to be phosphorylated (Eymann *et al.*, 2007; Lévine *et al.*, 2006; Macek *et al.*, 2007).

With the large number of proteins phosphorylated on serine, threonine or tyrosine, the identification of the responsible kinase(s) is getting into the spotlight. So far, the HPr kinase and the three kinases involved in controlling sigma factor activities have been studied. All these kinases seem to phosphorylate clearly defined sites and are therefore not candidates for the phosphorylation of novel targets. In addition, the protein kinase PrkC can phosphorylate several proteins, including elongation factor G and PrkC itself (Gaidenko *et al.*, 2002; Madec *et al.*, 2002). PrkC is located in the cell membrane of vegetative cells and in the inner spore membrane of spores (Madec *et al.*, 2002; Shah *et al.*, 2008). The *prkC* gene is part of the *prpC-prkC-cpgA* operon that is

constitutively expressed throughout growth (Iwanicki *et al.*, 2005). Recently, stimulation of PrkC activity by mucopeptides was reported. In spores, this activation of PrkC triggers germination, and *prkC* mutants are unable to germinate in response to mucopeptides (Shah *et al.*, 2008). Homologues of PrkC are widespread in both Gram-positive and Gram-negative bacteria (Fig. 14). This kinase is implicated in the phosphorylation of glycolytic enzymes and histone-like proteins as well as in pathogenicity in other Gram-positive bacteria (Jin and Pancholi, 2006; Kristich *et al.*, 2007; Lomas-Lopez *et al.*, 2007). It is interesting to note that *prkC* is encoded in an operon with a corresponding protein phosphatase, PrpC (Madec *et al.*, 2002). This phosphatase is able to dephosphorylate HPr(Ser-P) in *B. subtilis* and *Mycoplasma pneumoniae* (Halbedel *et al.*, 2006; Singh *et al.*, 2007).

We were interested in the regulation of carbon and nitrogen metabolism in *B. subtilis*. In an analysis of the transcriptome and metabolic flux responses to organic acids, we noticed that there are some cases where the changes in transcription do not match those in the metabolic fluxes. This is exemplified by the expression of the *alsSD* operon encoding acetolactate synthase and acetolactate decarboxylase and the corresponding acetoin production. Therefore, we considered posttranscriptional events to be important for metabolic adaptation (Schilling *et al.*, 2007). At the same time, phosphoproteome analyses demonstrated that indeed many enzymes of basic metabolism are subject to phosphorylation in *B. subtilis* (Eymann *et al.*, 2007; Lévine *et al.*, 2006; Macek *et al.*, 2007). Thus, protein phosphorylation might indeed play an important role for the adaptation of *B. subtilis* metabolism to changing conditions. However, the kinases responsible for these phosphorylation events have so far not been identified.

In this study, we intended to identify the kinase(s) for some of the enzymes of central metabolism by *in vitro* analysis of protein phosphorylation. Our work demonstrates that PrkC is able to phosphorylate several enzymes of different metabolic pathways. Moreover, PrkC was also responsible for a novel modification of the HPr protein of the PTS on Ser-12, an event previously observed *in vivo* (Macek *et al.*, 2007). Thus, PrkC may play an important role in phosphorylating proteins with different functions in *B. subtilis*.

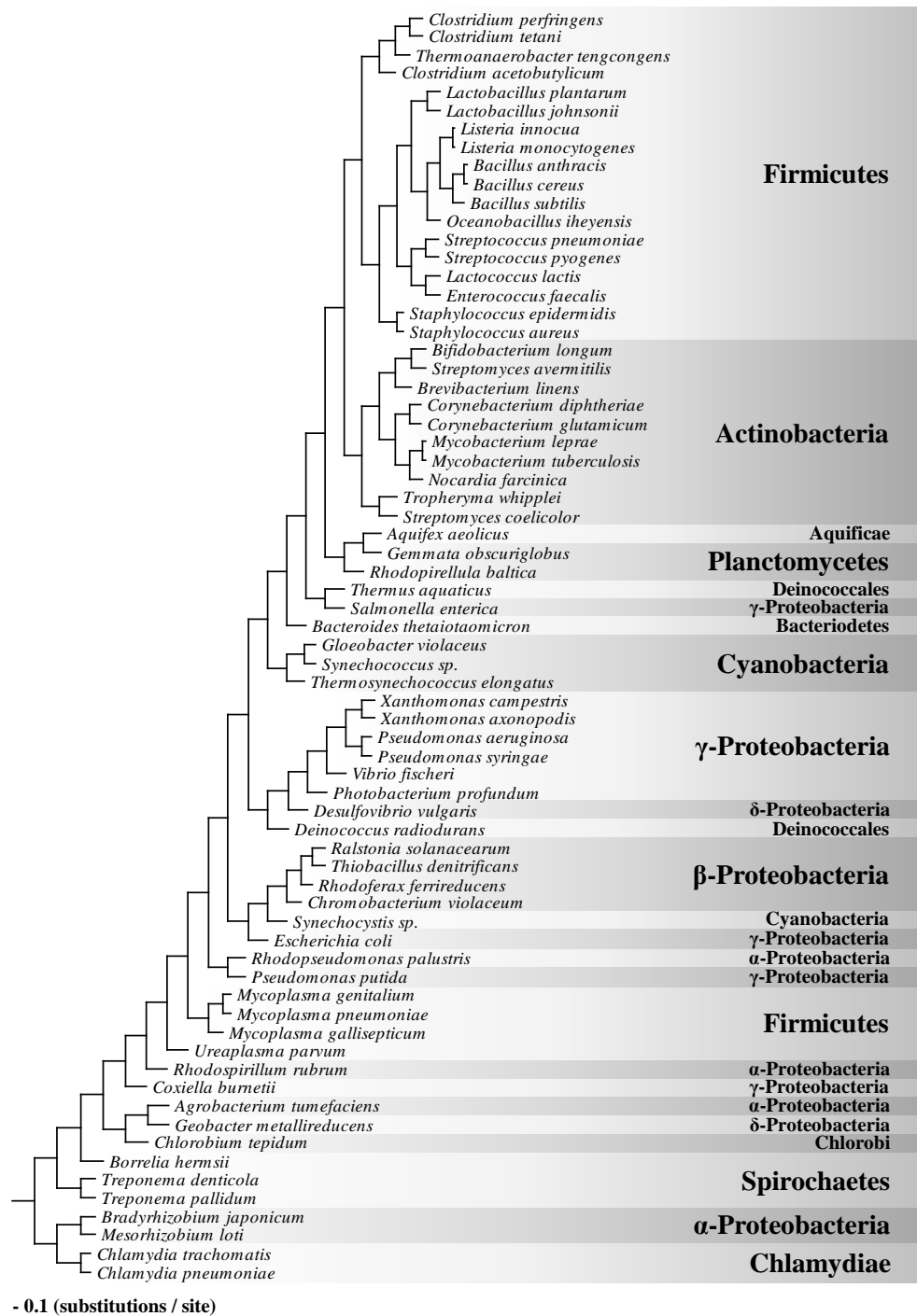


Fig. 14. Phylogenetic tree of PrkC homologues. The tree is based on a multiple alignment generated with the CLUSTAL X v2.0.12. program (Larkin *et al.*, 2007). The guide tree has been calculated using the UPGMA algorithm. The final phylogenetic tree was obtained using the Tree View X v0.5.0 program (<http://darwin.zoology.gla.ac.uk/~rpage/treeviewx/>).

Tab. 6. Plasmids used in this work.

Plasmid	Gene	Protein	Affinity tag	Oligonucleotides	Vector	References
pAG2	<i>ptsH</i>	HPr	His ₆ -tag	-	-	Galinier <i>et al.</i> (1997)
pGP174	<i>glnA</i>	Glutamine synthetase	<i>Strep</i> -tag	-	-	Heinrich <i>et al.</i> (2006)
pGP205	<i>hprK</i>	HPr kinase	His ₆ -tag	-	-	Hanson <i>et al.</i> (2002)
pGP371	<i>ptsH</i> ^a	HPr-S46A	His ₆ -tag	SH82/SH83	pWH844	This work
pGP563	<i>eno</i>	Enolase	His ₆ -tag	eno forw1/eno rev	pWH844	This work
pGP819	<i>ywjH</i>	Transaldolase	<i>Strep</i> -tag	NP11/NP12	pGP172	This work
pGP820	<i>tkt</i>	Transketolase	<i>Strep</i> -tag	NP05/NP06	pGP172	This work
pGP821	<i>prkD</i>	Protein kinase	<i>Strep</i> -tag	NP09/NP10	pGP172	This work
pGP822	<i>alsD</i>	α -acetolactate decarboxylase	<i>Strep</i> -tag	NP01/NP02	pGP172	This work
pGP823	<i>yabT</i>	Protein kinase	<i>Strep</i> -tag	NP07/NP08	pGP172	This work
pGP824	<i>ypaL</i>	Protein kinase	<i>Strep</i> -tag	NP13/NP14	pGP172	This work
pGP825	<i>prkC</i>	Protein kinase	<i>Strep</i> -tag	NP03/NP04	pGP172	This work
pGP931	<i>icd</i>	Isocitrate dehydrogenase	His ₆ -tag	FC17/FC18	pWH844	This work
pGP1100	<i>pyk</i>	Pyruvate kinase	His ₆ -tag	pyk forw1/pyk rev	pWH844	This work

^a Indicates mutant alleles.

Results

Identification of potential serine/threonine protein kinases in *B. subtilis*. The genome of *B. subtilis* encodes several proteins that are known or suspected to have serine/threonine kinase activity, among them the intensively studied HPr kinase/phosphorylase and the kinases involved in the control of sigma factor activities. In addition, the PrkC serine/threonine kinase has been studied before. Analysis of the annotated genome sequence revealed the presence of three additional potential kinases: PrkD that is similar to the kinase domain of PrkC (Madec *et al.*, 2002), YxaL and YabT.

Purification of selected potential protein kinases and phosphorylation targets. The four genes encoding the selected proteins were cloned into the expression vector pGP172, fusing them to an N-terminal *Strep*-tag. The proteins were expressed and purified using their affinity for Streptactin Sepharose. PrkC and PrkD were purified to apparent homogeneity. In contrast, we were unable to purify detectable amounts of YxaL. This may be due to the fact that YxaL is a secreted protein carrying a signal peptide (Tjalsma *et al.*, 2004). Similarly, only small amounts of YabT were obtained. Therefore, we concentrated our subsequent analyses on PrkC and PrkD.

Among the phosphoproteins that are involved in central metabolism, we selected glutamine synthetase (GlnA), enolase (Eno), transaldolase (YwjH), transketolase (Tkt), α -acetolactate decarboxylase (AlsD), isocitrate dehydrogenase (Icd), and pyruvate kinase (Pyk). These proteins were found to be phosphorylated *in vivo* on serine, threonine or tyrosine (Eymann *et al.*, 2007; Lévine *et al.*, 2006; Macek *et al.*, 2007). The corresponding genes were cloned into the expression vectors pWH844 and pGP172 to fuse the coding sequences to an N-terminal His₆- or *Strep*-tag, respectively (Table 6). All these proteins were expressed in *Escherichia coli* and were purified to apparent homogeneity by affinity chromatography.

Autophosphorylation of PrkC and PrkD. First, we analyzed the autophosphorylation of the selected serine/threonine kinases, PrkC and PrkD. For this purpose, we incubated the two proteins in the presence of [γ -³²P]ATP and analyzed them by SDS-PAGE. As shown in Fig. 15, both proteins exhibited autophosphorylation activity. This observation is in excellent agreement with a previous report on the autophosphorylation of PrkC (Madec *et al.*, 2003). To characterize these autophosphorylation events in more detail, we determined the phosphorylation sites by mass spectrometry using an LTQ Orbitrap mass spectrometer. For PrkC, we detected

six phosphorylation sites: Ser-214, Thr-290, Thr-313, Thr-320 in the cytoplasmic kinase domain, and Thr-417 and Thr-498 in the extracytoplasmic domain. The phosphorylation sites in the kinase domain were also detected in a previous study that was exclusively devoted to the analysis of this domain (Madec *et al.*, 2003). Moreover, phosphorylation of Thr-290 was found to take place *in vivo* (Macek *et al.*, 2007). For PrkD, we found one phosphorylation site, Thr-174. It is interesting to note that the region surrounding this site is not conserved in PrkC. Similarly, the regions encompassing the phosphorylation sites in PrkC are not conserved in PrkD. Thus, both PrkD and PrkC are mainly autophosphorylated on threonine residues, but the actual phosphorylation sites are not conserved even though 26 and 41% of identical and similar residues are conserved, respectively, for the N-terminal 200 amino acids of the two kinases.



Fig. 15. Autophosphorylation of the serine/threonine kinases PrkC and PrkD. Two micrograms of each purified protein were incubated with 0.4 mM [γ - 32 P]ATP (480 Ci/mmol) at 37°C for 30 min in assay buffer. The samples were then heated for 10 min at 95°C and loaded on a 16% SDS-PAGE gel. The gel was dried and analyzed by using a Storm 860 Molecular Imager, Molecular Dynamics.

Phosphorylation of the potential target proteins. The principal aim of this study was the investigation of phosphorylation of central metabolic enzymes of *B. subtilis*. To address this question, we incubated the putative kinase substrates with [γ - 32 P]ATP and either of the two kinases. Of the seven selected proteins, four were

phosphorylated by PrkC (Fig. 16). These were the transaldolase YwjH, the glutamine synthetase GlnA, the isocitrate dehydrogenase Icd, and the α -acetolactate decarboxylase AlsD. In contrast, enolase, transketolase, and the pyruvate kinase PykA were not substrates for PrkC-dependent phosphorylation (data not shown). However, the phosphorylation efficiency differed for the PrkC substrates: The phosphorylation efficiency of YwjH, GlnA, and Icd by PrkC was similar to that observed for HPrK-dependent phosphorylation of HPr (Fig. 16). In contrast, only weak signals were observed with AlsD (Fig. 16). This might be caused by differences in the number of phosphorylation sites or in different affinities of PrkC for its respective substrates. The kinase assays with PrkD revealed that only Icd and GlnA were phosphorylated by PrkD (data not shown). However, these phosphorylation signals were extremely faint, which questions their biological relevance. Thus, our analysis revealed selective phosphorylation of four enzymes of central metabolism by PrkC.

Determination of phosphorylation sites in the target proteins. In order to get new insights into PrkC substrates, we determined the phosphorylation sites of the proteins phosphorylated by PrkC. As observed for the autophosphorylation of PrkC, multiple phosphorylations with threonine as the major phosphoacceptor were observed. For the transaldolase YwjH, we observed six sites that were phosphorylated by PrkC. The phosphorylated amino acids were scattered throughout the protein. There was one phosphorylated serine residue, Ser-55, and five phosphothreonines, *i.e.* Thr-26, Thr-82, Thr-125, Thr-159, and Thr-184. Similar results were obtained with glutamine synthetase. This enzyme was phosphorylated on one serine residue, Ser-207, and three threonine residues, Thr-26, Thr-147, and Thr-286. It is interesting to note that Thr-26 is located in the N-terminal β -grasp domain of the enzyme that is thought to be involved in binding of small molecules (Burroughs *et al.*, 2007), whereas the other phosphorylation events take place in the catalytic domain of glutamine synthetase. Isocitrate dehydrogenase is phosphorylated by PrkC on three threonine residues, Thr-138, Thr-147, and Thr-396. In contrast to the other PrkC substrates (including PrkC autophosphorylation), the α -acetolactate decarboxylase AlsD was phosphorylated by PrkC on a single serine residue, Ser-88.

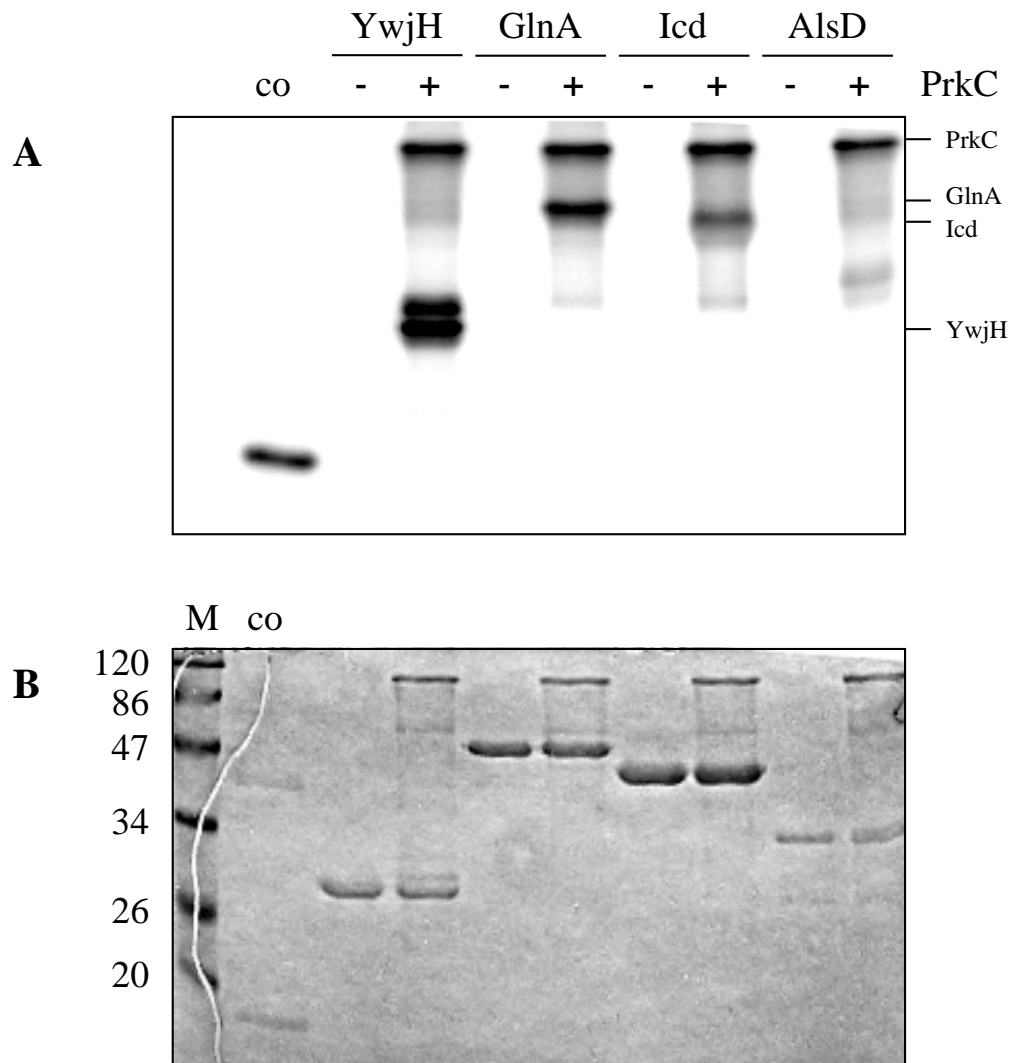


Fig. 16. Phosphorylation of potential target proteins by PrkC. Ten micrograms of the purified enzymes YwjH, GlnA, Icd, and AlsD were incubated with 0.4 mM [γ - 32 P]ATP (480 Ci/mmol) in the absence and in the presence of 2 μ g PrkC at 37°C for 30 min in assay buffer. The samples were heated for 10 min at 95°C and loaded on a 16% SDS-PAGE gel. To obtain the autoradiogram, the gel was dried and analyzed using a Storm 860 Molecular Imager, Molecular Dynamics. (A) In addition, the proteins were visualized by Coomassie staining. (B) co = Control (HPr phosphorylated by HPrK).

Phosphorylation of HPr by PrkC. A recent analysis of the *B. subtilis* phosphoproteome revealed a novel phosphorylation of the HPr protein of the PTS on Ser-12 (Macek *et al.*, 2007). However, the source of this phosphorylation is not known so far. We considered the possibility that this phosphorylation might be caused by PrkC. Therefore, we assayed the phosphorylation of HPr in the presence of PrkC and [γ - 32 P]ATP. The HPr kinase that phosphorylates HPr on Ser-46 served as a control. As shown in Fig. 17, HPr was efficiently phosphorylated by the HPr kinase. Similarly, PrkC was capable of phosphorylating HPr. Both HPrK (with its phosphorylase activity) and PrpC, a protein phosphatase encoded in an operon with PrkC, are able to dephosphorylate HPr(Ser-P) (Mijakovic *et al.*, 2002; Singh *et al.*, 2007). Therefore, we considered the possibility that Ser-46 of HPr was the phosphorylation site used by HPrK as well as by PrkC. To address this problem, we used a mutant variant of the HPr protein devoid of its HPrK-dependent phosphorylation site (HPr-S46A) and tested the phosphorylation of this protein by the two kinases. As expected, the mutant protein was no longer phosphorylated by HPr kinase, thus confirming the conclusion that Ser-46 is the only phosphorylation site in HPr used by HPr kinase. In contrast, the mutant protein was still phosphorylated by PrkC, and the intensity of the phosphorylation signal was similar to that observed with the wild type protein. These observations suggest that a site (or sites) distinct from Ser-46 are the primary target(s) of PrkC-dependent phosphorylation in HPr.

The use of a different phosphorylation site by PrkC may suggest that Ser-12, a site phosphorylated *in vivo* (Macek *et al.*, 2007), is the target of PrkC. This was verified by mass-spectrometric determination of the PrkC-dependent phosphorylation site (Fig. 18). Indeed, the only phosphorylated site detected in this study was Ser-12. Thus, the *in vitro* activity of PrkC on HPr reflects the *in vivo* situation. This observation suggests that PrkC is the kinase that phosphorylates HPr *in vivo* on Ser-12.

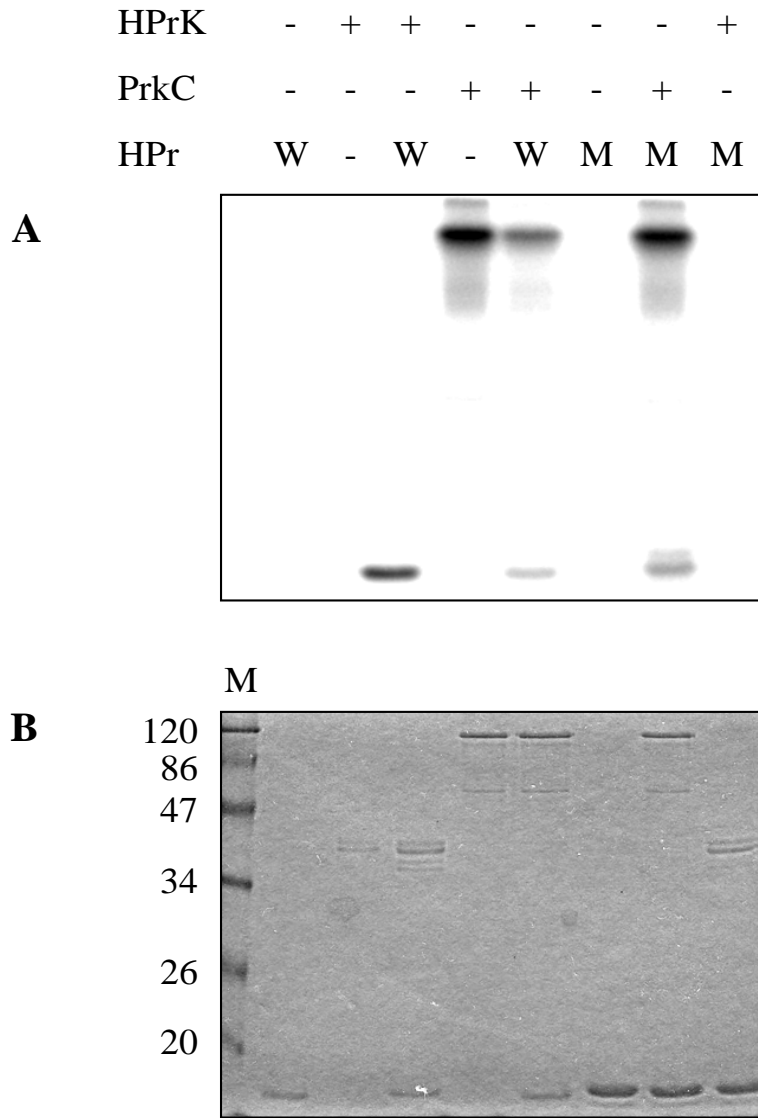


Fig. 17. Phosphorylation of wild type HPr and HPr-S46A by PrkC and HPrK. Ten micrograms of the purified wild type HPr (W) and HPr-S46A (M) were incubated with 0.4 mM [γ - 32 P]ATP (480 Ci/mmol) in the absence and in the presence of either 2 μ g PrkC or HPrK at 37°C for 30 min in assay buffer. The samples were heated for 10 min at 95°C and loaded on a 16% SDS-PAGE gel. The autoradiogram (A) and the Coomassie stained gel (B) were prepared as described in Fig. 15.

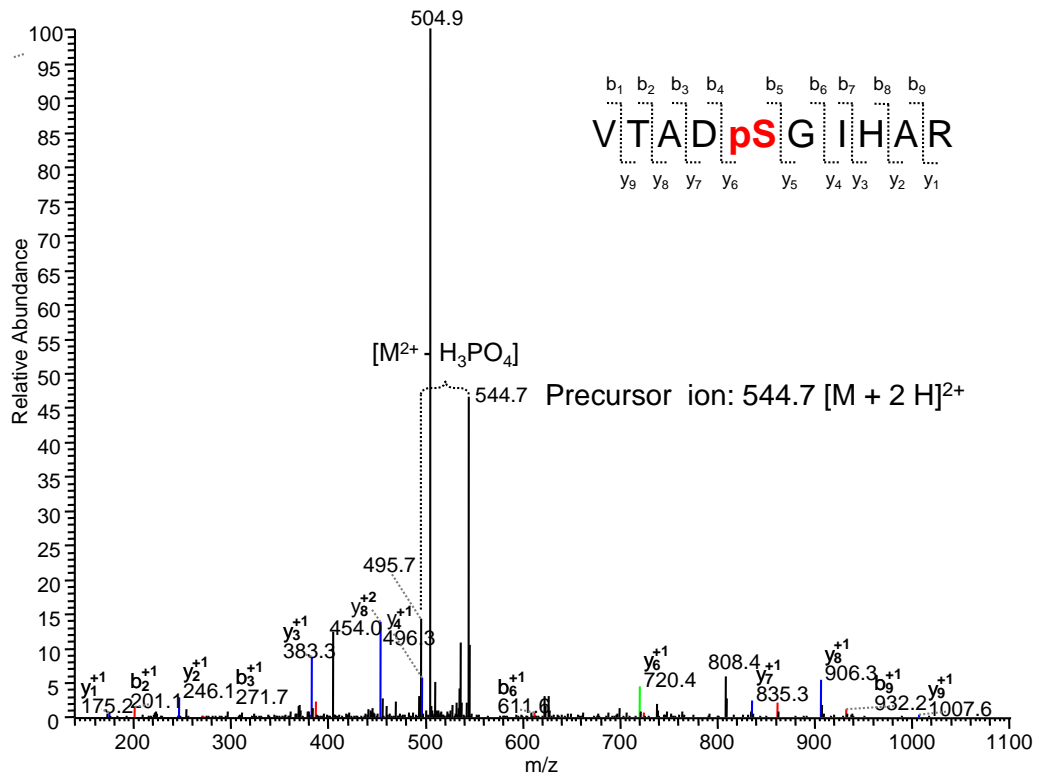


Fig. 18. Identification of the site of PrkC-dependent phosphorylation in HPr. The fragment ion spectrum of the HPr T2 peptide (VTADSGIHAR) with a precursor ion mass 544.7 [M + 2 H]²⁺ indicates a phosphate residue. The corresponding b- and y-ions and the formation of the ion corresponding to the neutral loss of phosphoric acid from the doubly-charged precursor ion are highlighted and demonstrate the Ser-12 phosphorylation of HPr.

Discussion

Protein phosphorylation is a very common event in all organisms (Eymann *et al.*, 2007; Ficarro *et al.*, 2002; Levine *et al.*, 2006; Macek *et al.*, 2007; Macek *et al.*, 2008). As much as about 5% of all proteins can be phosphorylated in organisms so different as the sporulating bacterium *B. subtilis* and the genome minimalist *Mycoplasma genitalium* (Su *et al.*, 2007). Two major questions remain to be answered: (1) Which kinases are responsible for these phosphorylation events, and (2) what is the effect of the phosphorylation on the activity of the target proteins?

In this work, we addressed the first of these questions. In *B. subtilis*, only five serine/threonine kinases have been studied so far. These are HPr kinase, RsbT kinase, RsbW kinase, and SpoIIAB kinase, involved in the control of sigma factor activities and PrkC (Reizer *et al.*, 1998; Madec *et al.*, 2002; Min *et al.*, 1993). In this work, we focused on PrkC and its relative, PrkD. Indeed, our *in vitro* experiments revealed that PrkC is able to phosphorylate several of the proteins that were found to exist as phosphoproteins *in vivo*.

PrkC is implicated in sporulation, biofilm formation, and germination (Gaidenko *et al.*, 2002; Madec *et al.*, 2002; Shah *et al.*, 2008), but only two substrates (EF-G and PrkC itself) have been identified. Our work confirms that PrkC might be of global importance as it phosphorylates enzymes from different pathways, such as transaldolase, glutamine synthetase, isocitrate dehydrogenase, α -acetolactate decarboxylase, and HPr. However, among the eight phosphoproteins tested for phosphorylation by PrkC, three were not targets of this kinase. A global role for PrkC is supported by studies with other bacteria. In *Staphylococcus aureus*, PrkC phosphorylates glycolytic enzymes (Lomas-Lopez *et al.*, 2007), whereas the α -subunit of RNA polymerase and the phosphoglucosamine mutase are substrates of the *Streptococcus pneumoniae* PrkC homolog, StkP (Nováková *et al.*, 2005). Moreover, PrkC homologs are important for virulence development and global gene expression in *S. pneumoniae*, *S. aureus*, *M. pneumoniae*, and *Bacillus anthracis* (Débarbouillé *et al.*, 2009; Sasková *et al.*, 2007; Schmidl *et al.*, 2010; Shakir *et al.*, 2010). Thus, PrkC can phosphorylate a wide range of proteins involved in a variety of cellular functions.

Another remarkable feature of PrkC is its obvious preference for threonine. This study presents a significant increase of the known phosphorylation sites used by PrkC. Of the sites identified here, 16 are threonines and only 5 are serine residues. In a previous study on PrkC autophosphorylation, 7 phosphorylated threonine residues and one serine residue were reported (Madec *et al.*, 2003). Our results confirm the autophosphorylation of Ser-214 as well as of Thr-290, Thr-313, and Thr-320. We failed to detect the phosphorylation of a stretch of multiple threonine residues in the N-terminal part of PrkC, but instead we detected two phosphorylation sites in the extracellular domain of PrkC that was not included in the previous study (Madec *et al.*, 2003). *In vivo* phosphorylation of PrkC was observed on Thr-290 (Macek *et al.*, 2007), thus providing a confirmation for our *in vitro* study. Studies on protein phosphorylation

by PrkC proteins from *Streptococcus pyogenes* also revealed the use of threonine as the preferred phosphorylation target by PrkC (Jin and Pancholi, 2006). The kinase domains of PrkC and PrkD are very similar to each other (about 30% identical residues). However, the sites of autophosphorylation were not conserved between the two proteins although the only phosphorylation site identified for PrkD was also a threonine. A comparison of the regions around the PrkC-dependent phosphorylation sites revealed little conservation of the primary sequences, suggesting that it is not the primary sequence context that serves for recognition by PrkC.

An interesting aspect of this work is the identification of HPr as a novel target for PrkC. HPr is a paradigm of protein phosphorylation with its His-15 and Ser-46 phosphorylated by enzyme I of the PTS and by the ATP-dependent HPr kinase, respectively (Reizer *et al.*, 1998). Analysis of the *B. subtilis* phosphoproteome revealed the phosphorylation of yet another site, Ser-12. We could attribute this phosphorylation event to the activity of PrkC. This finding suggests that our *in vitro* observations regarding PrkC-dependent protein phosphorylation reflect the *in vivo* activity of PrkC and the physiological interactions with the different target proteins. However, it is not known whether this phosphorylation affects the biological activity of HPr. The weak phosphorylation of Ser-12 by PrkC suggests that this phosphorylation does not affect the properties of the cellular HPr. Similar results have been obtained for the transcription antiterminator GlcT, which can be phosphorylated and inactivated to a minor degree by HPr under conditions in which its full activity is required. Again, this phosphorylation affects only a small fraction of the cellular GlcT pool and, therefore, does not influence GlcT-mediated regulation (Schmalisch *et al.*, 2003).

Our work suggests that PrkC is a protein kinase, which may have global importance in *B. subtilis*. However, important questions remain to be answered: Which other proteins does PrkC phosphorylate? Phosphoproteome studies with *prkC* mutants might be helpful to address this question. Does PrkC-dependent phosphorylation serve for fine-tuning of the metabolism, does it tag the proteins for degradation, or does it serve completely different purposes? Finding the answers to these questions is challenging, but these answers will have a significant impact on our understanding of microbial physiology.

Materials and Methods

Bacterial strains, oligonucleotides, and growth conditions. *B. subtilis* 168 (wild type, laboratory collection) and QB5223 (*ptsHI*) (Martin-Verstraete *et al.*, 1995) were used to isolate chromosomal DNA for the amplification of the desired genes. *E. coli* DH5 and BL21(DE3)/pLysS (Sambrook *et al.*, 1989) were used for cloning experiments and protein expression, respectively. *B. subtilis* was grown in TY medium (1% wt/vol tryptone, 0.5% wt/vol yeast extract, and 1% wt/vol NaCl). *E. coli* was grown in lysogeny broth medium (LB medium), and transformants were selected on plates containing ampicillin (100 g/ml). LB plates were prepared by the addition of 17 g Bacto agar (Difco) per liter of LB medium. The oligonucleotides used in this study are listed in Table 7.

DNA manipulation. Transformation of *E. coli* and plasmid DNA extraction were performed using standard procedures (Sambrook *et al.*, 1989). Restriction enzymes, T4 DNA ligase, and DNA polymerases were used as recommended by the manufacturers. DNA fragments were purified from agarose gels using the QIAquick PCR Purification kit (Qiagen, Germany). *Pfu* DNA polymerase was used for the polymerase chain reaction as recommended by the manufacturer. DNA sequences were determined using the dideoxy chain termination method (Sambrook *et al.*, 1989). All plasmid inserts derived from PCR products were verified by DNA sequencing. Chromosomal DNA of *B. subtilis* was isolated as described (Martin-Verstraete *et al.*, 1995).

Plasmid constructions. The plasmids used for the expression of tagged *B. subtilis* proteins in *E. coli* were constructed using the expression vectors pWH844 (Schirmer *et al.*, 1997) or pGP172 (Merzbacher *et al.*, 2004) that allow the fusion of the cloned proteins to an N-terminal His₆- or *Strep*-tag, respectively. These plasmids are listed in Table 6.

For the expression of the S46A mutant variant of the HPr proteins, plasmid pGP371 was constructed by cloning of the *ptsHI* DNA fragment from *B. subtilis* QB5223 (Table 6). *B. subtilis* HPr kinase and wild type HPr were expressed using pGP205 and pAG2, respectively (Galinier *et al.*, 1997; Hanson *et al.*, 2002).

Tab. 7. Oligonucleotides used in this study.

Oligonucleotide	Sequence (5'→3') ^a
CD13	AA <u>C</u> ATATGGCTAGCTGGAGCCACCCGCAGTTC
eno forw 1	AA <u>G</u> GATCCCATACATTGTTGATGTTTATGCAC
eno rev	TTTCTGCAGTTACTTGTTTAAGTTGTAGAAAGAGTTG
FC17	AA <u>G</u> GATCCGTTGGCACAAGGTGAAAAAATTAC
FC18	TTTCTGCAGTTATTAGTCCATGTTTTTGTAT
JS39	TCTATCAACAGGAGTCCAAGC
NP01	AA <u>A</u> GAGCTCCGATGAAACGAGAAAGCAACATTC
NP02	TTT <u>G</u> GATCCCTATTATTCAGGGCTTCCTTCAGT
NP03	AA <u>A</u> GAGCTCCGGTGCTAATCGGCAAGC
NP04	TTT <u>A</u> GATCTTCATTATTCATCTTTTCGGATACTCAAT
NP05	AA <u>A</u> GAGCTCGATGGATAACAATTGAAAAGAAATCAG
NP06	TTT <u>G</u> GATCCTCATTACTTATTGATTAATGCCTTAAC
NP07	AA <u>A</u> GAGCTCGATGATGAACGACGCTTTGAC
NP08	TTT <u>A</u> GATCTTCATTAGATTAAGAAAAAGATAATA
NP09	AA <u>A</u> GAGCTCGATGGCATTAAACTTCTAAAAAA
NP10	TTT <u>G</u> GATCCTCATTATGTGACCGATTGAATGGC
NP11	AA <u>A</u> GAGCTCGATGTTATTCTTTGTTGATACAG
NP12	TTT <u>G</u> GATCCTCATTATTTGTTCCAGTCTGCC
NP13	AA <u>A</u> GAGCTCGATGGTCAAGTCATTTTCG
NP14	TTT <u>G</u> GATCCTCATTATTTCCCAAAGCCATCAG
NP15	CCGGTGTTACGGTGGCGCCGCTTGG
NP16	CTCACCTGATTCTTTAACAGCTACAGCG
NP17	CTTGCTAAAGCTGCTGGCGAAAAGAAGCTG
NP18	ATCGTGAGCAAAACCCACGGCCAC
NP19	ATGTTACGCGATCAAACCGACGTC
NP20	GCAGCAGCCAACCTCAGCTTCCTTTTCGGGC
SH82	AT <u>G</u> GATCCATGGCACAAAAACATTTAAAG
SH83	ATA <u>A</u> AGCTTCTCGCCGAGTCCTTCG
pWH844 fw	TATGAGAGGATCGCATCACCAT
pyk forw 1	AA <u>G</u> GATCCAGAAAACTAAAATTGTTTGTACCATCGG
pyk rev	TTTCTGCAGTTAAAGAACGCTCGCACGG

^a The restrictions sites are underlined.

Overexpression and purification of recombinant proteins.

E. coli BL21(DE3)/pLysS was used as host for the overexpression of recombinant proteins. Expression was induced by the addition of IPTG (final concentration 1 mM) to exponentially growing cultures (OD₆₀₀ of 0.8). Cells were lysed using a French press (20,000 p.s.i., 138,000 kPa; Spectronic Instruments, UK). After lysis, the crude extracts were centrifuged at 15,000 g for 1 h. For purification of His₆-tagged proteins, the resulting supernatants were passed over an Ni²⁺ HiTrap chelating column (5 ml bed volume, Pharmacia) followed by elution with an imidazole gradient (from 0 to 500 mM imidazole in a buffer containing 10 mM Tris-HCl pH 7.5, 600 mM NaCl, 10 mM β-mercaptoethanol) over 30 ml at a flow rate of 0.5 ml/min. For proteins carrying an N-terminal *Strep*-tag, the crude extract was passed over a Streptactin column (IBA, Göttingen, Germany). The recombinant protein was eluted with desthiobiotin (Sigma, final concentration 2.5 mM).

After elution, the fractions were tested for the desired protein using 12.5% SDS-PAGE gels. The relevant fractions were combined and dialyzed overnight. Protein concentration was determined using the Bio-Rad dye-binding assay with bovine serum albumin serving as the standard.

Assays for protein phosphorylation. Activity assays of potential protein kinases were carried out with purified proteins in assay buffer [10 mM MgCl₂, 25 mM Tris-HCl pH 7.6, 1 mM dithiothreitol, 0.4 mM [γ-³²P]ATP (480 Ci/mmol)] using purified target proteins. For assays of HPr kinase activity, fructose 1,6-bisphosphate was added to a final concentration of 25 mM. The assays were carried out at 37°C for 30 min followed by thermal inactivation of the enzyme (10 min at 95°C). The assay mixtures were analyzed on 16% SDS-PAGE gels. Proteins were visualized by Coomassie staining.

Protein identification by mass spectrometry. Peptide preparation was carried out as recently described (Eymann *et al.*, 2007). Excised polyacrylamide gel pieces of stained protein bands were washed with 100 μl of 200 mM NH₄HCO₃ in 50% CH₃CN for 20 min at 37°C and dried in a vacuum centrifuge for 20 min. In-gel digestion with trypsin (Promega, Madison, Wisc., USA) was performed overnight at 37°C. After addition of 15 μl formic acid (5%, v/v), samples were incubated in an ultrasonic bath for 20 min. The supernatant was transferred into microsample vials and stored for LC-MS/MS analysis at 4°C.

LC-MS/MS analysis was performed using either an LTQ Orbitrap mass spectrometer (Thermo Electron, San Jose, Calif., USA) in conjunction with a nanoACQUITY UPLC™ system (Waters, Milford, Mass., USA) or a Q-Star Pulsar mass spectrometer (Applied Biosystems MDS Sciex) in conjunction with the Ettan MDLC system (GE Healthcare, Munich, Germany).

In the nanoACQUITY UPLC system, peptides were loaded onto a trapping column (nanoAcquity UPLC Column, Symmetry® C₁₈ 5 µm, 180 µm × 20 mm, Waters) and washed for 3 min with 99% buffer A (0.1% v/v formic acid) at a flow rate of 10 µl/min and separated on an analytical column (BEH130 C₁₈ 1.7 µm, 100 µm × 100 mm, Waters) in a linear gradient from 99% buffer A to 60% buffer B (90% v/v acetonitrile, 0.1% v/v acetic acid) in 80 min. The flow rate during elution was set to 1 µl/min. In the Ettan MDLC system, the peptides were loaded onto a trapping column (µ-Pre-column, PepMap™, C₁₈, 300-µm i.d. × 5 mm, LC Packings), washed for 15 min with buffer A and separated onto the analytical column (PepMap, C₁₈, 75-µm i.d. × 15 cm, LC Packings) by formation of a 70-min gradient of 99% buffer A to 60% buffer B at a flow rate of 200 nl/min.

The LTQ Orbitrap was employed to acquire a full Orbitrap survey scan in the range *m/z* 300-2,000. Subsequently, MS/MS experiments of the three most abundant precursor ions were carried out in the LTQ. Meanwhile, the masses of the precursor ions were determined with high accuracy via single-ion mode scans in the Orbitrap cell of the mass spectrometer. The Q-Star system was used to carry out a survey scan in the mass range of *m/z* 230-2,000 in the first step. In a second step, up to four precursor ions were selected for a fragmentation in MS/MS experiments. Product ions were detected in the range of *m/z* 70-2,000. The data were analyzed as described (Eymann *et al.*, 2007).

Acknowledgments

Oliver Schilling, Sven Halbedel, and Christina Herzberg are acknowledged for their help with some experiments. Finally, we wish to express our gratitude to Josef Deutscher and Boris Görke for their interest in this work and their valuable suggestions. This work was supported by grants of the Deutsche Forschungsgemeinschaft, the Fonds der Chemischen Industrie, and the BMBF (SYSMO, PtJ-BIUO/0313978D) to J. S.

Chapter 5

Upregulation of thymidine kinase activity compensates for loss of thymidylate synthase activity in *Mycoplasma pneumoniae*

The work described in this chapter was published in:

Wang, L., C. Hames, S. R. Schmidl, and J. Stülke. 2010. Upregulation of thymidine kinase activity compensates for loss of thymidylate synthase activity in *Mycoplasma pneumoniae*. *Mol. Microbiol.* **77**: 1502-1511.

Author contributions:

This study was designed and interpreted by LW. CH isolated the *thyA* transposon mutant. LW performed all experiments and SRS contributed to the slot blot analysis of the thymidine kinase gene. LW wrote the paper.

Summary

Thymidylate, an essential building block of DNA, is synthesized either from deoxyuridylate by thymidylate synthase (TS) or thymidine (dT) by thymidine kinase (TK). Thymidylate kinase (TMPK) phosphorylates dTMP to dTTP. Thymidine phosphorylase (TP) catalyses reversible phosphorolysis of dT. Using transposon mutagenesis, *Mycoplasma pneumoniae* TS gene (*thyA/mpn320*) was interrupted and requirement of this enzyme was studied. We found that TK activity and transcript levels and TP activity, but not TMPK or TS activity, are growth-phase-regulated, with induction at the exponential growth phase and a decline after the stationary phase. Inactivation of *thyA* results in upregulation of TK transcript and a 10-fold increase in TK activity, reduced TMPK level and it had no effect on TP activity. The level of [³H]-dT uptake and incorporation into DNA in the *thyA* mutant correlates with increases in TK activity, suggesting that dT uptake and metabolism is TK-dependent and that upregulation of TK activity in the *thyA* mutant compensates for the lack of ThyA activity. [³H]-dU uptake was low compared with dT, and incorporation of radioactivity into DNA in the *thyA* mutant indicates the presence of an alternative TS. Our results suggest that TK and TMPK are potential targets for the development of *Mycoplasma*-specific antibiotics.

Introduction

Mycoplasmas, of the class Mollicutes, phylogenetically belong to the family of Gram-positive bacteria and lack a cell wall. Several species are pathogenic to humans, including *M. pneumoniae*, *Mycoplasma genitalium* and *Ureaplasma urealyticum*. *M. pneumoniae* is spread through respiratory droplet transmission. Once attached to the mucosa, *M. pneumoniae* can cause pharyngitis, bronchitis, and pneumonia. *M. pneumoniae* has also been associated with a wide variety of extrapulmonary diseases, including central nerve system manifestation, such as encephalitis, aseptic meningitis, acute transverse myelitis, stroke, and polyradiculopathy (Narita, 2009; Narita, 2010; Tsiodras *et al.*, 2005; Waites and Talkington, 2004). Because of the lack of a cell wall, mycoplasmas are unaffected by antibiotics targeting cell wall synthesis, such as penicillin.

Thymidylate is an essential building block for DNA synthesis. In Mollicutes there is a general lack of enzymes in the *de novo* synthesis of purines and pyrimidines and therefore nucleotide biosynthesis begins with bases, nucleosides or deoxynucleosides, e.g. through the salvage pathway. As depicted in Fig. 19 thymidylate (dTMP) is synthesized either from deoxyuridylate (dUMP) by thymidylate synthase (TS), which catalyses the transfer of a methyl group from methylenetetrahydrofolate to dUMP, or from thymidine (dT) by thymidine kinase (TK), which catalyses the transfer of a gamma phosphate group from ATP to the 5'-OH group of dT to form dTMP. Deoxyuridine (dU) can also be phosphorylated by TK to generate dUMP. Thymidylate kinase (TMPK) phosphorylates dTMP to dTDP, which can be further phosphorylated to dTTP by pyruvate kinase (Pyk) (Pollack *et al.*, 2002) or TMPK (Wang, 2007). Both dT and dU can be degraded to their respective base by thymidine phosphorylase (TP) (Fig. 19). Pathway analysis of the *M. pneumoniae* genome by Pachkov *et al.* (2007) suggested that dTTP production can limit *M. pneumoniae* growth rate, even under optimal conditions, and pyrimidine metabolism appears to be more appropriate as a drug target due to its low plasticity.

A recent study using defined minimum medium showed that cytidine alone could provide all pyrimidines, and further addition of thymine promoted *M. pneumoniae* growth, but adding uracil had no such effect. Their study indicated that enzymes required for pyrimidine nucleotide biosynthesis, such as ribonucleotide reductase and thymidylate synthase, are active *in vivo* (Yus *et al.*, 2009). However, there are no experimental data regarding the activities of *M. pneumoniae* enzymes in dTTP synthesis pathway.

Thymidine kinase (Tdk, MPN044), TMPK (MPN006), TP (MPN064) and TS (ThyA, MPN320) have been annotated in the *M. pneumoniae* genome. The amino acid sequences of *M. pneumoniae* TK and TMPK show high identity (~40%) to *Ureaplasma* TK and TMPK, which have been characterized in detail (Carnrot *et al.*, 2003; Kosinska *et al.*, 2005; Wang, 2007; Welin *et al.*, 2004). *M. pneumoniae* TS (ThyA, MPN320) shows high sequence homology to mammalian and bacterial ThyA proteins. Previous studies demonstrated that TK and TMPK are essential for the survival of *M. genitalium* and *M. pneumoniae*, but that TP and TS are dispensable (Glass *et al.*, 2006; Hutchison *et al.*, 1999).

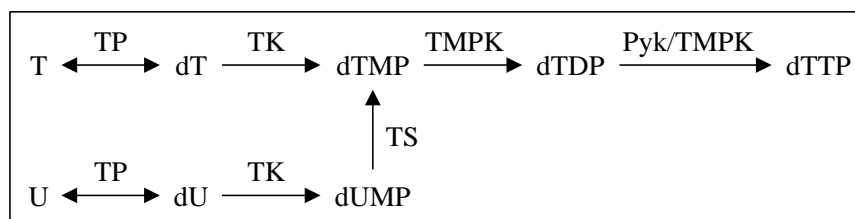


Fig. 19. Simplified dTTP synthesis pathway in mycoplasmas. In Mollicutes genomes nucleoside diphosphate kinase (Ndk), an enzyme responsible for the phosphorylation of nucleoside diphosphates to triphosphates has not been identified; however, it has been shown experimentally that glycolytic enzymes, such as Pyk (Pollack *et al.*, 2002), or TMPK (Wang, 2007) are able to phosphorylate dTDP to dTTP, and they were suggested to replace Ndk function in Mollicutes. dT, thymidine; T, thymine; dTMP, thymidine 5'-monophosphate; dTDP, thymidine 5'-diphosphate; dTTP, thymidine 5'-triphosphate; dU, deoxyuridine; U, uracil; dUMP, deoxyuridine 5'-monophosphate; TK, thymidine kinase; TMPK, thymidylate kinase; TS, thymidylate synthase; TP, thymidine phosphorylase; Pyk, pyruvate kinase.

The transposon mutagenesis technique was used to interrupt the *M. pneumoniae* TS gene (*thyA/mpn320*) to study the interactions of enzymes in the dTTP synthesis pathway in relation to *M. pneumoniae* growth. We found that TK and TP activities are closely regulated to *M. pneumoniae* growth but not TS and TMPK. Inactivation of the *thyA* gene resulted in upregulation of *tdk* (TK) gene transcription and increased TK activity and reduced TS and TMPK activity. Metabolic labelling with [³H]-dT shows a high level of [³H]-dT uptake and incorporation in the *thyA* mutant. However, [³H]-dU was primarily metabolized to ribonucleotides and incorporation into DNA was low. These data suggest that dT salvage through TK and TMPK is rate-limiting in dTTP synthesis and upregulation of TK activity compensated for the loss of ThyA activity in the *thyA* mutant.

Results

Characterization of the *thyA* mutant. The *thyA* (*mpn320*) mutant *M. pneumoniae* strain was generated by the global transposon mutagenesis procedure, as previously described (Halbedel *et al.*, 2006). Transposon insertion site into the *thyA* locus was after nucleotide 653. Wild type and the mutant strain were cultured according to standard protocol using modified Hayflick medium. Total proteins were extracted and TS activity was determined using [³²P]-dUMP as the substrate. TS activity was detected in both strains (Fig. 20A).

The presence and absence of ThyA protein was determined by labelling with radioactive 5-fluorodeoxyuridine monophosphate (5FdUMP), which forms a covalent complex with ThyA proteins together with methylenetetrahydrofolate. Total protein extracts were incubated in a reaction mixture containing [32 P]-5FdUMP and methylenetetrahydrofolate. The reactions were stopped by addition of Laemmli sample buffer, and the samples were analysed by SDS-PAGE and autoradiography. A radiolabeled protein band corresponding to the size of ThyA protein (MPN320, with calculated molecular weight of 33.46 kDa) was seen in the wild type but not in *thyA* mutant strain (Fig. 20B), as expected. The presence of TS activity but not ThyA protein in the *thyA* mutant strain indicates the presence of an alternative TS.

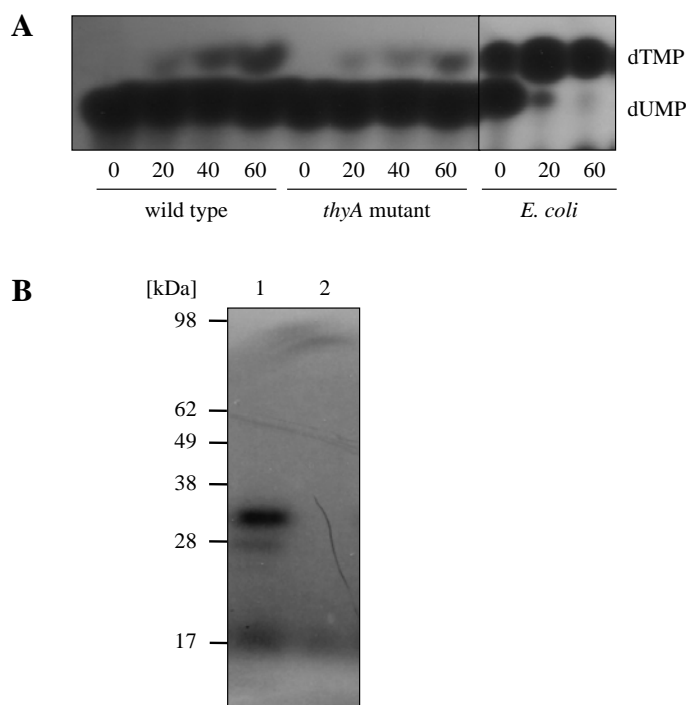


Fig. 20. Characterization of *thyA* mutant. (A) TS activity determined with [32 P]-dUMP as the labeled substrate. *E. coli* extracts was used as positive control. The reaction products were resolved by TLC and visualized by autoradiography. (B) Ternary complex formation of ThyA protein with [32 P]-5FdUMP and methylenetetrahydrofolate. Lane 1, wild type; Lane 2, *thyA* mutant.

The levels of TK, TP, TS, and TMPK activity. The activities of enzymes in dTTP synthesis were determined in protein extracts from both *M. pneumoniae* strains. TK activity was elevated (> 10-fold) in the *thyA* mutant, compared with the wild type (Table 8). TMPK activity was lower in the mutant strain as compared with wild type cells. The difference in TP activity in the *thyA* mutant and wild type strain was not statistically significant. There was also detectable TS activity in the *thyA* knockout strain (Table 8). We have also observed great variation in TK and TP activity in cultures that were harvested at different time points and/or had a different number of cells in the starting culture (inoculum size) (data not shown).

Tab. 8. Specific activities of enzymes in dTTP synthesis (nmol/(min mg)).

	Wild type	<i>thyA</i> mutant	<i>P</i> -value ^a
TK	1.10 ± 0.07	13.20 ± 0.30	< 0.001
TMPK	0.14 ± 0.01	0.083 ± 0.003	0.002
TP	2.65 ± 0.20	3.27 ± 0.09	0.170
TS	1.14 ± 0.10	0.0012 ± 0.0004	< 0.001

^a Statistical analysis was performed by Student's *t*-test and *P*-value < 0.05 indicates significant difference. Results are mean ± standard error from four to six measurements.

Activities of dTTP synthesis enzymes in relation to *M. pneumoniae* growth.

The above results warranted a further study of the levels of these enzymes at different phases of *M. pneumoniae* cell growth. Wild type and *thyA* mutant cells were cultured over an extended period (8 days) and harvested at 24 h intervals. *M. pneumoniae* growth was monitored daily by color change of the culture medium measured by OD₅₅₀ value, pH value of the medium, and cell pellet wet weight at harvest. There was no observable difference in growth between the two strains. Total proteins were extracted and enzyme activities and proteins levels were determined.

Thymidine kinase activity and transcript levels. There was a sharp increase in TK activity from day 2 to day 3 in wild type cells and activity peaked at day 4, decreasing to basal levels thereafter (Fig. 21A). In *thyA* mutant cells, TK activity increased at day 2 and reached the maximum level at day 3, remaining at this level until decreasing at day 6 (Fig. 21A). Interestingly, TK activity at each time point was 4-5 times higher in *thyA* mutant cells compared with wild type.

Thymidine kinase transcript levels, determined by slot blot analysis of total RNA, showed a similar pattern as TK activity profiles in both wild type and *thyA* mutant (Table 9 and Fig. 21B). In wild type cells there was a sharp increase in TK transcript from day 2, peaked at day 3, and then decreased. In *thyA* mutant cells TK transcript level increased from day 2, reached maximum at day 3, remained at relative high level at day 4 and 5, and then decreased to basal level at day 6 (Table 9 and Fig. 21B). At day 1 and day 2 TK transcripts in *thyA* mutant were at similar levels as wild type and upregulation of TK transcript levels in *thyA* mutant was observed from day 3 to day 6 with the exception that at day 4 the levels were similar in both strains (Table 9).

By comparing TK transcript and activity profiles, we observed that in wild type cells TK transcript levels peaked at day 3, but activity reached maximum at day 4 while in *thyA* mutant cells both TK transcript and activity reached maximum levels at day 3 and remained at high levels from day 3 through day 5, at day 6 TK transcript decreased to basal level, but TK activity still remained at highest level. These observations indicated that there is a clear difference in transcriptional and translational regulation as well as TK protein degradation in wild type and *thyA* mutant.

Thymidylate kinase activity. The TMPK activity increased approximately 25% from day 1 to 3 in wild type cells and stayed at a similar level throughout the culture period. In contrast, TMPK activity began decreasing in *thyA* mutant strains from day 3 resulting in about a 25% decrease from starting levels by the end of the culture period (Fig. 21C), and thus the mutant strain had lower TMPK activity at the end of the culture period compared with wild type cells (Fig. 21C). In general, TMPK activity was much lower compared with TK activity in both strains, suggesting that the second and third phosphorylation by TMPK is rate-limiting in dTTP synthesis.

The TMPK reaction products were analysed by the TLC technique and revealed that the majority (~75%) of the products were dTTP (data not shown). These data suggest that TMPK is capable of functioning as a nucleoside diphosphate kinase, as was demonstrated earlier with the *Ureaplasma* TMPK (Wang, 2007).

Thymidine phosphorylase activity. In both strains, TP activity increased during the exponential growth phase, reached a peak value at day 3, and then decreased to the end of the culture period. In wild type and *thyA* mutant cells the levels of TP activity were similar (Fig. 21D).

Tab. 9. TK transcript levels in different growth phases.

	Wild type ^a	<i>thyA</i> mutant ^a	Wild type/ <i>thyA</i> mutant ^b
Day 1	1.00	1.00	1.06 ± 0.06
Day 2	1.48 ± 0.07	1.53 ± 0.05	0.98 ± 0.09
Day 3	3.36 ± 0.10	5.04 ± 0.17	1.63 ± 0.12
Day 4	2.54 ± 0.08	2.55 ± 0.06	1.03 ± 0.05
Day 5	1.03 ± 0.08	2.48 ± 0.12	2.30 ± 0.10
Day 6	0.21 ± 0.14	0.47 ± 0.11	4.28 ± 0.24

^a TK transcript levels relative to day 1 (set to 1.00).

^b TK transcript levels in *thyA* mutant relative to wild type. Results are mean ± standard error from three measurements.

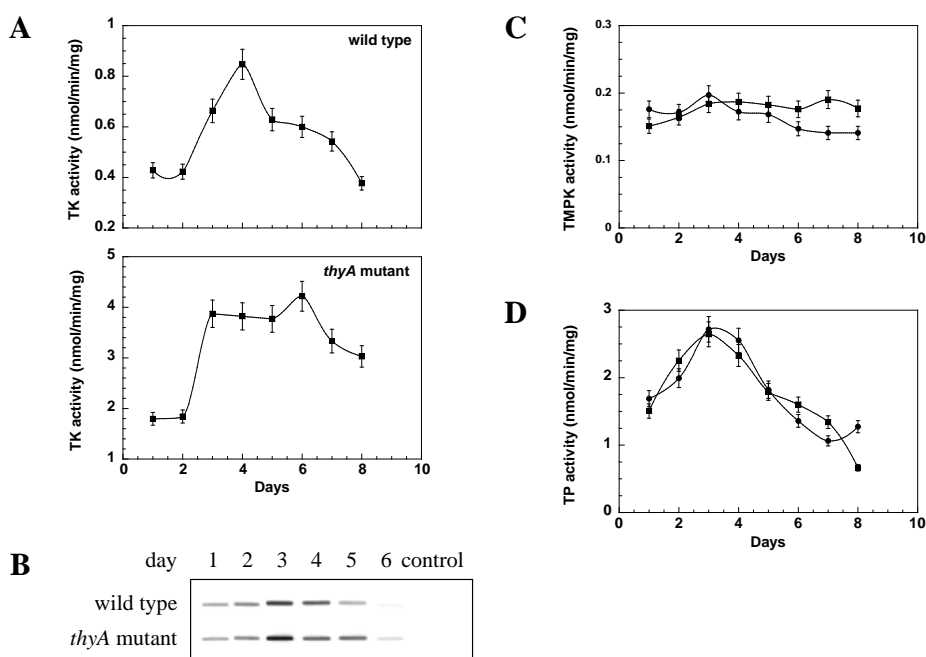


Fig. 21. TK activity (A) and transcript (B) levels in different growth phases. TK activity was determined using a radiochemical assay with [³H]-dT as substrate and total proteins extracts. TK transcript levels were determined by slot blot analyses of total RNA. A dilution series of RNA was blotted onto a positively charged nylon membrane and probed with a DIG-labeled riboprobe specific for an internal part of TK. Signals obtained with 1 µg of RNA are shown. Yeast tRNA (upper) and *M. pneumoniae* chromosomal DNA (lower) served as controls. TMPK (C) and TP (D) activity in different growth phases. Wild type (square) and *thyA* mutant (dot).

Thymidylate synthase activity and protein levels. The TS activity was measured by using the tritium-release assay with [5-³H]-dUMP as the labeled substrate. The activity levels in wild type cells decreased over the next 8 days, resulting in approximately 25% lower activity. In the *thyA* mutant strain there was detectable TS activity, approximately 0.1% of wild type TS activity in the starting cultures (Fig. 22A).

ThyA protein levels were determined by covalent labelling with [³²P]-5FdUMP. SDS-PAGE and autoradiography analysis revealed only one detectable radiolabeled band, which corresponded to the size of the ThyA protein in the wild type (Fig. 22B). The intensity of the ThyA protein band at each time point was similar, indicating that the ThyA protein is constitutively expressed. Therefore, the observed decrease in TS activity in wild type cells was not due to decreased protein expression. These data indicate that there may be other factors that are modulated during culture and regulate ThyA activity. As expected, no radiolabeled protein was detected in the *thyA* mutant strain (Fig. 22B).

[³H]-dT metabolism. The uptake and metabolism of dT was measured in both *M. pneumoniae* strains using tritium-labeled dT (Table 10). The level of uptake was high in the *thyA* mutant strain, approximately fourfold compared with wild type cells. In both strains, < 1% of total uptake radioactivity was detected in the soluble nucleosides and nucleotides, and > 99% was found in the insoluble fraction. High-performance liquid chromatography (HPLC) analysis of the soluble fractions revealed that the radiolabeled substances were thymine, dT, dTMP, dTDP, and dTTP (Fig. 23A). There was also an unidentified radiolabeled peak that eluted at an earlier time in both strains, possibly a degradation product of thymine.

The absolute levels of soluble nucleoside and nucleotides were approximately four times higher in *thyA* mutant cells compared with wild type cells. The absolute amount of radioactivity incorporated into DNA was three times higher in the *thyA* mutant compared with wild type strain (Table 10).

Analysis of the medium revealed that the majority of remaining unincorporated radiolabeled compounds was [³H]-thymine, indicating degradation of [³H]-dT by TP (Table 10).

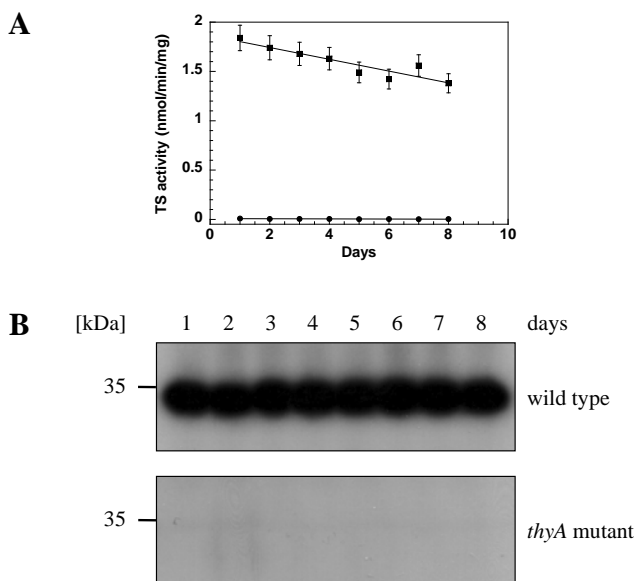


Fig. 22. TS activities (A) and protein levels (B) at different growth phases. TS activity determined using the tritium release assay. Wild type (square) and *thyA* mutant (dot). ThyA protein levels were determined by [³²P]-5FdUMP and methylenetetrahydrofolate labelling.

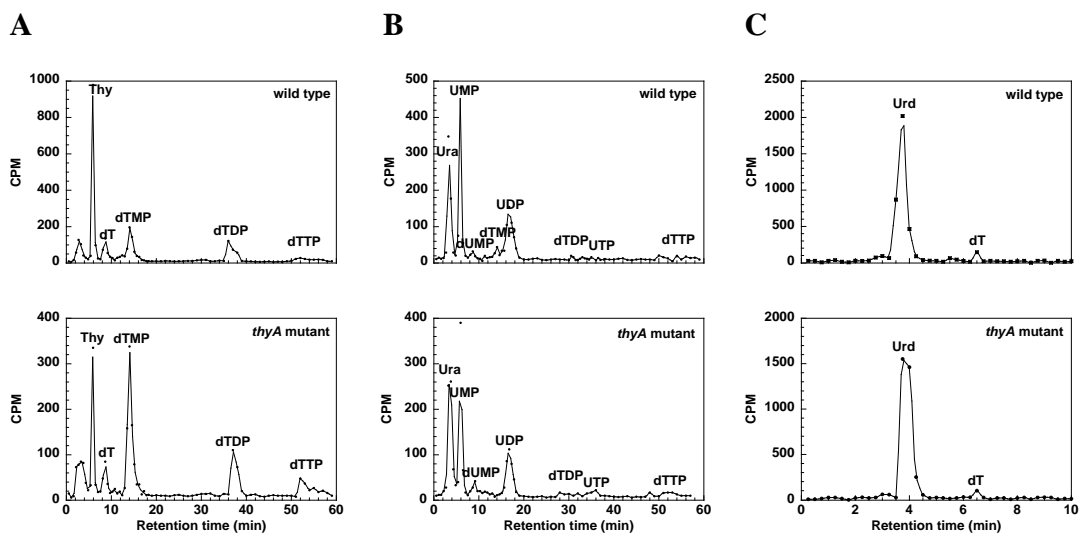


Fig. 23. HPLC analysis of acid soluble and insoluble extracts from wild type and *thyA* mutant strains. (A) [³H]-dT metabolism acid soluble extracts. (B) [⁶⁻³H]-dU metabolism acid soluble extracts. HPLC fractions (0.5 ml) were collected and the radioactivity was counted. (C) [⁶⁻³H]-dU metabolism acid insoluble fractions after treatment with NaOH and alkaline phosphatase. HPLC fractions (0.2 ml) were collected and the radioactivity was counted. Retention times for standards were: 3.23 min (uracil), 3.75 min (uridine), 4.58 min (dU), 5.80 min (UMP), 8.22 min (dUMP), 16.41 min (UDP), 36.7 min (UTP), 5.87 min (thymine), 8.75 min (dT), 14.35 min (dTMP), 31.9 min (dTDP), and 56.2 min (dTTP).

Tab. 10. [³H]-dT metabolism in wild type and *thyA* mutant *M. pneumoniae* strains^a.

	Wild type	<i>thyA</i> mutant
Total uptake (%)	19 ± 5	82 ± 2
PCA-soluble extracts (total counts)	16,830 ± 1,600	60,264 ± 6,500
% of total uptake	0.6 ± 0.3	0.7 ± 0.2
NaOH-soluble fraction (total counts)	1,455,915 ± 15,000	4,768,860 ± 45,000
% of total uptake	99.4 ± 0.3	99.3 ± 0.2
Medium analysis after removal of cells		
[³ H]-dT (%)	31 ± 13	15 ± 5
[³ H]-Thymine (%)	69 ± 12	85 ± 5

^a Data were from four independent incubations and represented as the mean ± standard error. Total uptake was calculated as radioactivity recovered in total extracts (soluble and insoluble) as compared with total radioactivity in the medium before incubation start.

[6-³H]-dU metabolism. A similar approach was performed using [6-³H]-dU to determine the role of TS in dTTP synthesis in wild type and *thyA* mutant strains (Table 11). The level of uptake was low in the *thyA* mutant strain at approximately 0.57%, while the level of uptake in wild type cells was at approximately 2.6%. In wild type strain, approximately 5% of total uptake was found in the soluble nucleosides and nucleotides, and approximately 95% was found in the insoluble fraction. In the *thyA* mutant strain, 10% of total uptake was incorporated into soluble nucleoside and nucleotides and 90% of the total radioactivity was recovered in the insoluble fraction. HPLC analysis of soluble nucleotides revealed that the radiolabeled compounds were predominantly uracil, UMP, and UDP, indicating that dU was degraded to uracil and further metabolized to ribonucleotides. Tritium-labeled dUMP and dTMP were detected at low levels in the wild type strain, but there was no detectable tritium-labeled dTMP in the *thyA* mutant strain (Fig. 23B). There was no [³H]-dU detected in the soluble fractions. Trace amounts of radiolabeled dTDP and dTTP were also detected (Fig. 23B).

The absolute levels of soluble nucleotides were low in *thyA* mutant compared with wild type cells (Table 10). The absolute amount of radioactivity in the insoluble fraction was six times lower in the *thyA* mutant than in wild type cells (Table 11).

The PCA-insoluble fractions were solubilized with NaOH, neutralized and treated with alkaline phosphatase before HPLC analysis. Two radioactive peaks were detected in both strains, one with a retention time of 3.95 min (Urd) and the other with a retention time of 6.35 min (dT), indicating that there was thymidylate incorporated into

DNA even in the *thyA* knockout strain (Fig. 23C). The amount of [³H]-dT recovered from HPLC analysis of PCA-insoluble fractions in both wild type and the *thyA* mutant were only ~1% of the total radioactivity in these fractions, which indicated that 99% of the radioactivity originated from [6-³H]-dU was incorporated into RNA as uridine ribonucleotide.

Analysis of the medium showed that the remaining radiolabeled compounds were [³H]-uracil and [³H]-dU, indicating that [³H]-dU had been degraded (Table 11).

Tab. 11. [³H]-dU metabolism in wild type and *thyA* mutant *M. pneumoniae* strains^a.

	Wild type	<i>thyA</i> mutant
Total uptake (%)	2.6 ± 0.1	0.57 ± 0.10
PCA-soluble extracts (total counts)	15,510 ± 987	6,435 ± 650
% of total uptake	4.3 ± 0.5	10.3 ± 0.2
NaOH-soluble fraction (total counts)	276,750 ± 2540	46,230 ± 2,347
% of total uptake	95.7 ± 0.7	90.3 ± 0.4
Medium analysis after removal of cells		
[³ H]-dU (%)	34 ± 6	48 ± 5
[³ H]-Uracil (%)	66 ± 7	52 ± 5

^a Data were from three independent experiments and given as mean ± standard error. Total uptake was calculated as radioactivity recovered in total extracts (soluble and insoluble) as compared with total radioactivity in the medium before incubation start.

Discussion

In mycoplasmas there are only a few enzymes involved in the biosynthesis of dTTP (Fig. 19), an essential precursor for DNA synthesis, as compared with their hosts. The corresponding mammalian enzymes, including TK, TMPK, TP, and TS, have been well studied, and their activity levels have been shown to be tightly regulated throughout the cell cycle, with the highest levels in S-phase (Gasparri *et al.*, 2009; Ke and Chang, 2004). However, little is known regarding cell cycle regulation of bacterial enzymes. Here we show that *M. pneumoniae* TK, at both activity and transcript levels, is regulated during the growth phase, with a clear induction in the exponential growth phase and a drastic decline during the stationary phase. The *M. pneumoniae* TK activity profile in wild type cells correlates with the rate of DNA synthesis (Yus *et al.*, 2009). Compared with wild type both TK activity and transcript levels were upregulated in *thyA* mutant, and the differences seen in TK expression profiles in wild type and *thyA*

mutant indicate that there is a cross-talk in transcriptional and translational regulation of *tdk* (TK) and *thyA* genes. Inactivation of *thyA* resulted in the upregulation of *tdk* gene transcription, which leads to induction of TK protein and increased TK activity, as a mechanism to compensate the loss of *thyA*. The upregulation and prolonged period of high TK activity in the *thyA* mutant strain indicates the importance of TK activity in dTTP synthesis and DNA replication in compensating for the lack of ThyA activity. In contrast to mammalian enzymes, *M. pneumoniae* TMPK activity varies only slightly during the culture period in both wild type and the *thyA* mutant strain. In wild type ThyA protein remained at similar levels during culture; however, TS activity decreased over time. In the *thyA* mutant a very low level of TS activity was detected, indicating the presence of an alternative TS enzyme. Similar to TK, TP activity was induced at the exponential growth phase and decreased at the stationary phase. The level of TP activity was similar in wild type and *thyA* mutant cells. Collectively, these results suggest that ThyA and TMPK are constitutively expressed and inactivation of the *thyA* gene results in the induction of TK.

Increased salvage of dT in *thyA* mutant compensates for the lack of ThyA activity. Metabolic labelling studies with dT and dU showed that both nucleosides or bases can be taken up, metabolized, and incorporated into DNA, confirming the activity of additional enzymes in the dTTP synthesis pathway. Furthermore, there was higher level of dT than dU uptake in wild type cells, indicating *M. pneumoniae* salvages dT more efficiently than dU. Radiolabeled dT was converted to the corresponding nucleotides and efficiently incorporated into DNA. However, [³H]-dU was recovered mainly as ribonucleotides and the amount of radioactivity in the form of dUMP and dTMP was < 5% of the total soluble fraction and total incorporation into DNA was only about 1%. These data indicate that the efficiency of ribonucleotide reduction and conversion of dUMP to dTMP was low.

The level of dT uptake and incorporation into DNA in the *thyA* mutant correlates with increases in TK activity, suggesting that dT uptake and metabolism is TK-dependent and upregulation of TK activity in *thyA* mutant cells is apparently compensating for the lack of ThyA activity. Our results also indicate that the efficiency of dTTP synthesis via UDP reduction was low compared with the direct salvage of dT, explaining why *thyA* is not essential.

Metabolism of dU and thymidylate synthases. The uptake of [³H]-dU was low compared with dT uptake in wild type cells, and uptake and incorporation of [³H]-dU into macromolecules were greatly reduced in the *thyA* knockout strain. HPLC analysis revealed that the radiolabeled compounds were mainly ribonucleotides and no detectable [³H]-dU was present in the soluble fractions, suggesting that [³H]-dU has been degraded to uracil and subsequently taken up and converted to ribonucleotides via uracil phosphoribosyltransferase (MPN033). The low level of uracil uptake in the *thyA* mutant indicates that inactivation of the *thyA* gene may affect uracil uptake and/or uracil phosphoribosyltransferase activity. This is the first experimental proof that connects the pentose phosphate pathway to nucleotide metabolism in *M. pneumoniae*. These results also explain why dU uptake is not TK-dependent.

The TS activity in the *thyA* mutant was only approximately 0.1% of activity in wild type cells. Incorporation of radioactive thymidylate into DNA originated from [³H]-dU in *thyA* mutant cells, indicating the presence of an alternative TS in *M. pneumoniae*. Nonetheless, our study indicates that dTTP synthesis via ribonucleotide reduction and methylation of dUMP by ThyA is not efficient in *M. pneumoniae*.

Thymidine/thymine, but not uracil, promotes *M. pneumoniae* growth. Yus *et al.* (2009) showed that purine and pyrimidine composition in the minimum defined medium can be replaced by ribonucleosides, but not deoxyribonucleosides, and that thymidine can be metabolized to some extent, but not thymine. Furthermore, addition of thymine increases *M. pneumoniae* growth when added with cytidine. In our metabolic study, we did not observe any difference in growth rate since we used enriched medium (modified Hayflick medium). When the medium was analysed at the end of the culture period most of the radiolabeled dT and dU were degraded; therefore, both thymine and uracil were present. We showed that dT, thymine, and uracil, but not dU, were taken up and metabolized. These data suggest that there may be specific transporters for bases and ribonucleosides and *M. pneumoniae* may lack such transporters for deoxynucleosides. Our study also indicates that the expression of TP may be influenced by nutrition status, since *M. pneumoniae* apparently was not able to degrade dT or dU and/or salvage thymine in the minimum defined medium (Yus *et al.*, 2009). The uptake of uracil was less efficient as compared with dT/thymine and the level of dTTP synthesized through UDP reduction was very low. However, thymine/dT can be efficiently salvaged to thymidine nucleotides (dTTP) through the combined

action of TP, TK, and TMPK, and increased dTTP synthesis promotes *M. pneumoniae* growth. Our results suggest that the slow division rate of *M. pneumoniae* is most likely due to inefficient dTTP synthesis.

Inhibition of *M. pneumoniae* dTTP synthesis as a therapeutic target. Mycoplasmas cause a wide variety of diseases and have also been associated with cancer (Narita, 2009; Narita, 2010; Waites and Talkington, 2004). Persistent *Mycoplasma* infection induced malignant transformation of human cells, as shown in a recent study (Namiki *et al.*, 2009). *Mycoplasma* infections can reduce the effect of anticancer nucleoside analogues due to degradation by *Mycoplasma* enzymes (Liekens *et al.*, 2009). Therefore, it may be beneficial to treat *Mycoplasma* infections in cancer patients who receive nucleoside analogues as chemotherapeutic agents. Current antibiotics used in treating *Mycoplasma* infections are effective but clinical antibiotic resistant *Mycoplasma* strains are emerging (Morozumi *et al.*, 2010). In addition, mycoplasmas are slow growing and therefore long-term treatment is required, which may lead to the emergence of antibiotic resistance in other bacteria species. Therefore, new targets for developing specific antibiotics against *Mycoplasma* are needed.

DNA synthesis requires dTTP, which is an essential building block, thus, blocking dTTP synthesis would lead to thymine deficiency-induced cell death. Inhibition of pyrimidine uptake and/or conversion to thymidine nucleotides would impair *Mycoplasma* dTTP synthesis and lead to cell death. Therefore, TK and TMPK are potential targets for future development of antibiotics against *Mycoplasma* infections.

Experimental procedures

Materials. Radiolabeled compounds [methyl-³H]-thymidine (dT, 20 Ci/mmol) and [γ -³²P]-ATP (3,000 Ci/mmol) were purchased from PerkinElmer. [5-³H]-dUMP (deoxyuridine 5'-monophosphate, 47 Ci/mmol) and [6-³H]-deoxyuridine (dU, 45 Ci/mmol) were bought from Moravek Biochemicals. [³²P]-5FdUMP, [³²P]-dUMP, and [³H]-dTTP were synthesized enzymatically using *Ureaplasma* thymidine kinase with [³²P]-ATP or [³H]-dT as the labeled substrate and purified (Carnrot *et al.*, 2003). Rabbit anti-MPN358 antibodies were produced by using synthetic peptides chosen from MPN358 sequence as antigens (GenScript Corp.) and antisera were used directly in Western blot analysis without further purification.

***Mycoplasma* culture and protein extraction.** *M. pneumoniae* wild type and the *thyA* mutant strains were cultured in modified Hayflick medium, as described previously (Halbedel *et al.*, 2004).

Time-course study. Culture was started (day 0) by the addition of 1 ml stock (OD₅₅₀, ~0.7) to a 25-cm² flask containing 25 ml fresh medium and incubated at 37°C with 5% CO₂. Culture optical density was monitored at 550 nm daily and cells harvested at 24 h intervals by centrifugation at 7,000 g for 30 min. Pellets were washed three times with phosphate-buffered saline (PBS) and then resuspended in protein extraction buffer. Total proteins were extracted as previously described (Wang *et al.*, 2001). Protein concentration was determined by Bio-Rad protein assay using BSA as a standard, according to the manufacturer's protocol.

Metabolic labelling with [methyl-³H]-dT and [6-³H]-dU. A stationary phase culture was resuspended in 6 ml fresh medium in a 25-cm² flask and used as stock. One milliliter stock culture was added to a 25-cm² flask containing 25 ml fresh medium with 1 µCi/ml [methyl-³H]-dT or [6-³H]-dU (1 µM dT or dU) and incubated at 37°C. After 5 days the cultures were harvested by centrifugation, washed three times with PBS, and divided into three aliquots and saved at -20°C for further analysis. Soluble nucleotides were extracted with 100 µl of 10% PCA (perchloric acid), followed by centrifuge at 16,000 g for 15 min. The supernatant was transferred to a new tube and neutralized with KOH and the insoluble salt (KClO₄) was removed by centrifugation. The supernatant containing nucleotides and nucleosides was analysed directly by TLC and/or HPLC to determine the amount of radiolabeled nucleoside tri-, di-, and monophosphates. To extract nucleotides from the insoluble fraction, pellets were washed twice with 10% PCA, followed by addition of 100 µl 1 M NaOH and incubation at 60°C for 2 h with shaking, and incorporation of radioactivity was then counted using a liquid scintillation counter (Beckman-Coulter). The NaOH-soluble fraction was treated with alkaline phosphatase after neutralization and analysed by HPLC and TLC. Non-radioactive nucleosides and/or nucleotides were used as internal standards in HPLC analysis. Culture medium before and after incubation was counted for radioactivity and the radioactive components were analysed by TLC and/or HPLC. Total uptake was calculated as radioactivity recovered in total extracts (soluble and insoluble) as compared with total radioactivity in the medium before incubation start.

The HPLC analysis was performed using reverse phase column (Source 5RPC, GE Healthcare) by isocratic elution in buffer containing 50 mM ammonium phosphate, pH 6.5, 5 mM tetrabutylammonium hydrogen sulphate and 12% methanol at a flow rate of 1 ml/min. Soluble nucleotide extracts were mixed with HPLC buffer (1:4) before injection. Fractions (0.5 ml or 0.2 ml) were collected and mixed with 2 ml scintillation fluid and counted. The radioactive peaks were compared with non-radioactive standards. Retention times for standards were 3.23 min (uracil), 3.75 min (uridine), 4.58 min (dU), 5.80 min (UMP), 8.22 min (dUMP), 16.41 min (UDP), 36.7 min (UTP), 5.87 min (thymine), 8.75 min (dT), 14.35 min (dTMP), 31.9 min (dTDP), and 56.2 min (dTTP). TLC analysis was performed with PEI-cellulose and developed in 0.1 M NaH_2PO_4 for separation of thymidine nucleotides and isobutyric acid/ H_2O /ammonia (66:33:1) for separation of Urd, dU from other nucleosides and nucleotides as previously described (Wang, 2007).

Labelling of ThyA protein with [^{32}P]-5FdUMP. *M. pneumoniae* protein extracts (30 mg) were added to a reaction mixture containing 25 mM MgCl_2 , 0.2 mM methylenetetrahydrofolate, 0.2 mM CMP, 20 mM DTT, and 5 μM [^{32}P]-5FdUMP in a total volume of 25 ml. The mixtures were incubated at 37°C for 2 h. The reaction was stopped by addition of Laemmli sample buffer (5 μl) and 15 μl (~15 μg protein) was resolved by 12% SDS-PAGE. After electrophoresis, gels were fixed in methanol/acetic acid and the radiolabeled protein bands were visualized by autoradiography.

Enzyme assays. The TK activity was assayed by a radiochemical method using [^3H]-dT as a substrate, essentially as described (Wang *et al.*, 2001). TMPK activity was determined by using [^3H]-dTMP as a substrate in a reaction mixture containing 50 mM Tris-HCl pH 8.0, 0.5 mg/ml BSA, 10 mM DTT, 5 mM MgCl_2 , 2 mM ATP, and 10 μM [^3H]-dTMP. The reaction was started by addition of *M. pneumoniae* protein extracts and incubated at 37°C. At 0, 10, 20, and 30 min intervals a 10 μl aliquot was removed and spotted onto DE-81 filter paper and allowed to dry. The unutilized substrate was removed by washing the filter papers three times in 50 mM ammonium formate solution. Finally, the products were eluted with 0.5 ml of 0.1 M HCl and 0.2 M KCl, and mixed with 2 ml scintillation fluid and the radioactivity counted. The specific activity was calculated as nmol/(min mg) protein.

The TS activity was determined by the tritium release assay with [5-³H]-dUMP as the labeled substrate, essentially as described (Armstrong and Diasio, 1982). TLC assay was performed with [³²P]-dUMP as the labeled substrate in a reaction mixture containing 50 mM Tris-HCl pH 7.5, 5 mM methylenetetrahydrofolate, 10 mM MgCl₂, 50 mM NADPH, 10 mM DTT, 50 mM FAD, 15 mM NaF, and 5 μM [³²P]-dUMP. The reaction was started by addition of *M. pneumoniae* extracts, incubated at 37°C, and at each time point a 1.5 μl aliquot was removed and spotted onto a PEI-cellulose sheet. The TLC sheet was developed in isobutyric acid/H₂O/ammonia (66:33:1, v/v). The products were visualized by autoradiography.

The TP activity was determined using [³H]-dT as substrate, as previously described (Mizutani *et al.*, 2003). The reaction mixture contained 100 mM potassium phosphate pH 7.4, 5 mM DTT, and 100 μM [³H]-dT.

Analysis of TK transcript levels. Total *M. pneumoniae* RNA was prepared as described previously (Halbedel *et al.*, 2004). For slot blot analysis serial twofold dilutions of the RNA in 10× SSC (2 mg to 0.25 mg) were blotted onto a positively charged nylon membrane using a PR 648 Slot Blot Manifold (Amersham Biosciences). Equal amounts of yeast tRNA (Roche) and *M. pneumoniae* chromosomal DNA served as controls. A DIG-labeled riboprobe were obtained by *in vitro* transcription of the PCR product with the primers SS32 (5'-GATTTGTGGGCCGATGTTTTCC) and SS33 (5'-CTAATACGACTCACTATAGGGAGACGGTTTCGTTGCTCTTGGAC) that cover a TK (*mpn044*) internal sequence using T7 RNA polymerase (Roche). The reverse primer SS33 used to generate the PCR product contained a T7 promoter sequence (underlined). The quantification was performed using the Image J software v1.44b (Abramoff *et al.*, 2004).

Acknowledgments

This work was supported by the Swedish Research Council for Environment, Agricultural Sciences, and Spatial Planning (to L. W.).

Chapter 6

Interactions between glycolytic enzymes of *Mycoplasma pneumoniae*

The work described in this chapter was published in:

Dutow, P., S. R. Schmidl, M. Ridderbusch, and J. Stülke. 2010. Interactions between glycolytic enzymes of *Mycoplasma pneumoniae*. J. Mol. Microbiol. Biotechnol. accepted.

Author contributions:

This study was designed by SRS and JS. MR constructed the mutated glycolytic enzyme alleles and PD performed the bacterial two-hybrid analysis. SRS designed the oligonucleotides and supervised the experimental work that was accomplished by MR and PD during their diploma theses. All authors were involved in the interpretation of the collected data. SRS and JS wrote the paper.

Abstract

With only 688 protein-coding genes, *Mycoplasma pneumoniae* is one of the smallest self-replicating organisms. These bacteria use glycolysis as the major pathway for ATP production by substrate-level phosphorylation suggesting that this pathway must be optimized to high efficiency. In this study, we have investigated the interactions between glycolytic enzymes using the bacterial adenylate cyclase-based two-hybrid system. We demonstrate that most of the glycolytic enzymes perform self-interactions suggesting that they form dimers or other oligomeric forms. In addition, enolase was identified as the central glycolytic enzyme of *M. pneumoniae* due to its ability to directly interact with each other glycolytic enzyme. Our results support the idea of the formation of a glycolytic complex in *M. pneumoniae* and we suggest that the formation of this complex might ensure higher fluxes through the glycolytic pathway than would be possible with isolated non-interacting enzymes.

Introduction

Mycoplasma pneumoniae, a cell wall-less pathogenic bacterium, is the best-studied representative of the class Mollicutes. These bacteria are derived from Gram-positive ancestors that are related to *Bacillus subtilis* and lactic acid bacteria. The evolution of the Mollicutes is characterized by substantial genome degeneration that reflects adaptation of the bacteria to a life in close association with eukaryotic hosts (Razin *et al.*, 1998; Stülke *et al.*, 2009).

M. pneumoniae causes usually mild diseases such as pneumonias: However, implication of this bacterium in arthritic, cutaneous or auto-immune diseases as well as in encephalitis was reported (Atkinson *et al.*, 2008; Domenech *et al.*, 2009; Jacobs, 1997; Schalock and Dinulos, 2009; Waites and Talkington, 2004). Although *M. pneumoniae* is highly adapted to a life on mucosal surfaces, the bacteria are able to live independently of host cells. With less than 700 genes, *M. pneumoniae* belongs to the smallest organisms that are capable of autonomous life (Himmelreich *et al.*, 1996).

The small genome of *M. pneumoniae* is also reflected by its limited metabolic capabilities. The bacteria can utilize glucose, fructose or glycerol as carbon sources (Halbedel *et al.*, 2004; Yus *et al.*, 2009). These carbohydrates are metabolized via the glycolytic pathway, leading to the concomitant generation of ATP by substrate-level

phosphorylation. However, *M. pneumoniae* does not possess an active citric acid cycle; similarly the pentose phosphate shunt is incomplete. While *M. pneumoniae* can produce ATP, nearly all anabolic pathways have been lost during degenerative evolution. Thus, *M. pneumoniae* depends heavily on the host cells or on organic nutrient supply from the artificial medium (Halbedel *et al.*, 2007; Miles, 1992).

We are interested in the glycolytic pathway. *M. pneumoniae* encodes all glycolytic enzymes. Interestingly, some of these enzymes have multiple functions: The glycolytic kinases are also active in nucleotide phosphorylation thus replacing the nucleoside diphosphate kinase (Pollack *et al.*, 2002). Moreover, several glycolytic enzymes are subject to phosphorylation. However, it is not known how these phosphorylation events are catalyzed and how they affect the enzymatic activities (Schmidl *et al.*, 2010). For the regeneration of NAD⁺, *M. pneumoniae* possesses a lactate dehydrogenase; alternatively the NAD⁺ oxidase may directly oxidize NADH, and the latter reaction is coupled to the production of hydrogen peroxide, the major virulence factor of *M. pneumoniae* (Cole *et al.*, 1968; Halbedel *et al.*, 2007; Low and Zimkus, 1973).

For a long time it was thought that metabolic pathways take place in an unorganized chaotic way in bacterial cells. However, at the same time there have been data indicating that, e.g. tryptophan metabolism in *Escherichia coli* involves protein complexes (Yanofsky and Rachmeler, 1958). Similarly, glycolytic protein complexes were reported for *E. coli* as well as for eukaryotic cells (Mowbray and Moses, 1976; Campanella *et al.*, 2005). The accumulating recent evidence suggests that enzymes of one pathway may be clustered to allow efficient metabolism. This was shown for purine biosynthesis and branched-chain amino acid catabolism in human cells as well as for glycolysis in *B. subtilis* (An *et al.*, 2008; Commichau *et al.*, 2009; Islam *et al.*, 2007). Moreover, a recent *in silico* study supports the idea that glycolytic flux is much more efficient if the enzymes form a complex as compared to free floating enzymes (Amar *et al.*, 2008). The analysis of protein complexes in *M. pneumoniae* suggests that glycolytic enzymes might also interact in this organism (Kühner *et al.*, 2009).

The analysis of primary protein-protein interactions in *M. pneumoniae* and other Mollicutes is hampered by an alteration of the genetic code in these organisms: They use the UGA codon for the incorporation of tryptophan, whereas it specifies a stop in most other organisms. Due to this problem, the interactions between *Mycoplasma*

proteins have so far never been studied using a two-hybrid system. We have developed a method for the quick replacement of stop codons (Hames *et al.*, 2005). Based on this method, we have studied the interactions between all glycolytic enzymes of *M. pneumoniae* using a bacterial two-hybrid (B2H) system. Our results support the idea that these enzymes interact, and that metabolism is well structured even in a seemingly primitive organism.

Results

Organization of glycolytic genes in *M. pneumoniae*. In *B. subtilis* and other Firmicutes, genes encoding glycolytic enzymes from phosphotransferase system (PTS) proteins for glucose transport and phosphorylation to the pyruvate kinase are clustered in five operons (Ludwig *et al.*, 2001). In contrast, the corresponding *M. pneumoniae* genes are scattered on the chromosome (Fig. 24). This is even the case for the PTS genes in *M. pneumoniae* that are clustered in most bacteria with a functional PTS sugar transport system (Barabote and Saier, 2005). In *M. pneumoniae*, three gene clusters with glycolytic genes are present: The *pfkA-pyk* cluster encodes the two glycolytic kinases. These genes also form an operon in *B. subtilis*. The second cluster is made up of the *pgk* and *gapA* genes encoding phosphoglycerate kinase and glyceraldehyde-3-phosphate dehydrogenase, respectively. These genes are clustered in most bacteria, and it has been suggested that the clustering of these genes might reflect physical interaction of the encoded enzymes, which catalyze consecutive reactions (Dandekar *et al.*, 1998). The third glycolytic cluster is formed by the *ptsI*, *pgm*, and *tpiA* genes encoding enzyme I of the PTS, phosphoglycerate mutase, and triose-phosphate isomerase, respectively. The *pgm* and *tpiA* genes are also part of one operon in *B. subtilis* (Ludwig *et al.*, 2001).

Interactions between glycolytic enzymes. In order to identify possible primary interactions between glycolytic enzymes, we made use of the B2H system. In this system, the T25 and the T18 fragments of the catalytic domain of the *Bordetella pertussis* adenylate cyclase were fused to full-length copies of all glycolytic enzymes of *M. pneumoniae*. The leucine zipper of the yeast GCN4 transcription factor served as a control (Karimova *et al.*, 1998). The results of the B2H analysis are shown in Fig. 25. As expected, the leucine zipper of GCN4 showed strong self-interaction.

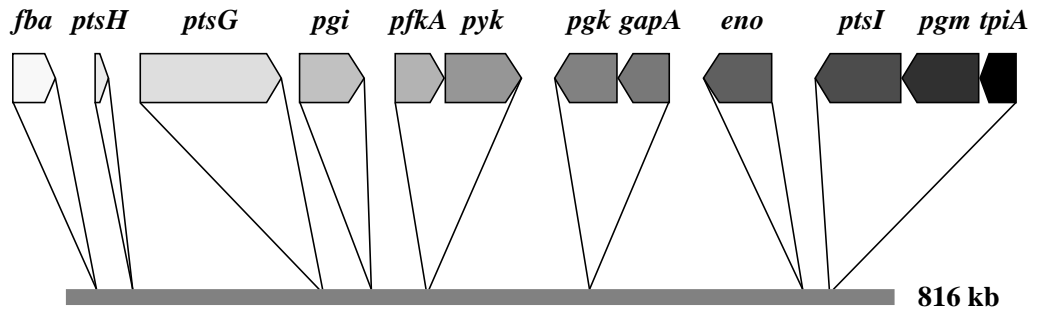


Fig. 24. Genomic localization of glycolytic genes in *M. pneumoniae*. The 816 kb genome of *M. pneumoniae* is shown true to scale in grey. Genes coding for glycolytic enzymes are illustrated relative to their position on the genome. *eno*, enolase; *fba*, fructose-bisphosphate aldolase; *gapA*, glyceraldehyde-3-phosphate dehydrogenase; *pfkA*, phosphofructokinase; *pgi*, glucose-6-phosphate isomerase; *pgk*, phosphoglycerate kinase; *pgm*, phosphoglycerate mutase; *ptsG*, PTS system glucose-specific EIICBA component; *ptsH*, phosphocarrier protein HPr; *ptsI*, enzyme I; *pyk*, pyruvate kinase; *tpiA*, triose-phosphate isomerase.

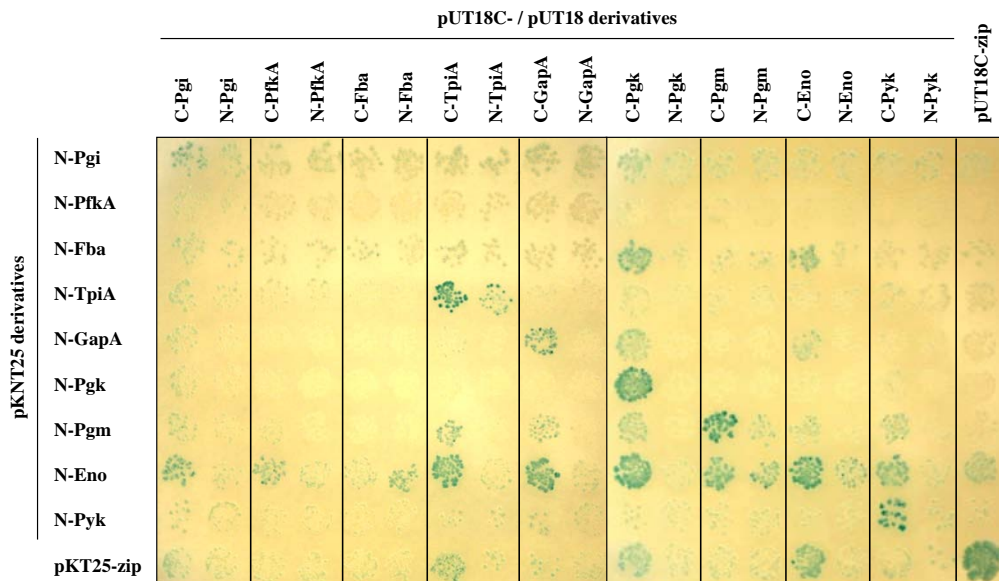


Fig. 25. Bacterial two-hybrid (B2H) analysis to identify interactions among glycolytic enzymes. All genes were cloned in the plasmids pUT18, pUT18C, and pKNT25. Plasmids pUT18 and pUT18C allow the expression of the selected enzymes fused either to the N- or the C-terminus of the T18 domain of the *B. pertussis* adenylate cyclase, respectively. Plasmid pKNT25 allows the expression of the selected enzymes fused either to the N-terminus of the T25 domain of the adenylate cyclase, respectively. The plasmids pKT25-zip and pUT18C-zip served as positive controls for complementation. The *E. coli* transformants were incubated for 48 h at 30°C. The level of protein-protein interaction was analyzed by observation of the blue coloration of the colonies.

As shown in Fig. 25, we observed self-interactions for all glycolytic enzymes with the exception of phosphofructokinase and fructose-bisphosphate aldolase. In addition to self-interactions, we detected several interactions between different glycolytic enzymes (see Fig. 25, Fig. 26). Of all glycolytic enzymes, enolase is involved in the largest number of interactions with other enzymes. We observed interactions of enolase with all other glycolytic enzymes. The strongest interactions were detected between enolase and triose-phosphate isomerase, glyceraldehyde-3-phosphate dehydrogenase, phosphoglycerate kinase, phosphoglycerate mutase, and pyruvate kinase. A strong interaction was also detected between phosphoglycerate kinase and fructose-bisphosphate aldolase. Weaker interactions were observed between enolase and glucose-6-phosphate isomerase, phosphofructokinase, and fructose-bisphosphate aldolase. Moreover, we observed weak interactions between glyceraldehyde-3-phosphate dehydrogenase and phosphoglycerate kinase as well as between triose-phosphate isomerase and phosphoglycerate mutase. These latter interactions reflect the genomic organization with *pgk-gapA* and *pgm-tpiA* gene clusters (see Fig. 24). Finally, faint interactions were observed between phosphoglycerate mutase on the one hand and glyceraldehyde-3-phosphate dehydrogenase, phosphoglycerate kinase, and pyruvate kinase on the other. A very weak interaction was also detectable between phosphoglycerate kinase and glucose-6-phosphate isomerase.

Thus, all glycolytic enzymes are involved in interactions with other enzymes of the pathway suggesting that glycolysis proceeds in a well organized and structured manner in *M. pneumoniae*.

Discussion

Glycolysis is the major pathway for the generation of energy by substrate-level phosphorylation in *M. pneumoniae* and most other Mollicutes. In good agreement with both the importance for cellular metabolism and the ancient origin of the glycolytic pathway is the observation that the genes encoding glycolytic enzymes are essential in many organisms and that these enzymes have additional functions that are completely unrelated to the biochemical pathway (Canback *et al.*, 2002; Commichau *et al.*, 2009; Kim and Kang, 2005).

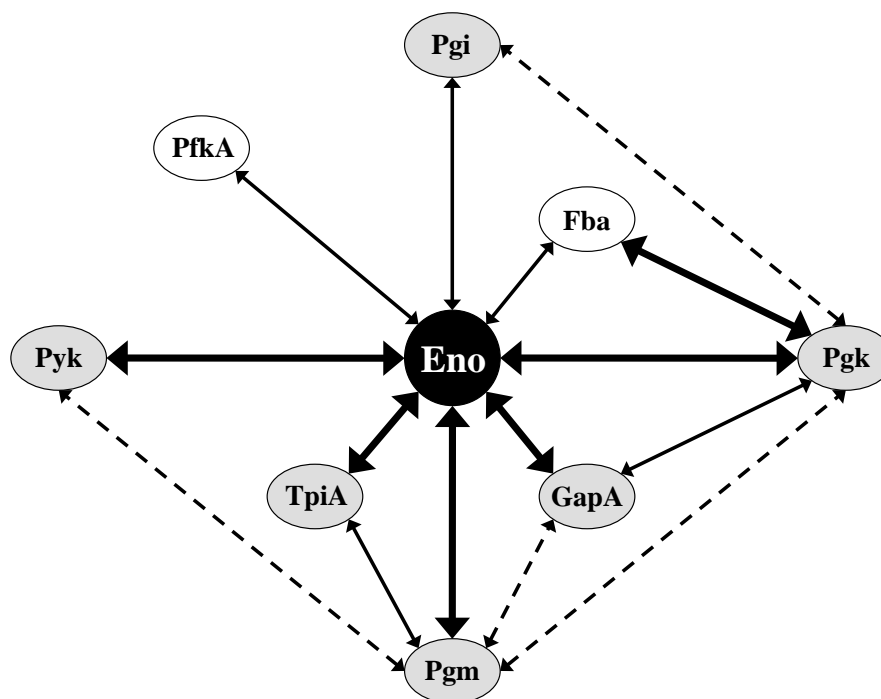


Fig. 26. Schematic summary of the outcome of the B2H analysis. The interaction network of glycolytic enzymes is depicted with the Enolase (Eno) as the core protein. Proteins that are able to form homomultimeric complexes are highlighted. Dashed arrows indicate weak interactions, whereas regular or bold black arrows point out moderate and strong interactions, respectively.

In this study, we have addressed the interactions between the glycolytic enzymes themselves. A recent proteome-level analysis of protein complexes in *M. pneumoniae* (Kühner *et al.*, 2009) as well as experiments with the Gram-positive model bacterium *B. subtilis* (Commichau *et al.*, 2009) provided indications for such interactions. In order to identify the primary interactions between the glycolytic enzymes, we applied the technique of two-hybrid analysis for the first time to proteins from a *Mycoplasma* species. Our studies revealed self-interactions that may correspond to the formation of dimers or other homo-oligomers for all glycolytic enzymes except phosphofruktokinase and fructose-bisphosphate aldolase. This observation is in good agreement with the known structures of glycolytic enzymes that indicate the formation of dimers or tetramers (Erlandsen *et al.*, 2000).

Our study indicates that enolase is of central importance in the organisation of glycolysis in *M. pneumoniae* since this is the only enzyme that is capable of interacting directly with any other glycolytic enzyme (see Fig. 26). Moreover, most of the strongest interactions involve enolase. Another interesting conclusion from this work is that the

enzymes of the lower part of glycolysis are much more strongly embedded in the interaction network than those of the hexose phosphate part (Fig. 26). This reflects that the triose-phosphate interconversion is the key module of the whole pathway in the living world, whereas the first intermediates of this part, glyceraldehyde 3-phosphate and dihydroxyacetone phosphate may be obtained from very different sources including the upper part of glycolysis, the pentose phosphate pathway, the Entner-Doudoroff pathway, or from glycerol phosphate dehydrogenase/oxidase.

In their proteome-level analysis, Kühner *et al.* (2009) proposed two glycolytic complexes in *M. pneumoniae*. One of these complexes consists of glyceraldehyde-3-phosphate dehydrogenase, phosphoglycerate kinase, and enolase. Our results are in support of this complex and provide compelling evidence that these three enzymes are capable of interacting directly with each other. The second complex was suggested to be composed of glyceraldehyde-3-phosphate dehydrogenase, pyruvate kinase and fructose-bisphosphate aldolase. We did not observe primary interactions between any couple of these three proteins. However, glyceraldehyde-3-phosphate dehydrogenase, as a member of the first complex, does directly bind to enolase, and we observe direct interaction between enolase and the two other enzymes. In any case, it seems difficult to name distinct complexes from *in vivo* pull-down studies that have the same members. Finally, Kühner *et al.* (2009) suggested a complex made up of enolase, triose-phosphate isomerase, a metalloprotease (MPN569), and an unknown protein (MPN316). The interactions between the two glycolytic enzymes is supported by our analysis. It is interesting to note that enolase may be involved in interactions that are not related to glycolysis. This has also been observed in *E. coli* and *B. subtilis*. In both organisms, enolase is part of the RNA-degrading multiprotein complex called RNA degradosome (Carpousis, 2007; Commichau *et al.*, 2009).

In conclusion, our results support the idea that glycolytic enzymes interact in *M. pneumoniae*. However, in contrast to previous findings, we suggest the presence of one complex of glycolytic enzymes that is organized around enolase. It is tempting to speculate that such a complex may be important for the efficiency of the glycolytic pathway, and thus for the efficiency of energy production in *M. pneumoniae*.

Experimental procedures

Bacterial strains and growth conditions. *E. coli* XL1-Blue (Stratagene) and BTH101 (Karimova *et al.*, 1998) were used for cloning experiments and B2H analyses, respectively. *E. coli* was grown in LB medium. LB plates were prepared by the addition of 18 g Bacto agar/liter (Difco) to LB medium.

DNA manipulation and transformation. Transformation of *E. coli* and plasmid DNA extraction were performed using standard procedures (Sambrook *et al.*, 1989). Restriction enzymes, T4 DNA ligase, and DNA polymerases were used as recommended by the manufacturers. DNA fragments were purified from agarose gels using the Nucleospin Extract Kit (Macherey and Nagel, Germany). Phusion DNA polymerase was used for the polymerase chain reaction as recommended by the manufacturer. All primer sequences are listed in the supplemental Table S7. DNA sequences were determined using the dideoxy chain termination method (Sambrook *et al.*, 1989). All plasmid inserts derived from PCR products were verified by DNA sequencing. *E. coli* transformants were selected on LB plates containing ampicillin (100 µg/ml) or kanamycin (50 µg/ml).

Plasmid constructions. The genes encoding the glycolytic enzymes from *M. pneumoniae* were first subcloned as follows. The coding sequence of each gene was amplified by PCR with gene specific primers using chromosomal DNA of *M. pneumoniae* M129 as the template. The PCR products were digested as appropriate with *Bam*HI and *Hind*III or with *Bam*HI and *Pst*I and cloned into the appropriately linearized expression vector pWH844 (Schirmer *et al.*, 1997). These plasmids allowed the expression of the glycolytic enzymes carrying a N-terminal His₆-tag. The resulting plasmids are listed in the supplemental Table S8. In *M. pneumoniae*, the UGA specifies a tryptophan; however, in *E. coli* it is a stop codon. With exception of *pfkA* and *pgm*, the glycolytic genes contain one to three UGA codons that were replaced by the multiple mutation reaction (Hames *et al.*, 2005) using phosphorylated mutagenic oligonucleotides and the former plasmids as template. The resulting final plasmids are listed in the supplemental material (see Table S8).

To obtain the plasmids for the B2H analyses, the coding sequences of the glycolytic genes were amplified by PCR using the latter plasmids. The PCR products were digested as shown in the supplemental material, and the resulting fragments were cloned into each of the three plasmids pKNT25, pUT18, and pUT18C (Claessen *et al.*,

2008; Karimova *et al.*, 1998), digested with the same enzymes. The resulting plasmids used for the B2H analyses are shown in the supplemental Table S8. All plasmid inserts were verified by DNA sequencing.

Bacterial two-hybrid analysis. Primary protein-protein interactions were identified by B2H analysis (Karimova *et al.*, 1998). The B2H system is based on the interaction-mediated reconstruction of adenylate cyclase (CyaA) activity from *B. pertussis* in *E. coli*. The CyaA enzyme consists of two complementary fragments T18 and T25 that are not active when physically separated. Fusion of these fragments to interacting proteins results in functional complementation between the T18 and T25 fragments and the synthesis of cAMP. cAMP production can be monitored by measuring the β -galactosidase activity of the cAMP-CAP-dependent promoter of the *E. coli lac* operon. Thus, a high β -galactosidase activity reflects the interaction between the hybrid proteins. Plasmids pUT18 and pKNT25 allow the expression of proteins fused to the N-terminus of the T18 and T25 fragments of the CyaA protein, respectively, and the plasmid pUT18C allows the expression of proteins fused to the C-terminus of the T18 fragment of the CyaA protein, respectively (Claessen *et al.*, 2008; Karimova *et al.*, 1998). The plasmids pKT25-*zip* and pUT18C-*zip* served as positive controls for complementation. These plasmids express T18-*zip* and T25-*zip* fusion proteins that can associate due to the leucine zipper motifs resulting in an active CyaA enzyme and a high β -galactosidase activity. The plasmids constructed for the B2H assay (see Table S8) were used for cotransformations of *E. coli* BTH101 and the protein-protein interactions were then analyzed by plating the cells on LB plates containing ampicillin (100 μ g/ml), kanamycin (50 μ g/ml), X-Gal (40 μ g/ml) and IPTG (0.5 mM). The plates were incubated for a maximum of 60 h at 30°C. The B2H assays were performed in triplicate.

Acknowledgments

We are grateful to Julia Busse, Henrike Pfortner, Martin Arnold, and Frederik Meyer for helpful discussions. This work was supported by Deutsche Forschungsgemeinschaft and the Fonds der Chemischen Industrie. S. R. S. was supported by a personal grant from the Studienstiftung des Deutschen Volkes.

Supplemental material

Tab. S7. Primers used in this study.

Primer	Sequence (5'→3') ^{ab}	Mutation	Resulting plasmid
Subcloning for multiple mutation reaction			
JS39	TCTATCAACAGGAGTCCAAGC	None	
MR04	AAAGGATCCATGGTTGACTTTAAAACAG TCCAAGC	None	pGP1006, pGP1010
MR05	TATAAAGCTTTTACTTTTTTTGAATATCG CTAATTCCCAC	None	pGP1006, pGP1010
MR06	P_GTTAGCACAGTTCTGGGCATCATTGGG	A441G	pGP1010
MR07	P_CCCAATGGCCAGCAGAACTTCAGG	A894G	pGP1010
MR08	AAAGGATCCATGCATAAGAAGGTCTTAC TAGCC	None	pGP1007
MR09	TATACTGCAGTTACTTTTTACTTATTTAA AGGGAGTTTGCG	None	pGP1007
MR10	AAAGGATCCATGAGTGCACAAACTGGA ACCGATCTTTTCAAG	None	pGP1008
MR11	TATACTGCAGTTAAGCTTTTTGCGTTTA ATGTTTTTAAAGGTGTTCCAACC	A1335G	pGP1008
MR19	AAAGGATCCATGGAAAGTAAATGGTTAA CAGTTGAC	None	pGP756, pGP762
MR20	TATAAAGCTTCTATTCACGACCAAGTTT AGCAAAC	None	pGP756, pGP762
MR21	P_GGGTAAATCATGGGCTTTGGTAGTAA CTTC	A393G	pGP762
MR22	P_CTGCTTTGCGTCACTGGCTTTACAC	A756G	pGP762
MR23	AAAGGATCCATGAGTCCAAAAACAACC AAAAAAATTGCC	None	pGP757
MR24	TATAAAGCTTTTAAATAATTTTTATTA ATGACTGCAATTAAAGCGC	None	pGP757
MR25	AAAGGATCCATGCTAGTAAACATCAAAC AAATGTTGCAAC	None	pGP758, pGP763
MR26	TATAAAGCTTCTAAGCCTTATTGGTTGA ACCACAG	None	pGP758, pGP763
MR27	P_GGCTTTACCCCGACAACCTGGAAGGG	A552G	pGP763
MR28	AAAGGATCCATGCGTACGAAATACCTAA TTGGTAACTGGAAG	A30G	pGP759, pGP764

Tab. S7. Continued.

Primer	Sequence (5'→3') ^{ab}	Mutation	Resulting plasmid
MR29	TATACTGCAGTTATGCATATACTTGTGCC ATTACTAAAAAGTCG	None	pGP759, pGP764
MR30	P_GTGATTGCTTACGAACCAATTTGGGCA ATTGGTACGG	A489G	pGP764
MR31	AAAGGATCCATGCTAGCAAAGAGTAAG ACTATCC	None	pGP760, pGP765
MR32	TATACTGCAGTTAAAGCTTGGCACAATA GTAACTAC	None	pGP760, pGP765
MR33	P_GCTAACCTGCCATGGGCAGAACAC	A270G	pGP765
MR34	AAAGGATCCATGATTCACCACCTAAAAC GCAC	None	pGP761, pGP766
MR35	TATACTGCAGTTATAAGCTAATGATCTT ATTGTGAAATACTC	None	pGP761, pGP766
MR36	P_GCTATGGACGCTAGCAATGTTAGATG AC	A69G	pGP766
MR37	P_CAAGGTGCCTTACTGGCAACGGTAC	A864G	pGP766
MR38	P_CAGTGAGTTTTGGAAGCAGGTGGTG	A1167G	pGP766
pWH844 fw	TATGAGAGGATCGCATCACCAT	None	
Bacterial two-hybrid analysis			
FC146	CGATGCGTTCGCGATCCAGGC	None	-
FC147	CCAGCCTGATGCGATTGCTGCAT	None	-
FC148	GTCACCCGGATTGCGGCGG	None	-
FC149	GCTGGCTTAACTATGCGGCATCAGA	None	-
M13 puc rev	GGAAACAGCTATGACCATG	None	-
PD05	AAATCTAGAGATGGAAAGTAAATGGTTA ACAGTTGACAC	None	pGP1553, pGP1563, pGP1573
PD06	TTTGGTACCCGTTACGACCAAGTTTAG CAAACATTAAC	None	pGP1553, pGP1563, pGP1573
PD07	AAATCTAGAGATGAGTCCAAAACAACC AAAAAAATTGCC	None	pGP1554, pGP1564, pGP1574
PD08	TTTGGTACCCGAATAATATTTTTATTAAT GACTGCAATTAAAGCGC	None	pGP1554, pGP1564, pGP1574
PD09	AAATCTAGAGATGCTAGTAAACATCAAA CAAATGTTGCAAC	None	pGP1555, pGP1565, pGP1575
PD10	TTTGAGCTCCGAGCCTTATTGGTTGAACC ACAGAG	None	pGP1555, pGP1565, pGP1575

Tab. S7. Continued.

Primer	Sequence (5'→3') ^{ab}	Mutation	Resulting plasmid
PD11	AAAT <u>CTAGAG</u> ATGCGTACGAAATACCTA ATTGGTAAC	None	pGP1556, pGP1566, pGP1576
PD12	TTTGGT <u>ACCCG</u> TGCATATACTTGTGCCAT TACTAAAAAGTC	None	pGP1556, pGP1566, pGP1576
PD13	AAAT <u>CTAGAG</u> ATGCTAGCAAAGAGTAA GACTATCCG	None	pGP1557, pGP1567, pGP1577
PD14	TTTGAAT <u>TCCGA</u> AGCTTGGCACAATAGT TAACTACCC	None	pGP1557, pGP1567, pGP1577
PD15	AAAT <u>CTAGAG</u> ATGGTTGACTTTAAAACA GTCCAAGC	None	pGP1558, pGP1568, pGP1578
PD16	TTTGAAT <u>TCCG</u> CTTTTTTTGAATATCGCT AATTCCCCTAG	None	pGP1558, pGP1568, pGP1578
PD17	AAAT <u>CTAGAG</u> ATGCATAAGAAGGTCTTA CTAGCC	None	pGP1559, pGP1569, pGP1579
PD18	TTTGAAT <u>TCCG</u> CTTTTTACTTATTTAAAAG GGAGTTTGCG	None	pGP1559, pGP1569, pGP1579
PD19	AAAT <u>CTAGAG</u> ATGAGTGCACAAACTGGA ACCG	None	pGP1560, pGP1570, pGP1580
PD20	TTTGAAT <u>TCCG</u> AGCTTTTTGCGGTTTAAT GTTTTTAAAGGTG	None	pGP1560, pGP1570, pGP1580
PD21	AAAT <u>CTAGAG</u> ATGATTCACCACCTAAAA CGCAC	None	pGP1561, pGP1571, pGP1581
PD22	TTTGGT <u>ACCCG</u> TAAGCTAATGATCTTATT GTGAAATACTCC	None	pGP1561, pGP1571, pGP1581

^a Restriction sites are underlined.

^b The “P” at the 5’ end of primer sequences indicates phosphorylation.

Tab. S8. Plasmids used for analysis of glycolytic enzymes.

Plasmid	Relevant characteristics ^a	Used restriction sites	Reference
Subcloning for multiple mutation reaction			
pGP756	pWH844- <i>pgi</i>	<i>Bam</i> HI + <i>Hind</i> III	This work
pGP757	pWH844- <i>pfkA</i>	<i>Bam</i> HI + <i>Hind</i> III	This work
pGP758	pWH844- <i>fba</i>	<i>Bam</i> HI + <i>Hind</i> III	This work
pGP759	pWH844- <i>tpiA</i> (A30G)	<i>Bam</i> HI + <i>Pst</i> I	This work
pGP760	pWH844- <i>gapA</i>	<i>Bam</i> HI + <i>Pst</i> I	This work
pGP761	pWH844- <i>pyk</i>	<i>Bam</i> HI + <i>Pst</i> I	This work
pGP762	pWH844- <i>pgi</i> (A393G+A756G)	<i>Bam</i> HI + <i>Hind</i> III	This work
pGP763	pWH844- <i>fba</i> (A552G)	<i>Bam</i> HI + <i>Hind</i> III	This work
pGP764	pWH844- <i>tpiA</i> (A30G+A489G)	<i>Bam</i> HI + <i>Pst</i> I	This work
pGP765	pWH844- <i>gapA</i> (A270G)	<i>Bam</i> HI + <i>Pst</i> I	This work
pGP766	pWH844- <i>pyk</i> (A69G+A864G+A1167G)	<i>Bam</i> HI + <i>Pst</i> I	This work
pGP1006	pWH844- <i>pgk</i>	<i>Bam</i> HI + <i>Hind</i> III	This work
pGP1007	pWH844- <i>pgm</i>	<i>Bam</i> HI + <i>Pst</i> I	This work
pGP1008	pWH844- <i>eno</i> (A1335G)	<i>Bam</i> HI + <i>Pst</i> I	This work
pGP1010	pWH844- <i>pgk</i> (A441G+A894G)	<i>Bam</i> HI + <i>Hind</i> III	This work
pWH844	Allows overexpression of N-terminal <i>His</i> ₆ -tag fusion proteins in <i>E. coli</i> DH5α (Amp ^R)	-	Schirmer <i>et al.</i> (1997)
Bacterial two-hybrid analysis			
pGP1553	pUT18C- <i>pgi</i> (A393G+A756G)	<i>Xba</i> I + <i>Kpn</i> I	This work
pGP1554	pUT18C- <i>pfkA</i>	<i>Xba</i> I + <i>Kpn</i> I	This work
pGP1555	pUT18C- <i>fba</i> (A552G)	<i>Xba</i> I + <i>Sac</i> I	This work
pGP1556	pUT18C- <i>tpiA</i> (A30G+A489G)	<i>Xba</i> I + <i>Kpn</i> I	This work
pGP1557	pUT18C- <i>gapA</i> (A270G)	<i>Xba</i> I + <i>Eco</i> RI	This work
pGP1558	pUT18C- <i>pgk</i> (A441G+A894G)	<i>Xba</i> I + <i>Eco</i> RI	This work
pGP1559	pUT18C- <i>pgm</i>	<i>Xba</i> I + <i>Eco</i> RI	This work
pGP1560	pUT18C- <i>eno</i> (A1335G)	<i>Xba</i> I + <i>Eco</i> RI	This work
pGP1561	pUT18C- <i>pyk</i> (A69G+A864G+A1167G)	<i>Xba</i> I + <i>Kpn</i> I	This work
pGP1563	pUT18- <i>pgi</i> (A393G+A756G)	<i>Xba</i> I + <i>Kpn</i> I	This work
pGP1564	pUT18- <i>pfkA</i>	<i>Xba</i> I + <i>Kpn</i> I	This work
pGP1565	pUT18- <i>fba</i> (A552G)	<i>Xba</i> I + <i>Sac</i> I	This work
pGP1566	pUT18- <i>tpiA</i> (A30G+A489G)	<i>Xba</i> I + <i>Kpn</i> I	This work
pGP1567	pUT18- <i>gapA</i> (A270G)	<i>Xba</i> I + <i>Eco</i> RI	This work
pGP1568	pUT18- <i>pgk</i> (A441G+A894G)	<i>Xba</i> I + <i>Eco</i> RI	This work
pGP1569	pUT18- <i>pgm</i>	<i>Xba</i> I + <i>Eco</i> RI	This work

Tab. S8. Continued.

Plasmid	Relevant characteristics ^a	Used restriction sites	Reference
pGP1570	pUT18- <i>eno</i> (A1335G)	<i>Xba</i> I + <i>Eco</i> RI	This work
pGP1571	pUT18- <i>pyk</i> (A69G+A864G+A1167G)	<i>Xba</i> I + <i>Kpn</i> I	This work
pGP1573	pKNT25- <i>pgi</i> (A393G+A756G)	<i>Xba</i> I + <i>Kpn</i> I	This work
pGP1574	pKNT25- <i>pfkA</i>	<i>Xba</i> I + <i>Kpn</i> I	This work
pGP1575	pKNT25- <i>fba</i> (A552G)	<i>Xba</i> I + <i>Sac</i> I	This work
pGP1576	pKNT25- <i>tpiA</i> (A30G+A489G)	<i>Xba</i> I + <i>Kpn</i> I	This work
pGP1577	pKNT25- <i>gapA</i> (A270G)	<i>Xba</i> I + <i>Eco</i> RI	This work
pGP1578	pKNT25- <i>pgk</i> (A441G+A894G)	<i>Xba</i> I + <i>Eco</i> RI	This work
pGP1579	pKNT25- <i>pgm</i>	<i>Xba</i> I + <i>Eco</i> RI	This work
pGP1580	pKNT25- <i>eno</i> (A1335G)	<i>Xba</i> I + <i>Eco</i> RI	This work
pGP1581	pKNT25- <i>pyk</i> (A69G+A864G+A1167G)	<i>Xba</i> I + <i>Kpn</i> I	This work
pKNT25	<i>P_{lac}-mcs-cyaA</i> (Kan ^R)	-	Claessen <i>et al.</i> (2008)
pKT25- <i>zip</i>	<i>P_{lac}-cyaA-<i>zip</i></i> (Kan ^R)	-	Karimova <i>et al.</i> (1998)
pUT18	<i>P_{lac}-mcs-cyaA</i> (Amp ^R)	-	Karimova <i>et al.</i> (1998)
pUT18C	<i>P_{lac}-cyaA-mcs</i> (Amp ^R)	-	Karimova <i>et al.</i> (1998)
pUT18C- <i>zip</i>	<i>P_{lac}-cyaA-<i>zip</i></i> (Amp ^R)	-	Karimova <i>et al.</i> (1998)

^a Resistance gene abbreviations as follows: Amp, ampicillin; Kan, kanamycin.

Chapter 7

The hidden pathway: Impact of the glycerophosphodiesterase GlpQ on virulence of *Mycoplasma pneumoniae*

The work described in this chapter was submitted for publication in:

Schmidl, S. R., A. Otto, M. Lluch-Senar, J. Piñol, J. Busse, D. Becher, and J. Stülke. The hidden pathway: Impact of the glycerophosphodiesterase GlpQ on virulence of *Mycoplasma pneumoniae*. PLoS Pathogens submitted.

Author contributions:

This study was designed and interpreted by SRS. The cell morphology experiments were accomplished by MLS and JP, University of Barcelona. SRS performed all biochemical and physiological researches, but JB contributed substantially to the slot blot analyses. The proteomic analysis was done in collaboration with AO and DB, University of Greifswald. SRS and JS wrote the paper.

Abstract

Mycoplasma pneumoniae is the causative agent of atypical pneumonia. The formation of hydrogen peroxide, a product of glycerol metabolism, is the major factor that damages the host cells. Phosphatidylcholine is the major carbon source available on lung epithelia, and their utilization requires the cleavage of deacylated phospholipids to glycerol 3-phosphate and choline. *M. pneumoniae* possesses two potential glycerophosphodiesterases, MPN420 (GlpQ) and MPN566. In this work, the function of these proteins was analyzed by biochemical, genetic, and physiological studies. The results indicate that only GlpQ is an active glycerophosphodiesterase. MPN566 has no enzymatic activity and the inactivation of the gene did not result in any detectable phenotype. Inactivation of the *glpQ* gene resulted in reduced growth in medium with glucose as the carbon source, in loss of hydrogen peroxide production when phosphatidylcholine was present, and in a complete loss of cytotoxicity toward HeLa cells. Moreover, the *glpQ* mutant strain exhibited a reduced gliding velocity. A comparison of the proteomes of the wild type and the *glpQ* mutant strain revealed that this enzyme is also implicated in the control of gene expression. Several proteins were present in higher or lower amounts in the mutant. This regulation by GlpQ is exerted at the level of transcription as determined by mRNA slot blot analyses. All genes subject to GlpQ-dependent control have a conserved potential *cis*-acting element upstream of the coding region. This element overlaps the promoter in the case of the genes that are repressed in a GlpQ-dependent manner and it is located upstream of the promoter for GlpQ-activated genes. We may suggest that GlpQ acts as a trigger enzyme that measures the availability of its product glycerol 3-phosphate and uses this information to differentially control gene expression.

Author summary

Mycoplasma pneumoniae serves as a model organism for bacteria with very small genomes that are nonetheless independently viable. These bacteria infect the human lung and cause a specific pneumonia. The major virulence determinant of *M. pneumoniae* is hydrogen peroxide that is generated during the utilization of glycerol 3-phosphate, which might be derived from free glycerol or from the degradation of phospholipids. Indeed, lecithin is the by far most abundant carbon source

on lung epithelia. In this study, we made use of the recent availability of methods to isolate mutants of *M. pneumoniae* and characterized the enzyme that generates glycerol 3-phosphate from deacylated lecithin (glycerophosphorylcholine). This enzyme, called GlpQ, is essential for the formation of hydrogen peroxide when the bacteria are incubated with glycerophosphorylcholine. Moreover, *M. pneumoniae* is unable to cause any damage to the host cells in the absence of GlpQ. This underlines the important role of phospholipid metabolism for the virulence of *M. pneumoniae*. We observed that GlpQ in addition to its enzymatic activity does also control the expression of several genes, among them the glycerol transporter. Thus, GlpQ is central to the normal physiology and to pathogenicity of the minimal pathogen *M. pneumoniae*.

Introduction

Pathogenic bacteria have developed a large battery of enzymes and mechanisms for extracting nutrients from their hosts, and the requirement for nutrient acquisition can be regarded as one of the driving forces for virulence (Eisenreich *et al.*, 2010; Görke and Stülke, 2008; Sonenshein, 2007). In consequence, the metabolic capabilities of a pathogen reflect its adaptation to a particular niche in a particular host.

Mycoplasma pneumoniae is the causative agent of atypical pneumonia and several additional infections including encephalitis, aseptic meningitis, acute transverse myelitis, stroke, and polyradiculopathy (Narita, 2009; Narita, 2010; Tsiodras *et al.*, 2005; Waites and Talkington, 2004). These bacteria are members of the phylogenetic group of Mollicutes that are characterized by an extreme reductive evolution that results in the smallest genomes that allow independent life. Moreover, the Mollicutes have lost the cell wall and most metabolic pathways, since they obtain the building blocks for their cellular macromolecules from the host tissue. However, even in these minimal pathogens, there is a close relation between metabolism and virulence [for review see Halbedel *et al.* (2007)]. *M. pneumoniae* thrives at the surfaces of lung epithelia. Thus, these bacteria must have evolved to utilize the carbon sources present in this niche. The pulmonary surfactant is composed of about 90% phospholipids and 10% proteins (Veldhuizen *et al.*, 1998). This suggests that phospholipids play a major role in the nutrition of *M. pneumoniae*.

Glycerophospholipids, the major building blocks of the cell membrane in bacteria and eukaryotes, are degraded in several steps. First, the fatty acids are cleaved off from the phospholipids resulting in the formation of glycerophosphodiester. In these molecules, the phosphate group of glycerol 3-phosphate is linked to another compound, called the head group. In eukaryotes, choline is by far the most abundant head group, and lecithin, the choline-containing phospholipid accounts for about 80% of all phospholipids in human lung cells (Veldhuizen *et al.*, 1998). In the second step, the choline head group is cleaved off due to the activity of a glycerophosphodiesterase resulting in the formation of glycerol 3-phosphate that can feed into glycolysis after oxidation to dihydroxyacetone phosphate (see Fig. 27). In *M. pneumoniae*, the latter reaction is catalyzed by the glycerol-3-phosphate oxidase GlpD (Hames *et al.*, 2009). GlpD transfers the electrons to water resulting in the formation of hydrogen peroxide, the major virulence factor of *M. pneumoniae* (Somerson *et al.*, 1965). In consequence, the virulence of *M. pneumoniae glpD* mutant cells is severely attenuated (Hames *et al.*, 2009).

While the metabolism of glycerol has been well studied in *M. pneumoniae* and other Mollicutes such as *Mycoplasma mycoides* (Bischof *et al.*, 2009; Hames *et al.*, 2009; Pilo *et al.*, 2005), only little is known about the glycerophosphodiesterases required for lipid utilization. Many bacteria encode multiple glycerophosphodiesterases. In *Escherichia coli*, both enzymes are enzymatically active in lipid degradation; however, they are differentially regulated, with GlpQ and UgpQ being induced in the presence of glycerol 3-phosphate and under conditions of phosphate starvation, respectively (Ohshima *et al.*, 2008; Wong and Kwan, 1992). In *Bacillus subtilis*, out of three putative glycerophosphodiesterases, only GlpQ has been studied. The corresponding gene is under dual control and its expression is induced when phosphate becomes limiting and glycerol is available (Antelmann *et al.*, 2000; Nilsson *et al.*, 1994). Moreover, *glpQ* expression is repressed if more favourable carbon sources such as glucose are present (Blencke *et al.*, 2003). In *Haemophilus influenzae*, another bacterium thriving in the respiratory tract, the glycerophosphodiesterase is involved in pathogenicity. The enzyme generates choline, which in turn is used for the biosynthesis of the bacterial lipopolysaccharide layer - a major virulence determinant of Gram-negative bacteria (Fan *et al.*, 2001; Forsgren *et al.*, 2008). Similarly, glycerophosphodiesterase activity is implicated on virulence of different *Borrelia*

species. The enzyme is only present in the relapsing fever group and may help the bacteria to reach a higher cell density in the blood of the host as compared to Lyme disease spirochetes (Schwan *et al.*, 2003).

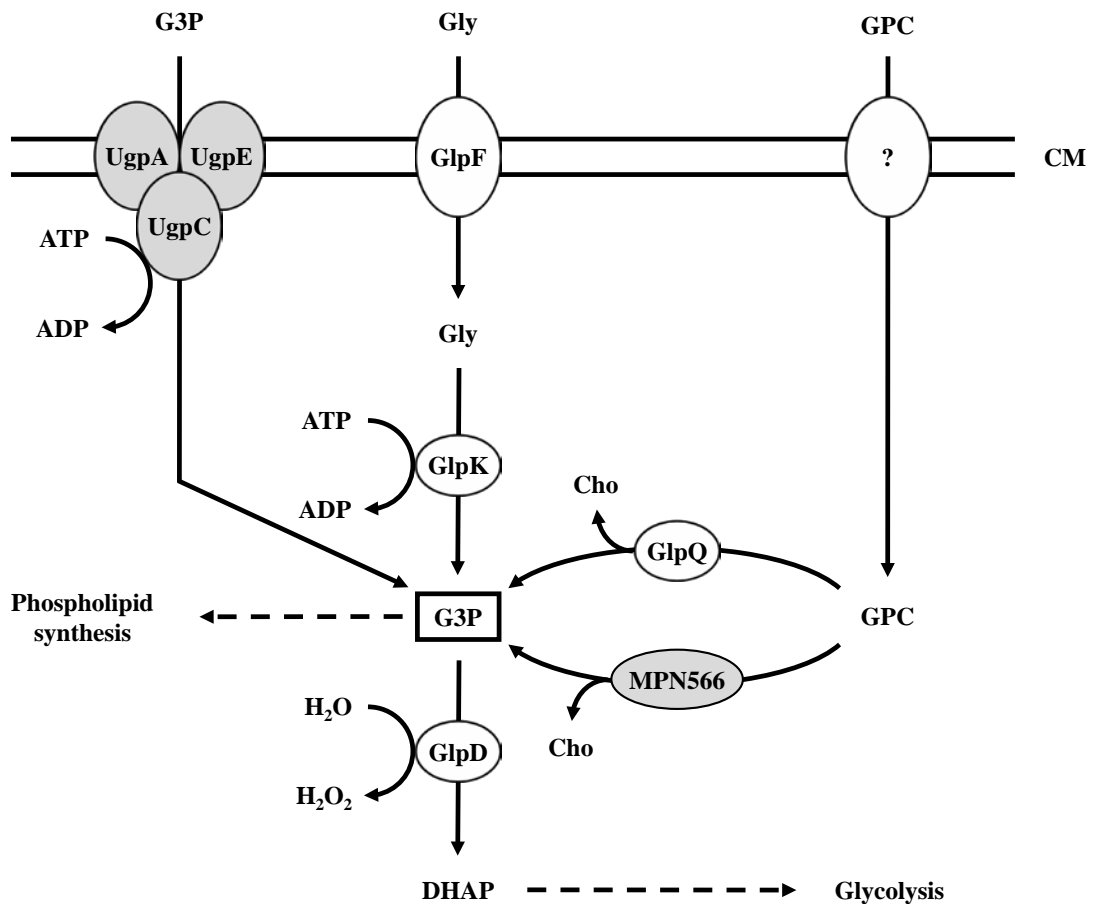


Fig. 27. Schematic illustration of the machinery for uptake and conversion of carbohydrates leading to the formation of glycerol 3-phosphate in *M. pneumoniae*. UgpC (MPN134), UgpA (MPN135), and UgpE (MPN136) form a ABC transport system for glycerol 3-phosphate, whereas GlpF (MPN043) is the glycerol uptake facilitator. The glycerol kinase GlpK (MPN050) and the glycerol-3-phosphate oxidase GlpD (MPN051) metabolize glycerol to the glycolytic intermediate dihydroxyacetone phosphate. Hydrogen peroxide formation by GlpD is crucial for the cytotoxic effects of *M. pneumoniae*. GlpQ (MPN420) and MPN566 encode two paralogous glycerophosphodiesterases that are able to metabolize glycerophosphorylcholine to glycerol 3-phosphate and choline. The uptake system for glycerophosphorylcholine is so far unknown. Proteins highlighted in grey seem not to fulfill the predicted function (this work). Cho, choline; CM, cell membrane; DHAP, dihydroxyacetone phosphate; G3P, glycerol 3-phosphate; GPC, glycerophosphorylcholine; Gly, glycerol.

In many bacteria, central enzymes of metabolism do not only serve their catalytic function, but in addition, they are also involved in signal transduction. In this way, the information on the availability of important metabolites can be directly determined by the enzyme in charge of their conversion, and this information is then often transferred to the transcription machinery. Collectively, such enzymes were termed trigger enzymes (Commichau and Stülke, 2008). They can control gene expression by directly acting as DNA- or RNA-binding transcription factors as the *E. coli* proline dehydrogenase and the aconitase or by controlling the activity of transcription factors by covalent modification or a regulatory protein-protein interaction as observed for several sugar permeases of the bacterial phosphotransferase system and the *B. subtilis* glutamate dehydrogenase, respectively (Beinert *et al.*, 1996; Commichau *et al.*, 2007; Schmalisch *et al.*, 2003; Zhu and Becker, 2003).

In this work, we have analyzed the role of the two potential glycerophosphodiesterases encoded in the genome of *M. pneumoniae*. Biochemical and physiological studies demonstrate that one of the two proteins, GlpQ, is a functional glycerophosphodiesterase. GlpQ is essential for hydrogen peroxide formation in the presence of deacylated phospholipids as the carbon source and, in consequence, for cytotoxicity. Moreover, GlpQ may act as a trigger enzyme by controlling the expression of a set of genes encoding lipoproteins, the glycerol facilitator, and a metal ion ABC transporter.

Results

Identification of *M. pneumoniae* genes encoding potential glycerophosphodiesterases. Since phospholipids are the most abundant potential carbon sources for *M. pneumoniae* living at lung epithelial surfaces, we considered the possibility that these bacteria synthesize enzymes that cleave the polar head groups from the glycerophosphodiesters to produce glycerol 3-phosphate that can be utilized by the enzymes of glycerol metabolism (Hames *et al.*, 2009) (Fig. 27). Two genes that potentially encode such enzymes are present in the genome of *M. pneumoniae*, *i.e.* *mpn420* (renamed to *glpQ*) and *mpn566*. An alignment of the corresponding proteins to glycerophosphodiesterases from other bacteria is shown in the supporting information (Fig. S4).

Enzymatic activities of the potential glycerophosphodiesterases. In order to assess the biochemical properties and physiological relevance of the putative glycerophosphodiesterases, their corresponding genes, *glpQ* and *mpn566*, were cloned into the expression vector pGP172, thus allowing a fusion of the proteins to a N-terminal *Strep*-tag facilitating purification. The recombinant proteins were purified and the activities were first determined using glycerophosphorylcholine (GPC) as the substrate and a set of divalent cations. As shown in Fig. 28, purified GlpQ was active against GPC, and the activity was highest in the presence of magnesium ions (10 mM). Manganese and zinc ions did also support activity, although to a lesser extent (Fig. 28). In contrast, the enzyme was inactive in the presence of calcium and cobalt ions (data not shown). The activity assay with purified MPN566 revealed no activity with GPC, irrespective of the cation present in the assay (data not shown). We did also test the activity of both proteins with glycerophosphorylethanolamine and glycerophosphorylglycerol. However, neither protein was active with any of these substrates. Thus, our data demonstrate that GlpQ is active as a glycerophosphodiesterase, whereas MPN566 does not exhibit such an activity.

The two proteins GlpQ and MPN566 share ~58% identical residues. Thus, it seems surprising that MPN566 was inactive in the enzymatic assay. However, several residues that are known to be important for the activity of glycerophosphodiesterases are conserved in GlpQ but not in MPN566 (Fig. S4). These residues include Trp-36 and Glu-38 as well as the conserved HD motif (Asn-51 and Leu-52 in MPN566) and Phe-110. Interestingly, a similar arrangement with two GlpQ-like proteins is also observed in *Mycoplasma genitalium*, and as in *M. pneumoniae*, one protein has all the conserved residues characteristic for glycerophosphodiesterases, whereas the second protein has similar deviations from the consensus as MPN566 (Fig. S4). In order to test whether a restoration of the conserved residues would also convert MPN566 to a biologically active glycerophosphodiesterase, we replaced the five amino acids that differ from the consensus by those residues present in GlpQ. The resulting mutant allele was cloned into pGP172, and the protein purified. Unfortunately, this protein was highly unstable and purification was impossible.

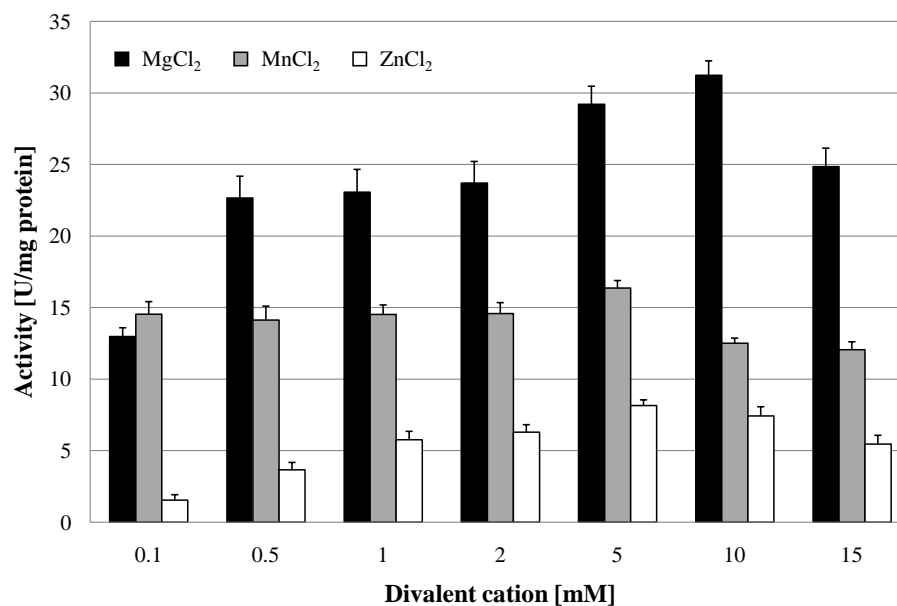


Fig. 28. Effect of divalent cations on GlpQ activity. GlpQ activity was measured in the presence of 0.5 mM glycerophosphorylcholine and various concentrations of divalent cations. Error bars indicate standard deviation (based on three independent experiments).

Construction of *glpQ* and *mpn566* mutants. The analysis of mutants is one of the most powerful tools for studying gene functions and bacterial physiology. The isolation of desired *M. pneumoniae* mutants became possible only recently by the introduction of the “Haystack mutagenesis” (Halbedel and Stülke, 2007). To get more insights into the physiological role of the glycerophosphodiesterases GlpQ and its paralogous MPN566, we attempted to isolate mutants affected in the corresponding genes.

The strategy of “Haystack mutagenesis” is based on an ordered collection of pooled random transposon insertion mutants that can be screened for junctions between the transposon and the gene of interest due to transposon insertion. The 64 pools were used in a PCR to detect junctions between the *glpQ* or *mpn566* genes and the mini-transposon using the oligonucleotides SS35 and SS40 (for the respective genes) and SH30 (for the mini-transposon) (Halbedel *et al.*, 2006) (Fig. 29). Positive signals were obtained for both genes. From pools that gave a positive signal, colony PCR with the 50 individual mutants resulted in the identification of the desired *glpQ* and *mpn566* mutants. The presence of the transposon insertion in both genes was verified by Southern blot analysis (Fig. 29). To test whether these strains contained only unique transposon insertions, we did another Southern blot using a probe specific for the

aac-aphD resistance gene present on the mini-transposon. As shown in Fig. 29, only one single band hybridizing with this probe was detected in each strain, moreover, this fragment had the same size as the *AgeI* or *PstI/SacI* fragment hybridizing to the *glpQ* and *mpn566* probe, respectively (Fig. 29). The isolated *glpQ* and *mpn566* mutant strains were designated as GPM81 and GPM82. The position of the transposon insertion in the two genes was determined by DNA sequencing. The *glpQ* gene was disrupted between nucleotides 517 and 518, resulting in a truncated protein of 172 amino acids with one additional amino acid and the following stop codon encoded by the inserted mini-transposon. The disruption of the *mpn566* gene was located between nucleotides 157 and 158, resulting in a truncated protein of 52 amino acids with one additional amino acid and the following stop codon.

Contributions of GlpQ and MPN566 to growth and motility. First, we compared the ability of the wild type strain and the two mutant strains to utilize glucose and glycerol as the single carbon sources (Fig. 30). As an additional control, we used the *glpD* mutant strain GPM52. This strain is defective in glycerol-3-phosphate oxidase and therefore unable to utilize glycerol as the only carbon source (Hames *et al.*, 2009). As shown in Fig. 30A, the wild type and the *glpD* and *mpn566* mutant strains grew well with glucose. In contrast, the *glpQ* mutant GPM81 grew more slowly and did not reach the final biomass as compared to the other strains. As reported previously, the wild type strain exhibited very slow growth with glycerol as the only carbon source (Halbedel *et al.*, 2004). In this respect, the *glpQ* and *mpn566* mutants were indistinguishable from the wild type. As reported previously, the *glpD* mutant strain did not grow at all in glycerol-containing medium (Hames *et al.*, 2009). In conclusion, the active glycerophosphodiesterase GlpQ is required for maximal growth in the presence of glucose, whereas its absence does not interfere with the slow growth in the presence of glycerol. It is therefore tempting to speculate that some glycerophosphodiesterases in the Hayflick medium support growth (see “Discussion”).

Since the disruption of *glpQ* affected the growth properties of the bacteria, we wondered whether this might reflect changes in cell morphology and in the movement of the bacteria. The morphology of the wild type and mutant bacteria was analyzed by scanning electron microscopy, and no significant differences were detected (Fig. S5). An analysis of the gliding velocities of the three strains revealed that the wild type strain glided with a velocity of $0.32 \pm 0.09 \mu\text{m/s}$, whereas the *glpQ* and *mpn566* mutants

exhibited velocities of $0.2 \pm 0.08 \mu\text{m/s}$ and $0.3 \pm 0.1 \mu\text{m/s}$, respectively. Thus, the active glycerophosphodiesterase GlpQ is required for efficient gliding movement of the bacteria.

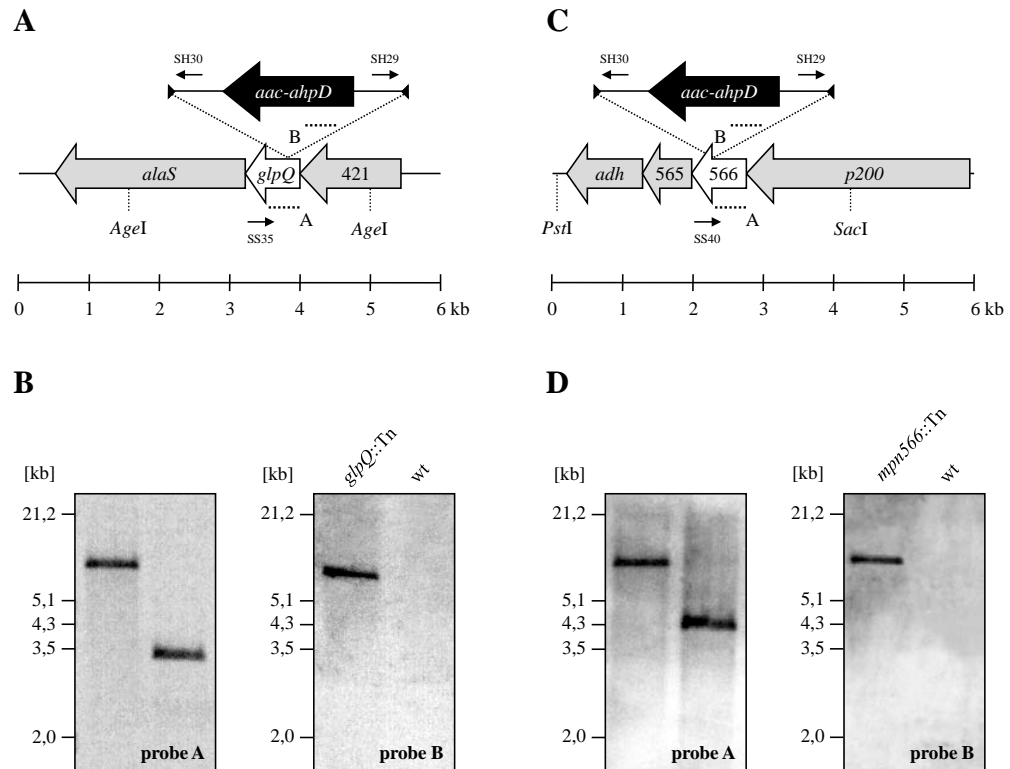


Fig. 29. Isolation of *M. pneumoniae* glycerophosphodiesterases transposon insertion mutants. (A, C) Schematic representation of the genomic region surrounding the *glpQ* and *mpn566* gene (both designated as glycerophosphodiesterases) in *M. pneumoniae* and site of the transposon insertion in the knockout strains GPM81 and GPM82, respectively. The annealing sites of oligonucleotides used for the determination of the transposon insertion site are indicated by arrows. Probes hybridizing to internal fragments of the glycerophosphodiesterases and the *aac-ahpD* genes are depicted as dotted lines. (B, D) Southern blot analysis to confirm the single insertion of the mini-transposon into the *glpQ* and *mpn566* gene of the strains GPM81 and GPM82, respectively. Chromosomal DNAs of the wild type and both glycerophosphodiesterases were digested as indicated. Blots were hybridized with the respective glycerophosphodiesterase-specific probe (left) and a probe hybridizing to the *aac-ahpD* gene of the mini-transposon (right).

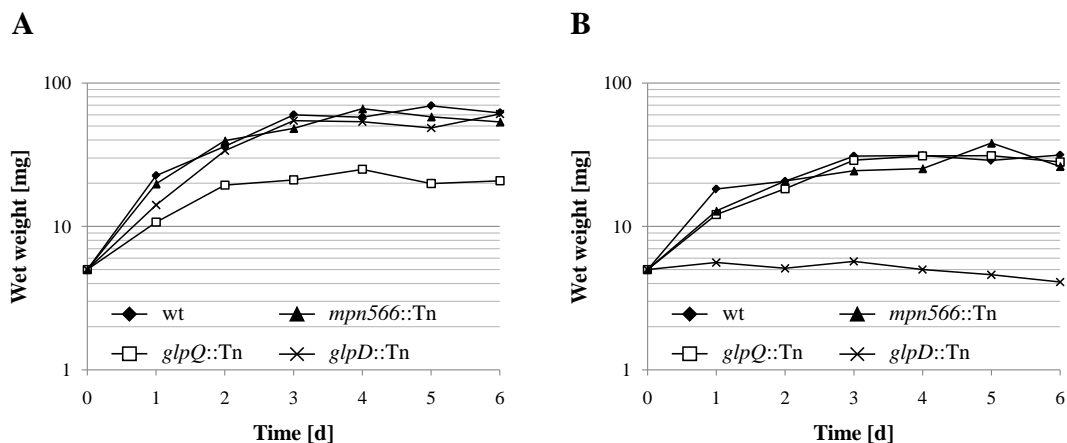


Fig. 30. Growth of *M. pneumoniae* in modified Hayflick medium containing different carbon sources. One hundred milliliters of medium were inoculated with 5 mg of *M. pneumoniae* wild type (wt), *glpQ*::Tn, *mpn566*::Tn, and *glpD*::Tn [control; Hames *et al.* (2009)] mutant cells and incubated for up to six days at 37°C in 150-cm² cell culture flasks. Glucose (A) and glycerol (B) were added to a final concentration of 1% (wt/vol). Attached cells were collected by scraping and growth was monitored by determination of the wet weight of the cell pellets. All measurements were done three times. Results are from a representative experiment.

Implication of GlpQ and MPN566 in hydrogen peroxide production and cytotoxicity. The utilization of glycerol or glycerophosphodiesteres results in the generation of hydrogen peroxide, the major cytotoxic product of *M. pneumoniae*. We asked therefore whether the *glpQ* and *mpn566* disruptions would affect hydrogen peroxide formation and if so, whether it also affects cytotoxicity. Hydrogen peroxide formation was assayed in *M. pneumoniae* cultures that contained glucose, glycerol, GPC, glycerol 3-phosphate or no carbon source. In the absence of an added carbon source, neither the wild type strain nor the mutants formed substantial amounts of hydrogen peroxide (Fig. 31). Similarly, essentially no hydrogen peroxide was produced in the presence of glucose. If glycerol was available, maximal hydrogen peroxide formation (9.5 mg/l) was observed in the wild type strain. In the *glpD* mutant that served as a control, no hydrogen peroxide was formed. This is in good agreement with previous reports on the increase of hydrogen peroxide generation in the presence of glycerol and its dependence on a functional glycerol-3-phosphate oxidase (Hames *et al.*, 2009). The hydrogen peroxide production in the *glpQ* and *mpn566* mutants was similar to that observed in the wild type strain. This result reflects that the metabolite glycerol is downstream from the glycerophosphodiesterase activity. In the presence of GPC, the

wild type strain produced similar amounts of hydrogen peroxide (9 mg/l) as in the presence of glycerol. In contrast, no hydrogen peroxide formation was detected for the *glpQ* mutant GPM81, whereas the disruption of *mpn566* did not have any effect on the production of hydrogen peroxide (Fig. 31). This result is in good agreement with the enzymatic activities of the two proteins: GlpQ is the only active glycerophosphodiesterase in *M. pneumoniae*, and no glycerol 3-phosphate, the substrate of GlpD, can be formed in its absence, whereas MPN566 is dispensable for the utilization of GPC. We also tested the ability of the *M. pneumoniae* strains to form hydrogen peroxide in the presence of glycerophosphorylethanolamine and glycerophosphorylglycerol. These compounds did not stimulate hydrogen peroxide in any of the strains tested (data not shown). This is in excellent agreement with the result of the enzyme assay that suggested that neither GlpQ nor MPN566 is able to degrade these substances. Finally, we tested whether hydrogen peroxide was formed in the presence of glycerol 3-phosphate. As shown in Fig. 31, no significant formation of hydrogen peroxide was observed in any of the strains tested. This suggests that the uptake of glycerol 3-phosphate is rather inefficient.

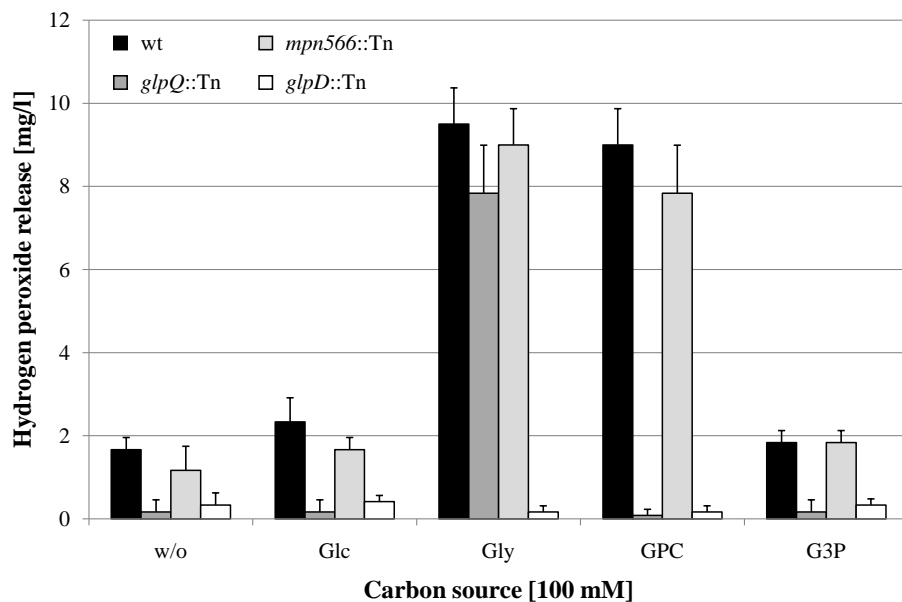


Fig. 31. Examination of *M. pneumoniae* hydrogen peroxide release. Hydrogen peroxide production of *M. pneumoniae* wild type (wt), *glpQ*::Tn, *mpn566*::Tn, and *glpD*::Tn [control; Hames *et al.* (2009)] mutant strains was measured in the presence of different carbon sources (100 μM) after 2 h. Error bars indicate standard deviation (based on three independent experiments). G3P, glycerol 3-phosphate; GPC, glycerophosphorylcholine; Glc, glucose; Gly, glycerol; w/o, without addition of any carbon source.

To assess the cytotoxicity of the different *M. pneumoniae* strains, we infected confluent HeLa cell cultures with *M. pneumoniae* cells (multiplicity of infection: 2). The cytotoxicity of the mutants was compared to that of the wild type strain and *M. pneumoniae* GPM52 that is affected in *glpD*. As shown in Fig. 32, the HeLa cells had undergone lysis after four days upon infection with wild type *M. pneumoniae*. As observed previously, a large portion of viable cells was observed after infection of the cell culture with the *glpD* mutant GPM52 (Hames *et al.*, 2009). For the *glpQ* mutant GPM81, nearly all HeLa cells had survived the infection suggesting that GlpQ is essential for cytotoxicity. In contrast, cytotoxicity induced by the *mpn566* mutant strain GPM82 was equivalent to that of the wild type strain (Fig. 32). These data clearly demonstrate that the active glycerophosphodiesterase GlpQ is required for host cell damage, whereas the inactive enzyme MPN566 is not. Moreover, they support the assumption that hydrogen peroxide formation is the major factor that contributes to host cell damage.

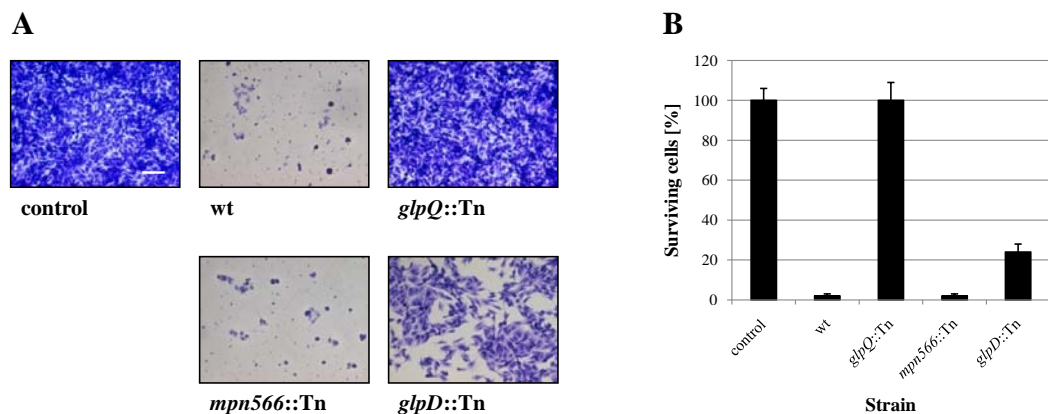


Fig. 32. Cytotoxicity of *M. pneumoniae* toward HeLa cell cultures. (A) Infection assay to verify cytotoxic effects of *M. pneumoniae* *glpQ::Tn* and *mpn566::Tn* mutant strains. HeLa cells were infected with *M. pneumoniae* wild type (wt), *glpQ::Tn*, and *mpn566::Tn* mutant cells. As control served two HeLa cell cultures: One without addition of *M. pneumoniae* cells and another after infection with the *glpD::Tn* mutant strain (Hames *et al.*, 2009). After four days, HeLa cell cultures were stained with crystal violet and photographed. All pictures are shown at the same magnification. Scale bar, 0.1 mm. (B) Quantification of HeLa cells after infection with different *M. pneumoniae* strains. The cell count of surviving cells is indicated in percent as the number of viable cells per field of view, quantified by crystal violet staining after four days of incubation. An uninfected HeLa cell culture served as control. Error bars indicate standard deviation (based on three independent experiments).

The role of GlpQ in gene expression. As reported above, the *glpQ* mutant exhibits multiple phenotypes related to motility, metabolism, and pathogenicity. We asked therefore whether some of the effects are due to changes in the proteome of the *glpQ* mutant GPM81. To answer this question, we compared the total protein profiles of the wild type strain and the *glpQ* and *mpn566* mutants, GPM81 and GPM82, respectively, after growth in glucose and glycerol (Fig. 33). While the protein patterns in the *mpn566* mutant were indistinguishable from the wild type strain under both conditions, several differences were noted for the *glpQ* mutant.

To identify those proteins that exhibit altered accumulation in the *glpQ* mutant, the total proteins of the wild type and the *glpQ* mutant strains were identified by mass spectrometry. For the protein extracts from glucose-grown cells, 532 different proteins were identified. This corresponds to about 77% of the theoretical proteome of *M. pneumoniae*. In the presence of glycerol, 473 proteins corresponding to 69% of the theoretical proteome were identified. The differences in protein expression between glucose- and glycerol-grown cells as well as proteins that could not be detected at all are summarized in Tables S9 and S10. A detailed list of the differences of the protein profiles between the wild type strain and the *glpQ* mutant is presented in Tables S11 and S12. As expected, the GlpQ protein was detected in the protein extracts of the wild type strain but not in those of the *glpQ* mutant strain. In glucose-grown cells, 33 and 21 proteins were in elevated and reduced amounts, respectively, in the *glpQ* mutant. The strongest increase was observed for the glycerol facilitator GlpF and the uncharacterized lipoprotein MPN162. A strongly reduced accumulation was observed for the lipoprotein MPN506. In the presence of glycerol, five induced and five repressed proteins were detected. These proteins were subject to a similar regulation as in glucose-grown cells and they are the only proteins with identical regulation under both conditions (Table 12).

It has been shown before that changes at the proteome level may result from altered gene expression or from changes in protein stability (Halbedel *et al.*, 2007; Schmidl *et al.*, 2010). Therefore, we studied the expression of the genes corresponding to the most prominently regulated proteins and of genes encoding potential regulators, transport systems, and potential pathogenicity factors. For this purpose, we isolated RNA from cultures grown in modified Hayflick medium supplemented with glucose and performed slot blot analyses (Fig. 34 and S6).

Table 12. Proteins with GlpQ-dependent expression pattern.

For detailed information on proteome and transcript changes in the *glpQ* mutant GPM81, see Tables S11 and S12.

Locus name	Protein name	Protein function	Fold-change in the presence of glucose ^a		Fold-change in the presence of glycerol ^a	
			Protein level	Transcript level	Protein level	Transcript level
MPN043	GlpF	Glycerol uptake facilitator	10.79 ± 1.06	5.69 ± 0.36	5.83 ± 0.76	3.32 ± 0.34
MPN162	-	Uncharacterized lipoprotein	9.96 ± 0.97	5.23 ± 0.23	5.41 ± 0.83	2.81 ± 0.47
MPN284	-	Uncharacterized lipoprotein	ns	0.25 ± 0.05	0.36 ± 0.02	0.35 ± 0.04
MPN433	CbiO	Metal ion ABC transporter ATP-binding protein	ns	7.56 ± 0.39	5.66 ± 0.49	2.92 ± 0.24
MPN506	-	Uncharacterized lipoprotein	0.10 ± 0.03	0.07 ± 0.05	0.18 ± 0.04	0.16 ± 0.02

^a Fold-change cut off ≥ 2.0 and ≤ 0.5 , respectively (*glpQ* mutant strain vs. wild type). Abbreviation: ns, no significant difference.

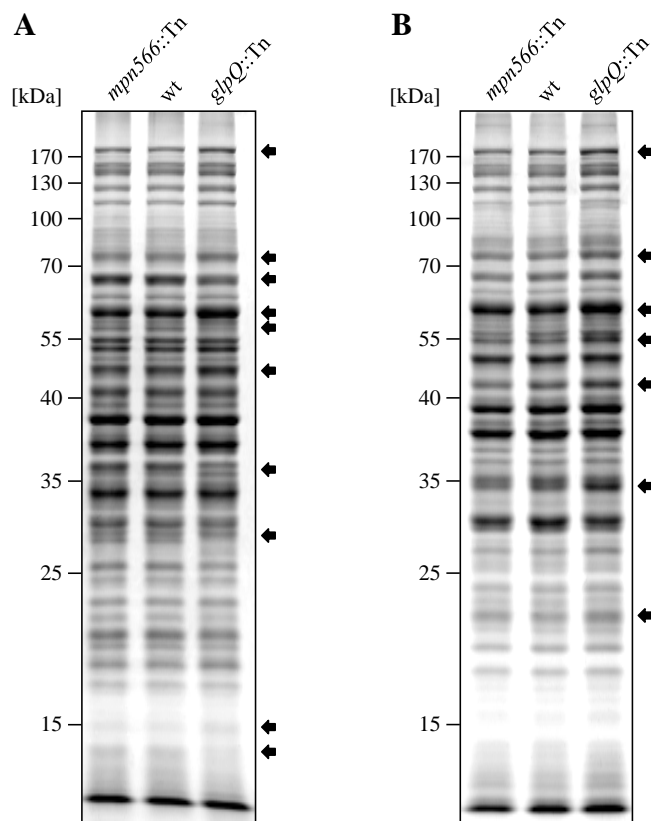


Fig. 33. Comparison of protein profile between *M. pneumoniae* wild type and both glycerophosphodiesterase mutant strains. Whole cell extracts of *M. pneumoniae* wild type (wt), *glpQ*::Tn, and *mpn566*::Tn mutant strains were analyzed by 12% SDS-PAGE and stained with Coomassie Brilliant Blue R250 dye (Serva) for visualization of proteins. 15 μ g of extract was applied to each lane. *M. pneumoniae* strains were grown in modified Hayflick medium containing either glucose (A) or glycerol (B) as sole carbon source (1% wt/vol). Complete lanes were cut out (into 15 pieces) and identified by mass spectrometry. Protein bands with prominent changes in the amount are indicated by arrows.

These studies demonstrated that the regulation of the glycerol facilitator GlpF and the lipoproteins MPN162 and MPN506 occurs at the level of transcription (Table 12). Moreover, our results confirmed the higher expression of *glpF* and *mpn162* and the repression of *mpn506* in the *glpQ* mutant. For the other proteins that were induced in the presence of glucose, with exception of *plsC* and *mpn566* (nearly twofold higher transcript levels), similar accumulation of the mRNAs compared to the protein amount was observed (Table S11 and Fig. S6). In contrast, for the proteins that were present in reduced amounts in glucose-grown cells, no changes of the corresponding mRNAs were observed for all transport proteins. Interestingly, the lipoprotein MPN083 showed a similar pattern at the level of transcription as the induced proteins and the

ribonucleoside-diphosphate reductase (encoded by *nrdFIE*) was the only protein with reduced mRNA amounts, however changes in transcript level were not significant (Table S11 and Fig. S6).

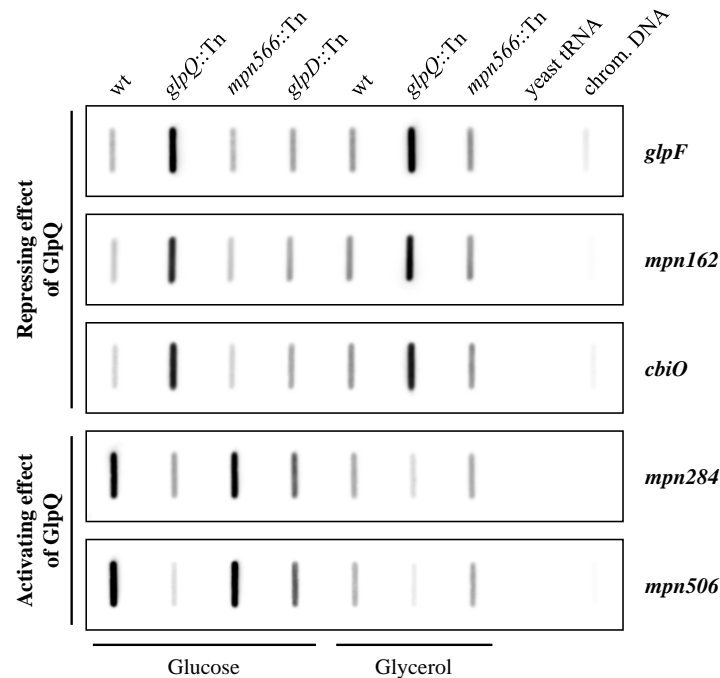


Fig. 34. Transcription analysis of GlpQ-dependent genes in *M. pneumoniae*. Slot blots were performed with whole RNA extracts of *M. pneumoniae* wild type (wt), *glpQ::Tn*, *mpn566::Tn*, and *glpD::Tn* [control; Hames *et al.* (2009)] mutant strains grown in modified Hayflick medium containing either glucose or glycerol as sole carbon source (1% wt/vol). A dilution series of RNA extracts was blotted onto a positively charged nylon membrane and probed with a DIG-labeled riboprobe specific for an internal part of a particular open reading frame. Names of riboprobes are given next to each blot. Signals obtained with 1 μ g of RNA are shown. Yeast tRNA and *M. pneumoniae* chromosomal DNA served as controls. For detailed information on differences of transcript levels see Tables 12, S11, and S12.

Identification of a potential target site for GlpQ-dependent regulation. The proteome and transcription analyses identified three genes that are significantly regulated - either induced or repressed - in a GlpQ-dependent manner. An inspection of the upstream region of these genes revealed the presence of a common palindromic DNA motif (Fig. 35). To exclude the possibility that this motif is randomly distributed in the genome of *M. pneumoniae* because of the extremely AT-rich consensus sequence, we tested its presence in the genome using the GLAM2SCAN algorithm (Frith *et al.*,

2008). In 15 cases (matching score cut ≥ 0.20), this potential motif was located upstream of open reading frames, among them the three genes mentioned above. Therefore, the expression of the remaining 12 genes was tested by slot blot analyses, and for two of these genes, *cbiO* and *mpn284*, a significant accumulation and reduction of the mRNA, respectively, was observed (data not shown; Fig. 34). Interestingly, the corresponding proteins, a subunit of a metal ion ABC transporter CbiO and the uncharacterized lipoprotein MPN284 were found to be present in higher or lower amounts in the *glpQ* mutant in glycerol-grown cell. Thus, there is a very good agreement between the regulatory effect of GlpQ at the proteome level, the regulation at the level of transcription, and the presence of the *cis*-acting element.

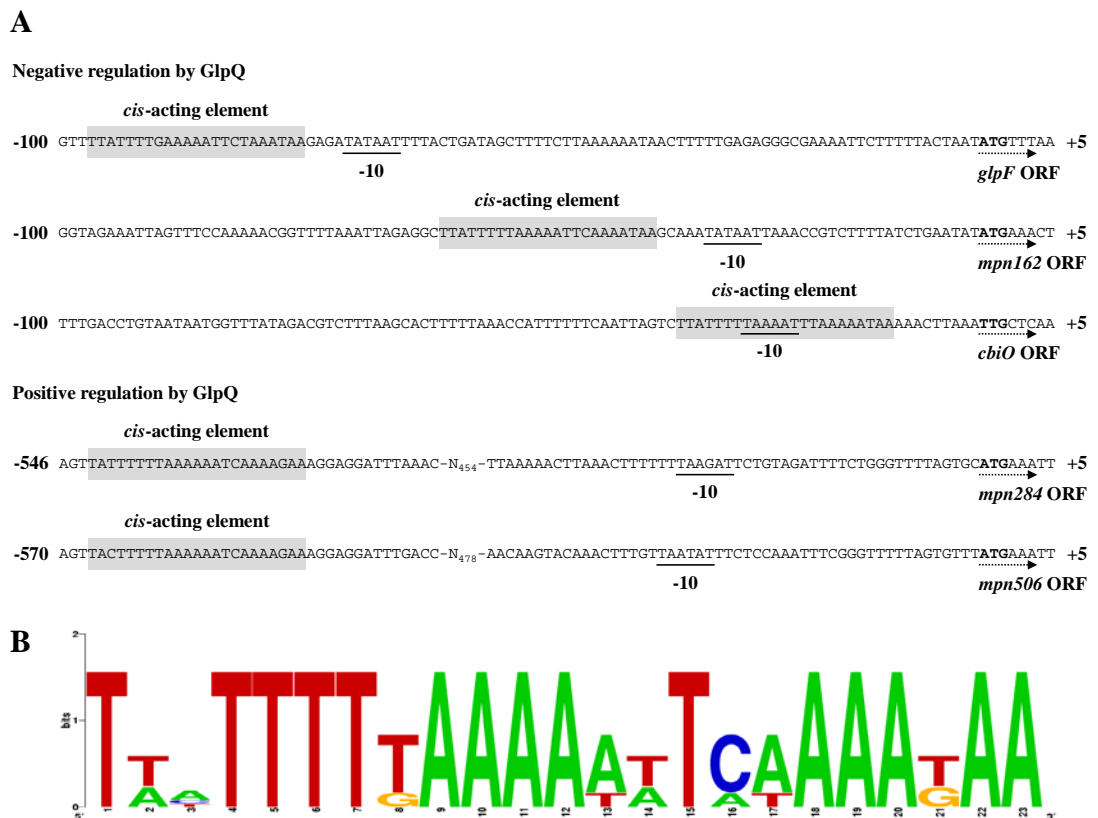


Fig. 35. Transcriptional organization of GlpQ-dependent genes in *M. pneumoniae*. (A) Nucleotide sequence of promoter regions of *M. pneumoniae glpF* (*mpn043*), *mpn162*, *cbiO* (*mpn433*), *mpn284*, and *mpn506* genes. Promoter sequences are numbered relative to the 5' end. Directions of the open reading frames (ORF) are indicated by dotted arrows and predicted ATG/TTG start codons are highlighted by bold type. The respective -10 motifs are underlined. GlpQ-dependent *cis*-acting elements (palindromic DNA motifs) are indicated by grey shading. (B) Consensus sequence of the GlpQ-dependent palindromic DNA motif in *M. pneumoniae*. The sequence logo was created using WebLogo v2.8.2 (Crooks *et al.*, 2004) based on all five *cis*-acting elements mentioned in A.

Discussion

This work establishes that the glycerophosphodiesterase GlpQ of *M. pneumoniae* is essential for cytotoxicity of these bacteria. This is in excellent agreement with previous reports that carbon metabolism is intimately linked to virulence in pathogenic bacteria, including *M. pneumoniae* and other Mollicutes (Görke and Stülke, 2008; Halbedel *et al.*, 2007; Sonenshein, 2007). The utilization of glycerol and phospholipids plays a particularly important role in virulence of *Mycoplasma* species: Hydrogen peroxide, the only known cytotoxic substance produced by these bacteria, is generated as a product of glycerol metabolism, and both *glpD* and *glpQ* mutants are severely affected in pathogenicity (Hames *et al.*, 2009; this work). In *M. mycoides*, pathogenicity is associated with the presence of a highly efficient ABC transporter for glycerol. Non-pathogenic strains of *M. mycoides* rely on the less efficient glycerol facilitator for glycerol uptake (Vilei and Frey, 2001).

In *M. pneumoniae*, GlpQ is not only important for virulence but also for growth in the commonly used medium in the laboratory, *i.e.* modified Hayflick medium with glucose as the added carbon source (see Fig. 30A). This observation is in good agreement with a recent analysis of the *M. pneumoniae* metabolism that suggested that glycerol is essential for growth of *M. pneumoniae* (Yus *et al.*, 2009). Accordingly, no difference between the wild type strain and the *glpQ* mutant was observed during growth in the presence of glycerol (see Fig. 30B).

In addition to GlpQ, *M. pneumoniae* encodes a second paralogous protein. However, as shown in this work, this protein does not exhibit enzymatic activity nor does the inactivation of the corresponding gene (*mpn566*) cause any detectable phenotypes. This lack of detectable activity of MPN566 is easily explained by the lack of conservation of amino acid residues that are essential for the activity as a glycerophosphodiesterase. Interestingly, a very similar arrangement with two *glpQ*-like genes is also present in *M. genitalium* and *Mycoplasma alligatoris*. Based on the conservation of the catalytically important residues (see Fig. S4), there is an active and an inactive enzyme in *M. genitalium*, as observed here for *M. pneumoniae*. In *M. alligatoris*, both potential glycerophosphodiesterases contain all the important amino acids suggesting that both proteins are enzymatically active. It is tempting to speculate that the possession of two active glycerophosphodiesterases is related to the fact that *M. alligatoris* is the only Mollicute that causes fatal infections (Brown *et al.*, 2001). In

the syphilis spirochete, *Treponema pallidum*, one *glpQ*-like gene is present, however, the encoded protein is not active as a glycerophosphodiesterase. Again, the inactivity is most likely caused by the lack of conservation of functionally important amino acids (Shevchenko *et al.*, 1997; Stebeck *et al.*, 1997). The presence of inactive GlpQ-like proteins in several pathogens, including a spirochete and *M. genitalium*, the bacterium with the smallest genome, suggests that these pseudo-enzymes have other functions that have yet to be identified. Unfortunately, the experiments reported in this study did not give any hints as to a putative function of MPN566.

Many proteins have activities in addition to their primary functions. On one hand, this allows gene duplication and specialization to non-related functions of similar proteins. On the other hand, a protein may acquire a second useful activity and act as a so-called moonlighting protein (Jeffery, 1999). The former is very common and might apply to the putative functional specialization of GlpQ and MPN566. In contrast, the latter phenomenon is true for all trigger enzymes that measure the availability of their respective metabolites and transduce this information to the regulatory machinery of the cell. In mammals, a glycerophosphodiesterase controls the development of skeletal muscles independent from its enzymatic activity (Okazaki *et al.*, 2010). Our results suggest that GlpQ might also have such a second activity. Indeed, the expression of the glycerol facilitator GlpF, a lipoprotein, and the ATP-binding subunit of a metal ion ABC transporter are strongly overexpressed in the *glpQ* mutant, whereas two uncharacterized lipoproteins are less expressed in the mutant. Interestingly, the genes that are under negative control of GlpQ are more strongly expressed in the presence of glycerol as the carbon source (as compared to glucose). In contrast, the two lipoprotein genes *mpn284* and *mpn506* that require GlpQ for expression are only weakly expressed in the presence of glycerol, but they are strongly induced if glucose is used as the carbon source. These observations might be explained as follows: In the presence of glucose, only little glycerol or glycerol 3-phosphate (the product of the reaction catalyzed by GlpQ) is present in the cell. Free GlpQ might then directly bind DNA or trigger the DNA-binding activity of another, yet unknown transcription factor, resulting in repression or activation of the two sets of genes. In the presence of glycerol, glycerol 3-phosphate would be formed due to the activity of glycerol kinase, and this metabolite might then prevent GlpQ from its regulatory activity. As a result, those genes that are subject to GlpQ-dependent repression (*glpF*, *mpn162*, and *cbiO*) are stronger

expressed than in the presence of glucose, whereas the GlpQ-activated genes (*mpn284* and *mpn506*) would be less expressed. Finally, in the *glpQ* mutant, the former set of GlpQ-repressed genes is highly constitutively expressed, and only a very low level of transcription can be detected for the two GlpQ-dependent lipoprotein genes. Since glycerol 3-phosphate is the product of the glycerophosphodiesterase reaction, this metabolite is an excellent candidate for detection by GlpQ. Moreover, the *glpQ* gene is constitutively expressed and the GlpQ protein was detected in *M. pneumoniae* cells irrespective of the carbon source used in similar amounts in this study (Güell *et al.*, 2009; this study). Thus, GlpQ is available in the cell under all conditions to cause regulation. In a recent study on the phosphoproteome of *M. pneumoniae*, phosphorylation of GlpQ was observed (Schmidl *et al.*, 2010), however, the functional relevance of this modification is unknown.

As observed for several other transcription regulators, GlpQ causes both transcription repression and transcription activation. The location of the putative *cis*-acting element correlates perfectly with the regulatory effect: Those genes that are subject to negative control by GlpQ have this element overlapping or in the very close vicinity of the -10 region of the promoters. This element is the only conserved promoter element in *M. pneumoniae* and it is sufficient for transcription initiation (Güell *et al.*, 2009; Halbedel *et al.*, 2007). Binding of GlpQ (or of a transcription factor that is controlled by GlpQ) would prevent a productive interaction with RNA polymerase and therefore cause transcription repression. On the other hand, the *cis*-acting elements that may be involved in the regulation of the GlpQ-activated genes are located upstream of the promoters. This is usually the case for binding sites of transcription activators and fits perfect with the observed regulation.

Our future work will focus on the elucidation of the mechanism(s) by which GlpQ controls gene expression. Moreover, we will address the functions of the lipoproteins that are subject by glycerol- and GlpQ-dependent regulation.

Materials and Methods

Bacterial strains and growth conditions. The *M. pneumoniae* strains used in this study were *M. pneumoniae* M129 (ATCC 29342) in the 32nd broth passage, and its isogenic mutant derivatives GPM52 (*glpD*::mini-Tn, Gm^R) (Hames *et al.*, 2009), GPM81 (*glpQ*::mini-Tn, Gm^R), and GPM82 (*mpn566*::mini-Tn, Gm^R). *M. pneumoniae* was grown at 37°C in 150-cm² tissue culture flasks containing 100 ml of modified Hayflick medium as described previously (Halbedel *et al.*, 2004). Carbon sources were added to a final concentration of 1% (wt/vol). Growth curves were obtained by determining the wet weight of *M. pneumoniae* cultures as described previously (Halbedel *et al.*, 2004). Strains harboring transposon insertions were cultivated in the presence of 80 µg/ml gentamicin. *Escherichia coli* DH5α and BL21(DE3)/pLysS (Sambrook *et al.*, 1989) were used as host for cloning and recombinant protein expression, respectively. The sequences of the oligonucleotides used in this study are listed in Table S13.

Construction of plasmids for the expression of potential glycerophosphodiesterases. The *M. pneumoniae* genes encoding proteins similar to glycerophosphodiesterases (*glpQ* and *mpn566*) were amplified with chromosomal DNA as the template and the primer pairs SS34/SS35 and SS39/SS40, respectively. The PCR products were digested with *Sac*I and *Bam*HI and cloned into the expression vector pGP172 that allows the fusion of the target proteins to a *Strep*-tag at their N-terminus (Merzbacher *et al.*, 2004). The resulting plasmids were pGP1018 and pGP1020. Since the *glpQ* gene contains three TGA codons that are recognized as stop codons in *E. coli*, these codons were replaced by TGG specifying tryptophan as in *M. pneumoniae*. For this purpose we applied the multiple mutation reaction (Hames *et al.*, 2005) using the phosphorylated mutagenesis primers SS36, SS37, and SS38 and the external primers SS34 and SS35. The PCR product was digested and cloned into pGP172 as described above. The resulting expression vector was pGP1019. The plasmids pGP1019 and pGP1020 allowed the purification of the potential *M. pneumoniae* glycerophosphodiesterases (GlpQ and MPN566) carrying a N-terminal *Strep*-tag.

A mutant variant of MPN566 was obtained by the multiple mutation reaction using pGP1020 as the template and the phosphorylated mutagenesis primers SS192, SS193, and SS194 and the external primers SS39 and SS40. The PCR product was cloned into pGP172 as described above and the resulting plasmid was pGP661.

Protein purification. The potential glycerophosphodiesterases were overexpressed in *E. coli* BL21(DE3)/pLysS. Expression was induced by the addition of IPTG (final concentration 1 mM) to exponentially growing cultures (OD₆₀₀ of 0.8). Cells were lysed using a french press (20.000 p.s.i., 138,000 kPa, two passes, Spectronic Instruments, UK). After lysis the crude extracts were centrifuged at 15,000 g for 60 min. The crude extract was passed over a Streptactin column (IBA, Göttingen, Germany). The recombinant proteins were eluted with desthiobiotin (IBA, final concentration 2.5 mM).

After elution the fractions were tested for the desired protein using 12% SDS-PAGE. The relevant fractions were combined and dialyzed overnight. Protein concentration was determined according to the method of Bradford using the Bio-Rad dye-binding assay where Bovine serum albumin served as the standard.

Assays of glycerophosphodiesterase enzymatic activity. Glycerophosphodiesterase activity was measured in a coupled spectrophotometric assay as described previously (Larson *et al.*, 1983). The enzyme assay is based on the formation of glycerol 3-phosphate and the subsequent oxidation by the glycerol-3-phosphate dehydrogenase and the formation of NADH. Briefly, 5 µg of glycerophosphodiesterase were incubated with 20 U of rabbit muscle glycerol-3-phosphate dehydrogenase (Sigma) in a 0.9 M glycine-hydrazine buffer containing 0.5 mM glycerophosphodiesterases and 0.5 mM NAD⁺ in a volume of 1 ml. Divalent cations were added as indicated. NADH formation was determined photospectrometrically at 340 nm.

Determination of *in vivo* hydrogen peroxide production. The hydrogen peroxide production in *M. pneumoniae* was determined using the Merckoquant peroxide test (Merck, Darmstadt, Germany) as previously described (Hames *et al.*, 2009). Briefly, growing cells were resuspended in assay buffer and after incubation for 1 h at 37°C, glucose, glycerol, glycerol 3-phosphate or glycerophosphodiesterases (final concentration 100 µM) were added to one aliquot. An aliquot without any added carbon source served as the control. The test strips were dipped into the suspensions for 1 s and subsequently read.

Preparation and separation of whole cell extracts. Whole cell extracts of the different *M. pneumoniae* strains were prepared as described previously (Schmidl *et al.*, 2010). In order to analyze the complete proteome, 15 µg of the cell extracts were separated by one-dimensional 12% SDS-PAGE and the gels subsequently stained with Coomassie Brilliant Blue R250 dye (Serva). For protein identification, each running lane was cut out into 15 pieces followed by a separate analysis by mass spectrometry. The proteome analyses were performed in triplicate.

Protein identification by mass spectrometry. Gel pieces were washed twice with 200 µl 20 mM NH₄HCO₃/30% (v/v) acetonitrile for 30 min, at 37°C and dried in a vacuum centrifuge (Concentrator 5301, Eppendorf). Trypsin solution (10 ng/µl trypsin in 20 mM ammonium bicarbonate) was added until gel pieces stopped swelling and digestion was allowed to proceed for 16 to 18 h at 37°C. Peptides were extracted from gel pieces by incubation in an ultrasonic bath for 15 min in 20 µl HPLC grade water and transferred into micro vials for mass spectrometric analysis.

The tryptic digested proteins obtained from the one-dimensional SDS-PAGE gel pieces were subjected to a reversed phase column chromatography (Waters BEH 1.7 µm, 100-µm i.d. × 100 mm, Waters Corporation, Milford, Mass., USA) operated on a nanoACQUITY UPLC™ (Waters Corporation, Milford, Mass., USA). Peptides were first concentrated and desalted on a trapping column (Waters nanoACQUITY UPLC column, Symmetry C₁₈, 5 µm, 180 µm × 20 mm, Waters Corporation, Milford, Mass., USA) for 3 min at a flow rate of 1 ml/min with 0.1% acetic acid. Subsequently the peptides were eluted and separated with a non-linear 80-min gradient from 5-60% acetonitrile in 0.1% acetic acid at a constant flow rate of 400 nl/min. MS and MS/MS data were acquired with the LTQ Orbitrap™ mass spectrometer (Thermo Fisher, Bremen, Germany) equipped with a nanoelectrospray ion source. After a survey scan in the Orbitrap (*r* = 30,000), MS/MS data were recorded for the five most intensive precursor ions in the linear ion trap. Singly charged ions were not taken into account for MS/MS analysis.

Tandem mass spectra were extracted using Sorcerer™ v3.5 (Sage-N Research). All MS/MS samples were analyzed using SEQUEST® (Thermo Fisher Scientific, San Jose, CA, USA; version 2.7, revision 11). Database searching was performed against a target decoy database of *M. pneumoniae* with added common laboratory contaminant proteins. Cleavage specificity for full tryptic cleavage and a maximum of 2 missed

cleavages was assumed. SEQUEST was run with a fragment ion mass tolerance of 1.00 Da and a parent ion tolerance of 10 ppm. Oxidation of methionine (+15.99492 Da) and phosphorylation of serine/threonine/tyrosine (+79.966331 Da) were specified in SEQUEST as variable modifications. Proteins were identified by at least two peptides applying a stringent SEQUEST filter (Xcorr vs. charge state: 1.8 for singly, 2.2 for doubly, 3.3 for triply, and 3.5 for higher charged ions). To address protein amount differences between the *M. pneumoniae* wild type and mutant strains, fold-changes were calculated by comparing number of assigned spectra for each protein (mutant vs. wild type strain).

Southern blot analysis. *M. pneumoniae* chromosomal DNA was prepared as described previously (Halbedel *et al.*, 2006). Finally, digests of chromosomal DNA were separated using 1% agarose gels and transferred onto a positively charged nylon membrane (Roche Diagnostics) (Sambrook *et al.*, 1989) and probed with Digoxigenin (DIG)-labeled riboprobes obtained by *in vitro* transcription with T7 RNA polymerase (Roche Diagnostics) using PCR-generated fragments as templates. Primer pairs for the amplification of *glpQ*, *mpn566*, and *aac-ahpD* gene fragments were SS42/SS43, SS44/SS45, and SH62/SH63, respectively (Table S13). The reverse primers contained a T7 RNA polymerase recognition sequence. *In vitro* RNA labelling, hybridisation, and signal detection were carried out according to the manufacturer's instructions (DIG RNA labeling Kit and detection chemicals, Roche Diagnostics).

Analysis of mRNA amounts. Preparation of total *M. pneumoniae* RNA was done as previously described (Halbedel *et al.*, 2004). For slot blot analysis, serial twofold dilutions of the RNA extract in 10× SSC (2 µg - 0.25 µg) were blotted onto a positively charged nylon membran using a PR 648 Slot Blot Manifold (Amersham Biosciences). Equal amounts of yeast tRNA (Roche) and *M. pneumoniae* chromosomal DNA served as controls. DIG-labeled riboprobes were obtained by *in vitro* transcription from PCR products that cover ORF internal sequences using T7 RNA polymerase (Roche). The reverse primers used to generate the PCR products contained a T7 promoter sequence (Table S13). The quantification was performed using the Image J software v1.44c (Abramoff *et al.*, 2004).

HeLa cell cytotoxicity assay. Infection of HeLa cell cultures with *M. pneumoniae* cells were done as described previously (Hames *et al.*, 2009; Schmidl *et al.*, 2010). After four days upon infection, HeLa cells cultures were stained with crystal violet and photographed. The cytotoxicity assays were performed in triplicate.

Scanning electron microscopy. After growing of *M. pneumoniae* cultures in 5 ml culture to mid-log phase, the cells were scraped off and passed ten times through a syringe. Then, 20 μ l of this cell suspension were inoculated to 2 ml of modified Hayflick medium in a Lab-Tek chamber slide (Nunc). After growing cells to mid-log phase, the medium was removed and the cells were washed three times with PBS and fixed with 1% glutaraldehyde for 1 h. The samples were washed three times with PBS and then dehydrated sequentially with 30, 50, 70, 90, and 100% ethanol for 10 min each. Immediately, the critical point dried of samples was performed (K850 critical point drier; Emitech Ashfort, United Kingdom) and sputter coated with 20 nm of gold. Samples were observed using a Hitachi S-570 (Tokyo, Japan) scanning electron microscope.

Microcinematography. After passing through a syringe, cells grown in a 5 ml culture, 20 μ l of disaggregated cells were inoculated to 2 ml of modified Hayflick medium including 3% gelatine in 14 mm glass bottom culture dishes plates (MatTek). Cell movement was examined at 37°C using a Nikon Eclipse TE 2000-E microscope, and images were captured at intervals of 2 s for a total of 2 min with a digital sight DS-SMC Nikon camera controlled by NIS-Elements BR software. Tracks from 50 individual motile cells corresponding to 2 min of observation and 2 separated experiments were analyzed to determine the gliding velocity and gliding motile patterns.

Acknowledgments

We are grateful to Stephanie Großhennig and Daniel Reuß for the help with some experiments. This work was supported by grants from the Deutsche Forschungsgemeinschaft and the Fonds der Chemischen Industrie. S. R. S. was supported by a personal grant from the Studienstiftung des Deutschen Volkes.

Supporting information

Table S9. Proteins with differential expression pattern.

Locus name	Protein name	UniProtKB accession number	Locus name	Protein name	UniProtKB accession number	Locus name	Protein name	UniProtKB accession number
Only identified in the presence of glucose								
MPN012	-	P75101	MPN293	LspA	P75484	MPN502	-	P75285
MPN030	-	P75084	MPN333	-	P75445	MPN504	-	P75282
MPN035	-	P75079	MPN339	-	P75439	MPN505	-	P75281
MPN068	SecE	P75048	MPN345	HsdR	P75433	MPN507	-	P75279
MPN074	SmpB	P75043	MPN350	PlsY	P75428	MPN512	-	P75274
MPN095	-	P75597	MPN351	-	P75427	MPN537	MucB	P75241
MPN096	-	P75596	MPN385	-	P75397	MPN564	Adh	P75214
MPN100	-	P75592	MPN404	-	P75380	MPN569	-	P75209
MPN116	RpmI	P75447	MPN406	-	P75378	MPN575	-	P75204
MPN130	-	P75345	MPN411	-	P75373	MPN582	-	P75198
MPN136	UgpE	P75262	MPN414	-	P75372	MPN588	-	Q50339
MPN137	-	P75261	MPN431	-	P75357	MPN589	-	Q50338
MPN138	-	P75260	MPN435	-	P75343	MPN603	AtpE	Q59550

Table S9. Continued.

Locus name	Protein name	UniProtKB accession number	Locus name	Protein name	UniProtKB accession number	Locus name	Protein name	UniProtKB accession number
MPN145	-	P75141	MPN440	-	P75338	MPN605	-	Q50325
MPN146	-	P75140	MPN450	-	Q50362	MPN615	HsdS	P75180
MPN151	-	P75035	MPN455	CtaD	P75328	MPN624	RpmB	P75171
MPN152	-	P75034	MPN460	KtrB	P75323	MPN651	MtlA	P75146
MPN163	-	P75582	MPN471	RpmG	P78015	MPN657	-	P75134
MPN178	RpsN	Q50305	MPN482	-	Q9EXD7	MPN659	TrmD	P75132
MPN214	-	P75555	MPN494	UlaC	P75292	MPN675	-	P75117
MPN222	TilS	P75549	MPN495	UlaB	Q9EXD8	MPN682	RpmH	P78006
MPN253	PgsA	P75520	MPN496	UlaA	P75291			
Only identified in the presence of glycerol								
MPN057	PotC	P75057	MPN365	-	P75416	MPN488	-	P75297
MPN114	Cpt2	P75448	MPN417	P69	P75369	MPN640	-	P75157

Table S10. Proteins not detected in proteome analysis.

Locus name	Protein name	UniProtKB accession number	Locus name	Protein name	UniProtKB accession number	Locus name	Protein name	UniProtKB accession number
MPN010	-	P75103	MPN206	-	P75570	MPN466	-	P75317
MPN014	DnaE	P75099	MPN212	-	P75557	MPN467	-	P75316
MPN037	-	P75077	MPN242	SecG	Q9EXD0	MPN468	-	P75315
MPN038	-	P75076	MPN249	EngC	P75523	MPN485	-	P75300
MPN039	-	P75075	MPN270	-	Q9EXD1	MPN486	-	P75299
MPN040	-	P75074	MPN274	-	P75503	MPN497	-	P75290
MPN041	-	P75073	MPN282	-	P75495	MPN500	-	P75287
MPN042	-	P75072	MPN283	-	P75494	MPN503	-	P75283
MPN048	-	P75066	MPN285	PrrB	P75492	MPN508	-	P75278
MPN049	-	P75065	MPN286	-	P75491	MPN510	-	P75276
MPN054	-	P75060	MPN289	HsdS1B	P75488	MPN511	-	P75275
MPN056	PotB	P75058	MPN290	-	P75487	MPN513	-	P75273
MPN069	RpmG2	P56850	MPN304	ArcA	P75475	MPN514	-	P75272
MPN085	-	P75608	MPN305	ArcA	P75475	MPN525	-	P75253
MPN086	-	P75607	MPN306	ArcB	P75473	MPN527	-	P75251
MPN087	-	P75606	MPN313	-	P75468	MPN534	-	P75244

Table S10. Continued.

Locus name	Protein name	UniProtKB accession number	Locus name	Protein name	UniProtKB accession number	Locus name	Protein name	UniProtKB accession number
MPN088	-	P75605	MPN334	BcrA	P75444	MPN535	RuvA	P75243
MPN089	HsdS	P75604	MPN335	-	P75443	MPN536	RuvB	P75242
MPN091	-	P75602	MPN343	-	P75435	MPN540	RpmF	P75238
MPN092	-	P75600	MPN346	-	P75432	MPN565	-	P75213
MPN093	-	P75599	MPN347	HsdR	P75431	MPN570	-	P75208
MPN097	-	P75595	MPN363	-	P75418	MPN571	LcnDR3	P75207
MPN098	-	P75594	MPN364	-	P75417	MPN577	-	P75203
MPN099	-	P75593	MPN366	-	P75415	MPN578	-	P75202
MPN101	-	P75568	MPN367	-	P75414	MPN579	-	P75201
MPN102	-	P75567	MPN369	-	P75412	MPN580	-	P75200
MPN103	-	P75566	MPN370	-	P75411	MPN581	-	P75199
MPN107	-	P75562	MPN371	-	P75410	MPN583	-	P75197
MPN108	-	P75561	MPN373	-	P75408	MPN584	-	P75196
MPN110	-	P75452	MPN374	-	P75407	MPN586	-	P75194
MPN111	-	P75451	MPN375	-	P75406	MPN587	-	P75193
MPN112	-	P75450	MPN388	-	Q9EXD4	MPN590	-	Q50337

Table S10. Continued.

Locus name	Protein name	UniProtKB accession number	Locus name	Protein name	UniProtKB accession number	Locus name	Protein name	UniProtKB accession number
MPN113	-	P75449	MPN403	-	P75381	MPN593	-	Q50334
MPN127	-	P75348	MPN405	-	P75379	MPN594	-	P75191
MPN128	-	P75347	MPN409	-	P75375	MPN612	-	P75183
MPN129	-	P75346	MPN412	-	Q9EXD5	MPN613	-	P75182
MPN131	-	P75267	MPN413	-	Q9EXD6	MPN614	-	P75181
MPN132	-	P75266	MPN437	-	P75341	MPN626	-	P75169
MPN143	-	P75143	MPN438	-	P75340	MPN633	-	P75164
MPN144	-	P75142	MPN439	-	P75339	MPN634	-	P75163
MPN147	-	P75139	MPN441	-	P75337	MPN635	-	P75162
MPN149	-	P75037	MPN442	-	P75336	MPN637	CdsA	P75160
MPN150	-	P75036	MPN448	-	Q50364	MPN644	-	P75153
MPN160	-	P75585	MPN451	Come3	Q50361	MPN648	-	P75149
MPN188	RpmJ	P52864	MPN457	-	P75326	MPN649	-	P75148
MPN201	-	Q50287	MPN458	-	P75325	MPN650	-	P75147
MPN202	-	Q50286	MPN462	-	P75321	MPN654	-	P75137
MPN203	-	Q50284	MPN463	-	P75320	MPN666	-	P75125

Table S10. Continued.

Locus name	Protein name	UniProtKB accession number	Locus name	Protein name	UniProtKB accession number	Locus name	Protein name	UniProtKB accession number
MPN204	-	P75572	MPN464	-	P75319	MPN676	-	P75116
MPN205	-	P75571	MPN465	-	P75318	MPN681	RnpA	P75111

Table S11. Summary of proteome and transcript analysis in the *glpQ* mutant GPM81 in the presence of glucose.

Locus name	Protein name	UniProtKB accession number	Protein function	COG ^a	Molecular weight (kDa)	Isoelectric point (pI)	Fold-change ^b	
							Protein level	Transcript level
Induced expression								
MPN023	MetG	P75091	Methionyl-tRNA synthetase	J	59.26	6.63	2.25 ± 0.22	na
MPN043	GlpF	P75071	Glycerol uptake facilitator	G	28.31	9.33	10.79 ± 1.06	5.69 ± 0.36
MPN060	MetK	P78003	S-adenosylmethionine synthetase	J	42.56	6.07	2.33 ± 0.11	na
MPN162	-	P75583	Uncharacterized lipoprotein	S	36.10	6.19	9.96 ± 0.97	5.23 ± 0.23
MPN179	RpsH	Q50304	30S ribosomal protein S8	J	15.88	10.32	2.63 ± 0.33	na
MPN191	RpoA	Q50295	RNA polymerase subunit α	K	36.66	6.98	2.30 ± 0.04	2.18 ± 0.17
MPN209	PacL	P78036	Cation-transporting P-type ATPase	P	94.97	6.38	2.49 ± 0.26	na
MPN221	Pth	P78034	Peptidyl-tRNA hydrolase	J	21.42	9.52	2.43 ± 0.14	na
MPN223	HPrK	P75548	HPr kinase phosphorylase	O	35.24	8.89	2.90 ± 0.29	2.83 ± 0.09
MPN239	-	P75532	HTH-type transcriptional regulator	K	25.85	9.50	2.53 ± 0.17	3.16 ± 0.14
MPN244	DisA	P75528	Uncharacterized protein	L	22.73	9.38	2.72 ± 0.30	3.39 ± 0.19
MPN247	PrpC	P75525	Protein phosphatase	O	29.69	8.57	2.43 ± 0.18	2.91 ± 0.12
MPN248	PrkC	P75524	Serine threonine-protein kinase	O	44.88	9.08	2.33 ± 0.11	na
MPN254	CinA	Q9EXC9	Uncharacterized protein	S	16.96	8.81	2.60 ± 0.27	2.11 ± 0.10
MPN266	Spx	P75509	Transcriptional regulator	K	16.81	9.81	2.71 ± 0.13	2.23 ± 0.07

Table S11. Continued.

Locus name	Protein name	UniProtKB accession number	Protein function	COG ^a	Molecular weight (kDa)	Isoelectric point (pI)	Fold-change ^b	
							Protein level	Transcript level
MPN279	LepA	P75498	GTP-binding protein	J	66.16	7.58	2.34 ± 0.18	na
MPN299	PlsC	P75479	1-acyl- <i>sn</i> -glycerol-3-phosphate acyltransferase	I	30.42	9.79	3.20 ± 0.35	6.43 ± 0.31
MPN300	ScpA	P75478	Segregation and condensation protein A	U	59.52	8.15	2.45 ± 0.18	na
MPN338	-	P75440	Uncharacterized protein	S	74.34	5.60	2.51 ± 0.23	na
MPN340	PcrA	P75438	DNA helicase II	L	60.53	6.23	2.43 ± 0.21	na
MPN357	LigA	P78021	DNA ligase	L	73.97	8.40	2.58 ± 0.30	na
MPN359	-	P75421	Uncharacterized protein	S	30.56	9.67	2.34 ± 0.24	na
MPN372	-	P75409	ADP-ribosylating toxin CARDS	V	68.06	5.63	2.91 ± 0.21	2.72 ± 0.20
MPN407	-	P75377	Lipase	I	101.09	5.81	2.13 ± 0.11	na
MPN408	-	P75376	Uncharacterized lipoprotein	S	83.35	9.16	3.57 ± 0.26	na
MPN425	FtsY	P75362	Cell division protein homolog	D	38.78	6.85	2.34 ± 0.21	na
MPN433	CbiO	P75355	Metal ion ABC transporter ATP-binding protein	P	30.77	8.41	ns	7.56 ± 0.39
MPN456	-	P75327	Uncharacterized lipoprotein	S	110.52	6.33	2.35 ± 0.18	na
MPN518	-	P75269	Uncharacterized protein	S	40.72	8.93	3.42 ± 0.12	na
MPN544	-	P75234	Uncharacterized protein	S	76.77	7.50	5.14 ± 0.48	na
MPN552	-	P75226	Uncharacterized protein	S	30.91	5.66	4.04 ± 0.41	na

Table S11. Continued.

Locus name	Protein name	UniProtKB accession number	Protein function	COG ^a	Molecular weight (kDa)	Isoelectric point (pI)	Fold-change ^b	
							Protein level	Transcript level
MPN566	-	P75212	Similar to glycerophosphoryldiester phosphodiesterase	S	27.72	9.24	2.89 ± 0.16	4.98 ± 0.24
MPN625	-	P75170	Osmotical inducible protein C-like protein	O	15.47	6.50	2.56 ± 0.13	na
MPN664	DegV	P75127	Uncharacterized protein	S	26.84	9.11	2.63 ± 0.30	na
Repressed expression								
MPN015	-	P75098	Uncharacterized protein	S	33.45	9.89	0.27 ± 0.02	na
MPN018	Pmd1	P75095	ABC transporter ATP-binding protein	S	68.93	9.07	0.20 ± 0.05	sa
MPN019	MsbA	P75094	ABC transporter ATP-binding protein	S	71.15	9.52	0.17 ± 0.04	na
MPN055	PotA	P75059	Spermidine putrescine import ATP-binding protein	E	65.13	9.10	0.26 ± 0.02	na
MPN083	-	P75610	Uncharacterized lipoprotein	S	59.97	7.69	nd	2.81 ± 0.16
MPN084	-	P75609	Uncharacterized lipoprotein	S	59.56	5.98	0.32 ± 0.03	na
MPN090	-	P75603	Adhesin P1	M	37.44	9.52	0.47 ± 0.03	na
MPN134	UgpC	P75264	<i>sn</i> -glycerol-3-phosphat transport system permease	G	66.47	9.11	0.39 ± 0.06	sa
MPN258	YjcW	P75516	Sugar ABC transporter ATP-binding protein	S	64.87	9.55	0.21 ± 0.04	sa
MPN259	-	P75515	Sugar ABC transporter permease	S	58.59	9.71	0.22 ± 0.06	na
MPN260	RbsC	P75514	Sugar ABC transporter permease	S	33.49	9.42	0.37 ± 0.01	na
MPN284	-	P75493	Uncharacterized lipoprotein	S	87.17	9.16	ns	0.25 ± 0.05

Table S11. Continued.

Locus name	Protein name	UniProtKB accession number	Protein function	COG ^a	Molecular weight (kDa)	Isoelectric point (pI)	Fold-change ^b	
							Protein level	Transcript level
MPN322	NrdF	P75461	Ribonucleoside-diphosphate reductase subunit β	F	39.41	5.47	0.38 \pm 0.05	ns
MPN323	NrdI	P75460	Ribonucleoside-diphosphate reductase stimulatory protein	F	17.15	7.79	0.29 \pm 0.06	na
MPN324	NrdE	P78027	Ribonucleoside-diphosphate reductase subunit α	F	82.38	6.63	0.40 \pm 0.05	na
MPN420	GlpQ	P75367	Glycerophosphoryldiester phosphodiesterase	C	28.37	6.32	nd	na
MPN449	-	Q50363	Uncharacterized protein	S	50.55	9.32	0.10 \pm 0.04	na
MPN498	UlaF	P75289	L-ribulose-5-phosphate 4-epimerase	C	27.09	6.44	0.20 \pm 0.04	sa
MPN506	-	P75280	Uncharacterized lipoprotein	S	87.50	9.24	0.10 \pm 0.03	0.07 \pm 0.05
MPN684	-	P75109	ABC transporter permease	S	209.45	8.23	0.32 \pm 0.03	sa
MPN685	CysA	Q50316	ABC transport ATP-binding protein	S	32.24	9.69	0.21 \pm 0.04	na

^a Abbreviations: COG, Cluster of orthologous groups of proteins; C, Energy production and conversion; D, Cell cycle control, cell division, and chromosome partitioning; E, Amino acid transport and metabolism; F, Nucleotide transport and metabolism; G, Carbohydrate transport and metabolism; I, Lipid metabolism; J, Translation, ribosomal structure, and biogenesis; K, Transcription; L, Replication, recombination, and repair; M, Cell wall, membrane, and envelope biogenesis; O, Posttranslational modification, protein turnover, and chaperones; P, Inorganic ion transport and metabolism; S, Function unknown; U, Intracellular trafficking, secretion, and vesicular transport; V, Defense mechanisms.

^b Fold-change cut off ≥ 2.0 and ≤ 0.5 , respectively (*glpQ* mutant strain vs. wild type). Abbreviations: na, not available; nd, not detectable; ns, no significant difference; sa, similar amount.

Table S12. Summary of proteome and transcript analysis in the *glpQ* mutant GPM81 in the presence of glycerol.

Locus name	Protein name	UniProtKB accession number	Protein function	COG ^a	Molecular weight (kDa)	Isoelectric point (pI)	Fold-change ^b	
							Protein level	Transcript level
Induced expression								
MPN043	GlpF	P75071	Glycerol uptake facilitator	G	28.31	9.33	5.83 ± 0.76	3.32 ± 0.34
MPN162	-	P75583	Uncharacterized lipoprotein	S	36.10	6.19	5.41 ± 0.83	2.81 ± 0.47
MPN433	CbiO	P75355	Metal ion ABC transporter ATP-binding protein	P	30.77	8.41	5.66 ± 0.49	2.92 ± 0.24
MPN444	-	P75334	Uncharacterized lipoprotein	S	146.28	7.89	2.74 ± 0.09	na
MPN489	-	P75296	Uncharacterized lipoprotein	S	143.06	9.14	2.40 ± 0.20	na
Repressed expression								
MPN284	-	P75493	Uncharacterized lipoprotein	S	87.17	9.16	0.36 ± 0.02	0.35 ± 0.04
MPN288	-	P75489	Uncharacterized lipoprotein	S	86.89	9.07	0.29 ± 0.03	na
MPN420	GlpQ	P75367	Glycerophosphoryldiester phosphodiesterase	C	28.37	6.32	nd	na
MPN506	-	P75280	Uncharacterized lipoprotein	S	87.50	9.24	0.18 ± 0.04	0.16 ± 0.02
MPN673	-	P75118	Uncharacterized protein	S	19.47	9.16	0.21 ± 0.03	na

^a Abbreviations: COG, Cluster of orthologous groups of proteins; C, Energy production and conversion; G, Carbohydrate transport and metabolism; P, Inorganic ion transport and metabolism; S, Function unknown.

^b Fold-change cut off ≥ 2.0 and ≤ 0.5 , respectively (*glpQ* mutant strain vs. wild type). Abbreviations: na, not available; nd, not detectable.

Table S13. Oligonucleotides used in this study.

Oligonucleotide	Sequence (5'→3') ^{ab}	Description
CH61	ATGCCAAATCCTGTTAGATTTGTTTAC	<i>mpn372</i> probe fw
CH63	<u>CTAATACGACTCACTATAGGGAGAGCCGGGTGGTGAGCATG</u>	<i>mpn372</i> probe rev
SH03	GAGTACCCGGATTAAGCGGG	<i>hprK</i> probe fw
SH04	<u>CTAATACGACTCACTATAGGGAGACATTA</u> ACTGGATTTCCGGTGCGCTG	<i>hprK</i> probe rev
SH05	CAGGTAACGGTGCTGGTTCG	<i>glpF</i> probe fw
SH06	<u>CTAATACGACTCACTATAGGGAGAATTGCAGTACCAGTAGCGGC</u>	<i>glpF</i> probe rev
SH29	ATGAGTGAGCTAACTCACAG	Screening primer for transposon insertions
SH30	CAATACGCAAACCGCCTC	Screening primer for transposon insertions
SH62	TAGAATTTTATGGTGGTAGAG	<i>aac-ahpD</i> probe fw
SH63	<u>CTAATACGACTCACTATAGGGAGAACACTATCATA</u> ACCACTACC	<i>aac-ahpD</i> probe rev
SH66	AAAGTCGACATGGACAGCACCAACCAAAAC	<i>prpC</i> probe fw (<i>Sal</i> I)
SH73	<u>CTAATACGACTCACTATAGGGAGAGACC</u> ATCAGAGCACAACAG	<i>prpC</i> probe rev
SS34	AAAGAGCTCGATGCTTAAACGACAACCTTCTGCTAGC	<i>glpQ</i> gene fw (<i>Sac</i> I)
SS35	TATAGGATCCTTACACTTCAAACCTTCTTGTTGGCAATTTG	<i>glpQ</i> gene rev (<i>Bam</i> HI)
SS36	P_GCCTTTTTGTTTTGGACGAAAAAGCAGTTCCAAG	<i>glpQ</i> A507G
SS37	P_CAGTATCTCCATCCCTGGACAAACATTTACG	<i>glpQ</i> A576G
SS38	P_CCTTTAGGGCTGTGGACGCTTAACAGTG	<i>glpQ</i> A639G
SS39	AAAGAGCTCGATGCGCAAACAGTTTTTAATTGCACAC	<i>mpn566</i> gene fw (<i>Sac</i> I)

Table S13. Continued.

Oligonucleotide	Sequence (5'→3') ^{ab}	Description
SS40	TATAGGATCCTTAGTAAAGTTGTGCTGCTATTTGAAATTTAAC	<i>mpn566</i> gene rev (<i>Bam</i> HI)
SS42	CAACTTCTGCTAGCACACCG	<i>glpQ</i> probe fw
SS43	<u>CTAATACGACTCACTATAGGGAGAGCTATTTGGTAGTTGGGGTTAATG</u>	<i>glpQ</i> probe rev
SS44	GCAAACAGTTTTTAATTGCACACCG	<i>mpn566</i> probe fw
SS45	<u>CTAATACGACTCACTATAGGGAGAGCTCTTAACTTTTCGTTGAGGTAC</u>	<i>mpn566</i> probe rev
SS123	GAATCAGTTTCTCCCTTAGAATATGC	<i>nrdF</i> probe fw
SS124	<u>CTAATACGACTCACTATAGGGAGAGTCTTCCCGGTGTAATAGGG</u>	<i>nrdF</i> probe rev
SS127	CCAACAGCGCTTTTATTCTCGG	<i>mpn083</i> probe fw
SS128	<u>CTAATACGACTCACTATAGGGAGAGGACATTAGGTTTGGTGTACTTAC</u>	<i>mpn083</i> probe rev
SS129	CCTTGTTAGTTGCGCCACAC	<i>mpn162</i> probe fw
SS130	<u>CTAATACGACTCACTATAGGGAGACACCTTCGTGGTGATCATGATC</u>	<i>mpn162</i> probe rev
SS131	GGCTTAGTCATCCACACTTGG	<i>ulaF</i> probe fw
SS132	<u>CTAATACGACTCACTATAGGGAGACCACTGCATCCTTGCCATTC</u>	<i>ulaF</i> probe rev
SS135	GGTTTACCCGTTTTTGTGTTAATGC	<i>plsC</i> probe fw
SS136	<u>CTAATACGACTCACTATAGGGAGAGCCCCGATTTAAACTCACCAATTTG</u>	<i>plsC</i> probe rev
SS137	CCGTTACATTCTCCTTAAAATTCAAAG	<i>mpn239</i> probe fw
SS138	<u>CTAATACGACTCACTATAGGGAGAGCTCTACCACAATGCCGTTG</u>	<i>mpn239</i> probe rev
SS139	ATGCTTAAGAAAAAAGTTAATAATGATGCTG	<i>spx</i> probe fw

Table S13. Continued.

Oligonucleotide	Sequence (5'→3') ^{ab}	Description
SS140	<u>CTAATACGACTCACTATAGGGAGATTACTTCTTTACTGTACGCACTTTAGG</u>	<i>spx</i> probe rev
SS141	CCGCTTTTCACCTTTGCACAG	<i>pmd1</i> probe fw
SS142	<u>CTAATACGACTCACTATAGGGAGAGAGTTAGTGGCAATAGCAAAGGC</u>	<i>pmd1</i> probe rev
SS143	GCTAATGTAGATGTTAACCTCACG	<i>yjcW</i> probe fw
SS144	<u>CTAATACGACTCACTATAGGGAGACTCAAAACAGCGGTTGGTTCATC</u>	<i>yjcW</i> probe rev
SS145	CCTGATTTATGACAAAGAAGGTAACC	<i>mpn684</i> probe fw
SS146	<u>CTAATACGACTCACTATAGGGAGAGGGATTAGTCTCTAACCAAAACTG</u>	<i>mpn684</i> probe rev
SS147	GAATATTGTAGTCGACTTTGGTGAG	<i>ugpC</i> probe fw
SS148	<u>CTAATACGACTCACTATAGGGAGAGGTTAGCTTCCAGTTCACTCTG</u>	<i>ugpC</i> probe rev
SS168	GCTAAATCATAAGCTCACCATTGC	<i>cinA</i> probe fw
SS169	<u>CTAATACGACTCACTATAGGGAGAGCTGCATCTTGTTCTCTTAAACC</u>	<i>cinA</i> probe rev
SS170	CTAACCCCAACTACGGCATC	<i>rpoA</i> probe fw
SS171	<u>CTAATACGACTCACTATAGGGAGACCCCAAAGAATTAATCATTTCACGG</u>	<i>rpoA</i> probe rev
SS172	CTTAATCTTAGCGCTTACCTTGTTG	<i>disA</i> probe fw
SS173	<u>CTAATACGACTCACTATAGGGAGAGTTTTTAATCACGCCGCGCAC</u>	<i>disA</i> probe rev
SS176	CTCAATTTTAGCCTCAAACCCAAC	<i>cbiO</i> probe fw
SS177	<u>CTAATACGACTCACTATAGGGAGACCGCTTTAGTTTGCTAGCTAGC</u>	<i>cbiO</i> probe rev
SS190	GCTGCCTGTGGTACAAAGG	<i>mpn506</i> probe fw

Table S13. Continued.

Oligonucleotide	Sequence (5'→3') ^{ab}	Description
SS191	<u>CTAATACGACTCACTATAGGGAGAGTACCTTCTTTCTTTT</u> AGCGTTGTTC	<i>mpn506</i> probe rev
SS192	P_GATGGTTTGGAGATGGATGTGCAACTCAC	<i>mpn566</i> T106G/G107A/A114T
SS193	P_CGTTTCGCTTCTCTTGCTTGAAATTAAGGGCG	<i>mpn566</i> T328G/T329A/T330A
SS194	P_GTAGTCACTCATGATGACAACATAAGGTAGGAAATAAAACC	<i>mpn566</i> A151C/T154G/T155A/A156T
SS199	CCAATTAAGCTCCTTCAAAGAATGG	<i>mpn284</i> probe fw
SS200	<u>CTAATACGACTCACTATAGGGAGACGATCGTATTGTTCGTCATTAATTTTG</u>	<i>mpn284</i> probe rev

^a Restriction sites and T7-promoters are underlined, respectively.

^b The “P” at the 5' end of primer sequences indicates phosphorylation.

Fig. S4. Multiple sequence alignment of GlpQ and MPN566 from *M. pneumoniae* with orthologous glycerophosphodiesterases of other bacteria. The multiple sequence alignment was performed using ClustalW (<http://www.ch.embnet.org/software/ClustalW.html>) and represented with BOXSHADE v3.21 (http://www.ch.embnet.org/software/BOX_form.html). Black shading indicates $\geq 80\%$ identity and grey shading stands for $\geq 80\%$ similarity. Amino acids that constitute to the strictly conserved active site structure are depicted by black arrows. The UniProtKB entry names of the aligned sequences are Y420_MYCPN (GlpQ, *M. pneumoniae*), Y566_MYCPN (MPN566, *M. pneumoniae*), Y293_MYCGE (MG_293, *M. genitalium*), Y385_MYCGE (MG_385, *M. genitalium*), D4XVJ7_9MOLU (MALL_0582, *M. alligatoris*), D4XVF1_9MOLU (MALL_0631, *M. alligatoris*), Q8XNB7_CLOPE (GlpQ, *Clostridium perfringens*), Q8XJ84_CLOPE (GlpQ, *C. perfringens*), YHDW_BACSU (YhdW, *B. subtilis*), GLPQ_BACSU (GlpQ, *B. subtilis*), YQIK_BACSU (YqiK, *B. subtilis*), GLPQ_TREPA (GlpQ, *T. pallidum*), GLPQ_HAEIN (GlpQ, *H. influenzae*), GLPQ_ECOLI (GlpQ, *E. coli*), and UGPQ_ECOLI (UgpQ, *E. coli*).

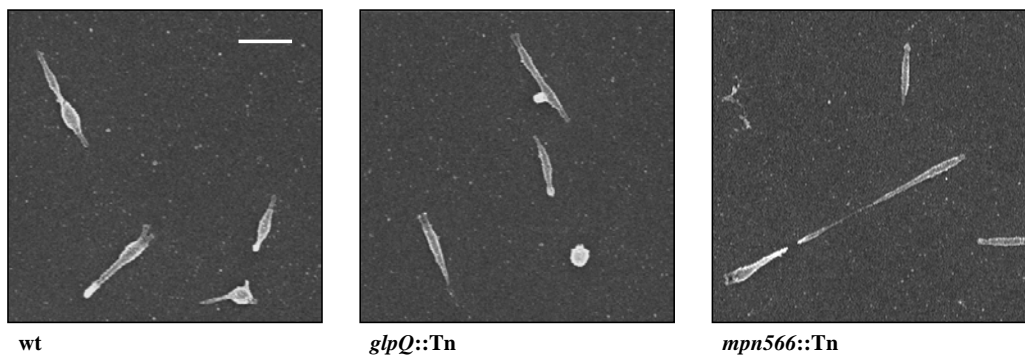


Fig. S5. Scanning electron microscopy analyses of *M. pneumoniae*. Morphology and cell division of *M. pneumoniae* wild type (wt), *glpQ::Tn*, and *mpn566::Tn* mutant strains were compared with each other. All pictures are shown at the same magnification. Scale bar, 1.0 μm .

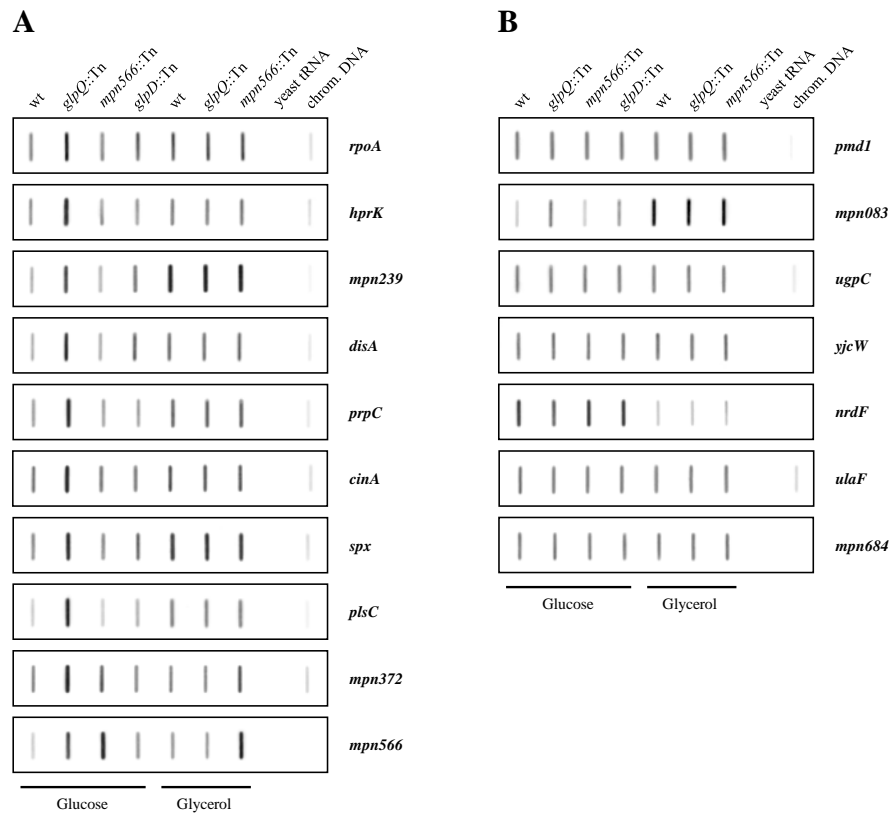


Fig. S6. Transcription analysis of interesting genes with protein amount changes in the *glpQ* mutant. Slot blots were performed with whole RNA extracts of *M. pneumoniae* wild type (wt), *glpQ*::Tn, *mpn566*::Tn, and *glpD*::Tn [control; Hames *et al.* (2009)] mutant strains grown in modified Hayflick medium containing either glucose or glycerol as sole carbon source (1% wt/vol). A dilution series of RNA extracts was blotted onto a positively charged nylon membrane and probed with a DIG-labeled riboprobe specific for an internal part of a particular open reading frame. Names of riboprobes are given next to each blot. Signals obtained with 1 µg of RNA are shown. Yeast tRNA and *M. pneumoniae* chromosomal DNA served as controls. Genes which had a significant higher protein amount in the *glpQ*::Tn mutant with glucose as carbon source are shown in (A) and genes with significant lower protein amounts in (B). For detailed information on changes of transcript levels see Table S11 and S12.

Chapter 8

Discussion

Protein phosphorylation in a minimal organism and its impact on virulence

Although much work has been devoted to the Mollicutes in the past few years, only little is known about their regulatory mechanisms. One major question is, how *Mycoplasma pneumoniae* cells recognize whether they are approaching a host tissue or not, and which changes in protein activities and/or gene expressions are caused. The most prominent regulatory mechanism both in bacteria and in eukaryotes is the control of protein activity by protein phosphorylation (Boekhorst *et al.*, 2008; Jers *et al.*, 2008). Bacteria possess two different classes of phosphorylation events. In addition to histidine and aspartate phosphorylation as part of two-component signal transduction (Hoch, 2000; Stock *et al.*, 2000), serine/threonine/tyrosine phosphorylation is also present and comes more and more into the spotlight. Phosphoproteome studies have been performed for several bacteria, including the model organisms *Escherichia coli* and *Bacillus subtilis* (Eymann *et al.*, 2007; Lévine *et al.*, 2006; Macek *et al.*, 2008; Macek *et al.*, 2007) or pathogens like *Klebsiella pneumoniae* or *Streptococcus pneumoniae* (Lin *et al.*, 2009; Sun *et al.*, 2010).

The analysis of the phosphoproteome of *M. pneumoniae* revealed substantial protein serine/threonine/tyrosine phosphorylation even in this minimal organism. In total 63 phosphorylated proteins could be identified that account for nearly 10% of all proteins encoded by *M. pneumoniae*. Compared to only 2.5% of all proteins of *B. subtilis* that are known to be phosphorylated on a serine, threonine or tyrosine residue (Eymann *et al.*, 2007; Lévine *et al.*, 2006; Macek *et al.*, 2007), it can be speculated that protein phosphorylation occurs more frequently in *M. pneumoniae* than in other bacteria. This might be related to the lack of an obvious transcription regulation machinery in *M. pneumoniae* (Dandekar *et al.*, 2000; Himmelreich *et al.*, 1996). Nevertheless, the size of all studied bacterial phosphoproteomes so far is remarkably similar suggesting a conservation of phosphorylated proteins. A comparison of the phosphoproteomes revealed a high proportion of phosphoproteins, including glycolytic enzymes and elongation factors that are conserved throughout the bacterial kingdom (Soufi *et al.*, 2008; this work). However, phosphorylation sites are hardly conserved and only one site, a serine residue of phosphosugar mutases, is actually identical in all living organisms from archaea and bacteria to man (Soufi *et al.*, 2008; this work). This observation might be due to the fact that site specific phosphorylation coevolved with

the adaptation of an organism to an individual ecological niche. Furthermore, the phosphorylation process might also partially result from gene transfer as many eukaryote-like kinases have been found in bacteria by metagenomic approaches (Yooseph *et al.*, 2007). This suggests that regulation via protein phosphorylation developed relatively late in the evolution. In general, eukaryotic phosphosites are more conserved throughout the eukaryotic domain (Gnad *et al.*, 2010). An explanation for this could be that in eukaryotes phosphorylation regulates many key processes including cell growth, proliferation, differentiation, and immune response (Hubbard and Miller, 2007; Pawson and Scott, 2005), processes which are not present in bacteria.

The knowledge about phosphorylation events and their regulation is crucial to understand the functional biology of an organism. *M. pneumoniae* contains two protein kinases, the HPr kinase (HPrK) and a serine/threonine protein kinase C (PrkC) (Steinhauer *et al.*, 2002; this work). For HPrK, only an implication in the phosphorylation of the HPr protein could be observed. In *B. subtilis* and other Firmicutes, the phosphorylation of HPr on Ser-46 is a major signal to trigger carbon catabolite repression (Görke and Stülke, 2008). In this case, HPr(Ser-P) acts as the cofactor for the pleiotropic transcription factor CcpA to regulate the expression of catabolic genes and operons. However, no such protein is encoded in the genome of *M. pneumoniae* suggesting a different role for HPr(Ser-P). This idea is supported by the fact that also the proteome of the *hprK* mutant was similar to the wild type strain.

The kinase PrkC is implicated in various cellular processes in different bacteria, among them spore germination, virulence, and control of glycolysis (Kristich *et al.*, 2007; Lomas-Lopez *et al.*, 2007; Shah *et al.*, 2008). In *M. pneumoniae*, six target proteins could be identified, including the major adhesin P1, two large cytoadherence proteins HMW1 and HMW2, the adhesin-related protein P41, the coiled coil surface protein MPN474, and a protein of unknown function MPN256 (Fig. 36A). Phosphorylation of most of these proteins was reported earlier (Krebes *et al.*, 1995; Su *et al.*, 2007). However, the corresponding kinase had not been identified. The HMW proteins and P1 are part of the so-called terminal organelle of *M. pneumoniae* that is involved in gliding motility, cell division, and adhesion to host epithelial tissues (Balish and Krause, 2006; Miyata, 2010). PrkC-dependent phosphorylation seems to be required for the stability of this protein complex due to the observation that an inactivation of the kinase led not only to a loss of protein phosphorylation, but also to a

decrease of the protein amount of the target proteins and also additional cytodherence proteins. It is known that the cytodherence proteins show a reciprocal dependency in their stabilities (Balish and Krause, 2006). Specifically, HMW1 was shown to be required for HMW2 and P1 localization and stability (Willby *et al.*, 2004). In turn, HMW2 is necessary for the stabilization of HMW3 and P65 (Fisseha *et al.*, 1999). As shown in this work, it has been suggested previously that the interdependence of the proteins of the attachment organelle is regulated posttranslationally (Popham *et al.*, 1997). In conclusion, PrkC is essential for cell adhesion in *M. pneumoniae*, which is also reflected by a nonadherent growth type of the *prkC* mutant strain. Furthermore, this mutant has lost cytotoxicity toward HeLa cells, most likely due to defects in cell adhesion. Interestingly, it has been reported that the *prpC* mutant has a reduced gliding velocity (Hasselbring *et al.*, 2006). Indeed, phosphorylation of the six PrkC target proteins was enhanced in the *prpC* mutant strain suggesting that PrpC is the protein phosphatase that reverses PrkC-dependent protein phosphorylation in *M. pneumoniae* (see Fig. 36A). Thus, the antagonistic PrkC/PrpC pair has a specific function in *M. pneumoniae* and phosphorylates/dephosphorylates a specific set of proteins. Nevertheless, PrpC is implicated in two more dephosphorylation events. First in the dephosphorylation of HPr(Ser-P) (Halbedel *et al.*, 2006) and in addition, PrpC seems also to dephosphorylate RpoE, the RNA polymerase subunit δ (Fig. 36B). Unfortunately, the role of both dephosphorylation events is unknown.

As already mentioned, HPrK and PrkC are the only two annotated protein kinases in *M. pneumoniae*. However, these known kinases were not responsible for the majority of phosphorylation events, since only seven phosphoproteins were affected by the loss of one of these two kinases. This suggests the existence of other, yet to be discovered protein kinases in *M. pneumoniae*. Alternatively, autophosphorylation of proteins might be more relevant than previously anticipated. Indeed, it could be shown in this work that the only universally conserved phosphorylation event in all living organisms is the result of an autophosphorylation in the catalytic site of phosphosugar mutases such as *B. subtilis* GlmM (Ser-100) and *M. pneumoniae* ManB (Ser-149). For the orthologue of both phosphosugar mutases in *E. coli*, it was established that the protein is only active in the phosphorylated form (Jolly *et al.*, 2000; Mengin-Lecreulx *et al.*, 1996). Thus, autophosphorylation is essential for the enzymatic activity of these enzymes. In general, mutases are widespread over all phyla of life

suggesting a conserved reaction mechanism. Therefore, it is not surprising to find autophosphorylation of mutases in other organisms like the archaeon *Sulfolobus solfataricus* or the mouse (Gururaj *et al.*, 2004; Potters *et al.*, 2003). Autophosphorylation was also identified for the GTP-binding protein Era in *E. coli* or the mammalian glyceraldehyde-3-phosphate dehydrogenase (Kawamoto and Caswell, 1986; Sood *et al.*, 1994). Another protein group where autophosphorylation events seem to be very common, are the chaperones. The ubiquitous heat shock protein DnaK (also called Hsp70) is present as a phosphoprotein in all studied organisms so far. In *E. coli* and mycobacteria, DnaK is capable of autophosphorylating at a strongly conserved threonine residue (McCarty and Walker, 1991; Peake *et al.*, 1998; Preneta *et al.*, 2004; Zylicz *et al.*, 1983). This site is also present in the DnaK protein of *M. pneumoniae* (Thr-182) suggesting a possible autophosphorylation mechanism.

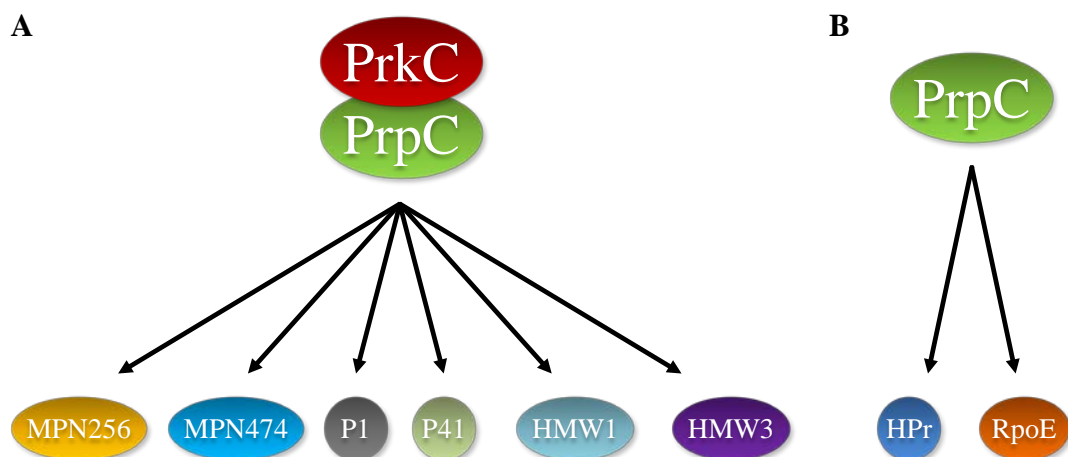


Fig 36. Overview of PrkC/PrpC-dependent phosphorylation events in *M. pneumoniae*. (A) Proteins affected by the antagonistic kinase/phosphatase pair. Loss of the Ser/Thr kinase PrkC results in an absence of protein phosphorylation probably leading to the observed decrease in protein amount of the proteins (protein amount of MPN474 is not influenced). In contrast, the proteins are more intensively phosphorylated in the *prpC* mutant. HMW1, cytoadherence high molecular weight protein 1; HMW3, cytoadherence high molecular weight protein 3; MPN256, uncharacterized protein; MPN474, coiled coil surface protein; P1, major adhesin; P41, adhesin-related protein. (B) Additional proteins dephosphorylated by PrpC. HPr is phosphorylated by HPrK at the conserved Ser-46 residue, whereas the phosphorylation mechanism of RpoE is unknown. HPr, phosphocarrier protein; RpoE, RNA polymerase subunit δ .

Glycerophosphodiesterases: Multiple roles for universal proteins

M. pneumoniae exhibits a hemolytic activity. While hemolysis by bacterial pathogens is usually caused by extracellular enzymes, the hemolysin of *M. pneumoniae* was identified as hydrogen peroxide (Somerson *et al.*, 1965). The synthesis of hydrogen peroxide by *M. pneumoniae* is strongly increased if the cells are supplied with glycerol (Low, 1971). This can be attributed to the oxidase activity of the glycerol-3-phosphate oxidase GlpD that oxidizes glycerol 3-phosphate (G3P). This enzyme uses molecular oxygen rather than NAD^+ (as in typical glycerol-3-phosphate dehydrogenases) as the sink for electrons (Hames *et al.*, 2009). Three potential pathways for the acquisition of G3P exist in *M. pneumoniae*. Glycerol may cross the cell membrane, mediated by the glycerol facilitator GlpF, and be phosphorylated by the glycerol kinase GlpK. Furthermore, *M. pneumoniae* can acquire G3P by direct uptake via the ABC transport system UgpAEC or hydrolysis of glycerophosphodiester, an abundant degradation product of phospholipids, by glycerophosphodiesterase activity. While the first pathway is thought to be the most prominent one, it could be shown in this work that direct uptake of G3P seems not to occur in *M. pneumoniae*. Nevertheless, two potential glycerophosphodiesterases are present in the genome of *M. pneumoniae*, *i.e.* *glpQ* (*mpn420*) and *mpn566* (Dandekar *et al.*, 2000; Himmelreich *et al.*, 1996). Interestingly, the pulmonary surfactant, the natural habitat of *M. pneumoniae*, is composed of about 90% phospholipids and 10% proteins (Veldhuizen *et al.*, 1998) indicating that glycerophosphodiesterases might play a major role in the life of this minimal organism.

A first attempt to characterize the two potential glycerophosphodiesterases of *M. pneumoniae* was to assess the biochemical properties of both enzymes. Enzymatic assays with the purified enzymes revealed that *M. pneumoniae* GlpQ has an enzymatic activity rather similar to the UgpQ of *E. coli* instead of the GlpQ of this organism (Larson *et al.*, 1983; Ohshima *et al.*, 2008; this work). In contrast, MPN566 was not active at all. *M. pneumoniae* GlpQ and *E. coli* UgpQ activity is highest in the presence of magnesium ions suggesting that this is the preferred cation (Ohshima *et al.*, 2008; this work). In general, glycerophosphodiesterases exhibit a calcium-dependent enzymatic activity as it has been reported for the GlpQ of *E. coli* and different *Borrelia* species or the so-called protein D of *Haemophilus influenzae* (Larson *et al.*, 1983; Munson and Sasaki, 1993; Schwan *et al.*, 2003). Nevertheless, the *E. coli* GlpQ is also active in the presence of magnesium ions but to a much lesser extent (Larson *et al.*,

1983), whereas *M. pneumoniae* GlpQ and *E. coli* UgpQ are completely inactive with calcium ions (Ohshima *et al.*, 2008; this work). While *E. coli* UgpQ accumulates under conditions of phosphate starvation (Ohshima *et al.*, 2008), both *M. pneumoniae* enzymes are constitutively expressed in the wild type strain (Güell *et al.*, 2009). Similar regulations compared to the UgpQ of *E. coli* were observed for the glycerophosphodiesterases of *B. subtilis*, *Corynebacterium glutamicum*, and *Streptomyces coelicolor* suggesting that the proteins allow the utilization of glycerophosphodiesters as a source of phosphate (Antelmann *et al.*, 2000; Ishige *et al.*, 2003; Santos-Beneit *et al.*, 2009). Moreover, *B. subtilis* *glpQ* expression is also induced when glycerol is available and repressed if a more favorable carbon sources such as glucose is present, respectively (Blencke *et al.*, 2003; Nilsson *et al.*, 1994). In *Staphylococcus aureus*, the GlpQ orthologue is regulated by the two-component system SaeRS, which is known to act on virulence gene expression (Rogasch *et al.*, 2006).

M. pneumoniae GlpQ and MPN566 share ~58% identical residues. It could be shown for the glycerophosphodiesterase of *Thermoanaerobacter tengcongensis* that amino acid mutations in the active site affect protein activity by interfering with metal ion or substrate binding (Shi *et al.*, 2007). In contrast to *M. pneumoniae* GlpQ, the active site structure is only poorly conserved in MPN566, not including all three essential metal ion binding residues. Thus, MPN566 does not seem to act as a glycerophosphodiesterase suggesting a different function in *M. pneumoniae* or the protein itself reflects the reductive evolution of this organism. The same phenomena were observed for the glycerophosphodiesterase of *Treponema pallidum*, whose active site is also poorly conserved (Shevchenko *et al.*, 1997; Stebeck *et al.*, 1997). It has been proposed that the *T. pallidum* GlpQ orthologue is a periplasmic lipoprotein associated with the spirochete's peptidoglycan-cytoplasmic membrane complex (Shevchenko *et al.*, 1999). Interestingly, most studied glycerophosphodiesterases are cytoplasmic or periplasmic enzymes. So far there are only two exceptions: Protein D of *H. influenzae*, which is membrane bound, and the extracellular GlpQ of *B. subtilis* (Janson *et al.*, 1992; Voigt *et al.*, 2009). This unusual localization could be explained by the fact that both proteins are synthesized as a precursor with a signal peptide (Wu and Tokunaga, 1986). In case of Protein D, the signal peptide is modified by covalent binding of fatty acids to a cysteine residue, which becomes the amino terminus after cleavage of the signal sequence (Janson *et al.*, 1992). In eukaryotes, glycerophosphodiesterases are also

membrane proteins that form a large family with roles in motor neuron differentiation, modulation of cell growth or amino acid homeostasis (Corda *et al.*, 2009; Kopp *et al.*, 2010; Van der Rest *et al.*, 2004; Yanaka, 2007).

To get more insights into the physiological role of the two paralogous glycerophosphodiesterases of *M. pneumoniae*, mutants lacking the ability to express either GlpQ or MPN566 were isolated in this work. No phenotypic differences could be detected between the *M. pneumoniae* wild type and the *mpn566* mutant strain. In contrast, GlpQ is crucial for the pathogenicity of *M. pneumoniae*, since a *glpQ* mutant exhibited a complete loss of cytotoxicity toward HeLa cells. This might be due to the enzymatic activity itself because hydrogen peroxide release in the presence of glycerophosphorylcholine was completely gone in this mutant suggesting rather deacylated phospholipids than glycerol are used for G3P production *in vivo*. An implication of glycerophosphodiesterases in the pathogenicity has also been reported for different *Borrelia* species (Schwan *et al.*, 2003). It is assumed that glycerophosphodiesterase activity permits only the relapsing-fever group of spirochetes to acquire G3P from phospholipids. This metabolic advantage may contribute in some extent to their ability to achieve higher cell densities in the blood than do the Lyme disease spirochetes (Schwan *et al.*, 2003). Similar effects are observed in *H. influenzae*. Here, protein D is involved in the pathogenesis of upper respiratory tract infections due to nontypeable *H. influenzae* (Forsgren *et al.*, 2008). A proposed mechanism is that the protein D glycerophosphodiesterase activity itself is the virulence factor, in this way that protein D hydrolyzes degraded phosphatidylcholine from host epithelia cells to obtain free choline for lipopolysaccharides on the bacteria cell surface that in turn contribute to pathogenicity (Fan *et al.*, 2001). In *M. pneumoniae*, G3P rather than choline is important for the pathogenicity of this organism but also for phospholipid synthesis. Two major phospholipids were detected in the membrane of *M. pneumoniae*, phosphatidylcholine and phosphatidylglycerol (Plackett *et al.*, 1969). However, only phosphatidylglycerol is synthesized *de novo* using G3P as precursor, whereas phosphatidylcholine seems to be directly integrated into the *M. pneumoniae* cell membrane from artificial media or host cells (Plackett *et al.*, 1969). The importance of G3P in phospholipid synthesis is also reflected by the proteome changes in *M. pneumoniae glpQ* mutant cells growing with glucose as sole carbon source. Under this condition, 33 and 21 proteins were present in elevated and reduced amounts,

respectively. In contrast, only five induced and five repressed proteins were detected in the presence of glycerol suggesting a complementation effect compared to glucose-grown cells. Indeed, nearly all proteins with reduced protein amounts in medium supplemented with glucose as carbon source are transport proteins indicating defects in cell membrane assembly, since transcription regulation of these proteins did not appear. Moreover, the *M. pneumoniae glpQ* mutant strain exhibited a growth defect in the presence of glucose and did not reach the final biomass as compared to the wild type strain, whereas growth with glycerol as sole carbon source was not affected. An implication of the glycerophosphodiesterase-like protein SHV3 in cell wall organization was already shown for the plant *Arabidopsis thaliana* (Hayashi *et al.*, 2008).

The protein amount of five proteins was up- or down-regulated in the *M. pneumoniae glpQ* mutant strain in a carbon source independent manner, including the glycerol facilitator GlpF, a subunit of a metal ion ABC transporter CbiO, and three lipoproteins (MPN162, MPN287, and MPN506). For these proteins, it could be shown that regulation appears on transcription level indicating a GlpQ-dependent regulon in *M. pneumoniae*. A possible explanation for this result could be that *M. pneumoniae* GlpQ acts as a trigger enzyme (Commichau and Stülke, 2008), which measures the availability of its product G3P and uses this information to differentially control gene expression by direct binding to DNA operator elements. Alternatively, the protein may bind as a cofactor to a transcription regulator to regulate gene expression similar to the role of HPr(Ser-P) in carbon catabolite repression in the Firmicutes (Görke and Stülke, 2008). Indeed, GlpQ was identified in the *M. pneumoniae* phosphoproteome analysis. However, the phosphorylation site and the function of this phosphorylation event is unknown. In addition, a recent analysis of protein-protein-interactions in *M. pneumoniae* provided no clear evidence for an interaction of GlpQ with other proteins. Only a self-interaction of this protein was reported (Kühner *et al.*, 2009). Non-enzymatic functions of glycerophosphodiesterases have also been reported for the mammalian GDE5. In this case, the protein negatively regulates skeletal muscle development even without enzymatic activity (Okazaki *et al.*, 2010).

GlpQ-dependent transcription regulation in *M. pneumoniae*: Mechanism and function?

In bacteria, regulation mostly appears on the transcription level (Campbel *et al.*, 2008; Hoskisson and Rigali, 2008; Segal and Ron, 1998). However, only two examples of transcription regulation are reported in the Mollicutes so far. This is the regulation of the *Spiroplasma citri* fructose operon by the transcription activator FruR (Gaurivaud *et al.*, 2001) and the control of heat shock genes in *M. pneumoniae* by the repressor protein HrcA and the DNA operator element CIRCE (Chang *et al.*, 2008; Weiner III *et al.*, 2003). Moreover, the induction of chaperone-encoding genes at elevated temperatures was also observed in several other *Mycoplasma* species (Dascher *et al.*, 1990; Madsen *et al.*, 2006; Musatovova *et al.*, 2006).

The analysis of the *M. pneumoniae glpQ* mutant strain revealed several differences in the protein amount of proteins, many triggered by changes at the transcription level. However, it was proposed that the higher proportion of regulatory events with glucose as sole carbon source are mostly due to a lack of G3P instead of the missing glycerophosphodiesterase GlpQ. Interestingly, the overlap of proteins and the corresponding genes, respectively, that exhibited a regulation independent from the carbon source, was relatively low. As mentioned before, these proteins were the glycerol facilitator GlpF, a subunit of a metal ion ABC transporter CbiO, and the three lipoproteins MPN162, MPN287, and MPN506. The observation that another way to acquire G3P from glycerol was strongly up-regulated in the *M. pneumoniae glpQ* mutant strain confirms the crucial factor of G3P accumulation in the life of this organism. Furthermore, CbiO and MPN162 showed an increase in transcription level, whereas the two other lipoproteins were down-regulated in the *M. pneumoniae glpQ* mutant strain. An inspection of the upstream region of all five genes revealed the presence of a common palindromic DNA motif, which has strong similarity to the motif of the virulence gene regulator CovR in group A *Streptococcus* (Churchward, 2007). A possible explanation for this differential regulation pattern of the five genes could be suspected in the localization of the inverted repeat sequence in relation to the -10 region of the gene. For all up-regulated genes, the motif adjoins or overlaps with the -10 region, whereas a ~500 bases spacer is present in case of the down-regulated ones. In addition to HrcA, the genome of *M. pneumoniae* encodes only two other typical transcription factors that belong to the GntR and the Fur family, respectively

(Dandekar *et al.*, 2000; Himmelreich *et al.*, 1996). However, it is open for speculation whether these two proteins are involved in this regulation process.

It is interesting to note that *M. pneumoniae* contains almost 70 potential lipoproteins (10% of all open reading frames) (Hallamaa *et al.*, 2006), whereas environmental bacteria such as *E. coli* and *B. subtilis* reserve less than one percent of their genetic capacity to encode these proteins (Blattner *et al.*, 1997; Kunst *et al.*, 1997). The high number of lipoproteins in *M. pneumoniae* might therefore reflect the close adaptation to the human host. It is reported that *M. pneumoniae* lipoproteins act as surface antigens because of their modulin activity, which makes them a preferred target of the host immune response (Chambaud *et al.*, 1999; You *et al.*, 2006; Zuo *et al.*, 2009). Similar lipoprotein functions were also documented in *S. aureus*, where lipoproteins seem to play an important role in pathogen recognition and host innate defense mechanisms against infections (Bubeck Wardenburg *et al.*, 2006). For *M. pneumoniae* MPN162 and its homologue in *Mycoplasma genitalium*, it could already be shown that these lipoproteins activate the nuclear factor κ B, a transcription regulator involved in immune response, through toll-like receptors (Shimizu *et al.*, 2007; Shimizu *et al.*, 2008). Moreover, MslA, the homologue of MPN284 and MPN506, which share a similarity of 76%, plays a role in *Mycoplasma gallisepticum* virulence, although the mechanism is unknown (Szczepek *et al.*, 2010). Further studies of lipoproteins in the Mollicutes suggest functions in adhesion and invasion of mammalian cells as well (Liu *et al.*, 2006; Zeiman *et al.*, 2008; Zimmermann *et al.*, 2010). Nevertheless, *Mycoplasma* lipoproteins seem not to be constitutively expressed as different expression patterns after contact with human host cells could be observed (Cecchini *et al.*, 2007; Hallamaa *et al.*, 2008; Madsen *et al.*, 2008).

In a first attempt to identify functions of GlpQ-dependent regulated proteins, *M. pneumoniae* mutant strains lacking the lipoproteins MPN161, MPN284 or MPN506 were isolated, while *glpF* and *cbiO* are essential (Hames *et al.*, 2009; unpublished data). It turned out that the *mpn284* mutant possessed a decreased cytotoxicity toward HeLa cells (Fig. 37A and B). Interestingly, this phenotype was very similar to that of the *M. pneumoniae glpD* mutant (Hames *et al.*, 2009). In addition, only the *mpn284* mutant exhibited an effect in hydrogen peroxide release, in that way that no formation occurred with glycerol as carbon source (Fig. 37C). This raises the question if decreased cytotoxicity toward HeLa cells is due to defects in hydrogen peroxide release with

glycerol. Nevertheless, deacylated phospholipids rather than glycerol are most likely available upon infection. A recent analysis of protein-protein-interactions in *M. pneumoniae* revealed also two potential interaction partners of MPN284, including the thymidylate synthase ThyA and a putative phosphosugar facilitator MPN076 (Kühner *et al.*, 2009). However, it is not known, how these three proteins are related to each other. Summing up, the first results showed that the lipoprotein MPN284 has a role in the pathogenicity of *M. pneumoniae*.

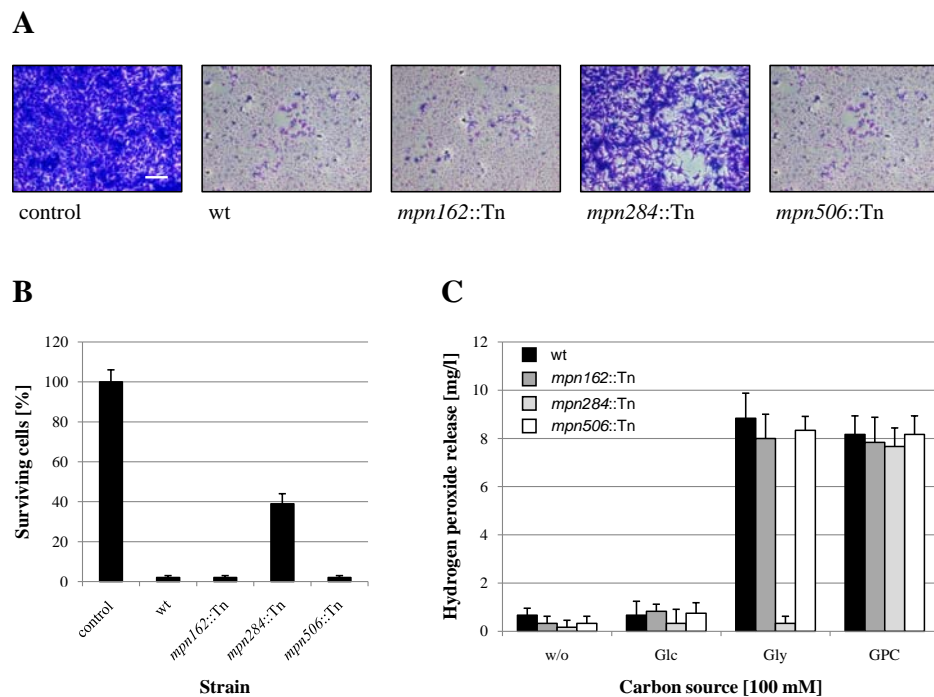


Fig. 37. Analysis of the pathogenicity of *M. pneumoniae* lipoprotein mutants. (A) Infection assay to verify cytotoxic effects of *M. pneumoniae* lipoprotein mutants. HeLa cells were infected with *M. pneumoniae* wild type (wt), *mpn162::Tn*, *mpn284::Tn*, and *mpn506::Tn* mutant cells. As control served a HeLa cell culture without addition of *M. pneumoniae* cells. After four days, HeLa cell cultures were stained with crystal violet and photographed. All pictures are shown at the same magnification. Scale bar, 0.1 mm. (B) Quantification of HeLa cells after infection with different *M. pneumoniae* strains. The cell count of surviving cells is indicated in percent as the number of viable cells per field of view, quantified by crystal violet staining after four days of incubation. An uninfected HeLa cell culture served as control. Error bars indicate standard deviation (based on three independent experiments). (C) Examination of *M. pneumoniae* hydrogen peroxide release. Hydrogen peroxide production of *M. pneumoniae* wild type (wt), *mpn162::Tn*, *mpn284::Tn*, and *mpn506::Tn* mutant strains were measured in the presence of different carbon sources (100 μ M) after 2 h. Error bars indicate standard deviation (based on three independent experiments). GPC, glycerophosphorylcholine; Glc, glucose; Gly, glycerol; w/o, without addition of any carbon source.

Outlook

The significance of PrkC/PrpC-dependent protein phosphorylation in the pathogenicity of *M. pneumoniae* was demonstrated in this work. In addition to one HPrK target protein, six proteins are phosphorylated by the kinase PrkC. However, this is only a small group of proteins compared to over 60 identified phosphoproteins in total. Thus, the genome of *M. pneumoniae* has to encode far more than the two annotated kinases or autophosphorylation as shown for the phosphosugar mutase ManB is more common as thought so far. To identify rather cryptic kinases or potential proteins with moonlighting functions in phosphorylation, it could be helpful to analyze the phosphoproteome of the smaller ancestor *M. genitalium*. The phosphoproteome overlap between these two minimal organisms might give hints for the identification of other phosphorylation mechanisms. An evidence for a prominent role of moonlighting proteins in minimal organisms give the current smallest cellular genome of the insect symbiont *Hodgkinia cicadicola*, which consists of just about 144 kb (McCutcheon *et al.*, 2009). Interestingly, the genome encodes for only 15 tRNAs to assemble the 20 amino acids required for protein synthesizes. It is difficult to understand, how this could work, but probably several tRNAs fulfill multiple functions in this organism.

A potential candidate of a moonlighting protein, in this special case a trigger enzyme, is the glycerophosphodiesterase GlpQ in *M. pneumoniae*. The current results indicate beside the enzymatic function a role in transcription regulation of a putative virulence regulon. Indeed, it could be shown that the protein binds DNA *in vitro*, but rather unspecific (unpublished data). Therefore, a useful approach should be the direct expression of a recombinant version of the protein in *M. pneumoniae* in order to elucidate the DNA-binding activity of the enzyme by techniques such as ChIP-chip. The use of a smaller protein-tag as the TAP-tag by Kühner *et al.* (2009) may also allow the identification of GlpQ interaction partners if the protein is not the direct transcription regulator. Moreover, the purification of GlpQ enhances the possibility to detect the phosphorylation site, which might allow a general knowledge of the regulation process itself.

For a more detailed understanding of the interconnection between the lipoprotein MPN284 and the pathogenicity of *M. pneumoniae*, the glycerol uptake system of *M. pneumoniae* should be reconstituted with or without MPN284 in a *B. subtilis glpF* mutant. This approach allows the verification, whether MPN284 modulates directly the glycerol uptake or later regulations are responsible for the absence of hydrogen peroxide formation with glycerol as carbon source. Furthermore, it might be interesting to compare the proteome of *mpn284* mutant cells grown in the presence of glycerol to the *M. pneumoniae* wild type strain.

Chapter 9

References

References

- Abramoff, M. D., P. J. Magelhaes, and S. J. Ram.** 2004. Image processing with ImageJ. *Biophotonics Internat.* **11**: 36-42.
- Absalon, C., M. Obuchowski, E. Madec, D. Delattre, I. B. Holland, and S. J. S  ror.** 2009. CpgA, EF-Tu and the stressosome protein YezB are substrates of the Ser/Thr kinase/phosphatase couple, PrkC/PrpC, in *Bacillus subtilis*. *Microbiology* **155**: 932-943.
- Aivaliotis, M., B. Macek, F. Gnad, P. Reichelt, M. Mann, and D. Oesterhelt.** 2009. Ser/Thr/Tyr protein phosphorylation in the archaeon *Halobacterium salinarum* - A representative of the third domain of life. *PLoS ONE* **4**: e4777.
- Allen, G. S., K. Steinhauer, W. Hillen, J. St  lke, and R. G. Brennan.** 2003. Crystal structure of HPr kinase/phosphatase from *Mycoplasma pneumonia*. *J. Mol. Biol.* **326**: 1203-1217.
- Amar, P., G. Legent, M. Thellier, C. Ripoll, G. Bernot, T. Nystrom, M. H. Saier Jr., and V. Norris.** 2008. A stochastic automaton shows how enzyme assemblies may contribute to metabolic efficiency. *BMC Syst. Biol.* **2**: 27.
- An, S., R. Kumar, E. D. Sheets, and S. J. Benkovic.** 2008. Reversible compartmentalization of *de novo* purine biosynthetic complexes in living cells. *Science* **320**: 103-106.
- Antelmann, H., C. Scharf, and M. Hecker.** 2000. Phosphate starvation-inducible proteins of *Bacillus subtilis*: Proteomics and transcriptional analysis. *J. Bacteriol.* **182**: 4478-4490.
- Armougom, F., S. Moretti, O. Poirot, S. Audic, P. Dumas, B. Schaeli, V. Keduas, and C. Notredame.** 2006. Espresso: Automatic incorporation of structural information in multiple sequence alignments using 3D-Coffee. *Nucleic Acids Res.* **34**: W604-608.
- Armstrong, R. D., and R. B. Diasio.** 1982. Improved measurement of thymidylate synthetase activity by a modified tritium-release assay. *J. Biochem. Biophys. Methods* **6**: 141-147.
- Atkinson, T. P., M. F. Balish, and K. B. Waites.** 2008. Epidemiology, clinical manifestations, pathogenesis and laboratory detection of *Mycoplasma pneumoniae* infections. *FEMS Microbiol. Rev.* **32**: 956-973.

- Balish, M. F., and D. C. Krause.** 2006. Mycoplasmas: A distinct cytoskeleton for wall-less bacteria. *J. Mol. Microbiol. Biotechnol.* **11**: 244-255.
- Balish, M. F., S. M. Ross, M. Fisseha, and D. C. Krause.** 2003. Deletion analysis identifies key functional domains of the cytoadherence-associated protein HMW2 of *Mycoplasma pneumoniae*. *Mol. Microbiol.* **50**: 1507-1516.
- Barabote, R. D., and M. H. Saier Jr.** 2005. Comparative genomic analyses of the bacterial phosphotransferase system. *Microbiol. Mol. Biol. Rev.* **69**: 608-634.
- Barré, A., A. de Daruvar, and A. Blanchard.** 2004. MolliGen, a database dedicated to the comparative genomics of Mollicutes. *Nucleic Acids Res.* **32**: D307-D310.
- Beinert, H., M. C. Kennedy, and C. D. Stout.** 1996. Aconitase as iron-sulfur protein, enzyme, and iron-regulatory protein. *Chem. Rev.* **96**: 2335-2374.
- Beltrao, P., J. C. Trinidad, D. Fiedler, A. Roguev, W. A. Lim, K. M. Shokat, A. L. Burlingame, and N. J. Krogan.** 2009. Evolution of phosphoregulation: Comparison of phosphorylation patterns across yeast species. *PLoS Biol.* **7**: e1000134.
- Bi, W., and P. J. Stambrook.** 1998. Site-directed mutagenesis by combined chain reaction. *Anal. Biochem.* **256**: 137-140.
- Bischof, D. F., E. M. Vilei, and J. Frey.** 2009. Functional and antigenic properties of GlpO from *Mycoplasma mycoides* subsp. *mycoides* SC: Characterization of a flavine adenine dinucleotide-binding site deletion mutant. *Vet. Res.* **40**: 35.
- Blattner, F. R., G. Plunkett III, C. A. Bloch, N. T. Perna, V. Burland, M. Riley, J. Collado-Vides, J. D. Glasner, C. K. Rode, G. F. Mayhew, et al.** 1997. The complete genome sequence of *Escherichia coli* K-12. *Science* **277**: 1453-1462.
- Blencke, H. M., G. Homuth, H. Ludwig, U. Mäder, M. Hecker, and J. Stülke.** 2003. Transcriptional profiling of gene expression in response to glucose in *Bacillus subtilis*: Regulation of the central metabolic pathways. *Metab. Engn.* **5**: 133-149.
- Boekhorst, J., B. van Breukelen, A. J. Heck Jr., and B. Snel.** 2008. Comparative phosphoproteomics reveals evolutionary and functional conservation of phosphorylation across eukaryotes. *Genome Biol.* **9**: R144.
- Boonmee, A., T. Ruppert, and R. Herrmann.** 2009. The gene *mpn310* (*hmw2*) from *Mycoplasma pneumoniae* encodes two proteins, HMW2 and HMW2-s, which differ in size but use the same reading frame. *FEMS Microbiol. Lett.* **290**: 174-181.

- Bové, J. M., J. Renaudin, C. Saillard, X. Foissac, and M. Garnier.** 2003. *Spiroplasma citri*, a plant pathogenic Mollicute: Relationship with its two hosts, the plant and the leafhopper vector. *Annu. Rev. Phytopathol.* **41**: 483-500.
- Brown, D. R., J. M. Farley, L. A. Zacher, J. M. Carlton, T. L. Clippinger, J. G. Tully, and M. B. Brown.** 2001. *Mycoplasma alligatoris* sp. nov., from American alligators. *Int. J. Syst. Evol. Microbiol.* **51**: 419-424.
- Bubeck Wardenburg, J., W. A. Williams, and D. Missiakas.** 2006. Host defenses against *Staphylococcus aureus* infection require recognition of bacterial lipoproteins. *Proc. Natl. Acad. Sci. USA* **103**: 13831-13836.
- Burroughs, A. M., S. Balaji, L. M. Iyer, and L. Aravind.** 2007. Small but versatile: The extraordinary functional and structural diversity of the beta-grasp fold. *Biol. Direct.* **2**: 18.
- Campanella, M. E., H. Chu, and P. S. Low.** 2005. Assembly and regulation of a glycolytic enzyme complex on the human erythrocyte membrane. *Proc. Natl. Acad. Sci. USA* **102**: 2402-2407.
- Campbel, E. A., L. F. Westblade, and S. A. Darst.** 2008. Regulation of bacterial RNA polymerase sigma factor activity: A structural perspective. *Curr. Opin. Microbiol.* **11**: 121-127.
- Canback, B., S. G. Andersson, and C. G. Kurland.** 2005. The global phylogeny of glycolytic enzymes. *Proc. Natl. Acad. Sci. USA* **99**: 6097-6102.
- Carnrot, C., R. Wehelie, S. Eriksson, G. Bölske, and L. Wang.** 2003. Molecular characterization of thymidine kinase from *Ureaplasma urealyticum*: Nucleoside analogues as potent inhibitors of *Mycoplasma* growth. *Mol. Microbiol.* **50**: 771-780.
- Carpousis, A. J.** 2007. The RNA degradosome of *Escherichia coli*: An mRNA-degrading machine assembled on RNase E. *Annu. Rev. Microbiol.* **61**: 71-87.
- Cecchini, K. R., T. S. Gorton, and S. J. Geary.** 2007. Transcriptional responses of *Mycoplasma gallisepticum* strain R in association with eukaryotic cells. *J. Bacteriol.* **189**: 5803-5807.
- Chambaud, I., H. Wróblewski, and A. Blanchard.** 1999. Interactions between *Mycoplasma* lipoproteins and the host immune system. *Trends Microbiol.* **7**: 493-499.

- Chang, L. J., W. H. Chen, F. C. Minion, and D. Shiuan.** 2008. Mycoplasmas regulate the expression of heat-shock protein genes through CIRCE-HrcA interactions. *Biochem. Biophys. Res. Commun.* **367**: 213-218.
- Christensen, N. M., K. B. Axelsen, M. Nicolaisen, and A. Schulz.** 2005. Phytoplasmas and their interactions with hosts. *Trends Plant Sci.* **10**: 526-535.
- Churchward, G.** 2007. The two faces of Janus: Virulence gene regulation by CovR/S in group A streptococci. *Mol. Microbiol.* **64**: 34-41.
- Ciccarelli, F. D., T. Doerks, C. von Mering, C. J. Creevey, B. Snel B, and P. Bork.** 2006. Toward automatic reconstruction of a highly resolved tree of life. *Science* **311**: 1283-1287.
- Claessen, D., R. Emmins, L. W. Hamoen, R. A. Daniel, J. Errington, and D. H. Edwards.** 2008. Control of the cell elongation-division cycle by shuttling of PBP1 protein in *Bacillus subtilis*. *Mol. Microbiol.* **68**: 1029-1046.
- Cole, B. C., J. R. Ward, and C. H. Martin.** 1968. Hemolysin and peroxide activity of *Mycoplasma* species. *J. Bacteriol.* **95**: 2022-2030.
- Commichau, F. M., and J. Stülke.** 2008. Trigger enzymes: Bifunctional proteins active in metabolism and in controlling gene expression. *Mol. Microbiol.* **67**: 692-702.
- Commichau, F. M., C. Herzberg, P. Tripal, O. Valerius, and J. Stülke.** 2007. A regulatory protein-protein interaction governs glutamate biosynthesis in *Bacillus subtilis*: The glutamate dehydrogenase RocG moonlights in controlling the transcription factor GltC. *Mol. Microbiol.* **65**: 642-654.
- Commichau, F. M., F. M. Rothe, C. Herzberg, E. Wagner, D. Hellwig, M. Lehnik-Habrink, E. Hammer, U. Völker, and J. Stülke.** 2009. Novel activities of glycolytic enzymes in *Bacillus subtilis*: Interactions with essential proteins involved in mRNA processing. *Mol. Cell. Proteomics* **8**: 1350-1360.
- Corda, D., T. Kudo, P. Zizza, C. Iurisci, E. Kawai, N. Kato, N. Yanaka, and S. Mariggìo.** 2009. The developmentally regulated osteoblast phosphodiesterase GDE3 is glycerophosphoinositol-specific and modulates cell growth. *J. Biol. Chem.* **284**: 24848-24856.
- Crooks, G. E., G. Hon, J. M. Chandonia, and S. E. Brenner.** 2004. WebLogo: A sequence logo generator. *Genome Res.* **14**: 1188-1190.

- Dandekar, T., B. Snel, M. Huynen, and P. Bork.** 1998. Conservation of gene order: A fingerprint of proteins that physically interact. *Trends Biochem. Sci.* **23**: 324-328.
- Dandekar, T., M. Huynen, J. T. Regula, B. Ueberle, C. U. Zimmermann, M. A. Andrade, T. Doerks, L. Sánchez-Pulido, B. Snel, M. Suyama, et al.** 2000. Re-annotating the *Mycoplasma pneumoniae* genome sequence: Adding value, function and reading frames. *Nucl. Acids Res.* **28**: 3278-3288.
- Dascher, C. C., S. K. Poddar, and J. Maniloff.** 1990. Heat shock response in mycoplasmas, genome-limited organisms. *J. Bacteriol.* **172**: 1823-1827.
- Débarbouillé, M., S. Dramsi, O. Dussurget, M. A. Nahori, E. Vaganay, G. Jouvion, A. Cozzone, T. Msadek, and B. Duclos.** 2009. Characterization of a serine/threonine kinase involved in virulence of *Staphylococcus aureus*. *J. Bacteriol.* **191**: 4070-4081.
- Deutscher, J., and M. H. Saier Jr.** 2005. Ser/Thr/Tyr phosphorylation in bacteria - For long time neglected, now well established. *J. Mol. Microbiol. Biotechnol.* **9**: 125-131.
- Dirksen, L. B., K. A. Krebs, and D. C. Krause.** 1994. Phosphorylation of cytoadherence-accessory proteins in *Mycoplasma pneumoniae*. *J. Bacteriol.* **176**: 7499-7505.
- Domenech, C., N. Leveque, B. Lina, F. Najjioullah, and D. Floret.** 2009. Role of *Mycoplasma pneumoniae* in pediatric encephalitis. *Eur. J. Clin. Microbiol. Infect. Dis.* **28**: 91-94.
- Dutow, P., S. R. Schmidl, M. Ridderbusch, and J. Stülke.** 2010. Interactions between glycolytic enzymes of *Mycoplasma pneumoniae*. *J. Mol. Microbiol. Biotechnol.* accepted.
- Eisenreich, W., T. Dandekar, J. Heesemann, and W. Goebel.** 2010. Carbon metabolism of intracellular bacterial pathogens and possible links to virulence. *Nat. Rev. Microbiol.* **8**: 401-412.
- Erlandsen, H., E. E. Abola, and R. C. Stevens.** 2000. Combining structural genomics and enzymology: Completing the picture in metabolic pathways and enzyme active sites. *Curr. Opin. Struct. Biol.* **10**: 719-730.
- Eymann, C., A. Dreisbach, D. Albrecht, J. Bernhardt, D. Becher, S. Gentner, T. Tam Le, K. Büttner, G. Buurman, C. Scharf, et al.** 2004. A comprehensive proteome map of growing *Bacillus subtilis* cells. *Proteomics* **4**: 2849-2876.

- Eymann, C., D. Becher, J. Bernhardt, K. Gronau, A. Klutzny, and M. Hecker.** 2007. Dynamics of protein phosphorylation on Ser/Thr/Tyr in *Bacillus subtilis*. *Proteomics* **7**: 3509-3526.
- Eymann, C., G. Homuth, C. Scharf, and M. Hecker.** 2002. *Bacillus subtilis* functional genomics: Global characterization of the stringent response by proteome and transcriptome analysis. *J. Bacteriol.* **184**: 2500-2520.
- Fabret, C., V. A. Feher, and J. A. Hoch.** 1999. Two-component signal transduction in *Bacillus subtilis*: How one organism sees its world. *J. Bacteriol.* **181**: 1975-1983.
- Faires, N., S. Tobisch, S. Bachem, I. Martin-Verstraete, M. Hecker, and J. Stülke.** 1999. The catabolite control protein CcpA controls ammonium assimilation in *Bacillus subtilis*. *J. Mol. Microbiol. Biotechnol.* **1**: 141-148.
- Fan, X., H. Goldfine, E. Lysenko, and J. N. Weiser.** 2001. The transfer of choline from the host to the bacterial cell surface requires *glpQ* in *Haemophilus influenzae*. *Mol. Microbiol.* **41**: 1029-1036.
- Faucher, S. P., C. Viau, P. P. Gros, F. Daigle, and H. Le Moual.** 2008. The *prpZ* gene cluster encoding eukaryotic-type Ser/Thr protein kinases and phosphatases is repressed by oxidative stress and involved in *Salmonella enterica* serovar Typhi survival in human macrophages. *FEMS Microbiol. Lett.* **281**: 160-166.
- Ficarro, S. B., M. L. McClelland, P. T. Stukenberg, D. J. Burke, M. M. Ross, J. Shabanowitz, D. F. Hunt, and F. M. White.** 2002. Phosphoproteome analysis by mass spectrometry and its application to *Saccharomyces cerevisiae*. *Nat. Biotechnol.* **20**: 301-305.
- Fisseha, M., H. W. Göhlmann, R. Herrmann, and D. C. Krause.** 1999. Identification and complementation of frameshift mutations associated with loss of cytoadherence in *Mycoplasma pneumoniae*. *J. Bacteriol.* **181**: 4404-4410.
- Forsgren, A., K. Riesbeck, and H. Janson.** 2008. Protein D of *Haemophilus influenzae*: A protective nontypeable *H. influenzae* antigen and a carrier for pneumococcal conjugate vaccines. *Clin. Infect. Dis.* **46**: 726-731.
- Frith, M. C., N. F. Saunders, B. Kobe, and T. L. Bailey.** 2008. Discovering sequence motifs with arbitrary insertions and deletions. *PLoS Comput. Biol.* **4**: e1000071.
- Gaidenko, T. A., T. J. Kim, and C. W. Price.** 2002. The PrpC serine-threonine phosphatase and PrkC kinase have opposing physiological roles in stationary-phase *Bacillus subtilis* cells. *J. Bacteriol.* **184**: 6109-6114.

- Galinier, A., J. Haiech, M. C. Kilhoffer, M. Jaquinod, J. Stülke, J. Deutscher, and I. Martin-Verstraete.** 1997. The *Bacillus subtilis crh* gene encodes a HPr-like protein involved in carbon catabolite repression. *Proc. Natl. Acad. Sci. USA* **94**: 8439-8444.
- Gasparri, F., N. Wang, S. Skog, A. Galvani, and S. Eriksson.** 2009. Thymidine kinase 1 expression defines an activated G1 state of the cell cycle as revealed with site-specific antibodies and ArrayScan assays. *Eur. J. Cell Biol.* **88**: 779-785.
- Gaurivaud, P., F. Laigret, M. Garnier, and J. M. Bové.** 2001. Characterization of FruR as a putative activator of the fructose operon of *Spiroplasma citri*. *FEMS Microbiol. Lett.* **198**: 73-78.
- Gibson, D. G., G. A. Benders, C. Andrews-Pfannkoch, E. A. Denisova, H. Baden-Tillson, J. Zaveri, T. B. Stockwell, A. Brownley, D. W. Thomas, M. A. Algire, et al.** 2008. Complete chemical synthesis, assembly, and cloning of a *Mycoplasma genitalium* genome. *Science* **319**: 1215-1220.
- Glass, J. I., N. Assad-Garcia, N. Alperovich, S. Yooseph, M. R. Lewis, M. Maruf, C. A. Hutchison III, H. O. Smith, and J. C. Venter.** 2006. Essential genes of a minimal bacterium. *Proc. Natl. Acad. Sci. USA* **103**: 425-430.
- Gnad, F., F. Forner, D. F. Zielinska, E. Birney, J. Gunawardena, and M. Mann.** 2010. Evolutionary constraints of phosphorylation in eukaryotes, prokaryotes, and mitochondria. *Mol. Cell. Proteomics* in press (PMID: 20688971).
- Görke, B., and J. Stülke.** 2008. Carbon catabolite repression in bacteria: Many ways to make the most out of nutrients. *Nat. Rev. Microbiol.* **6**: 613-624.
- Grangeasse, C., A. J. Cozzone, J. Deutscher, and I. Mijakovic.** 2007. Tyrosine phosphorylation: An emerging regulatory device of bacterial physiology. *Trends Biochem. Sci.* **32**: 86-94.
- Greenberg, E. P.** 2000. Bacterial genomics. Pump up the versatility. *Nature* **406**: 947-948.
- Güell, M., V. van Noort, E. Yus, W. H. Chen, J. Leigh-Bell, K. Michalodimitrakis, T. Yamada, M. Arumugam, T. Doerks, S. Kühner, et al.** 2009. Transcriptome complexity in a genome-reduced bacterium. *Science* **326**: 1268-1271.
- Guérout-Fleury, A. M., K. Shazand, N. Frandsen, and P. Stragier.** 1995. Antibiotic resistance cassettes for *Bacillus subtilis*. *Gene* **167**: 335-336.

- Guex, N., and M. C. Peitsch.** 1997. SWISS-MODEL and the Swiss-PdbViewer: An environment for comparative protein modeling. *Electrophoresis* **18**: 2714-2723.
- Gururaj, A., C. J. Barnes, R. K. Vadlamudi, and R. Kumar.** 2004. Regulation of phosphoglucomutase 1 phosphorylation and activity by a signaling kinase. *Oncogene* **23**: 8118-8127.
- Halbedel, S., and J. Stülke.** 2005. Dual phosphorylation of *Mycoplasma pneumoniae* HPr by Enzyme I and HPr kinase suggests an extended phosphoryl group susceptibility of HPr. *FEMS Microbiol. Lett.* **247**: 193-198.
- Halbedel, S., and J. Stülke.** 2006. Probing *in vivo* promoter activities in *Mycoplasma pneumoniae*: A system for generation of single-copy reporter constructs. *Appl. Environ. Microbiol.* **72**: 1696-1699.
- Halbedel, S., and J. Stülke.** 2007. Tools for the genetic analysis of *Mycoplasma*. *Int. J. Med. Microbiol.* **297**: 37-44.
- Halbedel, S., C. Hames, and J. Stülke.** 2004. *In vivo* activity of enzymatic and regulatory components of the phosphoenolpyruvate:sugar phosphotransferase system in *Mycoplasma pneumoniae*. *J. Bacteriol.* **186**: 7936-7943.
- Halbedel, S., C. Hames, and J. Stülke.** 2007. Regulation of carbon metabolism in the Mollicutes and its relation to virulence. *J. Mol. Microbiol. Biotechnol.* **12**: 147-154.
- Halbedel, S., C. Hames, and J. Stülke.** 2007. Regulation of carbon metabolism in the Mollicutes and its relation to virulence. *J. Mol. Microbiol. Biotechnol.* **12**: 147-154.
- Halbedel, S., H. Eilers, B. Jonas, J. Busse, M. Hecker, S. Engelmann, and J. Stülke.** 2007. Transcription in *Mycoplasma pneumoniae*: Analysis of the promoters of the *ackA* and *ldh* genes. *J. Mol. Biol.* **371**: 596-607.
- Halbedel, S., J. Busse, S. R. Schmidl, and J. Stülke.** 2006. Regulatory protein phosphorylation in *Mycoplasma pneumoniae*: A PP2C-type phosphatase serves to dephosphorylate HPr(Ser-P). *J. Biol. Chem.* **281**: 26253-26259.
- Hallamaa, K. M., G. F. Browning, and S. L. Tang.** 2006. Lipoprotein multigene families in *Mycoplasma pneumoniae*. *J. Bacteriol.* **188**: 5393-5399.

- Hallamaa, K. M., S. L. Tang, N. Ficorilli, and G. F. Browning.** 2008. Differential expression of lipoprotein genes in *Mycoplasma pneumoniae* after contact with human lung epithelial cells, and under oxidative and acidic stress. *BMC Microbiol.* **8**: 124.
- Hames, C., S. Halbedel, and J. Stülke.** 2005. Multiple-mutation reaction: A method for simultaneous introduction of multiple mutations into the *glpK* gene of *Mycoplasma pneumoniae*. *Appl. Environ. Microbiol.* **71**: 4097-4100.
- Hames, C., S. Halbedel, M. Hoppert, J. Frey, and J. Stülke.** 2009. Glycerol metabolism is important for cytotoxicity of *Mycoplasma pneumoniae*. *J. Bacteriol.* **191**: 747-753.
- Hanson, K. G., K. Steinhauer, J. Reizer, W. Hillen, and J. Stülke.** 2002. HPr kinase/phosphatase of *Bacillus subtilis*: Expression of the gene and effects of mutations on enzyme activity, growth, and carbon catabolite repression. *Microbiology* **148**: 1805-1811.
- Hasselbring, B. M., C. A. Page, E. S. Sheppard, and D. C. Krause.** 2006. Transposon mutagenesis identifies genes associated with *Mycoplasma pneumoniae* gliding motility. *J. Bacteriol.* **188**: 6335-6345.
- Hayashi, S., T. Ishii, T. Matsunaga, R. Tominaga, T. Kuromori, T. Wada, K. Shinozaki, and T. Hirayama.** 2008. The glycerophosphoryl diester phosphodiesterase-like proteins SHV3 and its homologs play important roles in cell wall organization. *Plant Cell Physiol.* **49**: 1522-1535.
- Hegermann, J., S. Halbedel, R. Dumke, J. Regula, R. R. Gaboulline, F. Mayer, J. Stülke, and R. Herrmann.** 2008. The acidic, glutamine-rich MPN474 protein of *Mycoplasma pneumoniae* is surface exposed and covers the complete cell. *Microbiology* **154**: 1185-1192.
- Heinrich, A., K. Woyda, K. Brauburger, G. Meiss, C. Detsch, J. Stülke, and K. Forchhammer.** 2006. Interaction of the membrane-bound GlnK-AmtB complex with the master regulator of nitrogen metabolism TnrA in *Bacillus subtilis*. *J. Biol. Chem.* **281**: 34909-34917.
- Himmelreich, R., H. Hilbert, H. Plagens, E. Pirkel, B. C. Li, and R. Herrmann.** 1996. Complete sequence analysis of the genome of the bacterium *Mycoplasma pneumoniae*. *Nucleic Acids Res.* **24**: 4420-4449.

- Hoch, J. A.** 2000. Two-component and phosphorelay signal transduction. *Curr. Opin. Microbiol.* **3**: 165-170.
- Holt, L. J., B. B. Tuch, J. Villén, A. D. Johnson, S. P. Gygi, and D. O. Morgan.** 2009. Global analysis of Cdk1 substrate phosphorylation sites provides insights into evolution. *Science* **325**: 1682-1686.
- Hoskisson, P. A., and S. Rigali.** 2008. Chapter 1: Variation in form and function the helix-turn-helix regulators of the GntR superfamily. *Adv. Appl. Microbiol.* **69**: 1-22.
- Hubbard, S. R., and W. T. Miller.** 2007. Receptor tyrosine kinases: Mechanisms of activation and signaling. *Curr. Opin. Cell Biol.* **19**: 117-123.
- Hutchison III, C. A., S. C. Peterson, S. R. Gill, R. T. Cline, O. White, C. M. Fraser, H. O. Smith, and J. C. Venter.** 1999. Global transposon mutagenesis and a minimal *Mycoplasma* genome. *Science* **286**: 2165-2169.
- Iakoucheva, L. M., P. Radivojac, C. J. Brown, T. R. O'Connor, J. G. Sikes, Z. Obradovic, and A. K. Dunker.** 2004. The importance of intrinsic disorder for protein phosphorylation. *Nucleic Acids Res.* **32**: 1037-1049.
- Ishige, T., M. Krause, M. Bott, V. F. Wendisch, and H. Sahm.** 2003. The phosphate starvation stimulon of *Corynebacterium glutamicum* determined by DNA microarray analyses. *J. Bacteriol.* **185**: 4519-4529.
- Islam, M. M., R. Wallin, R. M. Wynn, M. Conway, H. Fujii, J. A. Mobley, D. T. Chuang, and S. M. Hutson.** 2007. A novel branched-chain amino acid metabolon. Protein-protein interactions in a supramolecular complex. *J. Biol. Chem.* **282**: 11893-11903.
- Iwanicki, A., K. Hinc, S. Seror, G. Węgrzyn, and M. Obuchowski.** 2005. Transcription in the *prpC-yloQ* region in *Bacillus subtilis*. *Arch. Microbiol.* **183**: 421-430.
- Jacobs, E.** 1997. *Mycoplasma* infections of the human respiratory tract. *Wien. Klin. Wochenschr.* **109**: 574-577.
- Jaffe, J. D., H. C. Berg, and G. M. Church.** 2004. Proteogenomic mapping as a complementary method to perform genome annotation. *Proteomics* **4**: 59-77.
- Janson, H., L. O. Hedén, and A. Forsgren.** 1992. Protein D, the immunoglobulin D-binding protein of *Haemophilus influenzae*, is a lipoprotein. *Infect. Immun.* **60**: 1336-1342.

- Jeffery, C. J.** 1999. Moonlighting proteins. *Trends Biochem. Sci.* **24**: 8-11.
- Jers, C., B. Soufi, C. Grangeasse, J. Deutscher, and I. Mijakovic.** 2008. Phosphoproteomics in bacteria: Towards a systemic understanding of bacterial phosphorylation networks. *Exp. Rev. Proteomics* **5**: 619-627.
- Jin, H., and V. Pancholi.** 2006. Identification and biochemical characterization of a eukaryotic-type serine/threonine kinase and its cognate phosphatase in *Streptococcus pyogenes*: Their biological functions and substrate identification. *J. Mol. Biol.* **357**: 1351-1372.
- Johnson, L. N., and D. Barford.** 1993. The effects of phosphorylation on the structure and function of proteins. *Annu. Rev. Biophys. Biomol. Struct.* **22**: 199-232.
- Jolly, L., F. Pompeo, J. van Heijenoort, F. Fassy, and D. Mengin-Lecreulx.** 2000. Autophosphorylation of phosphoglucosamine mutase from *Escherichia coli*. *J. Bacteriol.* **182**: 1280-1285.
- Jordan, J. L., H. Y. Chang, M. F. Balish, L. S. Holt, S. R. Bose, B. M. Hasselbring, R. H. Waldo III, T. M. Krunkosky, and D. C. Krause.** 2007. Protein P200 is dispensable for *Mycoplasma pneumoniae* hemadsorption but not gliding motility or colonization of differentiated bronchial epithelium. *Infect. Immun.* **75**: 518-522.
- Jordan, S., A. Junker, J. D. Helmann, and T. Mascher.** 2006. Regulation of LiaRS-dependent gene expression in *Bacillus subtilis*: Identification of inhibitor proteins, regulator binding sites, and target genes of a conserved cell envelope stress-sensing two-component system. *J. Bacteriol.* **188**: 5153-5166.
- Karimova, G., J. Pidoux, A. Ullmann, and D. Ladant.** 1998. A bacterial two-hybrid system based on a reconstituted signal transduction pathway. *Proc. Natl. Acad. Sci. USA* **95**: 5752-5756.
- Kawamoto, R. M., and A. H. Caswell.** 1986. Autophosphorylation of glyceraldehydephosphate dehydrogenase and phosphorylation of protein from skeletal muscle microsomes. *Biochemistry* **25**: 657-661.
- Ke, P. Y., and Z. F. Chang.** 2004. Mitotic degradation of human thymidine kinase 1 is dependent on the anaphase-promoting complex/cyclosome-CDH1-mediated pathway. *Mol. Cell. Biol.* **24**: 514-526.

- Keller, A., A. I. Nesvizhskii, E. Kolker, and R. Aebersold.** 2002. Empirical statistical model to estimate the accuracy of peptide identifications made by MS/MS and database search. *Anal. Chem.* **74**: 5383-5392.
- Kennelly, P. J., and M. Potts.** 1996. Fancy meeting you here! A fresh look at “prokaryotic” protein phosphorylation. *J. Bacteriol.* **178**: 4759-4764.
- Kiefer, F., K. Arnold, M. Künzli, L. Bordoli, and T. Schwede.** 2009. The SWISS-MODEL Repository and associated resources. *Nucleic Acids Res.* **37**: D387-D392.
- Kim, J. W., and C. V. Dang.** 2005. Multifaceted roles of glycolytic enzymes. *Trends Biochem. Sci.* **30**: 142-150.
- Kobayashi, K., S. D. Ehrlich, A. Albertini, G. Amati, K. K. Andersen, M. Arnaud, K. Asai, S. Ashikaga, S. Aymerich, P. Bessieres, *et al.*** 2003. Essential *Bacillus subtilis* genes. *Proc. Natl. Acad. Sci. USA* **100**: 4678-4683.
- Kopp, F., T. Komatsu, D. K. Nomura, S. A. Trauger, J. R. Thomas, G. Siuzdak, G. M. Simon, and B. F. Cravatt.** 2010. The glycerophospho metabolome and its influence on amino acid homeostasis revealed by brain metabolomics of GDE1(-/-) mice. *Chem. Biol.* **17**: 831-840.
- Kosinska, U., C. Carnrot, S. Eriksson, L. Wang, and H. Eklund.** 2005. Structure of the substrate complex of thymidine kinase from *Ureaplasma urealyticum* and investigations of possible drug targets for the enzyme. *FEBS J.* **272**: 6365-6372.
- Krause, D. C., and M. F. Balish.** 2004. Cellular engineering in a minimal microbe: Structure and assembly of the terminal organelle of *Mycoplasma pneumoniae*. *Mol. Microbiol.* **51**: 917-924.
- Krauß, D., K. Hunold, B. Kusian, O. Lenz, J. Stülke, B. Bowien, and J. Deutscher.** 2009. Essential role of the *hprK* gene in *Ralstonia eutropha* H16. *J. Mol. Microbiol. Biotechnol.* **17**: 146-152.
- Krebes, K. A., L. B. Dirksen, and D. C. Krause.** 1995. Phosphorylation of *Mycoplasma pneumoniae* cytoadherence-accessory proteins in cell extracts. *J. Bacteriol.* **177**: 4571-4574.
- Kristich, C. J., C. L. Wells, and G. M. Dunny.** 2007. A eukaryotic-type Ser/Thr kinase in *Enterococcus faecalis* mediates antimicrobial resistance and intestinal persistence. *Proc. Natl. Acad. Sci. USA* **104**: 3508-3513.

- Kühner, S., V. van Noort, M. J. Betts, A. Leo-Macias, C. Batisse, M. Rode, T. Yamada, T. Maier, S. Bader, P. Beltran-Alvarez, et al.** 2009. Proteome organization in a genome-reduced bacterium. *Science* **326**: 1235-1240.
- Kunst, F., and G. Rapoport.** 1995. Salt stress is an environmental signal affecting degradative enzyme synthesis in *Bacillus subtilis*. *J. Bacteriol.* **177**: 2403-2407.
- Kunst, F., N. Ogasawara, I. Moszer, A. M. Albertini, G. Alloni, V. Azevedo, M. G. Bertero, P. Bessières, A. Bolotin, S. Borchert, et al.** 1997. The complete genome sequence of the Gram-positive bacterium *Bacillus subtilis*. *Nature* **390**: 249-256.
- Landry, C. R., E. D. Levy, and S. W. Michnick.** 2009. Weak functional constraints on phosphoproteomes. *Trends Genet.* **25**: 193-197.
- Larkin, M. A., G. Blackshields, N. P. Brown, R. Chenna, P. A. McGettigan, H. McWilliam, F. Valentin, I. M. Wallace, A. Wilm, R. Lopez, et al.** 2007. Clustal W and Clustal X version 2.0. *Bioinformatics* **23**: 2947-2948.
- Larson, T. J., M. Ehrmann, and W. Boos.** 1983. Periplasmic glycerophosphodiester phosphodiesterase of *Escherichia coli*, a new enzyme of the *glp* regulon. *J. Biol. Chem.* **258**: 5428-5432.
- Lee, I. M., R. E. Davis, and D. E. Gundersen-Rindal.** 2000. *Phytoplasma*: Phytopathogenic Mollicutes. *Annu. Rev. Microbiol.* **54**: 221-255.
- Lévine, A., F. Vannier, C. Absalon, L. Kuhn, P. Jackson, E. Scrivener, V. Labas, J. Vinh, P. Courtney, J. Garin, and S. J. Séror.** 2006. Analysis of the dynamic *Bacillus subtilis* Ser/Thr/Tyr phosphoproteome implicated in a wide variety of cellular processes. *Proteomics* **6**: 2157-2173.
- Li, X., S. A. Gerber, A. D. Rudner, S. A. Beausoleil, W. Haas, J. Villén, J. E. Elias, and S. P. Gygi.** 2007. Large-scale phosphorylation analysis of alpha-factor-arrested *Saccharomyces cerevisiae*. *J. Proteome Res.* **6**: 1190-1197.
- Liekens, S., A. Bronckaers, and J. Balzarini.** 2009. Improvement of purine and pyrimidine antimetabolite-based anticancer treatment by selective suppression of *Mycoplasma*-encoded catabolic enzymes. *Lancet Oncol.* **10**: 628-635.
- Lin, M. H., T. L. Hsu, S. Y. Lin, Y. J. Pan, J. T. Jan, J. T. Wang, K. H. Khoo, and S. H. Wu.** 2009. Phosphoproteomics of *Klebsiella pneumoniae* NTUH-K2044 reveals a tight link between tyrosine phosphorylation and virulence. *Mol. Cell. Proteomics* **8**: 2613-2623.

- Linding, R., L. J. Jensen, F. Diella, P. Bork, T. J. Gibson, and R. B. Russell.** 2003. Protein disorder prediction: Implications for structural proteomics. *Structure* **11**: 1453-1459.
- Liu, W. B., J. Z. Zhang, B. H. Jiang, T. T. Ren, M. M. Gong, L. Meng, and C. C. Shou.** 2006. Lipoprotein p37 from *Mycoplasma hyorhinis* inhibiting mammalian cell adhesion. *J. Biomed. Sci.* **13**: 323-331.
- Lomas-Lopez, R., P. Paracuellos, M. Riberty, A. J. Cozzone, and B. Duclos.** 2007. Several enzymes of the central metabolism are phosphorylated in *Staphylococcus aureus*. *FEMS Microbiol. Lett.* **272**: 35-42.
- Low, I. E.** 1971. Effect of medium on H₂O₂ levels and peroxidase-like activity by *Mycoplasma pneumoniae*. *Infect. Immun.* **3**: 80-86.
- Low, I. E., and S. M. Zimkus.** 1973. Reduced nicotinamide adenine dinucleotide oxidase activity and H₂O₂ formation of *Mycoplasma pneumoniae*. *J. Bacteriol.* **116**: 346-354.
- Ludwig, H., G. Homuth, M. Schmalisch, F. M. Dyka, M. Hecker, and J. Stülke.** 2001. Transcription of glycolytic genes and operons in *Bacillus subtilis*: Evidence for the presence of multiple levels of control of the *gapA* operon. *Mol. Microbiol.* **41**: 409-422.
- Macek, B., F. Gnad, B. Soufi, C. Kumar, J. V. Olsen, I. Mijakovic, and M. Mann.** 2008. Phosphoproteome analysis of *E. coli* reveals evolutionary conservation of bacterial Ser/Thr/Tyr phosphorylation. *Mol. Cell. Proteomics* **7**: 299-307.
- Macek, B., I. Mijakovic, J. V. Olsen, F. Gnad, C. Kumar, P. R. Jensen, and M. Mann.** 2007. The serine/threonine/tyrosine phosphoproteome of the model bacterium *Bacillus subtilis*. *Mol. Cell. Proteomics* **6**: 697-707.
- Madec, E., A. Laszkiewicz, A. Iwanicki, M. Obuchowski, and S. Séror.** 2002. Characterization of a membrane-linked Ser/Thr protein kinase in *Bacillus subtilis*, implicated in developmental processes. *Mol. Microbiol.* **46**: 571-586.
- Madec, E., A. Stensballe, S. Kjellström, L. Cladière, M. Obuchowski, O. N. Jensen, and S. Séror.** 2003. Mass spectrometry and site-directed mutagenesis identify several autophosphorylated residues required for the activity of PrkC, a Ser/Thr kinase from *Bacillus subtilis*. *J. Mol. Biol.* **330**: 459-472.

- Madsen, M. L., D. Nettleton, E. L. Thacker, R. Edwards, and F.C. Minion.** 2006. Transcriptional profiling of *Mycoplasma hyopneumoniae* during heat shock using microarrays. *Infect. Immun.* **74**: 160-166.
- Madsen, M. L., S. Puttamreddy, E. L. Thacker, M. D. Carruthers, and F. C. Minion.** 2008. Transcriptome changes in *Mycoplasma hyopneumoniae* during infection. *Infect. Immun.* **76**: 658-663.
- Martin-Verstraete, I., J. Stülke, A. Klier, and G. Rapoport.** 1995. Two different mechanisms mediate catabolite repression of the *Bacillus subtilis* levanase operon. *J. Bacteriol.* **177**: 6919-6927.
- Martin-Verstraete, I., M. Débarbouillé, A. Klier, and G. Rapoport.** 1994. Interaction of wild-type truncated LevR of *Bacillus subtilis* with the upstream activating sequence of the levanase operon. *J. Mol. Biol.* **241**: 178-192.
- McCarty, J. S., and G. C. Walker.** 1991. DnaK as a thermometer: Threonine-199 is site of autophosphorylation and is critical for ATPase activity. *Proc. Natl. Acad. Sci. USA* **88**: 9513-9517.
- McCutcheon, J. P., B. R. McDonald, and N. A. Moran.** 2009. Convergent evolution of metabolic roles in bacterial co-symbionts of insects. *Proc. Natl. Acad. Sci. USA* **106**: 15394-15399.
- Mengin-Lecreulx, D., and J. van Heijenoort.** 1996. Characterization of the essential gene *glmM* encoding phosphoglucosamine mutase in *Escherichia coli*. *J. Biol. Chem.* **271**: 32-39.
- Merzbacher, M., C. Detsch, W. Hillen, and J. Stülke.** 2004. *Mycoplasma pneumoniae* HPr kinase/phosphorylase: Assigning functional roles to the P-loop and the HPrK/P signature sequence motif. *Eur. J. Biochem.* **271**: 367-374.
- Mijakovic, I., S. Poncet, A. Galiner, V. Monedero, S. Fieulaine, J. Janin, S. Nessler, J. A. Marquez, K. Scheffzek, S. Hasenbein, et al.** 2002. Pyrophosphate-producing protein dephosphorylation by HPr kinase/phosphorylase: A relic of early life? *Proc. Natl. Acad. Sci. USA* **99**: 13442-13447.
- Miles, R. J.** 1992. Catabolism in Mollicutes. *J. Gen. Microbiol.* **138**: 1773-1783.
- Min, K. T., C. M. Hilditch, B. Diederich, J. Errington, and M. D. Yudkin.** 1993. Sigma F, the first compartment-specific transcription factor of *B. subtilis*, is regulated by an anti-sigma factor that is also a protein kinase. *Cell* **27**: 735-742.

- Miyata, M.** 2010. Unique centipede mechanism of *Mycoplasma* gliding. *Annu. Rev. Microbiol.* in press (PMID: 20533876).
- Mizutani, Y., H. Wada, O. Yoshida, M. Fukushima, M. Nakao, and T. Miki.** 2003. The significance of thymidine phosphorylase/platelet-derived endothelial cell growth factor activity in renal cell carcinoma. *Cancer* **98**: 730-736.
- Moreno, M. S., B. L. Schneider, R. R. Maile, W. Weyler, and M. H. Saier Jr.** 2001. Catabolite repression mediated by the CcpA protein in *Bacillus subtilis*: Novel modes of regulation revealed by whole-genome analysis. *Mol. Microbiol.* **39**: 1366-1381.
- Morozumi, M., T. Takahashi, and K. Ubukata.** 2010. Macrolide-resistant *Mycoplasma pneumoniae*: Characteristics of isolates and clinical aspects of community-acquired pneumonia. *J. Infect. Chemother.* **16**: 78-86.
- Mowbray, J., and V. Moses.** 1976. The tentative identification in *Escherichia coli* of a multi-enzyme complex with glycolytic activity. *Eur. J. Biochem.* **66**: 25-36.
- Munson Jr., R. S., and K. Sasaki.** 1993. Protein D, a putative immunoglobulin D-binding protein produced by *Haemophilus influenzae*, is glycerophosphodiester phosphodiesterase. *J. Bacteriol.* **175**: 4569-4571.
- Musatovova, O., S. Dhandayuthapani, and J. B. Baseman.** 2006. Transcriptional heat shock response in the smallest known self-replicating cell, *Mycoplasma genitalium*. *J. Bacteriol.* **188**: 2845-2855.
- Namiki, K., S. Goodison, S. Porvasnik, R. W. Allan, K. A. Iczkowski, C. Urbanek, L. Reyes, N. Sakamoto, and C. J. Rosser.** 2009. Persistent exposure to *Mycoplasma* induces malignant transformation of human prostate cells. *PLoS ONE* **4**: e6872.
- Narita, M.** 2009. Pathogenesis of neurologic manifestations of *Mycoplasma pneumoniae* infection. *Pediatr. Neurol.* **41**: 159-166.
- Narita, M.** 2010. Pathogenesis of extrapulmonary manifestations of *Mycoplasma pneumoniae* infection with special reference to pneumonia. *J. Infect. Chemother.* **16**: 162-169.
- Nesvizhskii, A. I., A. Keller, E. Kolker, and R. Aebersold.** 2003. A statistical model for identifying proteins by tandem mass spectrometry. *Anal. Chem.* **75**: 4646-4658.

- Nilsson, R. P., L. Beijer, and B. Rutberg.** 1994. The *glpT* and *glpQ* genes of the glycerol regulon in *Bacillus subtilis*. *Microbiology* **140**: 723-730.
- Nováková, L., L. Sasková, P. Pallová, J. Janecek, J. Novotná, A. Ulrych, J. Echenique, M. C. Trombe, and P. Branny.** 2005. Characterization of a eukaryotic type serine/threonine protein kinase and protein phosphatase of *Streptococcus pneumoniae* and identification of kinase substrates. *FEBS J.* **272**: 1243-1254.
- Ohshima, N., S. Yamashita, N. Takahashi, C. Kuroishi, Y. Shiro, and K. Takio.** 2008. *Escherichia coli* cytosolic glycerophosphodiester phosphodiesterase (UgpQ) requires Mg^{2+} , Co^{2+} or Mn^{2+} for its enzyme activity. *J. Bacteriol.* **190**: 1219-1223.
- Okazaki, Y., N. Ohshima, I. Yoshizawa, Y. Kamei, S. Mariggio, K. Okamoto, M. Maeda, Y. Nogusa, Y. Fujioka, T. Izumi, et al.** 2010. A novel glycerophosphodiester phosphodiesterase, GDE5, controls skeletal muscle development via a non-enzymatic mechanism. *J. Biol. Chem.* **285**: 27652-27663.
- Pachkov, M., T. Dandekar, J. Korbil, P. Bork, and S. Schuster.** 2007. Use of pathway analysis and genome context methods for functional genomics of *Mycoplasma pneumoniae* nucleotide metabolism. *Gene* **396**: 215-225.
- Pawson, T., and J. D. Scott.** 2005. Protein phosphorylation in signaling - 50 years and counting. *Trends Biochem. Sci.* **30**: 286-290.
- Peake, P., N. Winter, and W. Britton.** 1998. Phosphorylation of *Mycobacterium leprae* heat-shock 70 protein at threonine 175 alters its substrate binding characteristics. *Biochim. Biophys. Acta* **1387**: 387-394.
- Pietack, N., D. Becher, S. R. Schmidl, M. H. Saier, M. Hecker, F. M. Commichau, and J. Stülke.** 2010. *In vitro* phosphorylation of key metabolic enzymes from *Bacillus subtilis*: PrkC phosphorylates enzymes from different branches of basic metabolism. *J. Mol. Microbiol. Biotechnol.* **18**: 129-140.
- Pilo, P., E. M. Vilei, E. Peterhans, L. Bonvin-Klotz, M. H. Stoffel, D. Dobbelaere, and J. Frey.** 2005. A metabolic enzyme as a primary virulence factor of *Mycoplasma mycoides* subsp. *mycoides* small colony. *J. Bacteriol.* **187**: 6824-6831.

- Plackett, P., B. P. Marmion, E. J. Shaw, and R. M. Lemcke.** 1969. Immunochemical analysis of *Mycoplasma pneumoniae*. 3. Separation and chemical identification of serologically active lipids. *Aust. J. Exp. Biol. Med. Sci.* **47**: 171-195.
- Pollack, J. D.** 2001. *Ureaplasma urealyticum*: An opportunity for combinatorial genomics. *Trends Microbiol.* **9**: 169-175.
- Pollack, J. D., M. A. Myers, T. Dandekar, and R. Herrmann.** 2002. Suspected utility of enzymes with multiple activities in the small genome *Mycoplasma* species: The replacement of the missing “household” nucleoside diphosphate kinase gene and activity by glycolytic kinases. *OMICS* **6**: 247-258.
- Popham, P. L., T. W. Hahn, K. A. Krebes, and D. C. Krause.** 1997. Loss of HMW1 and HMW3 in noncytadhering mutants of *Mycoplasma pneumoniae* occurs post-translationally. *Proc. Natl. Acad. Sci. USA* **94**: 13979-13984.
- Potters, M. B., B. T. Solow, K. M. Bischoff, D. E. Graham, B. H. Lower, R. Helm, and P. J. Kennelly.** 2003. Phosphoprotein with phosphoglycerate mutase activity from the archaeon *Sulfolobus solfataricus*. *J. Bacteriol.* **185**: 2112-2121.
- Preneta, R., K. G. Papavinasasundaram, A. J. Cozzone, and B. Duclos.** 2004. Autophosphorylation of the 16 kDa and 70 kDa antigens (Hsp 16.3 and Hsp 70) of *Mycobacterium tuberculosis*. *Microbiology* **150**: 2135-2141.
- Razin, S., and R. Herrmann.** 2002. Molecular biology and pathogenicity of mycoplasmas (eds.), Kluwer Academic/Plenum Publishers, New York.
- Razin, S., D. Yogev, and Y. Naot.** 1998. Molecular biology and pathogenicity of mycoplasmas. *Microbiol. Mol. Biol. Rev.* **62**: 1094-1156.
- Regni, C., P. A. Tipton, and L. J. Beamer.** 2002. Crystal structure of PMM/PGM: An enzyme in the biosynthetic pathway of *P. aeruginosa* virulence factors. *Structure* **10**: 269-279.
- Regula, J. T., B. Ueberle, G. Boguth, A. Görg, M. Schnölzer, R. Herrmann, and R. Frank.** 2000. Towards a two-dimensional proteome map of *Mycoplasma pneumoniae*. *Electrophoresis* **21**: 3765-3780.
- Reizer, J., C. Hoischen, F. Titgemeyer, C. Rivolta, R. Rabus, J. Stülke, D. Karamata, M. H. Saier Jr., and W. Hillen.** 1998. A novel bacterial protein kinase that controls carbon catabolite repression. *Mol. Microbiol.* **27**: 1157-1169.

- Reizer, J., S. Bachem, A. Reizer, M. Arnaud, M. H. Saier Jr., and J. Stülke.** 1999. Novel phosphotransferase system genes revealed by genome analysis - The complete complement of PTS proteins encoded within the genome of *Bacillus subtilis*. *Microbiology* **145**: 3419-3429.
- Rogasch, K., V. Rühmling, J. Pané-Farré, D. Höper, C. Weinberg, S. Fuchs, M. Schmudde, B. M. Bröker, C. Wolz, M. Hecker, and S. Engelmann.** 2006. Influence of the two-component system SaeRS on global gene expression in two different *Staphylococcus aureus* strains. *J. Bacteriol.* **188**: 7742-7758.
- Sambrook, J., E. F. Fritsch, and T. Maniatis.** 1989. *Molecular cloning: A laboratory manual*, 2nd ed. Cold Spring Harbor Laboratory, Cold Spring Harbor, N.Y.
- Santos-Beneit, F., A. Rodríguez-García, A. K. Apel, and J. F. Martín.** 2009. Phosphate and carbon source regulation of two PhoP-dependent glycerophosphodiester phosphodiesterase genes of *Streptomyces coelicolor*. *Microbiology* **155**: 1800-1811.
- Sasková, L., L. Nováková, M. Basler, and P. Branny.** 2007. Eukaryotic-type serine/threonine protein kinase StkP is a global regulator of gene expression in *Streptococcus pneumoniae*. *J. Bacteriol.* **189**: 4168-4179.
- Schalock, P. C., and J. G. Dinulos.** 2009. *Mycoplasma pneumoniae*-induced cutaneous disease. *Int. J. Dermatol.* **48**: 673-680.
- Schilling, O., O. Frick, C. Herzberg, A. Ehrenreich, E. Heinzle, C. Wittmann, and J. Stülke.** 2007. Transcriptional and metabolic responses of *Bacillus subtilis* to the availability of organic acids: Transcription regulation is important but not sufficient to account for metabolic adaptation. *Appl. Env. Microbiol.* **73**: 499-507.
- Schirmer, F., S. Ehrt, and W. Hillen.** 1997. Expression, inducer spectrum domain structure, and function of MopR, the regulator of phenol degradation in *Acinetobacter calcoaceticus* NCIB8250. *J. Bacteriol.* **179**: 1329-1336.
- Schmalisch, M. H., S. Bachem, and J. Stülke.** 2003. Control of the *Bacillus subtilis* antiterminator protein GlcT by phosphorylation: Elucidation of the phosphorylation chain leading to inactivation of GlcT. *J. Biol. Chem.* **278**: 51108-51115.

- Schmidl, S. R., K. Gronau, C. Hames, J. Busse, D. Becher, M. Hecker, and J. Stülke.** 2010. The stability of cytoadherence proteins in *Mycoplasma pneumoniae* requires activity of the protein kinase PrkC. *Infect. Immun.* **78**: 184-192.
- Schmidl, S. R., K. Gronau, N. Pietack, M. Hecker, D. Becher, and J. Stülke.** 2010. The phosphoproteome of the minimal bacterium *Mycoplasma pneumoniae*: Analysis of the complete known Ser/Thr kinome suggests the existence of novel kinases. *Mol. Cell. Proteomics* **9**: 1228-1242.
- Schwan, T. G., J. M. Battisti, S. F. Porcella, S. J. Raffel, M. E. Schrupf, E. R. Fischer, J. A. Carroll, P. E. Stewart, P. Rosa, and G. A. Somerville.** 2003. Glycerol-3-phosphate acquisition in spirochetes: Distribution and biological activity of glycerophosphodiester phosphodiesterase (GlpQ) among *Borrelia* species. *J. Bacteriol.* **185**: 1346-1356.
- Segal, G., and E. Z. Ron.** 1998. Regulation of heat-shock response in bacteria. *Ann. NY Acad. Sci.* **851**: 147-151.
- Shah, I. M., M. H. Laaberki, D. L. Popham, and J. Dworkin.** 2008. A eukaryotic-like Ser/Thr kinase signals bacteria to exit dormancy in response to peptidoglycan fragments. *Cell* **135**: 486-496.
- Shakir, S. M., K. M. Bryant, J. L. Larabee, E. E. Hamm, J. Lovchik, C. R. Lyons, and J. D. Ballard.** 2010. Regulatory interactions of a virulence-associated serine/threonine phosphatase-kinase pair in *Bacillus anthracis*. *J. Bacteriol.* **192**: 400-409.
- Shevchenko, D. V., D. R. Akins, E. J. Robinson, M. Li, O. V. Shevchenko, and J. D. Radolf.** 1997. Identification of homologs for thioredoxin, peptidyl prolyl *cis-trans* isomerase, and glycerophosphodiester phosphodiesterase in outer membrane fractions from *Treponema pallidum*, the syphilis spirochete. *Infect. Immun.* **65**: 4179-4189.
- Shevchenko, D. V., T. J. Sellati, D. L. Cox, O. V. Shevchenko, E. J. Robinson, and J. D. Radolf.** 1999. Membrane topology and cellular location of the *Treponema pallidum* glycerophosphodiester phosphodiesterase (GlpQ) ortholog. *Infect. Immun.* **67**: 2266-2276.

- Shi, L., J. F. Liu, X. M. An, and D. C. Liang.** 2007. Crystal structure of glycerophosphodiester phosphodiesterase (GDPD) from *Thermoanaerobacter tengcongensis*, a metal ion-dependent enzyme: Insight into the catalytic mechanism. *Proteins* **72**: 280-288.
- Shimizu, T., Y. Kida, and K. Kuwano.** 2007. Triacylated lipoproteins derived from *Mycoplasma pneumoniae* activate nuclear factor-kappaB through toll-like receptors 1 and 2. *Immunology* **121**: 473-483.
- Shimizu, T., Y. Kida, and K. Kuwano.** 2008. A triacylated lipoprotein from *Mycoplasma genitalium* activates NF-kappaB through Toll-like receptor 1 (TLR1) and TLR2. *Infect Immun.* **76**: 3672-3678.
- Singh, K. D., S. Halbedel, B. Görke, and J. Stülke.** 2007. Control of the phosphorylation state of the HPr protein of the phosphotransferase system in *Bacillus subtilis*: Implication of the protein phosphatase PrpC. *J. Mol. Microbiol. Biotechnol.* **13**: 165-171.
- Sirand-Pugnet, P., C. Citti, A. Barré, and A. Blanchard.** 2007. Evolution of Mollicutes: Down a bumpy road with twists and turns. *Res. Microbiol.* **158**: 754-766.
- Somerson, N. L., B. E. Walls, and R. M. Chanock.** 1965. Hemolysin of *Mycoplasma pneumoniae*: Tentative identification as the peroxide. *Science* **150**: 226-228.
- Somerson, N. L., D. Taylor-Robinson, and R. M. Chanock.** 1963. Hemolytic production as an aid in the identification and quantitation of Eaton agent (*Mycoplasma pneumoniae*). *Am. J. Hyg.* **77**: 122-128.
- Sonenshein, A. L.** 2007. Control of key metabolic intersections in *Bacillus subtilis*. *Nat. Rev. Microbiol.* **5**: 917-927.
- Sood, P., C. G. Lerner, T. Shimamoto, Q. Lu, and M. Inouye.** 1994. Characterization of the autophosphorylation of Era, an essential *Escherichia coli* GTPase. *Mol. Microbiol.* **12**: 201-208.
- Soufi, B., F. Gnad, P. R. Jensen, D. Petranovic, M. Mann, I. Mijakovic, and B. Macek.** 2008. The Ser/Thr/Tyr phosphoproteome of *Lactococcus lactis* IL1403 reveals multiply phosphorylated proteins. *Proteomics* **8**: 3486-3493.

- Stebeck, C. E., J. M. Shaffer, T. W. Arroll, S. A. Lukehart, and W. C. van Voorhis.** 1997. Identification of the *Treponema pallidum* subsp. *pallidum* glycerophosphodiester phosphodiesterase homologue. FEMS Microbiol. Lett. **154**: 303-310.
- Steinhauer, K., T. Jepp, W. Hillen, and J. Stülke.** 2002. A novel mode of control of *Mycoplasma pneumoniae* HPr kinase/phosphatase activity reflects its parasitic lifestyle. Microbiology **148**: 3277-3284.
- Stock, A. M., V. L. Robinson, and P. N. Goudreau.** 2000. Two-component signal transduction. Annu. Rev. Biochem. **69**: 183-215.
- Stülke, J., H. Eilers, and S. R. Schmidl.** 2009. *Mycoplasma* and *Spiroplasma*. Encyclopedia of Microbiology (M. Schaechter, ed.), Elsevier, Oxford. p. 208-219.
- Su, H. C., C. A. Hutchison III, and M. C. Giddings.** 2007. Mapping phosphoproteins in *Mycoplasma genitalium* and *Mycoplasma pneumoniae*. BMC Microbiol. **7**: 63.
- Sun, X., F. Ge, C. L. Xiao, X. F. Yin, R. Ge, L. H. Zhang, and Q. Y. He.** 2010. Phosphoproteomic analysis reveals the multiple roles of phosphorylation in pathogenic bacterium *Streptococcus pneumoniae*. J. Proteome Res. **9**: 275-282.
- Szczepanek, S. M., S. Frasca Jr., V. L. Schumacher, X. Liao, M. Padula, S. P. Djordjevic, and S. J. Geary.** 2010. Identification of lipoprotein MslA as a neoteric virulence factor of *Mycoplasma gallisepticum*. Infect. Immun. **78**: 3475-3483.
- Tan, C. S., B. Bodenmiller, A. Pasculescu, M. Jovanovic, M. O. Hengartner, C. Jørgensen, G. D. Bader, R. Aebersold, T. Pawson, and R. Linding.** 2009. Comparative analysis reveals conserved protein phosphorylation networks implicated in multiple diseases. Sci. Signal. **2**: ra39.
- Tjalsma, H., H. Antelmann, J. D. H. Jongbloed, P. G. Braun, E. Darmon, R. Dorenbos, J. Y. Dubois, H. Westers, G. Zanen, W. J. Quax, et al.** 2004. Proteomics of protein secretion by *Bacillus subtilis*: Separating the “secrets” of the secretome. Microbiol. Mol. Biol. Rev. **68**: 207-233.
- Tsiodras, S., I. Kelesidis, T. Kelesidis, E. Stamboulis, and H. Giamarellou.** 2005. Central nervous system manifestations of *Mycoplasma pneumoniae* infection. J. Infect. **51**: 343-354.

- Van der Rest, B., N. Rolland, A. M. Boisson, M. Ferro, R. Bligny, and R. Douce.** 2004. Identification and characterization of plant glycerophosphodiester phosphodiesterase. *Biochem. J.* **379**: 601-607.
- Veldhuizen, R., K. Nag, S. Orgeig, and F. Possmayer.** 1998. The role of lipids in pulmonary surfactant. *Biochim. Biophys. Acta* **1408**: 90-108.
- Vilei, E. M., and J. Frey.** 2001. Genetic and biochemical characterization of glycerol uptake in *Mycoplasma mycoides* subsp. *mycoides* SC: Its impact on H₂O₂ production and virulence. *Clin. Diagn. Lab. Immunol.* **8**: 85-92.
- Voigt, B., H. Antelmann, D. Albrecht, A. Ehrenreich, K. H. Maurer, S. Evers, G. Gottschalk, J. M. van Dijl, T. Schweder, and M. Hecker.** 2009. Cell physiology and protein secretion of *Bacillus licheniformis* compared to *Bacillus subtilis*. *J. Mol. Microbiol. Biotechnol.* **16**: 53-68.
- Voisin, S., D. C. Watson, L. Tessier, W. Ding, S. Foote, S. Bhatia, J. F. Kelly, and N. M. Young.** 2007. The cytoplasmic phosphoproteome of the Gram-negative bacterium *Campylobacter jejuni*: Evidence for modification by unidentified protein kinases. *Proteomics* **7**: 4338-4348.
- Wach, A.** 1996. PCR-synthesis of marker cassettes with long flanking homology regions for gene disruptions in *S. cerevisiae*. *Yeast* **12**: 259-265.
- Waites, K. B., and D. F. Talkington.** 2004. *Mycoplasma pneumoniae* and its role as a human pathogen. *Clin. Microbiol. Rev.* **17**: 697-728.
- Wang, L.** 2007. The role of *Ureaplasma* nucleoside monophosphate kinases in the synthesis of nucleoside triphosphates. *FEBS J.* **274**: 1983-1990.
- Wang, L., C. Hames, S. R. Schmidl, and J. Stülke.** 2010. Upregulation of thymidine kinase activity compensates for loss of thymidylate synthase activity in *Mycoplasma pneumoniae*. *Mol. Microbiol.* **77**: 1502-1511.
- Wang, L., J. Westerberg, G. Bölske, and S. Eriksson.** 2001. Novel deoxynucleoside-phosphorylating enzymes in mycoplasmas: Evidence for efficient utilization of deoxynucleosides. *Mol. Microbiol.* **42**: 1065-1073.
- Weiner III, J., C. U. Zimmerman, H. W. Göhlmann, and R. Herrmann.** 2003. Transcription profiles of the bacterium *Mycoplasma pneumoniae* grown at different temperatures. *Nucleic Acids Res.* **31**: 6306-6320.

- Welin, M., U. Kosinska, N. E. Mikkelsen, C. Carnrot, C. Zhu, L. Wang, S. Eriksson, B. Munch-Petersen, and H. Eklund.** 2004. Structures of thymidine kinase 1 of human and mycoplasmic origin. *Proc. Natl. Acad. Sci. USA* **101**: 17970-17975.
- Willby, M. J., M. F. Balish, S. M. Ross, K. K. Lee, J. L. Jordan, and D. C. Krause.** 2004. HMW1 is required for stability and localization of HMW2 to the attachment organelle of *Mycoplasma pneumoniae*. *J. Bacteriol.* **186**: 8221-8228.
- Wong, K. K., and H. S. Kwan.** 1992. Transcription of *glpT* of *Escherichia coli* K12 is regulated by anaerobiosis and *fnr*. *FEMS Microbiol. Lett.* **73**: 15-18.
- Wu, H. C., and M. Tokunaga.** 1986. Biogenesis of lipoproteins in bacteria. *Curr. Top. Microbiol. Immunol.* **125**: 127-157.
- Yanaka, N.** 2007. Mammalian glycerophosphodiester phosphodiesterases. *Biosci. Biotechnol. Biochem.* **71**: 1811-1818.
- Yang, X., C. M. Kang, M. S. Brody, and C. W. Price.** 1996. Opposing pairs of serine protein kinases and phosphatases transmit signals of environmental stress to activate a bacterial transcription factor. *Genes Dev.* **10**: 2265-2275.
- Yanofsky, C., and M. Rachmeler.** 1958. The exclusion of free indole as an intermediate in the biosynthesis of tryptophan in *Neurospora crassa*. *Biochim. Biophys. Acta* **28**: 640-641.
- Yooseph, S., G. Sutton, D. B. Rusch, A. L. Halpern, S. J. Williamson, K. Remington, J. A. Eisen, K. B. Heidelberg, G. Manning, W. Li, et al.** 2007. The "Sorcerer II" global ocean sampling expedition: Expanding the universe of protein families. *PLoS Biol.* **5**: e16.
- You, X. X., Y. H. Zeng, and Y. M. Wu.** 2006. Interactions between *Mycoplasma* lipid-associated membrane proteins and the host cells. *J. Zhejiang Univ. Sci. B* **7**: 342-350.
- Yu, L. R., Z. Zhu, K. C. Chan, H. J. Issaq, D. S. Dimitrov, and T. D. Veenstra.** 2007. Improved titanium dioxide enrichment of phosphopeptides from HeLa cells and high confident phosphopeptide identification by cross-validation of MS/MS and MS/MS/MS spectra. *J. Proteome Res.* **6**: 4150-4162.

- Yus, E., T. Maier, K. Michalodimitrakis, V. van Noort, T. Yamada, W. H. Chen, J. A. Wodke, M. Güell, S. Martínez, R. Bourgeois, et al.** 2009. Impact of genome reduction on bacterial metabolism and its regulation. *Science* **326**: 1263-1268.
- Zeiman, E., M. Tarshis, and S. Rottem.** 2008. *Mycoplasma penetrans* under nutritional stress: Influence on lipid and lipoprotein profiles and on the binding to and invasion of HeLa cells. *FEMS Microbiol. Lett.* **287**: 243-249.
- Zhai, B., J. Villén, S. A. Beausoleil, J. Mintseris, and S. P. Gygi.** 2008. Phosphoproteome analysis of *Drosophila melanogaster* embryos. *J. Proteome Res.* **7**: 1675-1682.
- Zhu, W., and D. F. Becker.** 2003. Flavin redox state triggers conformational changes in the PutA protein from *Escherichia coli*. *Biochemistry* **42**: 5469-5477.
- Zimmerman, C. U., and R. Herrmann.** 2005. Synthesis of a small, cysteine-rich, 29 amino acids long peptide in *Mycoplasma pneumoniae*. *FEMS Microbiol. Lett.* **253**: 315-321.
- Zimmermann, L., E. Peterhans, and J. Frey.** 2010. RGD motif of lipoprotein T, involved in adhesion of *Mycoplasma conjunctivae* to lamb synovial tissue cells. *J. Bacteriol.* **192**: 3773-3779.
- Zuo, L. L., Y. M. Wu, and X. X. You.** 2009. *Mycoplasma* lipoproteins and Toll-like receptors. *J. Zhejiang Univ. Sci. B* **10**: 67-76.
- Zylicz, M., J. H. LeBowitz, R. McMacken, and C. Georgopoulos.** 1983. The DnaK protein of *Escherichia coli* possesses an ATPase and autophosphorylating activity and is essential in an *in vitro* DNA replication system. *Proc. Natl. Acad. Sci. USA* **80**: 6431-6435.

Chapter 10

Appendix

Oligonucleotides

Tab. S14. Oligonucleotides.

Name	Sequence (5'→3') ^{ab}	Description ^c
CD13	AAACATATGGCTAGCTGGAGCCACCCGCAGTTC	Sequencing of pGP172 constructs fw (<i>Nde</i> I)
CH35	GCTCAACTTGATTAATTTAAAACAATGG	Screening for <i>prkC</i> ::Tn strain fw
CH61	ATGCCAAATCCTGTTAGATTTGTTTAC	<i>mpn372</i> probe fw
CH63	CTAATACGACTCACTATAGGGAGAGCCGGGTGGTGA GCATG	<i>mpn372</i> probe rev
CH74	CTAATACGACTCACTATAGGGAGAGGTGTTCAAAC TGTGGAGG	<i>prkC</i> probe rev
eno forw1	AAGGATCCCCATACATTGTTGATGTTTATGCAC	<i>eno</i> _{Bsu} fw (<i>Bam</i> HI)
eno rev	TTTCTGCAGTTACTTGTTTAAGTTGTAGAAAGAGTTG	<i>eno</i> _{Bsu} rev (<i>Pst</i> I)
FC17	AAAGGATCCGTGGCACAAGGTGAAAAAATTAC	<i>icd</i> _{Bsu} fw (<i>Bam</i> HI)
FC18	TTTCTGCAGTTATTAGTCCATGTTTTTGTAT	<i>icd</i> _{Bsu} rev (<i>Pst</i> I)
FC146	CGATGCGTTCGCGATCCAGGC	Sequencing of pUT18 constructs fw
FC147	CCAGCCTGATGCGATTGCTGCAT	Sequencing of pKNT25 constructs fw
FC148	GTCACCCGGATTGCGGCGG	Sequencing of pUT18C constructs rev
FC149	GCTGGCTTAACTATGCGGCATCAGA	Sequencing of pUT18C constructs fw
JS39	TCTATCAACAGGAGTCCAAGC	Sequencing of pWH844 constructs rev
M13 puc rev	GGAAACAGCTATGACCATG	Sequencing pKNT25 and pUT18 constructs rev
MR04	AAAGGATCCATGGTTGACTTTAAAACAGTCCAAGC	<i>pgk</i> gene fw (<i>Bam</i> HI)
MR05	TATAAAGCTTTTACTTTTTTTGAATATCGCTAATTCCC AC	<i>pgk</i> gene rev (<i>Hind</i> III)
MR06	P_GTTAGCACAGTTCTGGGCATCATTGGG	<i>pgk</i> A441G
MR07	P_CCCAATGGCCAGCAGAACTTCAGG	<i>pgk</i> A894G
MR08	AAAGGATCCATGCATAAGAAGGTCTTACTAGCC	<i>pgm</i> gene fw (<i>Bam</i> HI)
MR09	TATACTGCAGTTACTTTTTACTTATTAAGGGAGTT TGCG	<i>pgm</i> gene rev (<i>Pst</i> I)
MR10	AAAGGATCCATGAGTGCACAACTGGAACCGATCTT TTCAAG	<i>eno</i> gene fw (<i>Bam</i> HI)

Tab. S14. Continued.

Name	Sequence (5'→3') ^{ab}	Description ^c
MR11	TATACTGCAGTTAAGCTTTTTGCGGTTAATGTTTTTA AAGGTGTTCCAACC	<i>eno</i> gene rev (<i>Pst</i> I) + A1335G
MR19	AAAGGATCCATGGAAAGTAAATGGTTAACAGTTGAC	<i>pgi</i> gene fw (<i>Bam</i> HI)
MR20	TATAAAGCTTCTATTACGACCAAGTTTAGCAAAC	<i>pgi</i> gene rev (<i>Hind</i> III)
MR21	P_GGGTAAATCATGGGCTTTGGTAGTAACTTC	<i>pgi</i> A393G
MR22	P_CTGCTTTGCGTCACTGGCTTTACAC	<i>pgi</i> A756G
MR23	AAAGGATCCATGAGTCCAAAAACAACCAAAAAAATT GCC	<i>pfkA</i> gene fw (<i>Bam</i> HI)
MR24	TATAAAGCTTTTAAATAATTTTTTATTAATGACTGC AATTAAAGCGC	<i>pfkA</i> gene rev (<i>Hind</i> III)
MR25	AAAGGATCCATGCTAGTAAACATCAAACAAATGTTG CAAC	<i>fba</i> gene fw (<i>Bam</i> HI)
MR26	TATAAAGCTTCTAAGCCTTATTGGTTGAACCACAG	<i>fba</i> gene rev (<i>Hind</i> III)
MR27	P_GGCTTTACCCCGACAACCTGGAAGGG	<i>fba</i> A552G
MR28	AAAGGATCCATGCGTACGAAATACCTAATTGGTAAC TGGAAG	<i>tpiA</i> gene fw (<i>Bam</i> HI) + A30G
MR29	TATACTGCAGTTATGCATATACTTGTGCCATTACTAA AAAGTCG	<i>tpiA</i> gene rev (<i>Pst</i> I)
MR30	P_GTGATTGCTTACGAACCAATTTGGGCAATTGGTAC GG	<i>tpiA</i> A489G
MR31	AAAGGATCCATGCTAGCAAAGAGTAAGACTATCC	<i>gapA</i> gene fw (<i>Bam</i> HI)
MR32	TATACTGCAGTTAAAGCTTGGCACAATAGTTAACTAC	<i>gapA</i> gene rev (<i>Pst</i> I)
MR33	P_GCTAACCTGCCATGGGCAGAACAC	<i>gapA</i> A270G
MR34	AAAGGATCCATGATTCACCACCTAAAACGCAC	<i>pyk</i> gene fw (<i>Bam</i> HI)
MR35	TATACTGCAGTTATAAGCTAATGATCTTATTGTGAAA TACTC	<i>pyk</i> gene rev (<i>Pst</i> I)
MR36	P_GCTATGGACGCTAGCAATGTTAGATGAC	<i>pyk</i> A69G
MR37	P_CAAGGTGCCTTACTGGCAACGGTAC	<i>pyk</i> A864G
MR38	P_CAGTGAGTTTTGGAAGCAGGTGGTG	<i>pyk</i> A1167G
NP01	AAAGAGCTCCGATGAAACGAGAAAGCAACATTC	<i>alsD</i> _{Bsu} fw (<i>Sac</i> I)
NP02	TTTGGATCCCTATTATTACAGGGCTTCCTCAGT	<i>alsD</i> _{Bsu} rev (<i>Bam</i> HI)
NP03	AAAGAGCTCCGGTGCTAATCGGCAAGC	<i>prkC</i> _{Bsu} fw (<i>Sac</i> I)
NP04	TTTAGATCTTCATTATTCATCTTTCGGATACTCAAT	<i>prkC</i> _{Bsu} rev (<i>Bgl</i> II)
NP05	AAAGAGCTCGATGGATACAATTGAAAAGAAATCAG	<i>tkl</i> _{Bsu} fw (<i>Sac</i> I)
NP06	TTTGGATCCCTCATTACTTATTGATTAATGCCTTAAC	<i>tkl</i> _{Bsu} rev (<i>Bam</i> HI)
NP07	AAAGAGCTCGATGATGAACGACGCTTTGAC	<i>yabT</i> _{Bsu} fw (<i>Sac</i> I)
NP08	TTTAGATCTTCATTAGATTAAGAAAAAGATAATA	<i>yabT</i> _{Bsu} rev (<i>Bgl</i> II)

Tab. S14. Continued.

Name	Sequence (5'→3') ^{ab}	Description ^c
NP09	AAAGAGCTCGATGGCATTAAAACTTCTAAAAAA	<i>prkD</i> _{Bsu} fw (<i>SacI</i>)
NP10	TTTGGATCCTCATTATGTGACCGATTGAATGGC	<i>prkD</i> _{Bsu} rev (<i>Bam</i> HI)
NP11	AAAGAGCTCGATGTTATTCTTTGTTGATACAG	<i>ywjH</i> _{Bsu} fw (<i>SacI</i>)
NP12	TTTGGATCCTCATTATTTGTTCCAGTCTGCC	<i>ywjH</i> _{Bsu} rev (<i>Bam</i> HI)
NP13	AAAGAGCTCGATGGTCAAGTCATTTCCG	<i>yxal</i> _{Bsu} fw (<i>SacI</i>)
NP14	TTTGGATCCTCATTATTTCCAAAAGCCATCAG	<i>yxal</i> _{Bsu} rev (<i>Bam</i> HI)
NP15	CCGGTGTTCACGGTGCGCCGCTTGG	<i>tkl</i> _{Bsu} sequencing fw
NP16	CTCACCTGATTCTTTAACAGCTACAGCG	<i>tkl</i> _{Bsu} sequencing rev
NP17	CTTGCTAAAGCTGCTGGCGAAAAGAAGCTG	<i>prkC</i> _{Bsu} sequencing fw
NP18	ATCGTGAGCAAACCCACGGCCAC	<i>prkC</i> _{Bsu} sequencing rev
NP19	ATGTTACGCGATCAAACCGACGTC	<i>yxal</i> _{Bsu} sequencing fw
NP20	GCAGCAGCCAACTCAGCTTCTTTTCGGGC	Sequencing of pGP172 constructs rev
NP108	AAAGGATCCCTCACTTATTTAAAGGAGGAAACAATC ATGGGCAAGTATTTTGAACAGACG	<i>glmM</i> _{Bsu} + RBS _{gapA} fw (<i>Bam</i> HI)
NP109	TTTGTGACCTATCACTCTAATCCCATTCTGACCGG	<i>glmM</i> _{Bsu} rev (<i>Sal</i> I)
NP110	GGCTATTCTCCGGAGCAGCCGATTGTCA	<i>glmM</i> _{Bsu} LFH-PCR fw (up-fragment)
NP111	CAGGAACGGACGACCAAAAGTTTTCCCG	<i>glmM</i> _{Bsu} LFH-PCR fw (up-fragment, sequencing)
NP112	CCTATCACCTCAAATGGTTCGCTGTAAAGGCCAGCTC AGGTGTAAGCTC	<i>glmM</i> _{Bsu} LFH-PCR rev (up-fragment)
NP113	CCGAGCGCCTACGAGGAATTTGTATCGAGCGAAGAC GAAAGAGCTGTGCGA	<i>glmM</i> _{Bsu} LFH-PCR fw (down-fragment)
NP114	CATCGCCATCGCATCAGATGCTACGACGT	<i>glmM</i> _{Bsu} LFH-PCR rev (down-fragment)
NP115	TATAAGACGCACGTGTAATCACGTCACCATC	<i>glmM</i> _{Bsu} LFH-PCR rev (down-fragment, sequencing)
NP116	P_GCAGAGGCGGGCGTCATGATTTCCGCTGCCATAA CCCAGTGCAGGATAACGGCATCAA	<i>glmM</i> _{Bsu} T298G
NP117	AAAGGATCCATGGGCAAGTATTTTGAACAGACG	<i>glmM</i> _{Bsu} fw (<i>Bam</i> HI)
PD05	AAATCTAGAGATGGAAAGTAAATGGTTAACAGTTGA CAC	<i>pgi</i> gene fw (<i>Xba</i> I)
PD06	TTTGGTACCCGTTACGACCAAGTTTAGCAAACATTA AC	<i>pgi</i> gene rev (<i>Kpn</i> I)

Tab. S14. Continued.

Name	Sequence (5'→3') ^{ab}	Description ^c
PD07	AAATCTAGAGATGAGTCCAAAAACAACCAAAAAAAT TGCC	<i>pfkA</i> gene fw (<i>Xba</i> I)
PD08	TTTGGTACCCGAATAATATTTTTATTAATGACTGCAA TTAAAGCGC	<i>pfkA</i> gene rev (<i>Kpn</i> I)
PD09	AAATCTAGAGATGCTAGTAAACATCAAACAAATGTT GCAAC	<i>fba</i> gene fw (<i>Xba</i> I)
PD10	TTTGAGCTCCGAGCCTTATTGGTTGAACCACAGAG	<i>fba</i> gene rev (<i>Sac</i> I)
PD11	AAATCTAGAGATGCGTACGAAATACCTAATTGGTAA C	<i>tpiA</i> gene fw (<i>Xba</i> I)
PD12	TTTGGTACCCGTGCATATACTTGTGCCATTACTAAAA AGTC	<i>tpiA</i> gene rev (<i>Kpn</i> I)
PD13	AAATCTAGAGATGCTAGCAAAGAGTAAGACTATCCG	<i>gapA</i> gene fw (<i>Xba</i> I)
PD14	TTTGAATTCCGAAGCTTGGCACAATAGTTAACTACCC	<i>gapA</i> gene rev (<i>Eco</i> RI)
PD15	AAATCTAGAGATGGTTGACTTTAAAACAGTCCAAGC	<i>pgk</i> gene fw (<i>Xba</i> I)
PD16	TTTGAATTCCGCTTTTTTTGAATATCGCTAATTCCCAC TAG	<i>pgk</i> gene rev (<i>Eco</i> RI)
PD17	AAATCTAGAGATGCATAAGAAGGTCTTACTAGCC	<i>pgm</i> gene fw (<i>Xba</i> I)
PD18	TTTGAATTCCGCTTTTTACTTATTTAAAGGGAGTTTG CG	<i>pgm</i> gene rev (<i>Eco</i> RI)
PD19	AAATCTAGAGATGAGTGCACAAACTGGAACCG	<i>eno</i> gene fw (<i>Xba</i> I)
PD20	TTTGAATTCCGAGCTTTTTGCGGTTTAATGTTTTTAAA GGTG	<i>eno</i> gene rev (<i>Eco</i> RI)
PD21	AAATCTAGAGATGATTCACCACCTAAAACGCAC	<i>pyk</i> gene fw (<i>Xba</i> I)
PD22	TTTGGTACCCGTAAGCTAATGATCTTATTGTGAAATA CTCC	<i>pyk</i> gene rev (<i>Kpn</i> I)
SH03	GAGTACCCGGATTAAAGCGGG	<i>hprK</i> probe fw
SH04	CTAATACGACTCACTATAGGGAGACATTAAGTGGAT TTCGGTGCGCTG	<i>hprK</i> probe rev
SH05	CAGGTAACGGTGCTGGTTTCG	<i>glpF</i> probe fw
SH06	CTAATACGACTCACTATAGGGAGAATTGCAGTACCA GTAGCGGC	<i>glpF</i> probe rev
SH29	ATGAGTGAGCTAACTCACAG	Screening primer for transposon insertions
SH30	CAATACGCAAACCGCCTC	Screening primer for transposon insertions
SH62	TAGAATTTTATGGTGGTAGAG	<i>aac-ahpD</i> probe fw

Tab. S14. Continued.

Name	Sequence (5'→3') ^{ab}	Description ^c
SH63	<u>CTAATACGACTCACTATAGGGAGAACACTATCATAA</u> CCACTACC	<i>aac-ahpD</i> probe rev
SH66	AAAG <u>TCGAC</u> ATGGACAGCACCAACCAAAC	<i>prpC</i> probe fw (<i>SalI</i>)
SH73	<u>CTAATACGACTCACTATAGGGAGAGACCATCAGAGC</u> ACAACAG	<i>prpC</i> probe rev
SH82	ATGGATCCATGGCACAAAAACATTTAAAG	<i>ptsH_{Bsu}</i> fw (<i>BamHI</i>)
SH83	ATA <u>AAGCTT</u> CTCGCCGAGTCCTTCG	<i>ptsH_{Bsu}</i> rev (<i>HindIII</i>)
SH89	TAGAGCTCGATGGCACTAAATTTAAAGATTGG	<i>prkC</i> probe fw
spec-fwd (kan)	CAGCGAACCATTTGAGGTGATAGGGACTGGCTCGCT AATAACGTAACGTGACTGGCAAGAG	Construction of <i>B. subtilis</i> mutants by LFH-PCR fw
spec-rev (kan)	CGATACAAATTCCTCGTAGGCGCTCGGCGTAGCGAG GGCAAGGGTTTATTGTTTTCTAAATCTG	Construction of <i>B. subtilis</i> mutants by LFH-PCR rev
SS29	AAAG <u>AGCTC</u> GATGATTAACATCGATCCCCATTTTATT C	<i>mpn549</i> gene fw (<i>SacI</i>)
SS30	TATAG <u>GATCCT</u> TAGCTGTTGACATGCTTTTTGTTTGG	<i>mpn549</i> gene rev (<i>BamHI</i>)
SS31	P_GAAGACATTAAGAAGTGGATTGGTTCCATTCG	<i>mpn549</i> A807G
SS32	GATTTGTGGGCCGATGTTTTCC	<i>tdk</i> probe fw
SS33	<u>CTAATACGACTCACTATAGGGAGACGGTTTCGTTGCT</u> CTTGGAC	<i>tdk</i> probe rev
SS34	AAAG <u>AGCTC</u> GATGCTTAAACGACAACCTTGCTAGC	<i>glpQ</i> gene fw (<i>SacI</i>)
SS35	TATAG <u>GATCCT</u> TACACTTCAAACCTTCTTGTTGGCAAT TTG	<i>glpQ</i> gene rev (<i>BamHI</i>)
SS36	P_GCCTTTTTGTTTTGGACGAAAAAGCAGTTCCAAG	<i>glpQ</i> A507G
SS37	P_CAGTATCTCCATCCCTGGACAAACATTTACG	<i>glpQ</i> A576G
SS38	P_CCTTTAGGGCTGTGGACGCTTAACAGTG	<i>glpQ</i> A639G
SS39	AAAG <u>AGCTC</u> GATGCGCAAACAGTTTTTAATTGCACA C	<i>mpn566</i> gene fw (<i>SacI</i>)
SS40	TATAG <u>GATCCT</u> TAGTAAAGTTGTGCTGCTATTTGAAA TTTAAC	<i>mpn566</i> gene rev (<i>BamHI</i>)
SS41	CGCAACAATTTAAAGAACTGACTTAGC	Screening for <i>mpn549::Tn</i> strain rev
SS42	CAACTTCTGCTAGCACACCG	<i>glpQ</i> probe fw
SS43	<u>CTAATACGACTCACTATAGGGAGAGCTATTTGGTAG</u> TTGGGGTTAATG	<i>glpQ</i> probe rev
SS44	GCAAACAGTTTTTAATTGCACACCG	<i>mpn566</i> probe fw

Tab. S14. Continued.

Name	Sequence (5'→3') ^{ab}	Description ^c
SS45	<u>CTAATACGACTCACTATAGGGAGAGCTCTTTAACTTT</u> TCGTTGAGGTAC	<i>mpn566</i> probe rev
SS46	5AAAGT <u>CGAC</u> CAGATAGATGGATGTGAGACAAACATG AAGAAGATTCAAGTAGTCGTTAAAG	<i>ptsH</i> gene fw (<i>SalI</i>)
SS47	5AA <u>ACTGCAGT</u> TAAATAACTTGGTGTTTTTCTAAAAC TGC	<i>ptsH</i> gene rev (<i>PstI</i>)
SS48	5AA <u>ACTGCAG</u> AGATAGATGGATGTGAGACAAACATG AAAAAGTTATTAGTCAAGGAGTTAATC	<i>hprK</i> gene fw (<i>PstI</i>)
SS49	AAAAAGCTTAGA <u>ACCGGTAGATCTAGACTGCTACTA</u> ACACTAGGATTCATC	<i>hprK</i> gene rev (<i>HindIII</i> / <i>BshTI/XbaI</i>)
SS50	<u>CTAATACGACTCACTATAGGGAGAGCACTAGCGGCA</u> ACGACG	<i>mpn162</i> promoter fragment probe (+56) rev
SS51	GGGAAGAAAAGATCCGTAAGTTTG	Screening for <i>mpn162::Tn</i> strain fw
SS52	GTTTGCCGCTTGCAGGCC	Screening for <i>mpn162::Tn</i> strain rev
SS53	AAAGGATCCTTGTCCATTCGTAAAACCTGGCATAGTAT TTC	<i>engC</i> gene fw (<i>BamHI</i>)
SS54	TATAAAGCTTTTAATTAATCAACTTTAGATAGCTCTC ATAAAGCCAC	<i>engC</i> gene rev (<i>HindIII</i>) + A804G
SS55	P_CTACAGTGGAAGCGCGATTTTAAACTGTTAGTTGG	<i>engC</i> A108G
SS56	P_CTAATTGAACCCAAGATTAAGTAACTGGCAACAGTTGTT TAAATTG	<i>engC</i> A267G
SS57	ATGAATGATACTGACAAGAAGTTCCC	Screening for <i>hmw2::Tn</i> strain fw 1
SS58	GATGAATCATCACGCCGAATTGC	Screening for <i>hmw2::Tn</i> strain fw 2
SS59	TTATTTAGCTGCTTTTTGGGCAATTAG	Screening for <i>hmw2::Tn</i> strain rev
SS60	GCTACTGCATACGATCCCAATC	<i>p65</i> probe fw
SS61	<u>CTAATACGACTCACTATAGGGAGACATAGTAAGCGT</u> TGGGATCGG	<i>p65</i> probe rev
SS62	GCACTGGGTTTGTATGATGGG	<i>hmw2</i> probe 1 fw
SS63	<u>CTAATACGACTCACTATAGGGAGACCTGGTTAGCTG</u> CAATCTGTTC	<i>hmw2</i> probe 1 rev
SS64	GAAGCGCAACCAACTAACGC	<i>hmw2</i> probe 2 fw

Tab. S14. Continued.

Name	Sequence (5'→3') ^{ab}	Description ^c
SS65	<u>CTAATACGACTCACTATAGGGAGAGTTGTTGGGACA</u> GATCAGCAC	<i>hmw2</i> probe 2 rev
SS66	GATGATGAAGCTGACATCATCATAG	<i>p41</i> probe fw
SS67	<u>CTAATACGACTCACTATAGGGAGAGTGTATTCCGTG</u> CCACCAATAAC	<i>p41</i> probe rev
SS68	CTAACACTAAAACGGGTACGAATTG	<i>p24</i> probe fw
SS69	<u>CTAATACGACTCACTATAGGGAGAGCCACAAGTGTT</u> TCTGATGTCAC	<i>p24</i> probe rev
SS70	CTGAGGAAAATCCCGAACAGATC	<i>hmw1</i> probe 1 fw
SS71	<u>CTAATACGACTCACTATAGGGAGAGCTGGTACATCT</u> GCTTCCAAAC	<i>hmw1</i> probe 1 rev
SS72	GCCAACAGCGACATTAACAGC	<i>hmw1</i> probe 2 fw
SS73	<u>CTAATACGACTCACTATAGGGAGACAGTATCACTGC</u> AGAGCTTATAAAC	<i>hmw1</i> probe 2 rev
SS74	GTATGGTAAGCTAGCACAAAAGATC	<i>hmw3</i> probe fw
SS75	<u>CTAATACGACTCACTATAGGGAGAGTTGATCAGCTT</u> GCTGTTCGG	<i>hmw3</i> probe rev
SS76	CTTGGATTCTCATCCTCACCG	<i>p1</i> probe 1 fw
SS77	<u>CTAATACGACTCACTATAGGGAGAGGTGCAGCCCCA</u> CTCAAAC	<i>p1</i> probe 1 rev
SS78	GCGAGCGGGTGGTTCCG	<i>p1</i> probe 2 fw
SS79	<u>CTAATACGACTCACTATAGGGAGAGCTTGTAAGCAC</u> TCGCTTCC	<i>p1</i> probe 2 rev
SS80	CCTGAATGCTAGTGCTGTTGAG	<i>p30</i> probe fw
SS81	<u>CTAATACGACTCACTATAGGGAGAGTTGAGGTGGGA</u> AACCAGTAC	<i>p30</i> probe rev
SS82	CAAAGGTAGTTAATGTAGATCAGGTAG	<i>engC</i> probe fw
SS83	<u>CTAATACGACTCACTATAGGGAGAGTTGGGCTGCTA</u> ATTGTTTGAGG	<i>engC</i> probe rev
SS84	GTTGCAGTAGATCAATAAAAAGAGGG	Screening for <i>chiO</i> ::Tn strain fw
SS85	GCTTTTATCAACAAAGACACTAAGATTG	Screening for <i>chiO</i> ::Tn strain rev
SS86	GCACGCATCTTAAAGCTGTTGG	<i>p28</i> probe fw
SS87	<u>CTAATACGACTCACTATAGGGAGACACTGTCAGCGT</u> GCTCTGC	<i>p28</i> probe rev
SS88	GCTTCTCCAATTCGCGGCG	<i>hmw2</i> sequencing rev 1

Tab. S14. Continued.

Name	Sequence (5'→3') ^{ab}	Description ^c
SS89	CGCCGCGAATTGGAGAAGC	<i>hmw2</i> sequencing fw 1
SS90	GTTCGATTTGCTGGAACCTCCTG	<i>hmw2</i> sequencing rev 2
SS91	CGCCAGTCTTTAGAGCATGAC	<i>hmw2</i> sequencing fw 2
SS92	GCTAGCTTCTTCACTTACCGG	<i>p40</i> probe fw
SS93	<u>CTAATACGACTCACTATAGGGAGGTTAACGTTCCCTT</u> CGTTACCATTG	<i>p40</i> probe rev
SS94	GCGTCAAAGTAGTACTTGGGAG	Screening for <i>mpn256::Tn</i> strain fw
SS95	GACATCAGGGTTAATTTGAGCAATC	Screening for <i>mpn256::Tn</i> strain rev
SS96	CGACTGATGGTTGGCTCTAC	Screening for <i>glpQ::Tn</i> strain fw
SS97	GCTAACCGTTTACTCGGTGG	Screening for <i>glpQ::Tn</i> strain rev
SS98	CAGTTAATAGGCAACGAAGACTATG	Screening for <i>mpn566::Tn</i> strain fw
SS99	CACTAGTAAGAACCACAGTAGTAC	Screening for <i>mpn566::Tn</i> strain rev
SS100	GAGTAGCTCACAATGACCCTG	Screening for <i>glpK::Tn</i> strain fw
SS101	GGTGGAGCAGAAGATAAGCAG	Screening for <i>glpK::Tn</i> strain rev
SS102	GTTAATTAATGGGAGGATAAGCAAGC	Screening for <i>glpF::Tn</i> strain fw
SS103	CCGACAAGATTTGTAAGTTAGATGC	Screening for <i>glpF::Tn</i> strain rev
SS104	<u>AAAGGATCCATGGCACTAAATTTAAAGATTGGTGAC</u>	<i>prkC</i> gene fw (<i>Bam</i> HI)
SS105	TATA <u>AAGCTTTT</u> TATAGGTAATTACTTACCATTAGTTC ACG	<i>prkC</i> catalytic domain rev (<i>Hind</i> III)
SS106	TATA <u>AAGCTTTT</u> TACGAATGGACAACACTACCCAG	<i>prkC</i> gene rev (<i>Hind</i> III)
SS107	<u>AAAGGATCCATGAACAGTAACGCATACTTGGGAAGC</u>	<i>manB</i> gene fw (<i>Bam</i> HI)
SS108	TATA <u>CTGCAGCTAAGCTTT</u> ATCGAGGTTGAGCAATC	<i>manB</i> gene rev (<i>Pst</i> I)
SS109	P_GAAAGTAAGGATACCTGGGAGTTAGCGCG	<i>manB</i> A846G
SS110	P_CTTTGCGATTGCCGAATGGAATCCGCAAAC	<i>manB</i> A936G
SS111	P_GATTACTATAACTGGACGGTACCACACACCATTC	<i>manB</i> A1356G
SS112	P_CGGTGAATGTCACTGCTGCTCATAATCCTAAAACC	<i>manB</i> A445G/G446C

Tab. S14. Continued.

Name	Sequence (5'→3') ^{ab}	Description ^c
SS113	CAAGGCCACAATTGATTATGTCTTTG	Screening for <i>manB</i> ::Tn strain fw
SS114	GGTAACTTAGTGGAAGTCCACTTAAC	Screening for <i>manB</i> ::Tn strain rev
SS115	GAATTAACAGTAAGCTAACCGGG	<i>mpn256</i> probe fw
SS116	<u>CTAATACGACTCACTATAGGGAGACAATAAACTTAG</u> AAAAGTCCATGGTTG	<i>mpn256</i> probe rev
SS117	GTATTTTGAGAGTTAGTGCCTTTCC	Screening for <i>ftsY</i> ::Tn strain fw
SS118	CTCGCGTAATTGGGGATCTG	Screening for <i>ftsY</i> ::Tn strain rev
SS119	GATCAGGAGACAAATACATTCGAAC	Screening for <i>mpn349</i> ::Tn strain fw
SS120	GTGCCTTGGTTAGATTACCTTTAC	Screening for <i>mpn349</i> ::Tn strain rev
SS121	CACTAAGGTGTACGGTGATTTAAG	<i>nrdE</i> probe fw
SS122	<u>CTAATACGACTCACTATAGGGAGAGACCAATTGATT</u> CCATGTTGTCTTC	<i>nrdE</i> probe rev
SS123	GAATCAGTTTCTCCCTTAGAATATGC	<i>nrdF</i> probe fw
SS124	<u>CTAATACGACTCACTATAGGGAGAGTCTTTCCCGGTG</u> TAATAGGG	<i>nrdF</i> probe rev
SS125	GATATCAAATAGTCGACGCTAGTG	<i>nrdI</i> probe fw
SS126	<u>CTAATACGACTCACTATAGGGAGACTTGTCTACATC</u> GTTTTTCGTGC	<i>nrdI</i> probe rev
SS127	CCAACAGCGCTTTTATTCTCGG	<i>mpn083</i> probe fw
SS128	<u>CTAATACGACTCACTATAGGGAGAGGACATTAGGTT</u> TGGTGTACTTAC	<i>mpn083</i> probe rev
SS129	CCTTGTTAGTTGCGCCACAC	<i>mpn162</i> probe fw
SS130	<u>CTAATACGACTCACTATAGGGAGACACCTTCGTGGT</u> GATCATGATC	<i>mpn162</i> probe rev
SS131	GGCTTAGTCATCCACACTTGG	<i>ulaF</i> probe fw
SS132	<u>CTAATACGACTCACTATAGGGAGACCACTGCATCCTT</u> GCCATTC	<i>ulaF</i> probe rev
SS133	CTGCTGTAGCTCATGTGGAAC	<i>licA</i> probe fw
SS134	<u>CTAATACGACTCACTATAGGGAGACTCAAAGTCAAT</u> TAAAACGACCTGC	<i>licA</i> probe rev
SS135	GGTTTTACCCGTTTTTGTGTTAATGC	<i>plsC</i> probe fw

Tab. S14. Continued.

Name	Sequence (5'→3') ^{ab}	Description ^c
SS136	<u>CTAATACGACTCACTATAGGGAGAG</u> GCCCGATTTAAA CTCACCAATTTG	<i>plsC</i> probe rev
SS137	CCGTTACATTCTCCTTAAAATTCAAAG	<i>mpn239</i> probe fw
SS138	<u>CTAATACGACTCACTATAGGGAGAG</u> GCTCTACCACAA TGCCGTTG	<i>mpn239</i> probe rev
SS139	ATGCTTAAGAAAAAAGTTAATAATGATGCTG	<i>spx</i> probe fw
SS140	<u>CTAATACGACTCACTATAGGGAG</u> ATTACTTCTTTACT GTACGCACTTTAGG	<i>spx</i> probe rev
SS141	CCGCTTTTCACCTTTGCACAG	<i>pmd1</i> probe fw
SS142	<u>CTAATACGACTCACTATAGGGAGAG</u> AGTTAGTGGA ATAGCAAAGGC	<i>pmd1</i> probe rev
SS143	GCTAATGTAGATGTTAACCTCACG	<i>yjcW</i> probe fw
SS144	<u>CTAATACGACTCACTATAGGGAG</u> ACTCAAACAGCG GTTGGTTCATC	<i>ycjW</i> probe rev
SS145	CCTGATTTATGACAAAGAAGGTAACC	<i>mpn684</i> probe fw
SS146	<u>CTAATACGACTCACTATAGGGAG</u> AGGGATTAGTCTC TAACCAAAACTG	<i>mpn684</i> probe rev
SS147	GAATATTGTAGTCGACTTTGGTGAG	<i>ugpC</i> probe fw
SS148	<u>CTAATACGACTCACTATAGGGAG</u> AGGTTAGCTTCCA GTTCACTCTG	<i>ugpC</i> probe rev
SS149	GTTCAAGGTCCGCGGTAGC	<i>oppF</i> probe fw
SS150	<u>CTAATACGACTCACTATAGGGAG</u> AGTAGGGCAAAC TGTTAATCGTAG	<i>oppF</i> probe rev
SS151	GCCTAGTGGGATAATTAATAGAAATAAG	<i>glpF</i> promoter fragment (-321) fw
SS152	CGGCACCAATCCAACGTGG	<i>glpF</i> promoter fragment (+49) rev
SS153	GAGTTAATGTTAGACAATGGGCAAG	<i>mpn239</i> promoter fragment (-247) fw
SS154	GGAGAATGTAACGGTAAATTATTTGAC	<i>mpn239</i> promoter fragment (+58) rev
SS155	AAAGAATTCGCTAGTGGGATAATTAATAGAAATAA G	<i>glpF</i> promoter fragment (-321) fw (<i>EcoRI</i>)
SS156	TATAGGATCCCCTAAAAATTCGGCACCAATCC	<i>glpF</i> promoter fragment (+59) rev (<i>BamHI</i>)
SS157	AAACAATTGGAGTTAATGTTAGACAATGGGCAAG	<i>mpn239</i> promoter fragment (-247) fw (<i>MfeI</i>)

Tab. S14. Continued.

Name	Sequence (5'→3') ^{ab}	Description ^c
SS158	TATAGGATCCCTTTGAATTTTAAGGAGAATGTAACG G	<i>mpn239</i> promoter fragment (+71) rev (<i>Bam</i> HI)
SS159	TATAGCGGCCGCTTACACTTCAAACCTTCTTGTTGGCA ATTTGTG	<i>glpQ</i> gene rev (<i>Not</i> I)
SS160	TATAGCGGCCGCTTAGTAAAGTTGTGCTGCTATTTGA AATTTAACAAAG	<i>mpn566</i> gene rev (<i>Not</i> I)
SS161	AAAGGATCCCGCAGGTTAGCTGATAAGTTTAGGAG	<i>glpQ</i> promoter fragment (-495) fw (<i>Bam</i> HI)
SS162	AAAGGATCCGGGGAATGGGTATGAGCTGG	<i>mpn566</i> promoter fragment (-492) fw (<i>Bam</i> HI)
SS163	AAAGGATCCGTTAATAATGATGATTGAAGC	<i>ackA</i> promoter fragment (-224) fw (<i>Bam</i> HI)
SS164	AAACTGCAGATGCTTAAACGACAACCTTCTGCTAGC	<i>glpQ</i> gene fw (<i>Pst</i> I)
SS165	AAACTGCAGATGCGCAAACAGTTTTTAATTGCACAC	<i>mpn566</i> gene fw (<i>Pst</i> I)
SS166	CTTCTACCGGGTTTTCCATGC	Screening for <i>deoA</i> ::Tn strain fw
SS167	CGCACTACGTTCCGCACAC	Screening for <i>deoA</i> ::Tn strain rev
SS168	GCTAAATCATAAGCTCACCATTGC	<i>cinA</i> probe fw
SS169	CTAATACGACTCACTATAGGGAGAGCTGCATCTTGTT CTCTTAAACC	<i>cinA</i> probe rev
SS170	CTAACCCCAACTACGGCATC	<i>rpoA</i> probe fw
SS171	CTAATACGACTCACTATAGGGAGACCCCAAAGAATT AATCATTTACGG	<i>rpoA</i> probe rev
SS172	CTAATCTTAGCGCTTACCTTGTTG	<i>disA</i> probe fw
SS173	CTAATACGACTCACTATAGGGAGAGTTTTAATCACG CCGCGCAC	<i>disA</i> probe rev
SS174	GAAATTTAAGTATGGTGCTACCC	<i>mpn363</i> probe fw
SS175	CTAATACGACTCACTATAGGGAGAGTTAGGTGATAA CTTGGAGAGATC	<i>mpn363</i> probe rev
SS176	CTCAATTTTAGCCTCAAACCCAAC	<i>cbiO</i> probe fw
SS177	CTAATACGACTCACTATAGGGAGACCGCTTTAGTTTG CTAGCTAGC	<i>cbiO</i> probe rev
SS178	GTTGGTGCCTTCTTTACCCTC	<i>mpn407</i> probe fw

Tab. S14. Continued.

Name	Sequence (5'→3') ^{ab}	Description ^c
SS179	<u>CTAATACGACTCACTATAGGGAGACTTACCTTCAA</u> CCGAGCACTAG	<i>mpn407</i> probe rev
SS180	CTGCATGTGGTGCTAGGGG	<i>mpn408</i> probe fw
SS181	<u>CTAATACGACTCACTATAGGGAGACTTTTAATCATTT</u> GAGCACCGTTTTCC	<i>mpn408</i> probe rev
SS182	CCGCTTATCATTCGCCGCAAC	<i>p37</i> probe fw
SS183	<u>CTAATACGACTCACTATAGGGAGACCTCTGTAGAAA</u> TTGATTAGTTTGTGTTG	<i>p37</i> probe rev
SS184	CTAGATAGTTTTTTACCAGCAATTGTG	<i>mtlF</i> probe fw
SS185	<u>CTAATACGACTCACTATAGGGAGACATTTAAAGGAC</u> AAGATGAACTTAGCC	<i>mtlF</i> probe rev
SS186	CCTTTTTGTACTATAAGCTTGCC	<i>lspA</i> probe fw
SS187	<u>CTAATACGACTCACTATAGGGAGACTGAATTAATAA</u> GGAGAGGAACAGAC	<i>lspA</i> probe rev
SS188	CGCCAAATCACGTCCTGTTC	<i>mpn294</i> probe fw
SS189	<u>CTAATACGACTCACTATAGGGAGACACAAGAATTGG</u> CACAACTAATAATG	<i>mpn294</i> probe rev
SS190	GCTGCCTGTGGTACAAAGG	<i>mpn506</i> probe fw
SS191	<u>CTAATACGACTCACTATAGGGAGAGTACCTTCTTTCT</u> TTTTAGCGTTGTTC	<i>mpn506</i> probe rev
SS192	P_GATGGTTTGGAGATGGATGTGCAACTCAC	<i>mpn566</i> T106G/G107A/ A114T
SS193	P_CGTTTCGCTTTCTCTTGCTTGAAATTAAGGGCG	<i>mpn566</i> T328G/T329A/ T330A
SS194	P_GTAGTCACTCATGATGACAACTATAAGGTAGGAA ATAAAACC	<i>mpn566</i> A151C/T154G/ T155A/A156T
SS195	CAAAGCCAATGTCAACGGCAC	<i>mpn131</i> probe fw
SS196	<u>CTAATACGACTCACTATAGGGAGACATTTTTGGTCCG</u> TGGAATTAACCTTAC	<i>mpn131</i> probe rev
SS197	GCTGTTGGTATTTTTATTCTTTCCTAAAC	<i>mpn149</i> probe fw
SS198	<u>CTAATACGACTCACTATAGGGAGAGAGGGAGCCACT</u> GTTAGTTG	<i>mpn149</i> probe rev
SS199	CCAATTAAGCTCCTTCAAAGAATGG	<i>mpn284</i> probe fw
SS200	<u>CTAATACGACTCACTATAGGGAGACGATCGTATTGTT</u> CGTCATTAATTTG	<i>mpn284</i> probe rev
SS201	CCAAACCCCAATCCCTCAAAC	<i>mpn370</i> probe fw

Tab. S14. Continued.

Name	Sequence (5'→3') ^{ab}	Description ^c
SS202	<u>CTAATACGACTCACTATAGGGAG</u> ACCGTGAGGGGA GGGAC	<i>mpn370</i> probe rev
SS203	GGAATGGATATAAGGGGGTTCG	<i>mpn468</i> probe fw
SS204	<u>CTAATACGACTCACTATAGGGAG</u> ACTTCTTGAACACT GATCGAATTACC	<i>mpn468</i> probe rev
SS205	GACATTGTTAAAAAGCTTGAATAAGGTTC	<i>mpn162</i> promoter fragment (-145) fw
SS206	GCACTAGCGGCAACGACG	<i>mpn162</i> promoter fragment (+56) rev
SS207	CACACAGGATCTAATAAATTTCAAGAG	Screening for <i>mpn506::Tn</i> strain fw
SS208	GGCTTTAAAAGAGCTCTTGCAAAC	Screening for <i>mpn506::Tn</i> strain rev
SS209	GGAAAATTCAAATAGAACTATAACACACAG	Screening for <i>mpn284::Tn</i> strain fw
SS210	GTAAGTTTTAATCTCCACGATAGTAAC	Screening for <i>mpn284::Tn</i> strain rev
SS211	<u>CTAATACGACTCACTATAGGGAG</u> ACGGCACCAATCC AACGTGG	<i>glpF</i> promoter fragment probe (+49) rev
pWH844 fw	TATGAGAGGATCGCATCACCAT	Sequencing of pWH844 constructs fw
pyk forw1	<u>AAGGATCC</u> CAGAAAACTAAAATTGTTTGTACCATCG G	<i>pyk</i> _{Bsu} fw (<i>Bam</i> HI)
pyk rev	TTT <u>CTGCAG</u> TAAAGAACGCTCGCACGG	<i>pyk</i> _{Bsu} rev (<i>Pst</i> I)

^a The sequence of the T7-promotor is underlined.

^b The "P" at the 5' end of primer sequences indicates phosphorylation.

^c Unless otherwise indicated, all genes are *M. pneumoniae* specific.

Plasmids

Tab. S15. Plasmids.

Name	Relevant characteristics ^{ab}	Used restriction sites	Reference
pAG2	pQE30- <i>ptsH</i> _{Bsu} (Amp ^R)	-	Galinier <i>et al.</i> (1997)
pBQ200	Allows expression of proteins in <i>B. subtilis</i> (Amp ^R /Erm ^R)	-	Martin-Verstraete <i>et al.</i> (1994)
pGP172	Allows overexpression of N-terminal <i>Strep</i> -tag fusion proteins in <i>E. coli</i> BL21(DE3)/pLysS (Amp ^R)	-	Merzbacher <i>et al.</i> (2004)
pGP174	pGP172- <i>glmA</i> _{Bsu}	-	Heinrich <i>et al.</i> (2006)
pGP205	pWH844- <i>hprK</i> _{Bsu}	-	Hanson <i>et al.</i> (2002)
pGP353	pMT85 with promoterless <i>lacZ</i> gene (Gm ^R /Kan ^R)	-	Halbedel and Stülke (2006)
pGP371	pWH844- <i>ptsH</i> _{Bsu} [S46A] (SH82+SH83)	<i>Bam</i> HI + <i>Hind</i> III	Pietack <i>et al.</i> (2010)
pGP400	pBQ200- <i>glmM</i> _{Bsu} (NP108/NP109)	<i>Bam</i> HI + <i>Sal</i> I	Schmidl <i>et al.</i> (2010)
pGP563	pWH844- <i>eno</i> _{Bsu} (<i>eno</i> forw1/ <i>eno</i> rev)	<i>Bam</i> HI + <i>Pst</i> I	Pietack <i>et al.</i> (2010)
pGP656	pWH844- <i>manB</i> (SS107/SS108)	<i>Bam</i> HI + <i>Pst</i> I	Schmidl <i>et al.</i> (2010)
pGP657	pWH844- <i>manB</i> ^c (SS107-SS111)	<i>Bam</i> HI + <i>Pst</i> I	Schmidl <i>et al.</i> (2010)
pGP658	pWH844- <i>manB</i> [S149A] ^c (SS107-SS112)	<i>Bam</i> HI + <i>Pst</i> I	Schmidl <i>et al.</i> (2010)
pGP659	pGP353- <i>glpF</i> (-321...+59) (SS155/SS156)	<i>Eco</i> RI + <i>Bam</i> HI	-
pGP660	pGP353- <i>mpn239</i> (-247...+71) (SS157/SS158)	<i>Eco</i> RI + <i>Bam</i> HI	-
pGP661	pGP172- <i>mpn566</i> [W36E/E38D/N51H/L52D/F110E] (SS39/SS40/SS192-SS194)	<i>Sac</i> I + <i>Bam</i> HI	This work
pGP756	pWH844- <i>pgi</i> (MR19/MR20)	<i>Bam</i> HI + <i>Hind</i> III	Dutow <i>et al.</i> (2010)
pGP757	pWH844- <i>pfkA</i> (MR23/MR24)	<i>Bam</i> HI + <i>Hind</i> III	Dutow <i>et al.</i> (2010)
pGP758	pWH844- <i>fba</i> (MR25/MR26)	<i>Bam</i> HI + <i>Hind</i> III	Dutow <i>et al.</i> (2010)
pGP759	pWH844- <i>tpiA</i> ^d (MR28/MR29)	<i>Bam</i> HI + <i>Pst</i> I	Dutow <i>et al.</i> (2010)
pGP760	pWH844- <i>gapA</i> (MR31/MR32)	<i>Bam</i> HI + <i>Pst</i> I	Dutow <i>et al.</i> (2010)
pGP761	pWH844- <i>pyk</i> (MR34/MR35)	<i>Bam</i> HI + <i>Pst</i> I	Dutow <i>et al.</i> (2010)
pGP762	pWH844- <i>pgi</i> ^c (MR19-MR22)	<i>Bam</i> HI + <i>Hind</i> III	Dutow <i>et al.</i> (2010)
pGP763	pWH844- <i>fba</i> ^c (MR25-MR27)	<i>Bam</i> HI + <i>Hind</i> III	Dutow <i>et al.</i> (2010)
pGP764	pWH844- <i>tpiA</i> ^c (MR28-MR30)	<i>Bam</i> HI + <i>Pst</i> I	Dutow <i>et al.</i> (2010)
pGP765	pWH844- <i>gapA</i> ^c (MR31-MR33)	<i>Bam</i> HI + <i>Pst</i> I	Dutow <i>et al.</i> (2010)

Tab. S15. Continued.

Name	Relevant characteristics ^{ab}	Used restriction sites	Reference
pGP766	pWH844- <i>pyk</i> ^c (MR34-MR38)	<i>Bam</i> HI + <i>Pst</i> I	Dutow <i>et al.</i> (2010)
pGP819	pGP172- <i>ywjH</i> _{Bsu} (NP11/NP12)	<i>Sac</i> I + <i>Bam</i> HI	Pietack <i>et al.</i> (2010)
pGP820	pGP172- <i>tkf</i> _{Bsu} (NP05/NP06)	<i>Sac</i> I + <i>Bam</i> HI	Pietack <i>et al.</i> (2010)
pGP821	pGP172- <i>prkD</i> _{Bsu} (NP09/NP10)	<i>Sac</i> I + <i>Bam</i> HI	Pietack <i>et al.</i> (2010)
pGP822	pGP172- <i>alsD</i> _{Bsu} (NP01/NP02)	<i>Sac</i> I + <i>Bam</i> HI	Pietack <i>et al.</i> (2010)
pGP823	pGP172- <i>yabT</i> _{Bsu} (NP07/NP08)	<i>Sac</i> I + <i>Bam</i> HI	Pietack <i>et al.</i> (2010)
pGP824	pGP172- <i>yxaL</i> _{Bsu} (NP13/NP14)	<i>Sac</i> I + <i>Bam</i> HI	Pietack <i>et al.</i> (2010)
pGP825	pGP172- <i>prkC</i> _{Bsu} (NP03/NP04)	<i>Sac</i> I + <i>Bam</i> HI	Pietack <i>et al.</i> (2010)
pGP931	pWH844- <i>icd</i> _{Bsu} (FC17/FC18)	<i>Bam</i> HI + <i>Pst</i> I	Pietack <i>et al.</i> (2010)
pGP1006	pWH844- <i>pgk</i> (MR04/MR05)	<i>Bam</i> HI + <i>Hind</i> III	Dutow <i>et al.</i> (2010)
pGP1007	pWH844- <i>pgm</i> (MR08/MR09)	<i>Bam</i> HI + <i>Pst</i> I	Dutow <i>et al.</i> (2010)
pGP1008	pWH844- <i>eno</i> ^c (MR10/MR11)	<i>Bam</i> HI + <i>Pst</i> I	Dutow <i>et al.</i> (2010)
pGP1010	pWH844- <i>pgk</i> ^c (MR04-MR07)	<i>Bam</i> HI + <i>Hind</i> III	Dutow <i>et al.</i> (2010)
pGP1016	pGP172- <i>mpn549</i> (SS29/SS30)	<i>Sac</i> I + <i>Bam</i> HI	-
pGP1017	pGP172- <i>mpn549</i> ^c (SS29-SS31)	<i>Sac</i> I + <i>Bam</i> HI	-
pGP1018	pGP172- <i>glpQ</i> (SS34/SS35)	<i>Sac</i> I + <i>Bam</i> HI	This work
pGP1019	pGP172- <i>glpQ</i> ^c (SS34-SS38)	<i>Sac</i> I + <i>Bam</i> HI	This work
pGP1020	pGP172- <i>mpn566</i> (SS39/SS40)	<i>Sac</i> I + <i>Bam</i> HI	This work
pGP1100	pWH844- <i>pyk</i> _{Bsu} (<i>pyk</i> forw1/ <i>pyk</i> rev)	<i>Bam</i> HI + <i>Pst</i> I	Pietack <i>et al.</i> (2010)
pGP1401	pWH844- <i>glmM</i> _{Bsu} (NP109/NP117)	<i>Bam</i> HI + <i>Sal</i> I	Schmidl <i>et al.</i> (2010)
pGP1403	pBQ200- <i>glmM</i> _{Bsu} [S100A] (NP108/NP109/NP116)	<i>Bam</i> HI + <i>Sal</i> I	Schmidl <i>et al.</i> (2010)
pGP1405	pWH844- <i>glmM</i> _{Bsu} [S100A] (NP108/NP116/NP117)	<i>Bam</i> HI + <i>Sal</i> I	Schmidl <i>et al.</i> (2010)
pGP1553	pUT18C- <i>pgi</i> ^c (PD05/PD06)	<i>Xba</i> I + <i>Kpn</i> I	Dutow <i>et al.</i> (2010)
pGP1554	pUT18C- <i>pfkA</i> (PD07/PD08)	<i>Xba</i> I + <i>Kpn</i> I	Dutow <i>et al.</i> (2010)
pGP1555	pUT18C- <i>fbA</i> ^c (PD09/PD10)	<i>Xba</i> I + <i>Sac</i> I	Dutow <i>et al.</i> (2010)
pGP1556	pUT18C- <i>tpiA</i> ^c (PD11/PD12)	<i>Xba</i> I + <i>Kpn</i> I	Dutow <i>et al.</i> (2010)
pGP1557	pUT18C- <i>gapA</i> ^c (PD13/PD14)	<i>Xba</i> I + <i>Eco</i> RI	Dutow <i>et al.</i> (2010)
pGP1558	pUT18C- <i>pgk</i> ^c (PD15/PD16)	<i>Xba</i> I + <i>Eco</i> RI	Dutow <i>et al.</i> (2010)
pGP1559	pUT18C- <i>pgm</i> (PD17/PD18)	<i>Xba</i> I + <i>Eco</i> RI	Dutow <i>et al.</i> (2010)
pGP1560	pUT18C- <i>eno</i> ^c (PD19/PD20)	<i>Xba</i> I + <i>Eco</i> RI	Dutow <i>et al.</i> (2010)
pGP1561	pUT18C- <i>pyk</i> ^c (PD21/PD22)	<i>Xba</i> I + <i>Kpn</i> I	Dutow <i>et al.</i> (2010)
pGP1563	pUT18- <i>pgi</i> ^c (PD05/PD06)	<i>Xba</i> I + <i>Kpn</i> I	Dutow <i>et al.</i> (2010)
pGP1564	pUT18- <i>pfkA</i> (PD07/PD08)	<i>Xba</i> I + <i>Kpn</i> I	Dutow <i>et al.</i> (2010)
pGP1565	pUT18- <i>fbA</i> ^c (PD09/PD10)	<i>Xba</i> I + <i>Sac</i> I	Dutow <i>et al.</i> (2010)
pGP1566	pUT18- <i>tpiA</i> ^c (PD11/PD12)	<i>Xba</i> I + <i>Kpn</i> I	Dutow <i>et al.</i> (2010)

Tab. S15. Continued.

Name	Relevant characteristics ^{ab}	Used restriction sites	Reference
pGP1567	pUT18- <i>gapA</i> ^c (PD13/PD14)	<i>Xba</i> I + <i>Eco</i> RI	Dutow <i>et al.</i> (2010)
pGP1568	pUT18- <i>pgk</i> ^c (PD15/PD16)	<i>Xba</i> I + <i>Eco</i> RI	Dutow <i>et al.</i> (2010)
pGP1569	pUT18- <i>pgm</i> (PD17/PD18)	<i>Xba</i> I + <i>Eco</i> RI	Dutow <i>et al.</i> (2010)
pGP1570	pUT18- <i>eno</i> ^c (PD19/PD20)	<i>Xba</i> I + <i>Eco</i> RI	Dutow <i>et al.</i> (2010)
pGP1571	pUT18- <i>pyk</i> ^c (PD21/PD22)	<i>Xba</i> I + <i>Kpn</i> I	Dutow <i>et al.</i> (2010)
pGP1573	pKNT25- <i>pgi</i> ^c (PD05/PD06)	<i>Xba</i> I + <i>Kpn</i> I	Dutow <i>et al.</i> (2010)
pGP1574	pKNT25- <i>pfkA</i> (PD07/PD08)	<i>Xba</i> I + <i>Kpn</i> I	Dutow <i>et al.</i> (2010)
pGP1575	pKNT25- <i>fba</i> ^c (PD09/PD10)	<i>Xba</i> I + <i>Sac</i> I	Dutow <i>et al.</i> (2010)
pGP1576	pKNT25- <i>tpiA</i> ^c (PD11/PD12)	<i>Xba</i> I + <i>Kpn</i> I	Dutow <i>et al.</i> (2010)
pGP1577	pKNT25- <i>gapA</i> ^c (PD13/PD14)	<i>Xba</i> I + <i>Eco</i> RI	Dutow <i>et al.</i> (2010)
pGP1578	pKNT25- <i>pgk</i> ^c (PD15/PD16)	<i>Xba</i> I + <i>Eco</i> RI	Dutow <i>et al.</i> (2010)
pGP1579	pKNT25- <i>pgm</i> (PD17/PD18)	<i>Xba</i> I + <i>Eco</i> RI	Dutow <i>et al.</i> (2010)
pGP1580	pKNT25- <i>eno</i> ^c (PD19/PD20)	<i>Xba</i> I + <i>Eco</i> RI	Dutow <i>et al.</i> (2010)
pGP1581	pKNT25- <i>pyk</i> ^c (PD21/PD22)	<i>Xba</i> I + <i>Kpn</i> I	Dutow <i>et al.</i> (2010)
pKNT25	<i>P_{lac}-mcs-cyaA</i> (Kan ^R)	-	Claessen <i>et al.</i> (2008)
pKT25- zip	<i>P_{lac}-cyaA-zip</i> (Kan ^R)	-	Karimova <i>et al.</i> (1998)
pMT85	Mini-transposon delivery vector for <i>M. pneumoniae</i> (Gm ^R /Kan ^R)	-	Zimmerman and Herrmann (2005)
pUT18	<i>P_{lac}-mcs-cyaA</i> (Amp ^R)	-	Karimova <i>et al.</i> (1998)
pUT18C	<i>P_{lac}-cyaA-mcs</i> (Amp ^R)	-	Karimova <i>et al.</i> (1998)
pUT18C- zip	<i>P_{lac}-cyaA-zip</i> (Amp ^R)	-	Karimova <i>et al.</i> (1998)
pWH844	Allows overexpression of N-terminal His ₆ -tag fusion proteins in <i>E. coli</i> DH5α (Amp ^R)	-	Schirmer <i>et al.</i> (1997)

^a Resistance abbreviations as follows: Amp, ampicillin; Erm, erythromycin; Gm, gentamicin; Kan, kanamycin.

^b Unless otherwise indicated, all genes are *M. pneumoniae* specific.

^c All TGA opal codons in the wild type gene are mutated to TGG.

^d Only one TGA opal codon in the forward primer region is mutated to TGG.

Strains

Tab. S16. Strains.

Name	Genotype ^a	Reference/Construction ^b
<i>Bacillus subtilis</i>		
168	<i>trpC2</i>	Laboratory collection
GP588	<i>trpC2</i> Δ <i>glmM::spec</i> ; complemented with pGP400	Schmidl <i>et al.</i> (2010)
<i>Escherichia coli</i>		
BL21(DE3)/pLysS	F- <i>ompT hsdSB</i> (rB ⁻ mB ⁻) <i>gal dcm</i> (DE3) pLysS (Cam ^R)	Sambrook <i>et al.</i> (1989)
BTH101	F- <i>cya-99 araD139 galE15 galK16 rpsL1</i> (Str ^R) <i>hsdR2 mcrA1 mcrB1</i>	Karimova <i>et al.</i> (2005)
DH5 α	F- Φ 80 <i>lacZ</i> Δ <i>M15</i> Δ (<i>lacZYA-argF</i>) U169 <i>recA1 endA1 hsdR17</i> (rK ⁻ mK ⁺) <i>phoA supE44</i> λ - <i>thi-1 gyrA96 relA1</i>	Sambrook <i>et al.</i> (1989)
XL1-Blue	<i>recA1 endA1 gyrA96 thi-1 hsdR17 supE44 relA1 lac</i> [F' <i>proAB lacI</i> ^q Δ <i>M15 Tn10</i> (Tet ^R)]	Stratagene
<i>Mycoplasma pneumoniae</i>		
GPM09	M129 <i>thyA::Tn4001m</i>	Wang <i>et al.</i> (2010)
GPM11	M129 <i>prkC::Tn4001m</i>	Schmidl <i>et al.</i> (2010)
GPM51	M129 <i>hprK::Tn4001m</i>	Halbedel <i>et al.</i> (2006)
GPM52	M129 <i>glpD::Tn4001m</i>	Hames <i>et al.</i> (2009)
GPM68	M129 <i>prpC::Tn4001m</i>	Halbedel <i>et al.</i> (2006)
GPM70	M129 <i>mpn474::Tn4001m</i>	Hegermann <i>et al.</i> (2008)
GPM80	M129 <i>mpn256::Tn4001m</i>	pMT85 \rightarrow M129
GPM81	M129 <i>mpn420::Tn4001m</i>	This work
GPM82	M129 <i>mpn566::Tn4001m</i>	This work
GPM84/1...GPM84/10	1-5 Glc <i>glpF</i> (-321...+59)- <i>lacZ</i> 6-10 Gly <i>glpF</i> (-321...+59)- <i>lacZ</i>	pGP659 \rightarrow M129
GPM85/1...GPM85/9	1-5 Glc <i>mpn239</i> (-247...+71)- <i>lacZ</i> 6-9 Gly <i>mpn239</i> (-247...+71)- <i>lacZ</i>	pGP660 \rightarrow M129
GPM86	M129 <i>mpn162::Tn4001m</i>	pMT85 \rightarrow M129
GPM87	M129 <i>mpn284::Tn4001m</i>	pMT85 \rightarrow M129
GPM88	M129 <i>mpn506::Tn4001m</i>	pMT85 \rightarrow M129
M129 (ATCC 29342)	Wild type	Somerson <i>et al.</i> (1963)

^a Resistance abbreviations as follows: Cam, chloramphenicol; Spec, spectinomycin; Str, streptomycin; Tet, tetracycline.

^b The arrow indicates transformation.

Curriculum vitae

Personal information

Name: Sebastian Schmidl
 Date of birth: 27th July, 1981
 Place of Birth: Bad Hersfeld, Germany
 Nationality: German
 Parents: Roland Schmidl and Petra Schmidl, née Haas
 Sibling: Saskia Schmidl

School education

1988 - 1992 Grundschule Friedlos, Ludwigsau
 1992 - 1998 Gesamtschule Geistal, Bad Hersfeld
 1998 - 2001 Modellschule Obersberg, Bad Hersfeld
 06/2001 University-entrance diploma (Abitur)

Community service

2001-2002 Deutsches Rotes Kreuz, Bad Hersfeld

Scientific education

10/2002 - 09/2007 Study of biology, University of Göttingen
 Diploma thesis in the group of Prof. Dr. Jörg Stülke,
 University of Göttingen
 Thesis title: “Control of the HPr kinase activity of
Mycoplasma pneumoniae”

11/2007 - 11/2010 PhD project:
 “Pathogenicity of a minimal organism: Role of protein
 phosphorylation in *Mycoplasma pneumoniae*”
 Dept. of General Microbiology (Prof. Dr. Jörg Stülke),
 University of Göttingen

03/2008 - 11/2010 Awarded a grant from the Studienstiftung des deutschen
 Volkes